UNITED STATES DEPARTMENT OF COMMERCE
HARRY L. HOPKINS, Secretary
NATIONAL BUREAU OF STANDARDS
Lyman J. Briggs, Director

✦

Journal of Research

of the

National Bureau of Standards

✦

Volume 22, No. 2
February 1939

[Published with approval of the Director of the Budget]

UNITED STATES
GOVERNMENT PRINTING OFFICE
WASHINGTON : 1939

For sale by the Superintendent of Documents, Washington, D. C. - - - - - - Price 30 cents
$3.50 per year on subscription

The prices of the separate Research Papers appearing in this JOURNAL are given on the front cover page. If 100 or more copies of any separate are ordered, a discount of 25 percent is allowed. Those who desire copies of separate Research Papers should send their orders and remittances without delay to the Superintendent of Documents, U. S. Government Printing Office, Washington, D. C. This will aid him to determine the number of copies to be printed for sale. Research Papers are not printed from electrotypes, and usually no more reprints can be had when the first and only printing is exhausted.

U. S. Department of Commerce National Bureau of Standards

RESEARCH PAPER RP1172

Part of Journal of Research of the National Bureau of Standards, Volume 22, February 1939

THERMAL-EXPANSION CHARACTERISTICS OF SOME GROUND-COAT ENAMEL FRITS

By William N. Harrison, Benjamin J. Sweo, and Stephen M. Shelton

ABSTRACT

Thermal-expansion determinations were made on 11 sheet-iron ground-coat frits of the single-frit type, using the interferometer and also a quartz-tube dial-indicator apparatus. "Critical" temperatures for both heating and cooling were determined. Mean coefficients of expansion from 25° to 400° C, and total contraction from the critical temperatures to 25° C during cooling were correlated with variations in composition. Total differential contractions between enameling-type iron and the frits were also computed and correlated with variations in composition. Constants were determined which, when substituted in simple first-order equations, permit the computation of the expansivity of each frit at any temperature or temperature interval between 25° C and the critical temperatures. The observed difference in the critical temperature on heating and that on cooling, the difference in the temperature-expansion curve of highly strained specimens below the critical temperature in heating, and the shrinkage of annealed specimens when held 30° C below the critical temperature for heating, are explained by the work of Tool, Lloyd, and Merritt on glass.

CONTENTS

	Page
I. Introduction	127
II. Methods of testing	128
1. Dial method	128
2. Interferometer method	129
III. Results and discussion	129
1. Expansivity to 400° C	129
2. "Critical" temperatures	130
3. Expansion constants	132
4. Application of conclusions of Tool, Lloyd, and Merritt to frits studied	134
IV. Conclusions	135

I. INTRODUCTION

A series of 11 ground coats for sheet iron of the single-frit type were studied at this Bureau, and reports on their fusion properties,[1] strength, and elasticity [2] have been published. Subsequently, determinations on their thermal expansions were completed and considerable work done in comparing the results obtained by different methods of test and of analyzing the data. Further, some experiments were

[1] W. N. Harrison and B. J. Sweo, *Some fusion properties of ground coat enamels as influenced by composition.* BS J. Research **10**, 189 (1933) RP524.

[2] W. N. Harrison, S. M. Shelton, and W. H. Wadleigh, *Strength and Young's modulus of some ground coat enamels for sheet iron.* J. Am. Ceram. Soc. **18**, 100 (1935).

conducted to obtain confirmation of the logical presumption that the temperature-time-volume relations, which, according to the work of Tool, Lloyd, and Merritt [3] apply to glasses studied by them, also apply to the enamel frits used in this investigation, which were essentially homogeneous glasses. This paper is a report of these studies.

The method of preparation of the frits, and also their compositions, both as computed from batch weights and as determined by chemical analysis, have been published.[4] The scheme of variation in compositions is shown in table 1.

TABLE 1.—*Scheme of variation in composition of frits and data on critical temperatures and thermal-expansion characteristics*

Enamel designation	Variable constituents [1]				Coefficient of linear thermal expansion 25° to 400° C. $\times 10^6$		Critical [2] temperatures (heating)	Expansion constants from interferometer data		Coefficients of linear expansion $\times 10^6$ computed from constants		Total linear expansion, 25° C to "critical temperature on heating"	Total linear contraction from "critical temperature on cooling" to 25° C		
	Feldspar	Flint	Sodium oxide	Boric oxide	Dial	Interferometer		$a \times 10^6$	$b \times 10^6$	25° to 200° C	25° to 400° C		Enamel frit	Enameling-type iron	Difference
	%	%	%	%			°C					μ/cm	μ/cm	μ/cm	μ/cm
A	35	25	17	13	11.5	11.8	437	9.78	0.00484	10.9	11.8	49.6	41.3	47.9	6.6
B	35	25	14	16	10.7	10.9	475	9.08	.00431	10.1	10.9	50.6	42.8	53.9	11.1
C	35	25	11	19	9.6	9.9	483	8.45	.00347	9.2	9.9	46.7	39.8	55.1	15.3
D	30	30	17	13	11.4	11.6	438	9.75	.00440	10.7	11.6	48.7	40.6	48.0	7.4
E	30	30	14	16	10.5	10.7	480	9.10	.00387	10.0	10.7	50.2	42.7	54.7	12.0
F	30	30	11	19	9.4	9.7	490	8.57	.00262	9.2	9.7	46.1	39.5	56.2	16.7
G	25	35	17	13	11.0	11.3	447	9.38	.00444	10.4	11.3	48.4	40.5	49.4	8.9
H	25	35	14	16	10.2	10.4	482	8.92	.00351	9.7	10.4	48.9	41.6	55.0	13.4
I	25	35	11	19	9.1	9.5	488	7.92	.00362	8.7	9.5	45.3	38.5	56.0	17.5
J	27	27	17	19	11.0	11.5	450	9.66	.00427	10.6	11.5	49.8	41.7	49.9	8.2
K	33	33	11	13	9.6	9.9	488	8.84	.00249	9.4	9.9	46.8	40.2	55.8	15.6

[1] Each frit contained, in addition to the tabulated constituents, 7.7 percent of fluorspar, 1.7 percent of manganese oxide, and 0.6 percent of cobalt oxide.

[2] The values for cooling may be obtained by subtracting 60° C from those determined for heating, an approximation which is explained in the text.

II. METHODS OF TESTING

1. DIAL METHOD

The apparatus used was similar to that described by Hidnert and Sweeney,[5] with the following refinements. A sensitive dial indicator, which could be read to 0.0001 inch and estimated to an additional decimal, was used. To minimize temperature gradients, the furnace winding was tapped to divide it into three sections. The middle section was the same length as the specimen and inclosed it during a test. The two end sections were each about half the length of the specimen. Current could be shunted through variable resistances in parallel with the respective sections of the winding. Correction for the ex-

[3] *Dimensional changes caused in glass by heating cycles.* BS J. Research **5**, 632 (1930) RP219. Also J. Am. Ceram. Soc. **13**, 4 (Sept. 1930).

[4] W. N. Harrison and B. J. Sweo, *Some fusion properties of ground coat enamels as influenced by composition.* BS J. Research **10**, 189 (1933) RP524.

[5] Peter Hidnert and W. T. Sweeney, *Thermal expansion of magnesium and some of its alloys.* BS J. Research **1**, 771 (1928) RP29.

pansivity of the particular fused quartz used, and for temperature gradients in the quartz tubes during test, was made by calibration against a specimen of porcelain, the expansivity of which had been accurately determined at this Bureau. It was established that the expansivity of this specimen did not change in repeated determinations up to 400° C.

The dial was read when the furnace was at room temperature and at 100°, 200°, 300°, and 400° C, respectively. At each temperature the dial reading used in computing expansion had remained constant over a 20-minute period, during which the temperature of the furnace was held constant, the resistance being adjusted so that the temperature was uniform within 1° C from top to bottom of the specimen.

The requisite 8-inch specimens were cast in molds made from blocks of electrode carbon. Side-opening molds were used so that the vessel from which the molten frit was poured could be moved from one end of the mold to the other during the pouring process. Each mold was preheated to about 600° C and, after the specimen was cast, was returned to the furnace, held at 550° C for 1 hour and allowed to cool with the furnace. While in the furnace the molds were encased in sheet-iron jackets buried in mixtures of sand and graphite to retard oxidation. Expansion curves on specimens prepared in this way indicated a satisfactory quality of annealing.

2. INTERFEROMETER METHOD

The construction and operation of the apparatus used for measuring expansion by the interferometer method are described by Merritt.[6] The test specimens were made from rods approximately 3 mm in diameter drawn from the molten frit. A blunt point was formed at one end of each specimen, and three short legs formed on the opposite end, by grinding. These specimens were approximately 5 mm long, over-all. The temperature was increased continuously in these tests at the rate of 3° C per minute, as indicated by the average of two Chromel-Alumel thermocouples, the junction of one being placed just above the cover plate, and the junction of the other just below the base plate. The cup in which the specimens were placed during test was made of aluminum. Tests were made on unannealed specimens cooled from the molten state in air to determine their "softening temperatures." [7] They were then annealed by heating for 3 hours at a temperature about 5° C below their respective softening temperatures, and cooling in the furnace. These annealed specimens were used for expansivity determinations.

III. RESULTS AND DISCUSSION

1. EXPANSIVITY TO 400° C

The coefficients of linear thermal expansion from 25° to 400° C, as determined by both the dial and the interferometer methods, are given in table 1. The initial temperature in each case was approximately 25° C and the values were all corrected to 25° C in order that they might be comparable. The coefficient of expansion values given in

[6] G. E. Merritt, *The interference method of measuring thermal expansion.* BS J. Research **10**, 59 (1933) RP515.

[7] W. N. Harrison and B. J. Sweo, *Some fusion properties of ground coat enamels as influenced by composition.* BS J. Research **10**, 189 (1933) RP524.

this table represent averages of determinations on three separately prepared batches of frit. Individual deviations from the reported values averaged less than 0.1×10^{-6}, the maximum deviation being 0.3×10^{-6}.

The values obtained with the interferometer are 0.2 to 0.5×10^{-6} higher than those obtained with the dial apparatus. A number of experiments made to determine the source of this difference failed to reveal the cause of the discrepancy.

From table 1 it may be seen that the assumption commonly used in calculating expansivity from factors, namely, that the expansivity is an additive function of the constituent parts, held approximately true for these frits. Each of the six substitutions of 3 percent of boric oxide for 3 percent of sodium oxide, with other constituents unchanged, resulted in a decrease of about 1.0×10^{-6} in the coefficient of expansion, the extremes being 0.8 and 1.1×10^{-6}. The substitution of 10 percent of flint for 10 percent of feldspar produced a decrease of about 0.5×10^{-6}.[8] The *J–K* change in composition resulted in a substantial reduction in the coefficient of expansion.

2. "CRITICAL" TEMPERATURES

It is recognized that the real importance of the thermal expansivity of enamels lies in the differential contraction between the enamel and the underlying metal as an enameled article cools after firing, and this differential depends not only upon the difference in expansivity but also upon the temperature at which the enamel becomes sufficiently stiff to set up strains in cooling. Hence it is obvious that the coefficient of expansion alone, whether computed or determined experimentally, does not give all of the required information.

The temperatures at which these strains were initiated were not determined directly. However, the "critical" temperatures[9] of the frits were determined because it was thought that a knowledge of the total contraction from these temperatures to room temperature would be helpful in estimating the relative amounts of residual strain after firing. In locating these critical temperatures, only the interferometer method was used. No attempt was made to carry the observations with the dial apparatus up to such temperatures, as the use of the large specimens, and the accompanying necessity for holding the temperature constant at each observation level, render this method unsuitable for the purpose. Data obtained during cooling were compared with those obtained during heating and, for greater accuracy, new determinations were made, using a more sensitive potentiometer, the precision of the new pyrometer being better than 0.01°C. The cooling rate of the furnace was approximately 2°C per minute through that temperature range which included the critical temperatures, becoming slower as the temperature decreased.

Figure 1 is indicative of the results that were obtained. In the upper curves, expansion and contraction with change of temperature are plotted in the usual manner. In the lower curves the rates (coefficients) of expansion (or contraction) for the small temperature intervals between pairs of adjacent interference bands are plotted against the corresponding mean temperatures. Since the lower curves

[8] This 10-percent change in batch composition entailed a much smaller change in chemical composition.

[9] C. G. Peters and C. H. Cragoe, *Measurements on the thermal dilatation of glass at high temperatures*, BS Sci. Pap. 15, 445 (1920) S393.

are the first derivatives of the upper ones, they accentuate changes in rate of expansion or contraction. Straight lines fitted the points on the derivative curves sufficiently well up to approximately the critical temperature, which may be defined for the purpose of this work as the temperature at which a smooth curve drawn through the plotted points diverges or "breaks away" from the straight line.[10] That this "break" was sharper and that it occurred at a substantially higher temperature on heating than on cooling, as shown in figure 1, held true for every frit tested.

Even with the breaks accentuated by this system of plotting the data, it was not possible to determine the exact temperature at which

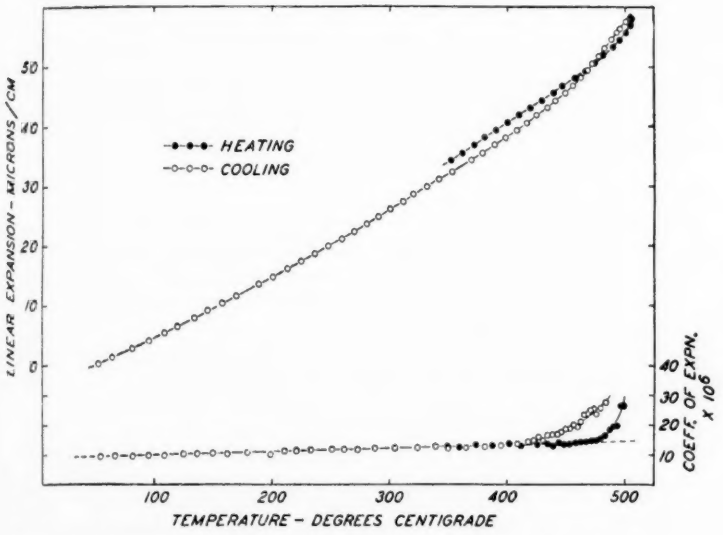

FIGURE 1.—*Curves showing the expansion and contraction of frit B.*

The upper curves show the expansion from 350° to 500° C and contraction from 500° to 50° C. The lower curves were obtained from the same data and show the change in coefficient of expansion (or contraction) with temperature under the conditions of test. To avoid confusion, not all of the data are plotted, except at the high-temperature end of the lower curves.

each break occurred, but it is thought that the uncertainty of the values obtained from the heating curves is within ±5° C. However, it is believed that the differences between the critical temperatures of different enamels were obtained with greater accuracy, since all were judged in the same way. The critical temperatures given in table 1 are those for heating data. Because of the greater difficulty in locating the critical temperatures for cooling from the data as plotted in figure 1, an estimate was made of the average difference, and this value (60° C) was subtracted from the critical temperature obtained from a heating curve to obtain the critical temperature for the corresponding cooling curve.

One correlation between change in composition and resultant change in critical temperature is very striking. The *A-B*, *D-E*, and *G-H*

[10] Although the points of divergence will not be accentuated to the same degree as in the described procedure, the same principle can be used by fitting a curve to expansion (or contraction) data from the constants referred to further on in this paper, and noting the temperatures at which smooth lines drawn through the data points diverge from such curves.

changes in critical temperatures (see table 1) are about four times as large as the *B-C*, *E-F*, and *H-I* changes, although the changes in composition are in the same direction and are of the same magnitude. The first three pairs all involve an increase of boric oxide from 13 to 16 percent and a reduction of sodium oxide from 17 to 14 percent. The second three pairs involve a further increase in the boric oxide to 19 percent, with corresponding decrease in sodium oxide to 11 percent. The average effect of increasing flint from 25 to 35 percent, at the same time reducing feldspar from 35 to 25 percent (the *A-G*, *B-H*, and *C-I* changes), was to increase the critical temperature only about 7° C.[11] The *J-K* change in composition resulted in an increase of 38° C in critical temperature.

3. EXPANSION CONSTANTS

The following equation has frequently been used to express changes of length with temperature, as graphically illustrated in the upper curves of figure 1.

$$L/L_0=1+at+bt^2 \tag{1}$$

in which:

L=length of specimen at the temperature, t.

L_0=length of specimen at the temperature, 0° C. (No appreciable error is introduced if this length is measured at room temperature.)

a and b are constants.

The instantaneous coefficient of expansion, C_t, at any temperature, t, is therefore given by the derivative of eq 1.

$$C_t=\frac{dL}{dt}\times\frac{1}{L_0}=a+2bt, \tag{2}$$

from which it follows that the mean coefficient between two temperatures, t_1 and t_2, is:

$$C_{t_1t_2}=\frac{C_{t_1}+C_{t_2}}{2}=a+b(t_1+t_2) \tag{3}$$

The constants, a and b, for the enamels studied are given in table 1. Although these constants are empirical, and small variations in the data may make relatively large percentage differences in their values, they are, nevertheless, useful in several ways. Various investigators have reported thermal expansions of enamels and similar materials between different limits of temperature, and hence it is sometimes difficult to compare the results reported by different authors. The constants given in table 1, when used in eq 3, make it possible to compute the coefficient of expansion of the enamels within any desired temperature range up to the critical temperature of a frit by a very simple calculation. Furthermore, unless elaborate precautions are taken, it is difficult to obtain accurate data on thermal expansion near room temperature when a schedule of continuous increase in temperature is used.[12] This difficulty may be largely remedied by use of the constants, as indicated in the following discussion.

[11] See footnote 8, p. 130.

[12] G. E. Merritt, *The interference method of measuring thermal expansion.* BS J. Research **10**, 59 (1933) RP515.

In this study determinations of total expansion from 25° to 400° C (and hence mean coefficient of expansion) were in satisfactory agreement whether obtained in heating or in cooling. However, the agreement was not satisfactory at the lower temperatures, notably from 50° to 150° C. Below 50° C no readings were taken in cooling. Since temperature measurements were made from two thermocouples, one above and one below the quartz plates, and a quartz thermometer was not used, it was concluded that the temperature readings may have differed significantly from the true temperature of the specimen during heating. In the cooling tests the average rate of change of temperature in the 50° to 150° C interval was about 0.3° C per minute, as compared with a rate of 3° C per minute in heating, and because of this slower rate, the temperature gradients were presumably smaller. When a very slow heating schedule was tried, a higher apparent rate of expansion was observed, as in cooling. Hence, in computing the constants given in table 1, the data obtained in cooling were used in establishing the lower end of the expansion curves down to 50° C. Extrapolations from 50° C down to 25° C by means of the constants used in eq 3, are thought to be more reliable than the observed data in that range.

In table 1, in addition to the constants for eq 3, the mean linear coefficients of expansion computed from these constants are given for the following temperature ranges: 25° to 200° C, 25° to 400° C, 25° C to the critical temperature, as determined from heating data, and 25° C to the critical temperature, as determined from cooling data.

Concerning the total expansions to the critical temperatures in heating, or total contraction from critical temperatures in cooling, a reversal of trend takes place as sodium oxide is substituted for boric oxide. Increasing the sodium oxide content from 11 to 14 percent and decreasing boric oxide from 19 to 16 percent (the *C–B*, *F–E*, and *I–H* changes shown in table 1) caused a substantial increase in total expansion to (or contraction from) the critical temperatures, as well as in the average coefficient of expansion. A further 3-percent increase of sodium oxide at the expense of boric oxide (the *B–A*, *E–D*, and *H–G* changes shown in table 1) increased the coefficient of expansion, as in the first substitution, but the accompanying reduction in critical temperatures more than compensated the effect of this increase in average coefficient of expansion on the total length change between 25° C and the critical temperatures.[13]

It would be a mistake, however, to deduce that the total differential contraction between iron and enamel in the temperature ranges under discussion undergoes a reversal, as boric oxide and sodium oxide are varied between the indicated limits. From values given in table 1 it is apparent that the differential contraction increases without reversal as the coefficient of expansion of the frits decreases. The total contraction of the iron to 25° C from the respective critical temperatures of the frits in cooling, given in table 1, was computed from constants which were experimentally established for one specimen of enameling-type iron in the range 25° to 400° C, namely, $a=11.4\times10^{-6}$ and $b=0.0055\times10^{-6}$.

[13] A nonlinear effect on the properties of glasses caused by intersubstitution of boric oxide for silica was noted by W. E. S. Turner, J. Glass Tech. **7**, 155 (1923).

4. APPLICATION OF CONCLUSIONS OF TOOL, LLOYD, AND MERRITT TO FRITS STUDIED

The described shift in the "critical" temperature obtained on cooling, as compared with that obtained on heating (fig. 1), has been explained by Tool, Lloyd, and Merritt.[14] The critical temperature observed on heating indicates a behavior analogous to that occurring in superheating and the critical temperature observed on cooling bears a similar analogy to under cooling. In either case the high rates of change of volume with respect to temperature illustrated by the lower curves in figure 1, between 400° and 500° C indicate drifts toward the equilibrium volumes, for the temperatures involved, which proceed at insignificant rates in lower temperature ranges, because of the higher viscosity of the specimens. The familiar dip in the expansion curve of highly strained specimens of enamel frit (or glass), which begins as much as 100° C below the critical temperature in heating, is also explained by those authors in the same way. Figure 2

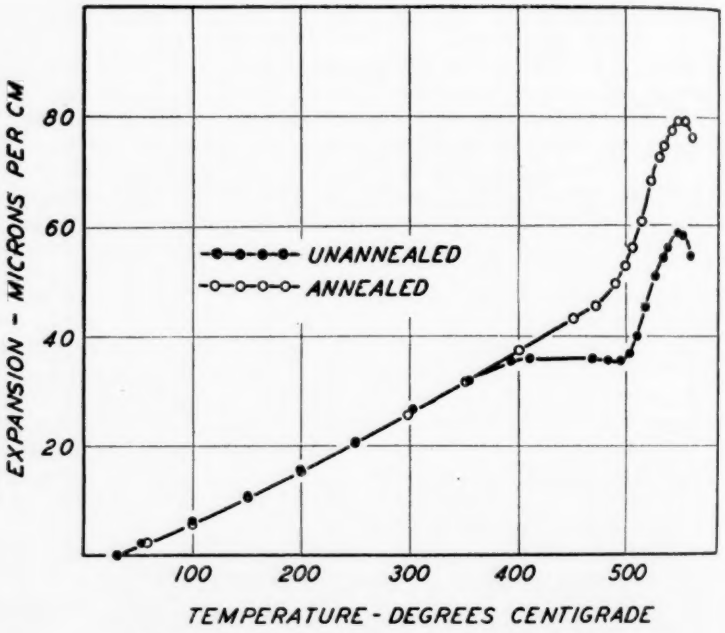

FIGURE 2.—*Thermal expansion curves for frit H.*

Drawn from molten frit and cooled in air (solid circles) and the same specimens after annealing (open circles).

shows typical heating curves for specimens of frit *H* in the annealed and the unannealed conditions. The relatively flat portion of the latter curve between 400° and 500° C reflects a drift toward the equilibrium volume-temperature line. The forces tending toward equilibrium volume are larger in the highly strained specimens and hence can operate more rapidly against high viscosities.

[14] *Dimension changes caused in glass by heating cycles.* BS J. Research **5**, 627 (1930) RP219. Also J. Am. Ceram. Soc. **13**, 4 (Sept. 1930).

The fact that even annealed specimens will undergo such drifts if given sufficient time was shown by Tool, Lloyd, and Merritt. In the present study, annealed specimens of enamel frit *E* were held for 5 hours at 450° C, which is 30° C below the critical temperature obtained on heating and 30° C above that on cooling. The drift toward equilibrium volume at that temperature resulted in a decrease in length equal to 13 percent of the expansion from 25° to 450° C (see fig. 3). Upon subsequent reheating no significant change in coefficient of expansion was detected.

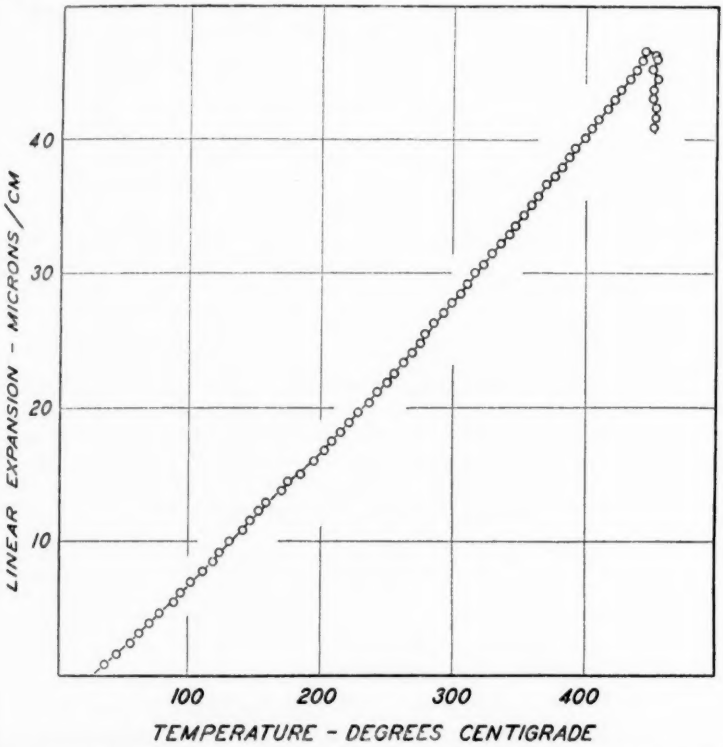

FIGURE 3.—*Curve showing the expansion of annealed specimens of frit E heated at 3° C per minute to 450° C and subsequent contraction on holding at that temperature for 5 hours.*

IV. CONCLUSIONS

A consistent difference of about 3 percent was observed between the expansivities from 25° to 400° C, as determined with the interferometer, using specimens 5 mm tall and 3 mm in diameter, and those determined with a quartz-tube and indicating-dial apparatus, using specimens 8 inches long and ⅝ inch square in cross section. Since interferometer specimens cut from the larger specimens gave the same difference in results, it was concluded that this difference was inherent in the methods of test and may have been related to the difference in size of the specimens. Because the smaller specimens are better

adapted for determining change of length with continuous change in temperature, especially through the "critical" range, the interferometer method is preferred.

Equal substitutions of boric oxide for sodium oxide in the range studied caused approximately equal decreases in coefficient of expansion, but caused unequal increases in "critical" temperature, the first 3-percent substitution causing about four times as much change in this property as a further 3-percent substitution in the same direction. The total expansion to critical temperature underwent an actual reversal in the same range of substitutions, that for the intermediate composition being greater than that for either higher or lower sodium oxide content. Computation from data of effective differential contractions between the frits and a typical enameling-type iron indicated, however, that this important relation followed a continuous trend, increasing with decreasing sodium oxide content.

From expansion constants and a simple first-order equation which are given, the coefficients of expansion of the frits studied can be easily computed for any desired temperature or any temperature interval between 25° C, and the critical temperatures.

The report of Tool, Lloyd, and Merritt on the dimensional changes resulting from heating cycles in glasses explains why the data obtained in the present study indicate that the critical temperature for cooling was lower than that for heating and also explains the shrinkage of annealed specimens of enamel frit held for 5 hours at a temperature 30° C below the critical temperature for heating. The difference between the critical temperatures was about 60° C and the shrinkage was about 6 μ/cm. Both of these phenomena, as well as the familiar dip in the expansion curve of a highly strained specimen, which occurs well below the critical temperature observed in heating, apparently result from drifts toward the equilibrium temperature-volume conditions which those authors reported for glasses.

WASHINGTON, October 16, 1938.

U. S. Department of Commerce National Bureau of Standards

RESEARCH PAPER RP1173

Part of Journal of Research of the National Bureau of Standards, Volume 22, February 1939

SEPARATION OF 1,2,4-TRIMETHYLCYCLOHEXANE AND AN ISONONANE FROM A MIDCONTINENT PETROLEUM[1]

By Joseph D. White,[2] and Augustus R. Glasgow, Jr.[3]

ABSTRACT

A fraction of Oklahoma petroleum boiling at 141° C, from which the aromatic hydrocarbons previously had been removed, was separated by distillation at 215 mm Hg into a fraction containing the bulk of a naphthene constituent and one enriched in paraffins. From the former, nearly pure 1,2,4-trimethylcyclohexane was isolated by crystallization from solution in liquid dichlorodifluoromethane. Continued distillation of the paraffinic fraction at normal pressure, alternated with distillation at 215 mm Hg, yielded a fraction containing 85 mole percent of an isononane, probably 2,3-dimethylheptane. The 1,2,4-trimethylcyclohexane constitutes about 0.1 percent, and the isononane about 0.05 percent of the original petroleum.

Effective separation of a paraffin-naphthene mixture, constant-boiling at normal pressure, by distillation at a different pressure arises from the greater change in boiling point with pressure of the naphthene component. For hydrocarbons normally boiling near 140° C, the mean interval between boiling points at 760 mm Hg and 215 mm Hg is about 42° C for paraffins, and about 43.2° C for naphthenes. The boiling points at the two pressures were determined for six hydrocarbons, 2,6-dimethylheptane, a nonanaphthene (boiling at 136.7° C), 1,2,4-trimethylcyclohexane, 4-methyloctane, 3-methyloctane, and 2-methyloctane. The boiling points at these pressures for the "2,3-dimethylheptane" were estimated from values for an impure sample.

The boiling point, freezing point, density, refractive index, and critical solution temperature in aniline have been determined for the 1,2,4-trimethylcyclohexane and the isononane. Comparison of the properties of the 1,2,4-trimethylcyclohexane with those reported for its synthetic stereoisomers indicates that the petroleum hydrocarbon is either 1_{cis}, 2_{trans},4_{cis}-trimethylcyclohexane or 1_{cis},2_{trans}, 4_{trans}-trimethylcyclohexane.

CONTENTS

	Page
I. Introduction	138
II. Previous fractionation of the petroleum distillate	138
III. Composition and properties of the fraction boiling between 98° and 99° C at 215 mm Hg	139
IV. Isolation and identification of 1,2,4-trimethylcyclohexane	142
V. Composition and properties of the material distilling between 98.8° and 100.8° C at 215 mm Hg, after partial removal of 1,2,4-trimethylcyclohexane	145
VI. Separation of paraffin-naphthene mixtures by alternate distillation at normal and reduced pressures	147
VII. Separation of the paraffin-naphthene mixture boiling between 98.8° and 99.8° C at 215 mm Hg	148

[1] Financial assistance has been received from the research fund of the American Petroleum Institute. This work is part of Project 6, The Separation, Identification, and Determination of the Constituents of Petroleum.

[2] Formerly Research Associate at the National Bureau of Standards, representing the American Petroleum Institute; now with the W. C. Hardesty Co., Dover, Ohio.

[3] Research Associate at the National Bureau of Standards, representing the American Petroleum Institute.

Page
VIII. Properties of the isomeric nonane fraction and the probable identity of the nonane with 2,3-dimethylheptane 151
IX. Content of 1,2,4-trimethylcyclohexane and the isononane in the petroleum 152
X. References 152

I. INTRODUCTION

In 1883 Markownikoff and Ogloblin [1][4] identified 1,2,4-trimethylcyclohexane (hexahydropseudocumene) in Caucasian petroleum from the product of its nitration. Since then, frequent allusions have been made to the presence of nonanaphthenes (C_9H_{18}) in petroleum without specific reference to 1,2,4-trimethylcyclohexane. Recently, however, Kasansky and Eliséeva [2] dehydrogenated the nonanaphthene fraction, distilling between 135° and 138° C, of Baku petroleum into aromatic material, and, by brominating the portion of the product which boiled at 170° C, obtained some tribromopseudocumene. From this experiment, they concluded that 1,2,4-trimethylcyclohexane was a constituent of the original petroleum fraction.

The present investigation has resulted in the isolation of 1,2,4-trimethylcyclohexane and the partial separation of a nonane, probably 2,3-dimethylheptane, from the methyloctane fraction [3] of an Oklahoma petroleum. Until now, the presence in petroleum of the isononane (boiling point, 140.7° C) appears to have escaped detection.

II. PREVIOUS FRACTIONATION OF THE PETROLEUM DISTILLATE

After a systematic distillation of the whole naphtha fraction of the petroleum, the material boiling between 130° and 145° C was treated with liquid sulfur dioxide to extract the bulk of the aromatic hydrocarbons [4]. To complete the removal of aromatic material, the immiscible portion was redistilled, and the large-volume fraction boiling between 140° and 145° C was treated with silica gel [3]. The residual oil consisting of paraffins and naphthenes was then distilled at a pressure of 215 mm Hg through a fractionating column, packed with jeweler's locket chain, having the equivalent of about 60 theoretical plates [5]. The distilled material was recovered in 50-ml fractions. After the measurement of their boiling points and refractive indices, fractions boiling within a range of 0.2° C were combined. The distillation separated the material into two main portions, each with a boiling range (at 215 mm Hg) of about 1° C. The larger, boiling between 101° C and 102.2° C (143° and 144.2° C at 760 mm Hg), contained the three methyloctanes. The isolation of these hydrocarbons from the petroleum has already been described [3]. The other portion distilled chiefly between 98° and 99° C. The volumes and refractive indices of the combined fractions comprising this portion are given in figure 1.

[4] Figures in brackets indicate the literature references at the end of this paper.

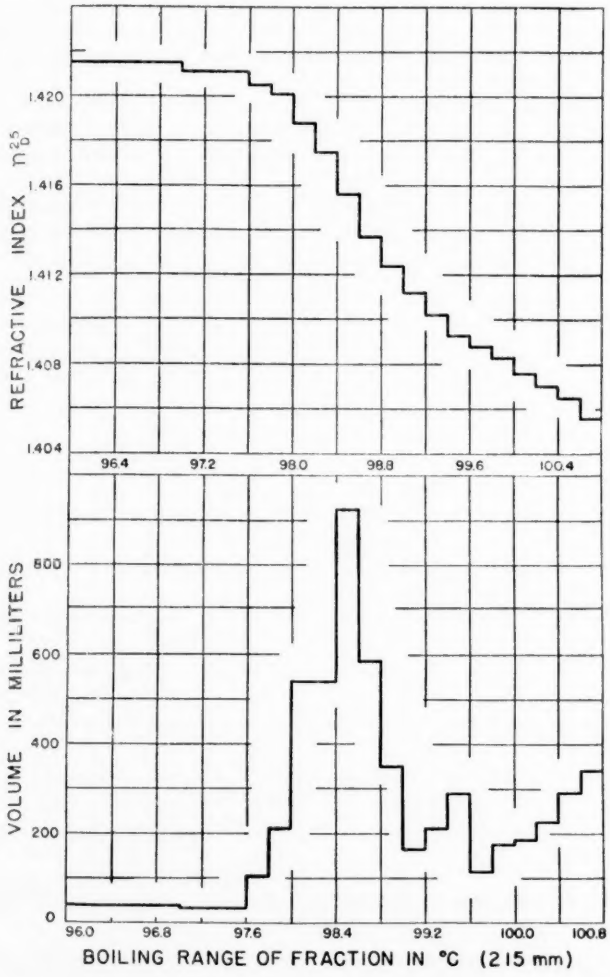

FIGURE 1.—*Volumes and refractive indices of the petroleum fractions, boiling between 96.0° and 100.8° C at 215 mm* Hg, *after removal of aromatic hydrocarbons and subsequent distillation.*

Lower graph, volume distribution with respect to boiling range; upper graph, refractive indices.

III. COMPOSITION AND PROPERTIES OF THE FRACTION BOILING BETWEEN 98° AND 99° C AT 215 mm Hg

In figure 2 the boiling points and refractive indices of the material represented in figure 1 are plotted against the volume distilled. The refractive indices are those for the 50-ml fractions which marked a rise of 0.2° C in the boiling point of the distillate. The plateau in the boiling-point curve between 98° and 99° C represents nearly 3 liters of material whose gradual change in properties indicated it to be a mixture. The values of the boiling points and refractive indices signi-

fied that the material was composed of nonanaphthenes and isononanes. As disclosed by the high refractive index of the lower-boiling material, the naphthenes were more volatile than the paraffins at a pressure of 215 mm Hg.

To determine the degree of separation of the material into its components when distilled at normal pressure, a 1,200-ml portion boiling between 98.4° and 98.8° C at 215 mm Hg was distilled at atmospheric pressure in the column used before. The results of the distillation are given in figure 3. The boiling-point curve (labeled 760 mm) shows that fully half of the material distilled between 141.0° and 141.1° C. Somewhat more surprising was the fact, as indicated by the

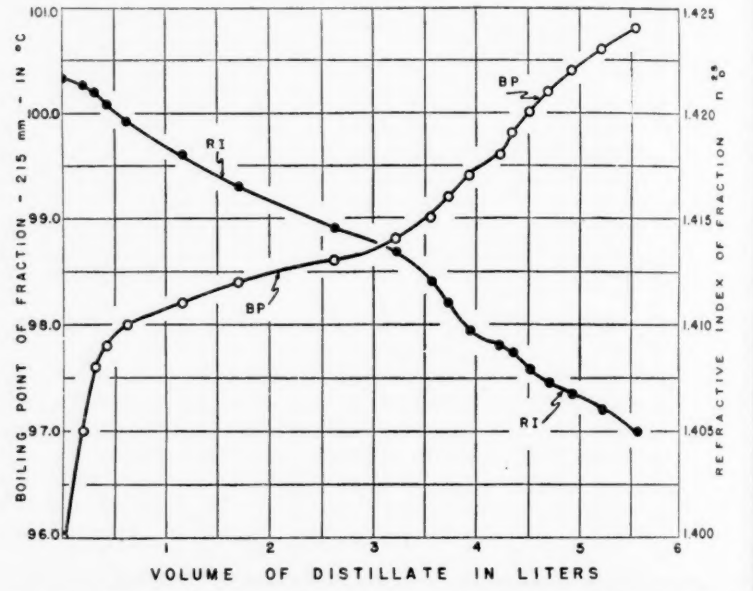

FIGURE 2.—*Fractionation by distillation of the material represented by the graphs in figure 1.*

Boiling points and refractive indices are plotted against the volume of material distilled. The individus points are those for 50-ml fractions which marked a rise of 0.2° C in the boiling point of the material.

refractive-index curve drawn through the open circles, that at 760 mm Hg the order of distillation of the constituents was the reverse of that at 215 mm Hg. At normal pressure the paraffinic material was more volatile than the naphthene and tended to concentrate in the lower-boiling fractions.[5] It was hoped that the normal boiling points of the component hydrocarbons could be located by the atmospheric distillation and compared with those of known hydrocarbons to obtain a clue as to what compounds might be present. Little knowledge was obtained concerning the boiling points of the constituents. What fractionation there was indicated that the naphthene present boiled above 141.0° C and the paraffin below.

[5] Prior to this experiment, S. T. Schicktanz had observed similar behavior of material from the "isodecane" fraction of this petroleum.

Since it was difficult to fractionate the material at normal pressure, the fractions were combined and distilled again at 215 mm Hg. The change in composition of the material as the distillation progressed is indicated by the curves passing through the solid circles in figure 3. The continual rise in boiling point and the marked change in refractive index indicated that better separation took place at the reduced pressure.

By combustion analysis the composition of a fraction of the distillate boiling at 98.4$_5$° C (n_D^{25}=1.4151) was 48 mole percent of naphthenes and 52 mole percent of isononanes. The cooling curve of a

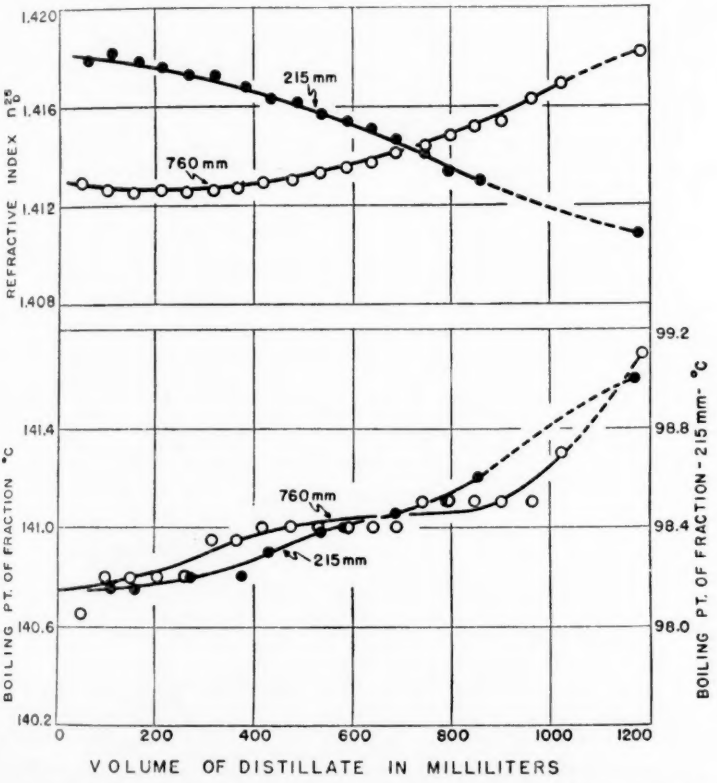

FIGURE 3.—*Fractionation of the paraffin-naphthene mixture by distillation at normal pressure contrasted to that obtained by distillation at 215 mm* Hg.

Curves passing through the open circles represent the change in boiling point and refractive index of the fractions obtained from the distillation at 760 mm Hg. Curves passing through the solid circles denote the fractionation at 215 mm Hg.

50-ml fraction boiling at 98.4$_5$° C, (n_D^{25}=1.4154) is shown in figure 4. By repeatedly plunging a metal rod, chilled with liquid air, into the material as it was cooled, freezing was finally induced at −120° C. On warming the partially frozen mass, a rapid change from a higher to a lower viscosity took place around −115° C, and at −104° C the last of the crystals melted. The cooling and warming behavior indicated that the material was substantially a binary mixture. As de-

termined later, the portion of the melting curve, figure 4, extending from −115° C to −104° C represents the melting of the naphthene component, while the break in the curve at −115° C is attributed to a change in state of the isomeric nonane present (see section VII).

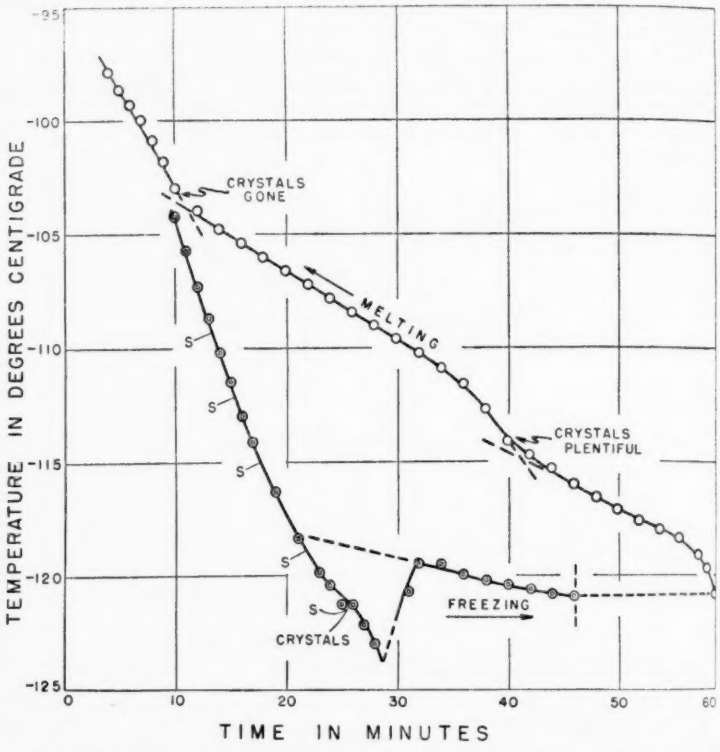

FIGURE 4.—*Cooling and warming curves of a distillation fraction boiling at 98.4° C at 215 mm* Hg.

S, stirred with a cold rod to induce crystallization.

IV. ISOLATION AND IDENTIFICATION OF 1,2,4-TRIMETHYLCYCLOHEXANE

When the material boiling at 98.4° C was mixed with liquid dichlorodifluoromethane, Freon 12, and cooled, a crystal fraction was produced which was found to be enriched in a naphthene having a normal boiling point of approximately 141.3° C. Systematic crystallization from this solvent, alternated with distillation, yielded from the material boiling between 97.0° and 98.8° C at 215 mm Hg somewhat more than a liter of the impure naphthene.[6] This was subjected to further fractional crystallization to yield a 95-ml fraction of "best"

[6] The lowest-boiling mother liquor contained another naphthene, probably 1,3,5-trimethylcyclohexane. The higher-boiling mother liquors were rich in paraffins.

naphthene. After distillation through a small fractionating column and filtration through silica gel to remove remaining traces of solvent, this fraction had the following properties: [7]

Normal boiling point, °C	141. 22
Pressure coefficient, °C/mm Hg at 760 mm	0. 051
Melting point, °C	−86. 4
Density at 20° C, g/ml	0. 7720
Refractive index, n_D^{20}	1. 4266
Critical solution temperature in aniline, °C	59. 0

The freezing range of 1° C in the cooling curve, figure 5, showed that the compound was sufficiently pure for use in identification. Combustion analysis indicated that its chief impurity was an isomeric nonane. As a result of three determinations by the procedure described by Rossini [6], the mean ratio, moles H_2O/moles CO_2, was found to be 1.0060 ±0.0004. Compared with the theoretical value of 1.0000 for a naphthene, C_nH_{2n}, and 1.1111 for a nonane, C_9H_{20}, the combustion analysis indicated that the material was composed of 94.6 mole percent of a naphthene and 5.4 mole percent of an isononane.

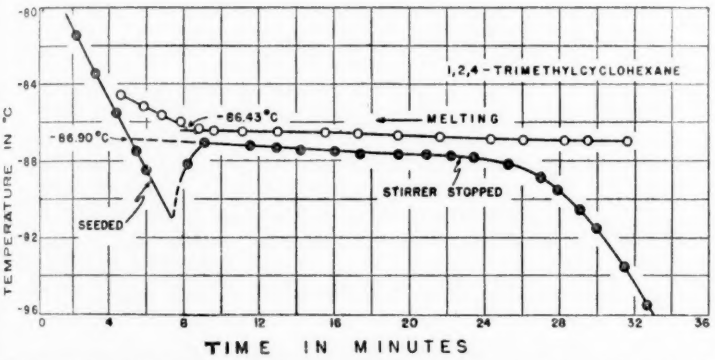

FIGURE 5.—*Time-temperature cooling and warming curves of the 1,2,4-trimethylcyclohexane isolated from petroleum.*

The molecular weight of the fraction, determined by the lowering in freezing point of cyclohexane,[8] was 128.5, which agrees within the error of the method with the theoretical value of 126.2 for a nonanaphthene, C_9H_{18}.

The nonanaphthene was identified as 1,2,4-trimethylcyclohexane by dehydrogenation over palladinized asbestos (20 percent of palladium). The catalyst was prepared by the method described by Zelinsky and Borisoff [7]. A 5-ml portion of the petroleum hydrocarbon, having $n_D^{25}=1.4229$, was vaporized at the rate of six drops a minute and passed through a tube containing a 50-cm section of the catalyst held at a temperature of 340° to 380° C. The passage required 25 minutes, during which time hydrogen was constantly evolved. A hydrocarbon product of 3.2 ml was obtained which had a refractive index at 25° C of 1.4827, and smelled strongly of pseudocumene (1,2,4-trimethylbenzene). This aromatic material was sulfon-

[7] The boiling point was measured in a Świętosławski ebulliometer. The difference between the boiling and condensing points was found to be 0.013° C. The density was determined by the Division of Weights and Measures of this Bureau.

[8] A value of 7.4 cal/g was used for the heat of fusion of cyclohexane. See Parks and Huffman, Ind. Eng. Chem. 23, 1138 (1931).

ated at 45° C with a mixture of 20 ml of concentrated sulfuric acid and 1 ml of fuming sulfuric acid (30 percent of free SO_3) and then hydrolyzed by steam distillation. After rejecting the oil distilling near 100° C as unsulfonated material, 1.3 ml of hydrocarbon was produced by hydrolysis of the sulfonated material at 145° C. The product had a refractive index at 25° C of 1.5022, as compared with an observed index of 1.5017 for a reference sample of pseudocumene [14]. Confirmatory evidence of the identity of the dehydrogenated naphthene with pseudocumene was obtained by comparing the melting point of the former's nitro derivative with that of pure trinitropseudocumene, and by determining the melting point of a mixture of the two nitro compounds. Comparative values for the three melting points were as follows:

(1) From the dehydrogenated naphthene ..... 180° C.
(2) From pseudocumene ..... 180° C.
(3) For a mixture of (1) and (2) ..... 180° C.

The results of the dehydrogenation and nitration experiments leave little doubt that the petroleum naphthene is hexahydropseudocumene, namely, 1,2,4-trimethylcyclohexane. However, further information regarding the naphthene's identity is obtained by comparing its physical properties with those reported for the synthetic stereoisomers of 1,2,4-trimethylcyclohexane. Of the four stereoisomers possible, three have been prepared and two identified [8]. The properties of these and the properties of the petroleum compound are given in table 1. The comparison shows that the 1,2,4-trimethylcyclohexane from petroleum is not the "*cis*" stereoisomer boiling at 146° C and, also, that it differs appreciably in properties from the $1_{cis},2_{cis},4_{trans}$-trimethylcyclohexane prepared by Skita and Schneck [8]. The compound therefore is probably either $1_{cis},2_{trans},4_{cis}$-trimethylcyclohexane or $1_{cis},2_{trans},4_{trans}$-trimethylcyclohexane. In the absence of critical data, it is not possible to state which of the two it is.

TABLE 1.—*Comparison of the properties of 1,2,4-trimethylcyclohexane from petroleum with those reported for three of the four stereoisomers of 1,2,4-trimethylcyclohexane*[a]

Compound	Boiling point (760 mm Hg)	Density at 20° C	Refractive index
	° *C*	*g/ml*	n_D^{20}
1,2,4-Trimethylcyclohexane from Oklahoma petroleum; White and Glasgow	141.2	0.7720	1.4266
$1_{cis},2_{trans},4_{?}$[b]-Trimethylcyclohexane; Von Auwers [9]	140 to 141	.777	1.4292
$1_{cis},2_{cis},4_{trans}$-Trimethylcyclohexane; Skita and Schneck [8]	142	.786	1.4321
$1_{cis},2_{cis},4_{cis}$-Trimethylcyclohexane; Skita and Schneck [8]	146	.790	1.4331

[a] The data for the properties of the synthetic compounds have been taken at their face value. Since the values were determined on small samples (5 to 10 g) whose purity was not specified, they are not necessarily accurate values.

[b] If the compound prepared by Von Auwers is $1_{cis},2_{trans},4_{trans}$-trimethylcyclohexane, the fourth, and unknown, stereoisomer is $1_{cis},2_{trans},4_{cis}$-trimethylcyclohexane.

V. COMPOSITION AND PROPERTIES OF THE MATERIAL DISTILLING BETWEEN 98.8° AND 100.8° C AT 215 mm Hg, AFTER PARTIAL REMOVAL OF 1,2,4-TRIMETHYLCYCLOHEXANE

Figure 6 shows the boiling-point and refractive-index curves of 2.3 liters of material obtained by redistilling a mixture of 0.6 liter of the higher-boiling mother liquors from the crystallization of 1,2,4-trimethylcyclohexane and the 2 liters of petroleum distillate boiling between 98.8° and 100.8° C.[9] The comparatively low refractive index indi-

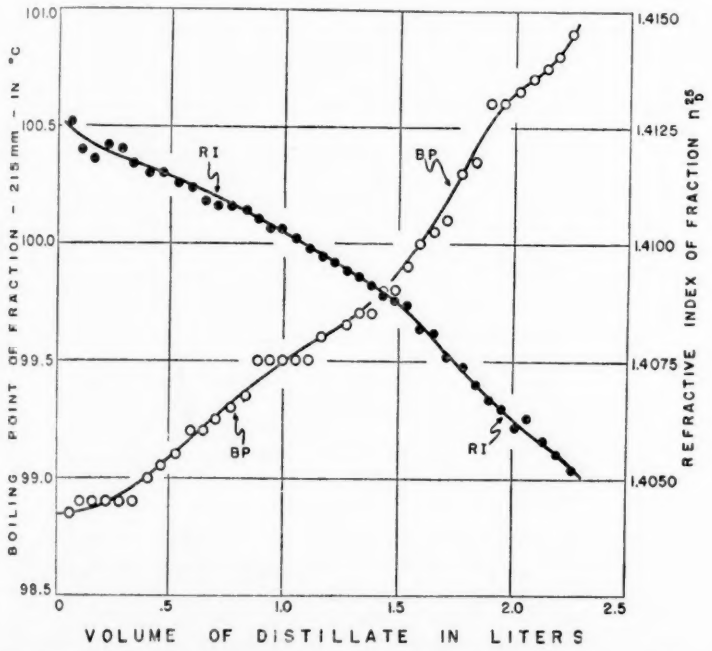

FIGURE 6.—*Fractionation by distillation of crystallization residues and petroleum fractions boiling directly above 1,2,4-trimethylcyclohexane.*

The circles on the two curves represent, respectively, the boiling points and refractive indices of successive fractions of distillate.

cated that the redistilled material, while still containing some 1,2,4-trimethylcyclohexane, was largely composed of paraffinic hydrocarbons. The shape of the boiling-point curve suggested the presence of at least two paraffins. The indications were that the bulk of the paraffin previously encountered as a binary mixture with the isolated trimethylcyclohexane had been concentrated in the distillate boiling between 98.8° and 99.8° C, and that another paraffin had accumulated in the fractions boiling near 100.7° C. The presence of two paraffins could not be clearly established, however, until the amount of naphthene present had been determined with accuracy. Naph-

[9] Material boiling above 100.8° C had been set aside for the separation of its chief constituent, 2-methyloctane.

thenes differ distinctly from paraffins in the magnitude of their refractive indices, but the amount of naphthene in the apparently three-component system under consideration could not be determined by measuring the refractive index alone, because of a possible difference in refractive index of the paraffinic material in the successive fractions of the distillate. Since, however, the two paraffins had the same molecular weight,[10] the content of the naphthene in the fractions could be determined by combustion analysis, and from the known refractive index of the distillate and the assumption that the naphthene was 1,2,4-trimethylcyclohexane, a refractive index of the residual paraffinic material could be computed. Combustion analyses of representative fractions are given in table 2. The figures in the last column indicate clearly that the paraffinic material in the fractions boiling at 99.05° and 99.5° C differed in composition from that boiling at 100.4° C. The analysis was confirmed when 4-methyloctane was later separated from the material distilling between 100° and 101° C.

TABLE 2.—*Properties and composition of fractions of petroleum distilling between 99° and 100.5° C at 215 mm* Hg

Boiling point of fraction (215 mm Hg)	Boiling point of fraction (760 mm Hg)	Δt (boiling point) [a]	Refractive index	$\frac{\text{Moles } H_2O}{\text{Moles } CO_2}$	Estimated mole percentage		Estimated refractive index of paraffin constituent [b]
					Paraffin C_9H_{20}	Naphthene C_9H_{18}	
°C	°C	°C	n_D^{25}				n_D^{25}
99.0$_5$	141.3	42.3	1.4115	1.0740 (1 experiment)	67	33	1.4047
99.5$_0$	141.6	42.1	1.4101	(1) 1.0862	77.5	22.5	1.4059
				(2) 1.0861	77.5	22.5	1.4059
100.3$_5$	142.4	42.1	1.4070	1.0890 (1 experiment)	80	20	1.4026

[a] Difference between the boiling point at 760 and 215 mm Hg.

[b] Assuming n_D^{25} for the naphthene to be 1.4250.

Attempts were made to separate the lower-boiling paraffin from the fractions boiling near 99.5° C by crystallization from dichlorodifluoromethane, and from propane, but, although the distillate contained 75 mole percent of the paraffinic material, only a tacky mass was obtained when the solutions were cooled to low temperatures. At −170° C the glue-like material appeared to be insoluble in the solvents used. An effort to fractionate the material which boiled at 98.8° C by distilling it with excess glacial acetic acid [10, 11] was also unsuccessful. Apparently the composition of the fraction was not as simple as was supposed or else the azeotropic properties of the component hydrocarbons were too much alike. A system of fractionation by distillation at normal pressure, alternated with distillation at a pressure of 215 mm Hg, was then tried and found to be fairly successful in separating the chief paraffinic constituent from the fraction boiling between 98.8° and 99.8° C.

[10] It is almost axiomatic that paraffins from petroleum which boil near 140° C are nonanes.

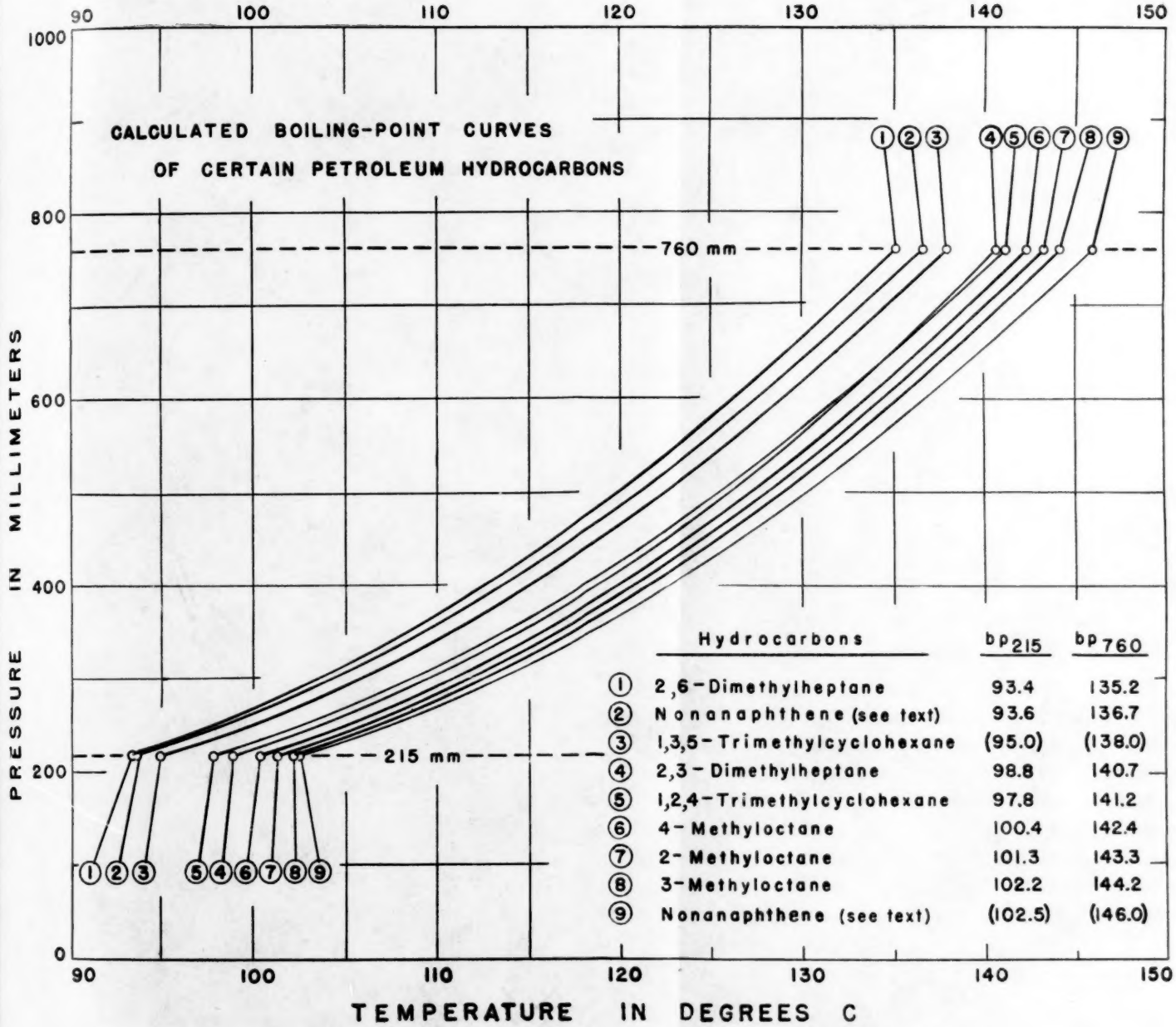

FIGURE 7.—*Calculated vapor pressure curves of certain hydrocarbons found in Oklahoma petroleum.*

The numbers in circles refer to the curves of the numbered hydrocarbons in the table at the lower right of the figure. The table gives the boiling points, at 760 mm and at 215 mm Hg, of the listed hydrocarbons. Those without parentheses are experimentally determined values, those in parentheses are values estimated from the boiling points of impure fractions. For the mode of construction of the curves, see text.

118273—39 (Face p. 146)

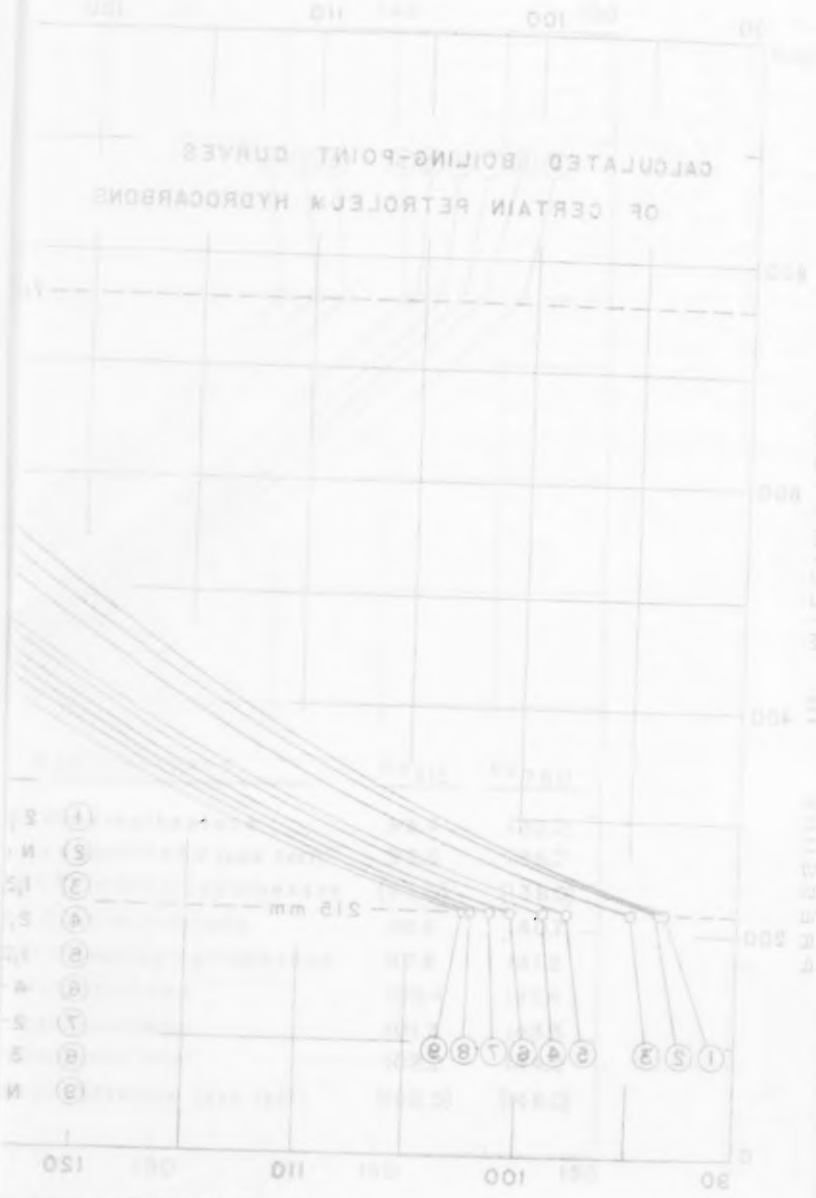
215 mm
1
2
3
4
5
6
7
8
9
120
110
100
90

VI. SEPARATION OF PARAFFIN-NAPHTHENE MIXTURES BY ALTERNATE DISTILLATION AT NORMAL AND REDUCED PRESSURES

As pointed out in section III, 1, 2, 4-trimethylcyclohexane has a higher volatility at a pressure of 215 mm Hg than the paraffin associated with it in the petroleum, and a correspondingly lower volatility at 760 mm Hg. This behavior illustrates the general principle that, with paraffins, naphthenes, and aromatic hydrocarbons which boil at nearly the same temperature, members of one class differ materially from those of another class in the change of their vapor pressures with temperature. Because of this, a binary mixture consisting of a paraffin and a naphthene boiling close together can have the partial pressures of its components so altered as to enhance their separation by fractional distillation, or to reverse the order in which they distil [18].[11] Figure 7 shows calculated vapor-pressure curves of the paraffin and naphthene hydrocarbons in the fraction of this petroleum which normally boils between 135° and 145° C. In the lower right of the figure the boiling points at 215 mm and 760 mm Hg are given for the hydrocarbons.[12] The values for boiling points were experimentally determined, except those in parentheses. These were estimated from the boiling points of impure fractions by correcting for the effect of the major impurity. To construct the vapor-pressure curves of figure 7, the reciprocals of the absolute boiling points of 1,2,4-trimethylcyclohexane and of 2-methyloctane were first plotted with respect to the logarithm of the corresponding pressures for the two experimental points (at 215 and 760 mm Hg). Intermediate values for boiling points and pressures were then obtained from the straight line connecting the experimental points. With these additional values, the vapor-pressure curves of the two hydrocarbons were drawn. Lines for the other paraffins were drawn with the same curvature as that for 2-methyloctane, and those for the naphthenes with the same curvature as that for 1,2,4-trimethylcyclohexane. This was permissible because the difference between the boiling points at 760 and 215 mm Hg for each of the paraffins was quite close to the mean value of 42° C, and for each of the naphthenes, close to the mean value of 43.2° C. It should be noted that the curves as constructed may not correspond exactly with the actual vapor pressure curves of the individual hydrocarbons, but they nevertheless illustrate the relative change in vapor pressure with temperature of the two classes of hydrocarbons. All of the curves have been useful in the analysis of the distillate boiling between 135° and 145° C. Curves 1 and 2, for example, indicate the substantial difference between the boiling points at normal pressure of 2,6-dimethylheptane and a nonanapthene, and the close proximity of

[11] A practical demonstration of the possibilities of the principle is afforded by the experiments of S. T. Schicktanz mentioned in footnote 4. The results of the experiments were kindly called to the attention of the authors by Schicktanz, prior to the present investigation.

[12] The hydrocarbons used for the boiling-point determinations were, with the exception of 4-methyloctane, the best fractions prepared from petroleum. The sample of 4-methyloctane was supplied by George Calingaert of the Ethyl Gasoline Corporation. Properties of the samples used are listed in the following papers relating to 2,6-dimethylheptane, J. Research NBS **17,** 952 (1936) RP955; nonanaphthene, 136.7° C, J. Research NBS **13,** 808 (1934) RP745; isononane (probably 2, 3-dimethylheptane), 140.7° C, described in this paper; 1,2,4-trimethylcyclohexane, described in this paper; and 4-methyloctane (Calingaert), 2-methyloctane, and 3-methyloctane, J. Research NBS **19,** 423 (1937) RP1033. The fractions containing the nonanaphthene (probably 1,3,5-trimethylcyclohexane) boiling at 138° C, and the nonanaphthene boiling at 146° C, had refractive indices at 25° C of 1.4233 and 1.4263, respectively. The isolation of these compounds from the petroleum has not been completed.

their boiling points at 215 mm Hg. It would be expected that a mixture of these two hydrocarbons could be separated by fractional distillation at 760 mm Hg, but not at 215 mm, at which pressure a constant-boiling mixture would result. This was found to be the case when a fraction of the petroleum composed of these two hydrocarbons was resolved into its constituents [12]. Similarly, use was made of the pressure-temperature relationships depicted in curves 8 and 9, in separating 3-methyloctane from the petroleum [3]. Special attention, however, is called to curves 4 and 5, which concern the present work. Curve 4 crosses curve 5 at a pressure of about 650 mm. In this region of pressure the pair of hydrocarbons form a mixture which is constant-boiling at about 135° C. At higher or lower pressures, the mixture would distil over a definite temperature range. It follows that constant-boiling mixtures of naphthene and paraffin hydrocarbons are only incidental, and that such mixtures may be resolved into their components by distillation at a pressure somewhat removed from that causing the constant-boiling behavior. Closer inspection of curves 4 and 5 indicates that a binary mixture of 1,2,4-trimethylcyclohexane and the "2,3-dimethylheptane" could be separated more readily by distillation at 215 mm Hg than at 760 mm. The present problem, however, was to separate a three-component mixture which contained, besides these two compounds, 4-methyloctane (curve 6). It was believed that by fractionally distilling the mixture at atmospheric pressure, the 4-methyloctane could be removed by rejecting the end fractions and residue which, from the order of distillation of the constituents, would contain the 4-methyloctane and some of the naphthene. The bulk of the lower-boiling paraffin would be concentrated in the initial fractions as a binary mixture with the naphthene which afterwards could be removed by fractionation at a pressure of 215 mm Hg.

VII. SEPARATION OF THE PARAFFIN-NAPHTHENE MIXTURE BOILING BETWEEN 98.8° AND 99.8° C AT 215 mm Hg

Using the procedure outlined above, the 1600-ml fraction shown in figure 6 to boil between 98.9° and 100° C was mixed with 400 ml of paraffinic mother liquors obtained from further crystallization of the 1,2,4-trimethylcyclohexane stock, and redistilled at 760 mm. The boiling-point and refractive-index curves of the distillate are shown in figure 8. The individual points denote the boiling points and refractive indices of successive 50-ml fractions. The curves show that the first liter of distillate was almost constant-boiling at 141.0° to 141.1° C, and changed but little in refractive index, 1.409 to 1.410. Both properties indicate a constancy in composition of the material. The 50-ml fraction taken after 900 ml had distilled (bp 141.1° C, $n_D^{25}=1.4101$) contained 20 mole percent of a naphthene and 80 mole percent of a nonane. From the composition, the nonane was calculated to have an index of 1.4065 at 25° C. From this point in the distillation, the remaining material distilled at increasingly higher temperatures and exhibited a steady increase in refractive index. For the 50-ml fraction which marked the 1,750-ml point in the distillation (bp 141.9° C, $n_D^{25}=1.4130$), the naphthene content was 40 mole percent. The calculated refractive index of the paraffinic material in this fraction

was 1.4046 at 25° C as compared with 1.4036 for pure 4-methyloctane. From the analysis it was evident that the naphthene and 4-methyloctane had collected in the end fractions of the distillation, and for this reason the last 400 ml of distillate and the residue were rejected. The first 1,400 ml to distil, which was rich in the lower-boiling paraffin, was redistilled at 215 mm Hg.

As a result of this second distillation at reduced pressure, much of the naphthene still present collected in the first portion to distil, and most of the 4-methyloctane which remained was held in the residue. The 850 ml of oil representing the middle portion of the distillate consisted chiefly of the desired isononane. The individual fractions comprising the middle portion ranged in boiling point from 98.7°

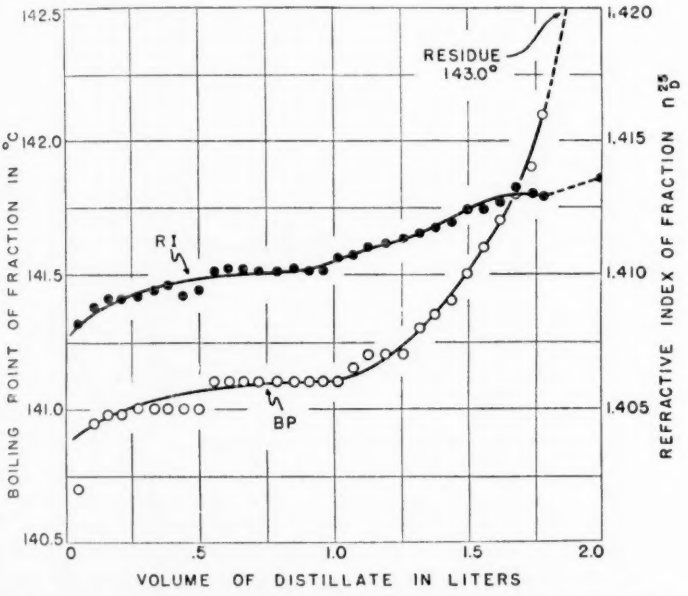

FIGURE 8.—*Fractionation by distillation at normal pressure of the petroleum fraction enriched in 2,3-dimethylheptane.*

The points on the curves indicate the boiling points and refractive indices of successive fractions.

to 98.9° C and varied in refractive index (in the order distilled) from 1.4125 to 1.4087. By combustion analysis, the naphthene content was 30 mole percent for a fraction with $n_D^{25}=1.4122$ and 15 mole percent for one with $n_D^{25}=1.4087$. The paraffinic material in most of the distillate had a calculated refractive index of 1.406 at 25° C. In the last fractions, however, the index of the paraffinic material had decreased to 1.405.

As a final step in the separation of the isononane, the middle portion (850 ml) of the distillate described above was redistilled in the same column, at 760 mm Hg. The boiling points of the successive fractions from this final distillation were measured at 760 mm and at 215 mm Hg in order to determine the nature of the distillate.

The boiling-point curves for the two sets of data are shown in the lower part of figure 9. The curve at the top of the figure indicates the range in refractive index of the distillate. Barring the first 100 ml of oil distilled, the gradual rise in refractive index of the

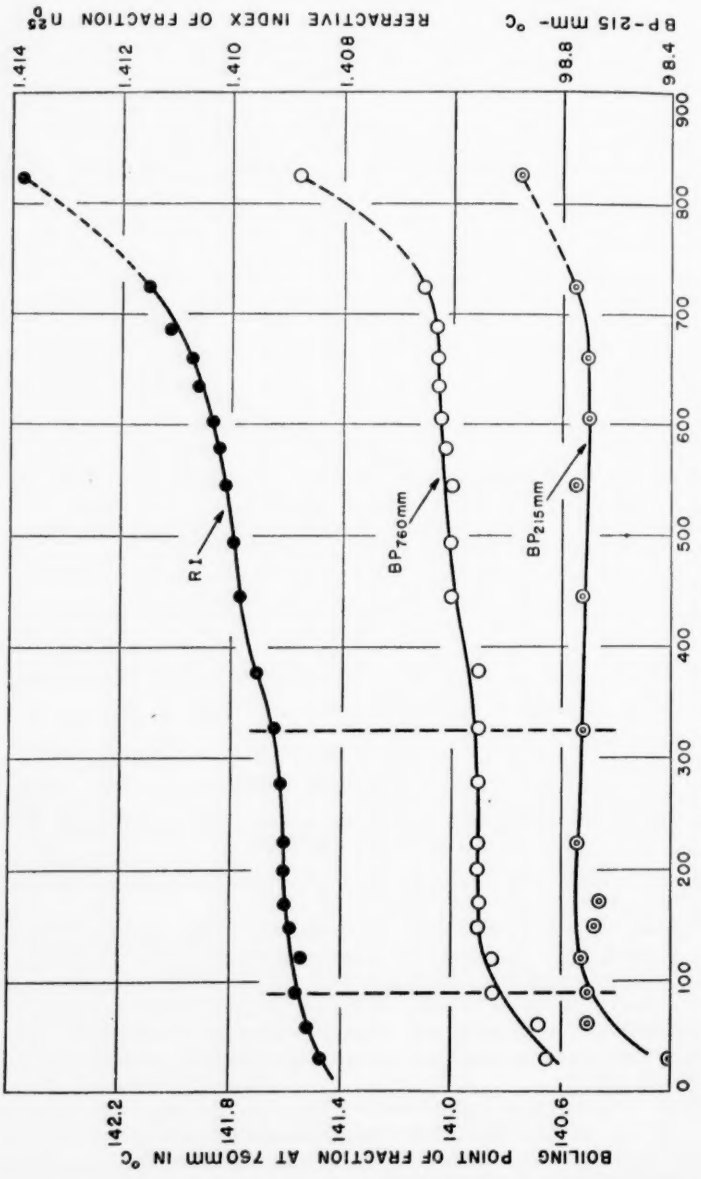

FIGURE 9.—*Final fractionation by distillation of the 2,3-dimethylheptane concentrate.*

Top curve, refractive indices; middle curve, boiling points at 760 mm Hg; and bottom curve, boiling points at 215 mm Hg of successive fractions. The vertical dotted lines bound the portion of the distillate later subjected to fractional crystallization.

distillate, together with the divergence of the boiling-point curves, shown by the steady increase in boiling point at 760 mm Hg (middle curve) and the steady decrease in boiling point of the fractions when

measured at 215 mm Hg (bottom curve), is regarded as substantial evidence that the major portion of the distillate was composed of a binary mixture of the unidentified nonane and 1,2,4-trimethylcyclohexane.

Although the mean refractive index of the material, 1.4095, signified that the isononane was the chief constituent, none of the distillation fractions would freeze. A 240-ml portion, characterized by a constant boiling point of 140.9° C and a constant refractive index of 1.4090, was subjected to a fractional crystallization from its solution in propane and methane [13]. Apparently a crystalline phase formed, but when separated and freed from solvent it had the same physical properties as the oil in the mother liquid, indicating that no fractionation had taken place.[13]

VIII. PROPERTIES OF THE ISOMERIC NONANE FRACTION AND THE PROBABLE IDENTITY OF THE NONANE WITH 2,3-DIMETHYLHEPTANE

The properties of the recombined material from the crystallization experiment are as follows: Boiling point at 760 mm Hg, 140.80° C; congeals to a glass at −119° C; density at 20° C, 0.7340 g/ml; refractive index, $n_D^{20}=1.4121$; critical solution temperature in aniline, 71° C. From two determinations by combustion, the ratio of moles of H_2O to moles of CO_2 was found to be 1.0950 ± 0.0002. From this it was estimated that the petroleum fraction contained 85.5 mole percent of the nonane and 14.5 mole percent of 1,2,4-trimethylcyclohexane.

The properties of the constituent isononane, calculated from those of the petroleum fraction by correcting for the effect of the 1,2,4-trimethylcyclohexane present, are given in table 3. That the compound is related to, if not identical with 2,3-dimethylheptane, is indicated in the table by the similarity in their physical properties. Of the 16 isomeric nonanes which have been prepared (chiefly the substituted octanes and heptanes) 2,3-dimethylheptane is the only one which has properties similar to those of the petroleum hydrocarbon. However, in the absence of specific information concerning the properties of other possible isomers of nonane, it cannot be stated definitely that the two compounds are identical. General knowledge relating the properties of paraffin hydrocarbons to their molecular structure [15] indicates that only a few of the 19 unreported nonanes can be closely related to the nonane in question. From such a correlation, all of the trimethylhexanes and tetramethylpentanes may be expected to boil below 140° C and all of the dimethylethylpentanes may be expected to have densities greater than that of the isolated hydrocarbon. Some of the methylethylhexanes, however, as well as some of the dimethylheptanes, can be expected to have properties similar in magnitude to those of the nonane from petroleum. These include, 3,5-, 3,4-, and 4,4-dimethylheptane and 3,3-, and 3,4- methylethylhexane.

[13] A method was considered for purifying the material by dehydrogenation of the naphthene present, followed by adsorption of the aromatic product, but time was not available to make an adequate study of its possibilities.

TABLE 3.—*Comparison of the properties of an isomeric nonane from petroleum with those of 2,3-dimethylheptane*

Nonane, C_9H_{20}	Boiling point (760 mm Hg)	Behavior on cooling	Density at 20° C	Refractive index
	°C	°C	g/ml	n_D^{20}
Petroleum fraction, corrected for naphthene content	140.7	glass at −116.7	0.727	1.4095
2,3-Dimethylheptane, Whitmore and Southgate [a]	[b]140.65		.7235	1.4085

[a] Private communication from F. C. Whitmore and H. A. Southgate, Pennsylvania State College.
[b] Initial boiling point. dp/dt=0.049.

IX. CONTENT OF 1,2,4-TRIMETHYLCYCLOHEXANE AND THE ISONONANE IN THE PETROLEUM

Of the 3 liters of petroleum shown in figure 2 to boil between 98° and 99° C at 215 mm Hg, nearly 2 liters was 1,2,4-trimethylcyclohexane and somewhat less than a liter was the isomeric nonane. It is estimated that the percentage of 1,2,4-trimethylcyclohexane in the petroleum is about 0.1, and that of the isononane about 0.05, by volume.[14]

X. REFERENCES

[1] W. Markownikoff and W. Ogloblin, J. Russ. Phys. Chem. Soc. **15,** 331 (1883); Ber. deut. chem. Ges. **16B**, 1877 (1883).
[2] B. A. Kasansky and M. P. Eliséeva, J. Gen. Chem. (U. S. S. R.) **6,** 888 (1936); Chem. Abs. **30,** 6930 (1936).
[3] J. D. White and A. R. Glasgow, Jr., J. Research NBS **19,** 423 (1937) RP1033.
[4] J. D. White and F. W. Rose, Jr., BS J. Research **9,** 711 (1932) RP501.
[5] S. T. Schicktanz, BS J. Research **11,** 89 (1933) RP579.
[6] F. D. Rossini, BS J. Research **8,** 121 (1932) RP405.
[7] N. Zelinsky and T. Borisoff, Ber. deut. chem. Ges. **57,** 150 (1924).
[8] A. Skita and A. Schneck, Ber. deut. chem. Ges. **55I,** 144 (1922).
[9] K. Von Auwers, Liebigs Ann. Chem. **420,** 97 (1919).
[10] J. D. White and F. W. Rose, Jr., J. Research NBS **17,** 943 (1936) RP955.
[11] S. T. Schicktanz, J. Research NBS **18,** 129 (1937) RP967.
[12] J. D. White and F. W. Rose, Jr., J. Research NBS **13,** 799 (1934) RP745.
[13] R. T. Leslie, BS J. Research **10,** 609 (1933) RP552.
[14] B. J. Mair and S. T. Schicktanz, BS J. Research **11,** 665 (1933) RP614.
[15] G. Calingaert and J. W. Hladky, J. Am. Chem. Soc. **58,** 153 (1936).
[16] R. T. Leslie and J. D. White, J. Research NBS **15,** 218 (1935) RP824.
[17] F. D. Rossini, Proc. Am. Petroleum Inst. **18III,** 36 (1937); Oil and Gas J. **36,** No. 26, 193 (1937); Refiner Natural Gasoline Mfr. **16,** 545 (1937).
[18] E. W. Washburn, Ind. Eng. Chem. **25,** 891 (1933).

WASHINGTON, October 4, 1938.

[14] See references [16, 17] for a discussion as to the accuracy of these estimates.

U. S. DEPARTMENT OF COMMERCE NATIONAL BUREAU OF STANDARDS

RESEARCH PAPER RP1174

Part of Journal of Research of the National Bureau of Standards, Volume 22, February 1939

SUMMARY OF AN INVESTIGATION OF THE COMPOSITION OF A MIDCONTINENT PETROLEUM DISTILLATE, BOILING BETWEEN 100° AND 130° C. [1]

By Robert T. Leslie [2]

ABSTRACT

The results of 7 years of investigation of the composition of the naphtha fraction of petroleum boiling between 100° and 130° C are summarized. Of the 130 liters found to boil in this range after the first laboratory distillation, the constituents of about one-sixth of the volume were identified or characterized by physical properties, isolated or concentrated, and their concentration in the petroleum roughly estimated. About one-fourth of the volume remains as unidentified distillate. This is composed in part of material of which the constitution is only predicted (about one-twelfth of the volume) and of additional quantities of the constituents which were isolated previously (about one-sixth of the volume). The remainder was lost during the investigation or distilled out of the range on subsequent distillations. Photomicrographic studies were made of those concentrations of distillate which could be crystallized. There is given a bibliography of the physical constants of hydrocarbons reported to boil within this range.

CONTENTS

	Page
I. Introduction	153
II. Study of the composition of the distillate	164
1. Distillate between 98° and 102° C	164
2. Distillate between 103° and 106° C	164
3. Distillate between 108.5° and 110.5° C	165
4. Distillate between 112° and 116° C	166
5. Distillate between 117° and 124° C	166
6. Distillate between 125° and 126° C	167
7. Distillate between 127° and 130° C	168
III. Probable composition of a midcontinent petroleum boiling between 100° and 130° C	168

I. INTRODUCTION

This paper summarizes the work done to date since 1929 with the portion of midcontinent petroleum distilling between 100° and 130° C and includes some new information obtained since the publication of a previous summary paper [3] and two subsequent specialized papers.[4 5]

[1] Financial assistance has been received from the research fund of the American Petroleum Institute. This work is part of Project 6, The Separation, Identification, and Determination of the Constituents of Petroleum.

[2] Research Associate at the National Bureau of Standards, representing the American Petroleum Institute.

[3] R. T. Leslie and J. D. White, J. Research NBS **15**, 211 (1935) RP824.

[4] R. T. Leslie, J. Research NBS **17**, 761 (1936) RP943.

[5] R. T. Leslie and W. W. Heuer, J. Research NBS **18**, 639 (1937) RP1000.

About 6 percent of the total volume of the crude petroleum distilled between 100° and 130° C and, of this, by far the largest volume distilled between 117° and 128° C. Curves A_1 and A_2 of figure 1 show, respectively, the refractive indices and the distribution of volumes after four distillations in the laboratory, before the removal of any of the constituents. Curves B_1 and B_2 of the same figure show the distillate still remaining after the removal of seven hydrocarbons and the distillation of the residual material. This is composed of the unidentified constituents and of unisolated residues of the identified compounds. Although unidentified constituents which boil chiefly between 101.5° and 116° C still remain, the constituents present in the largest proportions have been removed. The paper includes, besides a summary of the compounds actually isolated, all the information concerning the material represented by curves B_1 and B_2 of figure 1. In addition, the values of physical constants for the hydrocarbons reported in the literature to boil within the range are given in table 1. This information was obtained by surveying the literature up to 1937, including standard works of reference. The values were selected from publications dealing with the preparation of pure compounds or apparently reliable measurements of the properties of nearly pure compounds. Where necessary, the only available data were included. The best values, in the author's opinion, have been plotted in figure 1, and are numbered for convenient reference to the table.[6]

[6] Figures in brackets throughout the paper are the reference numbers given in figure 1 and table 1.

TABLE 1.—*Properties of known paraffinic, naphthenic, and aromatic hydrocarbons boiling between 98° and 130° C.*

(Compounds are arranged in order of increasing boiling points)

Reference number	Normal boiling point	Freezing point	Specific gravity	Refractive index	Heat of fusion	Literature references
			***n*-Heptane**			
	°C	°C	d_4^{20}	n_D^{20}	cal/g	
	98.4	−90.5	0.6836	1.38777		G. Edgar, G. Calingaert, and R. E. Marker, J. Am. Chem. Soc. **51**, 1483 (1929).
	98.38	−90.65	.68378	1.38775		A. F. Shepard, A. L. Henne, and T. Midgley, Jr., J. Am. Chem. Soc. **53**, 1948 (1931).
1	98.38	−90.62		1.38510^{25}		B. J. Mair, BS J. Research **9**, 457 (1932) RP482.
		−90.9			33.78	H. M. Huffman, G. S. Parks, and S. B. Thomas, J. Am. Chem. Soc. **52**, 3241 (1930).
	98.36[5]					M. Wojciechowski, J. Research NBS **17**, 453 (1936) RP921.
	98.41[1]					E. R. Smith and H. Matheson, J. Research NBS **20**, 641 (1938) RP1097.
			2,2,4-Trimethylpentane			
	99.3		0.6914_{20}^{20}	1.3921		G. Edgar, Ind. Eng. Chem. **19**, 145 (1927).
		−107.8			2160 cal/mole	G. S. Parks and H. M. Huffman, Ind. Eng. Chem. **23**, 1138 (1931).
2		−107.41				J. H. Bruun and M. M. Hicks-Bruun, BS J. Research **9**, 269 (1932).
	99.3		.6918	1.3916		K. C. Laughlin and F. C. Whitmore, J. Am. Chem. Soc. **55**, 2608 (1933).
	99.23[4]					E. R. Smith and H. Matheson, J. Research NBS **20**, 641 (1938) RP1097.
			Methylcyclohexane			
	101.20	−126.4	0.7734^{15}	1.42535^{15}		J. Timmermans and F. Martin, J. chim. phys. **23**. 747 (1926).
	99.8 to 100.8		$.769_{20}^{20}$	1.4230		F. K. Signaigo and P. L. Cramer, J. Am. Chem. Soc. **55**, 3326 (1933).
3	101.0 ±0.5		.7696	1.4239		F. H. Garner and E. B. Evans, J. Inst. Petroleum Tech. **18**, 751 (1932).
		−126.85				J. Timmermans, Comm. Phys. Lab. Univ. Leiden, Suppl. **64**, 3 (1929).
		−126.9			16.24	G. S. Parks and H. M. Huffman, J. Am. Chem. Soc. **52**, 4385 (1930).
	102.8		.7963	1.4232		E. C. Bromiley and D. Quiggle, Ind. Eng. Chem. **25**, 1136 (1933).

TABLE 1.—*Properties of known paraffinic, naphthenic, and aromatic hydrocarbons boiling between 98° and 130° C.*—Continued

Reference number	Normal boiling point	Freezing point	Specific gravity	Refractive index	Heat of fusion	Literature references
			Ethylcyclopentane			
	°C	°C	d_4^{20}	n_D^{20}	cal/g	
4	103.0 ±0.5		0.7695	1.4201[20.4]		F. H. Garner and E. B. Evans, J. Inst. Petroleum Tech. **18**, 751 (1932).
		−137.9				J. Timmermans, Bul. soc. chim. Belg. **36**, 502 (1927).
			1,1,2-Trimethyl-2-ethylcyclopropane			
5	103.5 to 104.5		0.7418[20.4]	1.4129		R. Lespieau and R. Wakeman, Bul. soc. chim. **51**, 392 (1932). (Only 1 ml of product.)
			1,2-Dimethyl-1-ethylcyclopropane			
6	104		0.7418	1.4129		R. Lespieau and R. Wakeman, Bul. soc. chim. **51**, 399 (1932).
			2, 2, 3, 3-Tetramethylbutane			
7	106 to 107	+103 to 104				A. Richard, Ann. chim. phys. [8] **21**, 357 (1910).
	106 to 107 [765]	+103 to 104				L. Henry, Compt. rend. **142**, 1075 (1906).
	104 to 105.2	+100.7 to 101.4				D. T. Flood and G. Calingaert, J. Am. Chem. Soc. **56**, 1211 (1934).
		+104			14.9	G. S. Parks and H. M. Huffman, Ind. Eng. Chem. **23**, 1138 (1931).
			2, 2,-Dimethylhexane			
8	106 to 107		0.6967	1.3931		C. R. Noller, J. Am. Chem. Soc. **51**, 594 (1929).

9	107 [747] 108.25 109.2 ±0.1		0.6937 $^{20}_{20}$ .6991 $^{15}_{15}$ .6986 $^{20}_{20}$	1.3922 1.3930 [25] 1.3932		M. Tuot, Compt. rend. **197**, 1434 (1933). L. Clarke, J. Am. Chem. Soc. **33**, 520 (1911). H. Graef, Bul. soc. chim. Belg. **40**, 315 (1931).
	1-Methyl-1, 2-diethylcyclopropane					
10	108 to 109		0.7382 $^{20}_{0}$	1.4102		N. Kishner, J. Russ. Phys. Chem. Soc. **44**, 179; Chem. Zentr. **1912** I, 2025 (listed in Beilsteins Ergänzungsband 4th ed, **5**). Also listed by R. Lespieau and R. Wakeman, Bul. soc. chim. **51**, 399 (1932).
	2, 4-Dimethylhexane					
11	108 [750] 110.0 [763] 110 to 111		0.6986 $^{20}_{20}$ .7083 $^{15}_{15}$ .703 $^{21}_{4}$	1.3950 1.3986 [25]		M. Tuot, Compt. rend. **197**, 1434 (1933). L. Clarke, J. Am. Chem. Soc. **33**, 520 (1911). P. A. Levene and R. E. Marker, J. Biol. Chem. **91**, 405 (1931).
	1-Methyl-2-isobutylcyclopropane					
12	109.5 to 110.5		0.7403	1.4088		N. D. Zelinsky and A. E. Upenski, J. Russ. Phys. Chem. Soc. **45**, 839; Ber. deut. Chem. Ges. **46**, 1472 (1913) (Listed in Beilsteins Ergänzungsband 4th ed., **5**). Also listed by R. Lespieau and R. Wakeman, Bul. soc. chim. **51**, 399 (1932).
	Toluene					
13	110.614 110.4 ±0.2 110.80	 −95	 0.8652 .87160 [15]	1.4961 1.4947 1.49985 [18]	 90.5	W. Świętosławski, Ann. acad. sci. tech. Varsovie, **3**, 28 (1936). F. H. Garner and E. B. Evans, J. Inst. Petroleum Tech. **18**, 751 (1932). J. Timmermans and F. Martin, J. chim. phys. **23**, 747 (1926). M. Schmitt, Compt. rend. **199**, 1299 (1934).
	2, 2, 3-Trimethylpentane					
14	110.5 to 110.8 110.2 (Cottrell)		0.7219 $^{15}_{15}$ .7173	1.4164 [25] 1.4030		L. Clarke and W. N. Jones, J. Am. Chem. Soc. **34**, 174 (1912). K. C. Laughlin and F. C. Whitmore, J. Am. Chem. Soc. **55**, 2608 (1933).

118273—39——3

TABLE 1.—*Properties of known paraffinic, naphthenic, and aromatic hydrocarbons boiling between 98° and 130° C.*—Continued

Reference number	Normal boiling point	Freezing point	Specific gravity	Refractive index	Heat of fusion	Literature references
			Dextro-3, 5-dimethylhexane (α_D^{20}+2.99)			
	°C	°C	d_4^{20}	n_D^{20}	cal/g	
15	111 to 112		0.696 $^{20}_{4}$			P. A. Levene and R. E. Marker, J. Biol. Chem. **95**, 23 (1932).
			3, 3-Dimethylhexane			
16	111 to 112		0.7116	1.3998		C. R. Noller, J. Am. Chem. Soc. **51**, 594 (1929).
			1,2,3-Trimethylcyclopentane			
17	111.5 to 114 114 to 115		0.7688 ^{19}	1.42591 1.4230 ^{19}		A. W. Crossley and N. Renouf, J. Chem. Soc. **89**, 27, 40 (1906). N. D. Zelinsky and N. Lepeschkin, J. Russ. Phys. Chem. Soc. **33**, 549 (1902); Chem. Zentr. **1902**, I, 33. (Listed in Beilsteins Handbuch 4th ed., 5.)
			2,3,4-Trimethylpentane			
18	112.8		0.7197	1.4045		K. C. Laughlin and F. C. Whitmore, J. Am. Chem. Soc. **55**, 2608 (1933).
			1,2,4-Trimethylcyclopentane			
19	112.5 to 113		0.7565	1.4156		N. D. Zelinsky, J. Russ. Phys. Chem. Soc. **35**, 565. (Listed in Beilsteins Ergänzungsband, 4th ed. 5.)
			2,3,3-Trimethylpentane			
20	113.6		0.7258	1.4074		K. C. Laughlin and F. C. Whitmore, J. Am. Chem. Soc. **55** 2608 (1933).

20	113.6		0.7258	1.4074		R. C. Laughlin and F. C. Whitmore, J. Am. Chem. Soc. 58, 2658 (1936).

2,3-Dimethylhexane

21	113.9		0.7246^{18}_{18}	1.4075^{25}		L. Clarke, J. Am. Chem. Soc. **33**, 520 (1911).

2-Methyl-3-ethylpentane

22	114		0.7084^{15}	1.3996^{25}		L. Clarke Am. Chem. J. **39**, 578 (1908). Reported in Beilsteins Handbuch, 3d ed., **I**.

1,1,2-Trimethylcyclopentane

23	113 to 114^{749}		0.7661^{20}_{0}	1.4199		N. Kishner, J. Russ. Phys. Chem. Soc. **43**, 1211; Chem. Zentr. **1911**, I, 543. (Listed in Beilsteins Ergänzungsband, 4th ed., **5**.)

1,1,3-Trimethylcyclopentane

24	115 to 116		0.7703	1.4223		N. D. Zelinsky and A. E. Upenski, J. Russ. Phys. Chem. Soc. **45**, 839; Ber. deut. chem. Ges. **46**, 1472 (1913). (Listed in Beilsteins Ergänzungsband, 4th ed., **5**.)

3,3-Dimethylbicyclo-(0,1,3) hexane

25	115		0.7962	1.4331		N. D. Zelinsky and A. E. Upenski, J. Russ. Phys. Chem. Soc. **45**, 839; Ber. deut. chem. Ges. **46**, 1466 (1923). (Listed in Beilsteins Ergänzungsband, 4th ed. **5**.)
	115.2 to 115.4		.8125	1.4385		A. E. Upensky, J. Russ. Phys. Chem. Soc. **51**, 259; Chem. Zentr. **1923**, III, 757.

2-Methylheptane

26	116		0.7035^{18}_{18}	1.3944^{25}		L. Clarke, J. Am. Chem. Soc. **33**, 520 (1911).
	117.2	−111.3	$.7035^{20}_{20}$	1.3949	2,200 cal/g mole	R. T. Leslie, BS J. Research **10**, 617 (1933) RP552.

TABLE 1.—*Properties of known paraffinic, naphthenic, and aromatic hydrocarbons boiling between 98° and 130° C.*—Continued

Reference number	Normal boiling point	Freezing point	Specific gravity	Refractive index	Heat of fusion	Literature references
			3,4-Dimethylhexane			
	°C	°C	d_4^{20}	n_D^{20}	cal/g	
27	116.5		0.7270_{15}^{15}	1.4038^{25}		L. Clarke, J. Am. Chem. Soc. **33,** 520 (1911).
	118.7	"glassy"				J. Timmermans, Bul. soc. chim. Belg. **36,** 502 (1927).
			3-Methylheptane			
28	116.5[746]		0.7033_{20}^{20}	1.3982		M. M. Tuot, Compt. rend. **197,** 1434 (1933).
	119.0 ±0.05[760]		$.7095_4^{15}$	$1.3987_{\text{red line of He}}^{15}$		H. Van Rissenghem, Bul. soc. chim. Belg. **39,** 369 (1930).
	117.6		$.7167_{15}^{15}$	1.4022^{25}		L. Clarke, J. Am. Chem. Soc. **33,** 520 (1911).
			3-Ethylhexane			
29	118.8 to 119[760]		0.7175_{15}^{15}	1.3993^{25}		L. Clarke and R. Riegel, J. Am. Chem. Soc. **34,** 674 (1912).
			Cycloheptane			
30	118 to 120		0.8099	1.4440		N. A. Rosanow, J. Russ. Phys. Chem. Soc. **48,** 318; Chem. Zentr. **1924** I, 2425. (Listed in Beilsteins Ergänzungsband, 4th ed. **5,** 29).
	118[736]	−12 to −13	.8108	1.44521		R. Willstatter and T. Kametaka, Ber. deut. chem. Ges. **41,** 1483. (Listed in Beilsteins Ergänzungsband, 4th ed. **5,** 29).
	117 to 117.3[736]		$.8093_0^{20}$			W. Markownikow, J. Russ. Phys. Chem. Soc., **34,** 908; Chem. Zentr. **1903** I, 568. (Listed in Beilsteins Ergänzungsband, 4th ed. **5,** 29).

				4-Methylheptane		
31	118		0.7217^{15}_{15}	1.3978^{25}		L. Clarke, J. Am. Chem. Soc. **33**, 520 (1911).
				3-Methyl-3-ethylpentane		
32	118.5 to 119^{760}		0.713^{19}	1.4028^{19}		J. Tafel and W. Jurgens, Ber. deut. chem. Ges. 1909, **42**, 2548.
				trans-1, 4-Dimethylcyclohexane		
33	119.63	−37.2	0.76264	$1.42160^{18.8}$ J line of He		O. Miller, Bul. soc. chim. Belg. **44**, 513 (1935).
				1,4-Dimethylcyclohexane		
33	121.7 ±1.0	−59	0.7727	1.4253		F. H. Garner and E. B. Evans, J. Inst. Petroleum Tech. **18**, 764 (1932).
	122 to 124		$.777^{20}_{20}$	1.4271		F. K. Signaigo and P. L. Cramer, J. Am. Chem. Soc. **55**, 3326 (1933).
				1,1-Dimethylcyclohexane		
34	119.8	−34.1	0.78073	$1.42959^{18.8}$ J line of He		O. Miller, Bul. soc. chim. Belg. **44**, 513 (1935).
	119.2 to 119.7		$.7843^{15}$	1.4320^{15}		N. D. Zelinsky and A. E. Upenski, Ber. deut. chem. Ges. **46**, 1466 (1923).
				1-Methyl-3-ethylcyclopentane		
35	120.5 to 121^{736}			1.4214^{15}		N. D. Zelinsky, Ber. deut. chem. Ges. **35**, 2679 (1902).
				trans-1,3-Dimethylcyclohexane		
36	120.40	−79.4	0.76628	$1.43254^{18.8}$ J line of He		O. Miller, Bul. soc. chim. Belg. **44**, 513 (1935).

TABLE 1.—*Properties of known paraffinic, naphthenic, and aromatic hydrocarbons boiling between 98° and 130° C.*—Continued

Reference number	Normal boiling point	Freezing point	Specific gravity	Refractive index	Heat of fusion	Literature references
			1,3-Dimethylcyclohexane			
	°C	°C	d_4^{20}	n_D^{20}	cal/g	
36	120.9 to 122.5		0.774 $^{20}_{20}$	1.4253		F. K. Signaigo and P. L. Cramer, J. Am. Chem. Soc. **55,** 3326 (1933).
	121.6 ± 1.0		.7723	1.4255		F. H. Garner and E. B. Evans, J. Inst. Petroleum Tech. **18,** 751 (1932).
			2,2,4,4-Tetramethylpentane			
37	122.30	−66.9 to −67.1	0.7185	1.40695		Private communication from H. A. Southgate and F. C. Whitmore, Pennsylvania State College.
			2,2,5-Trimethylpentane			
38	121 to 123		0.7091	1.3997		C. R. Noller, J. Am. Chem. Soc. **51,** 594 (1929).
	126.764		.7082 $^{20}_{0}$	1.3987		N. Kishner, J. Russ. Phys. Chem. Soc. **45,** 954; Chem. Zentr. **1913** II, 2130. (Listed in Beilsteins Ergänzungsband, 4th ed. **5.**
			trans-1,2-Dimethylcyclohexane			
39	123.70	−89.4	0.77601	1.42768 $^{18.8}_{\text{D line of He}}$		O. Miller, Bul. soc. chim. Belg. **44,** 513 (1935).
			1,2-Dimethylcyclohexane			
39	126.4 to 128.9		0.792 $^{20}_{20}$	1.4332		F. K. Signaigo and P. L. Cramer, J. Am. Chem. Soc. **55,** 3326 (1933).
	127.9 ± 1.0		.7874	1.4314		F. H. Garner and E. B. Evans, J. Inst. Petroleum Tech. **18,** 764 (1932).
			Isopropylcyclopentane			
40	123 to 124.731.6		0.7785 ^{18}	1.4273 ^{18}		B. A. Kazanskii, A. F. Plate, and G. M. Gnatenko, Ber. deut. chem. Ges. **69B,** 954 (1936).

40	123 to 124 $^{731.5}$		0.7785 ^{15}	1.4273 ^{15}		B. A. Kazanskii, A. F. Plate, and G. M. Gnatenko, Ber. deut. chem. Ges. **69B,** 954 (1936).
41	124					T. R. Marshal and W. H. Perkin, J. Chem. Soc. **57,** 250 (1890).

1,1,3,3-Tetramethyl-2,4-diethylcyclobutane

42	124 to 125					E. Wedekind and M. Miller, Ber. deut. chim. Soc. **44,** 3286 (1911).

cis-1,4-Dimethylcyclohexane

43	124.59	−91.6	0.78271	1.43029 $^{15.5}$ J line of He		O. Miller, Bul. soc. chim. Belg. **44,** 513 (1935).

n-Octane

44	125.59	−56.82		1.39509 ^{25}		B. J. Mair, BS J. Research **9,** 457 (1932) RP482.
	125.59	−56.90	0.70279	1.39760		A. F. Shepard and A. L. Henne, J. Am. Chem. Soc. **53,** 1948 (1931).
	125.65 [8]					M. Wojciechowski, J. Research NBS **17,** 453 (1936) RP921.
	124.7		.7068 $^{15}_{15}$	1.3963 ^{25}		L. Clarke, J. Am. Chem. Soc. **33,** 520 (1911).
		−57.3			43.2	G. S. Parks and H. M. Huffman, Ind. Eng. Chem. **23,** 1138 (1931).

2,3,5-Trimethylhexane

45	129 ^{738}		0.7171 $^{20}_{20}$	1.4051 ^{20}		M. M. Tuot, Compt. rend. **197,** 1434 (1933).

cis-1,2-Dimethylcyclohexane

46	130.04	−50.1	0.79625	1.43663 $^{15.5}$ J line of He		O. Miller, Bul. soc. chim. Belg. **44,** 513 (1935).

n-Propylcyclopentane

47	130.6 ± 0.2		0.7766	1.4269		F. H. Garner and E. B. Evans, J. Inst. Petroleum Tech. **18,** 761 (1932).
		−120.3				J. Timmermans, Bul. soc. chim. Belg. **36,** 502 (1927).

II. STUDY OF THE COMPOSITION OF THE DISTILLATE

1. DISTILLATE BETWEEN 98° AND 102° C

In earlier work on the portion of petroleum boiling between 60° and 100° C, a large quantity of a nearly constant-boiling mixture of *n*-heptane and methylcyclohexane was found just below 100° C. The material also contained, as did all the distillate boiling between 95° and 108° C, a considerable quantity of toluene.

Further systematic distillation, after the removal of the major portion of these constituents,[7] [8] probably resulted in the reappearance at about 98° and 102° C of the concentration shown by curve B_2 of figure 1. The maximum volume was found to distil between 100° to 100.5° C, and this coincides with the temperature at which a maximum in the refractive-index curve (1.422_D^{20}) appears. The boiling range and refractive index correspond very nearly to the properties of methylcyclohexane [3]. The photomicrographs of crystals of the material boiling at 101.2° C (fig. 1) support this conclusion.[9]

The material distilling just below this peak shows a rapidly decreasing refractive index, the minimum index (1.3925_D^{20}) occurring at 97.5° to 98° C. This indicates that the lower-boiling constituent of the large-volume fraction was chiefly a paraffin hydrocarbon. Table 1 lists two hydrocarbons, *n*-heptane [1] and 2,2,4-trimethylpentane [2], which are reported to have approximately the properties of this fraction. Comparison of photomicrographs of the crystals from the material at 98.3° C (fig. 1) with photomicrographs of pure *n*-heptane and 2,2,4-trimethylpentane show that the chief constituent was *n*-heptane.[10]

2. DISTILLATE BETWEEN 103° AND 106° C

No great effort was made to separate the constituents other than toluene from the material boiling between 102° and 106° C, because of the relatively small quantities present and because the fractions of distillate did not crystallize readily.

Curve B_2 of figure 1 shows about 4 liters of material boiling between 102.5° and 105.5° C after the toluene was removed. The fact that the refractive-index curve slopes down more gradually above 101° C than it does below that temperature indicates either the presence of one or more naphthenic hydrocarbons boiling just above methylcyclohexane, such as ethylcyclopentane [4], 1,1,2-trimethyl-2-ethylcyclopropane [5], or 1,2-dimethyl-1-ethylcyclopropane [6], or the presence of a paraffin, such as 2,2,3,3-tetramethylbutane [7] or 2,2-dimethylhexane [8], which tended to form a constant-boiling mixture with methylcyclohexane. At 105° to 105.5° C the refractive index has dropped to a value which shows that the distillate was largely paraffinic. Attempts to crystallize fractions in this range by cooling without dilution with solvents resulted in clear glasses. When a fraction distilling at 105.2° to 105.3° C was diluted with propane and poured into liquid methane, cooled by liquid nitrogen, two liquid layers appeared. These layers were separated by using a separatory funnel constructed

[7] M. M. Hicks-Bruun and J. H. Bruun, BS J. Research **8**, 525 (1932) RP432.
[8] J. H. Bruun, R. T. Leslie, and S. T. Schicktanz, BS J. Research **6**, 363 (1931) RP280.
[9] [10] R. T. Leslie, and W. W. Heuer, J. Research NBS **18**, 639 (1937) RP1000.

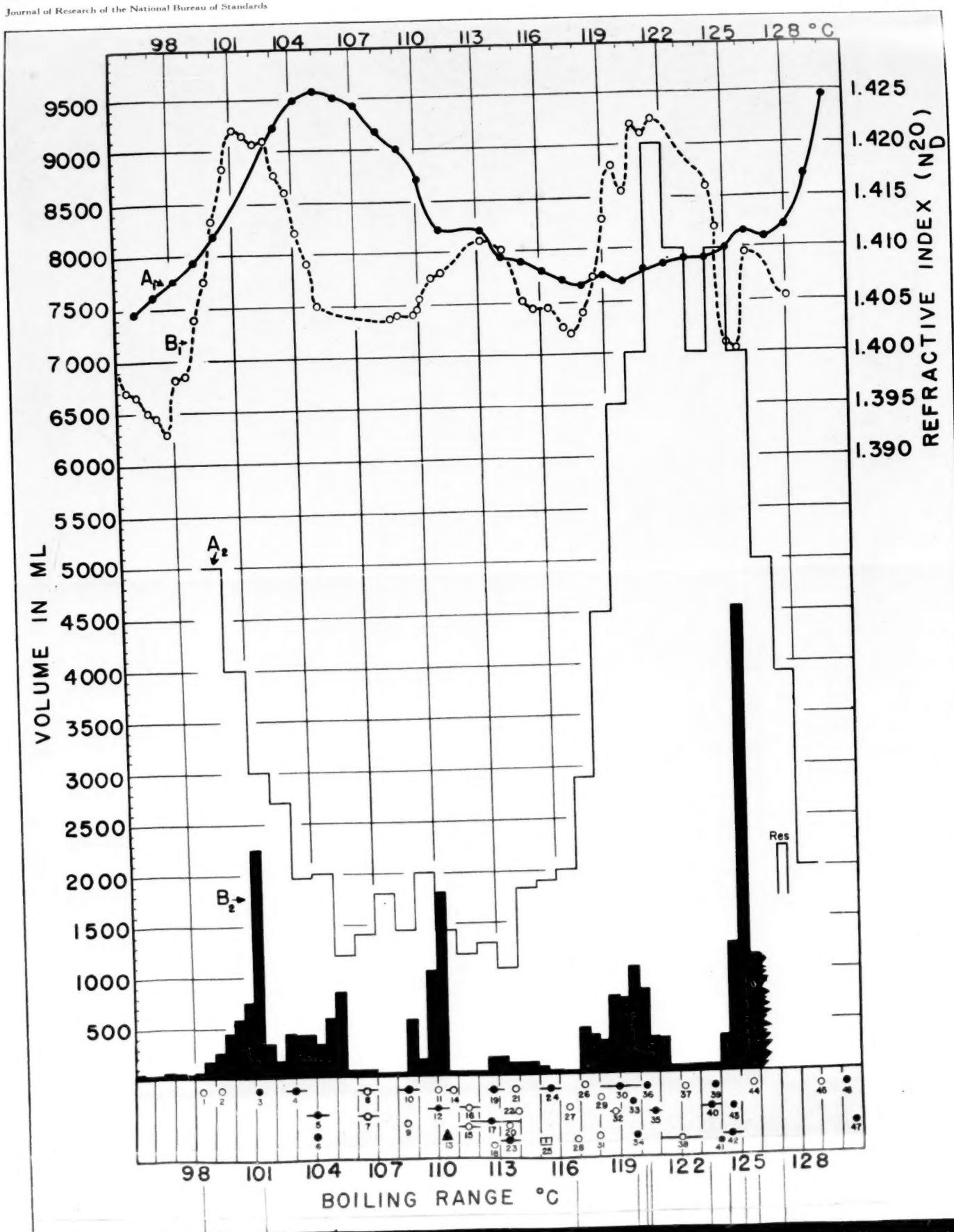
98 101 104 107 110 113 116 119 122 125 128 °C
9500
9000
8500
8000
7500
7000
6500
6000
5500
5000
4500
4000
3500
3000
2500
2000
1500
1000
500
VOLUME IN ML
1.425
1.420
1.415
1.410
1.405
1.400
1.395
1.390
REFRACTIVE INDEX (N_D^{20})
A_1
B_1
A_2
B_2
Res
98 101 104 107 110 113 116 119 122 125 128
BOILING RANGE °C

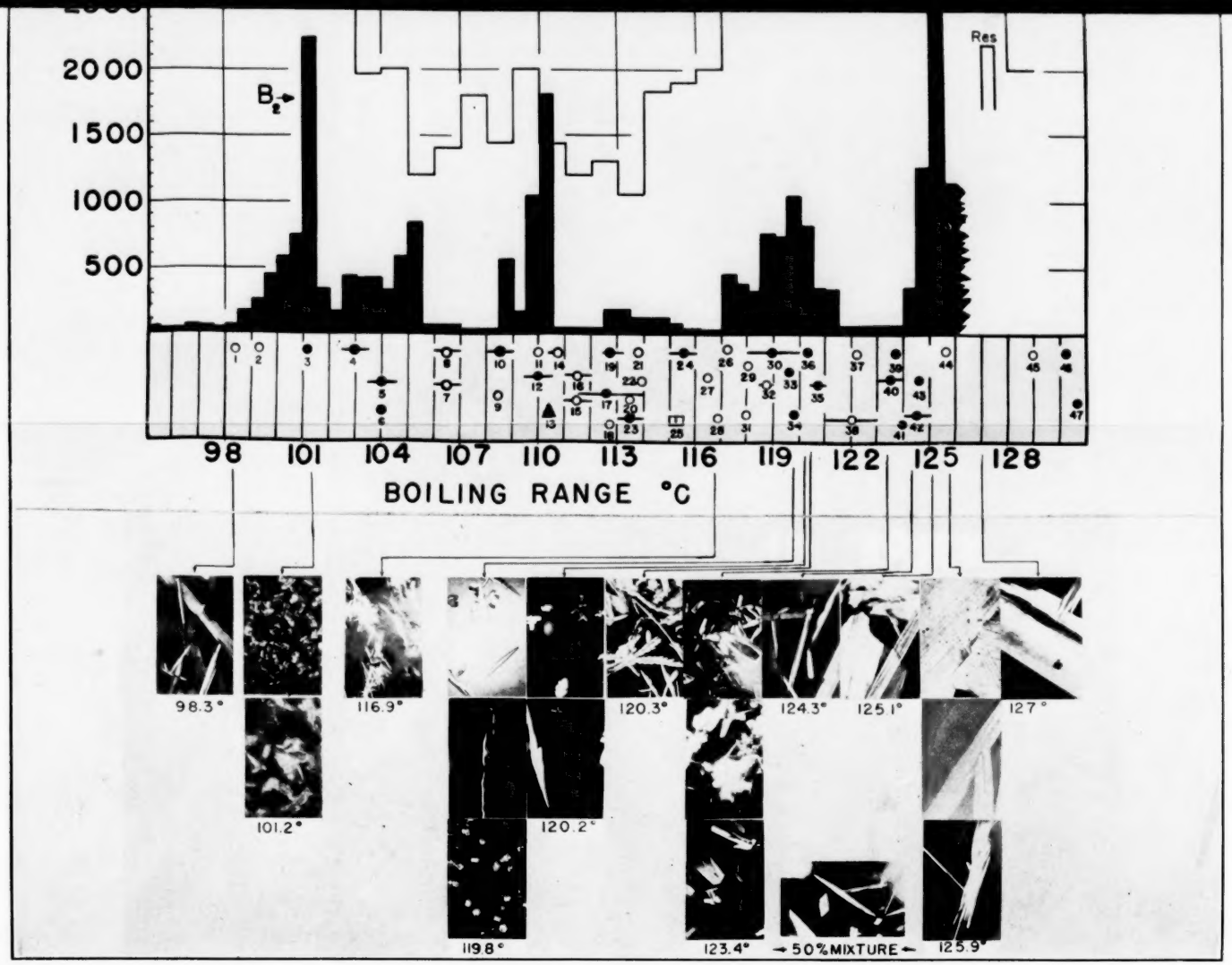

FIGURE 1.—*Volume and refractive index of fractions distilling between 95° and 130° C.*

A, status of material in 1929, after careful distillation but before removal of any constituents; *B*, status of material in 1936, after isolation or concentration and removal of seven hydrocarbons. Below the shaded graph the known hydrocarbons are indicated by the numbers referring to table 1 and the following symbols: open circles, paraffin hydrocarbons; solid disks, monocyclonaphthenes; triangle, aromatics; double square, bicyclonaphthenes; horizontal lines through circles indicate boiling range. The micrographs are of crystals from fractions of distillate; magnified about 30 times.

as shown in figure 2. The residue obtained from each layer, after boiling off the solvents, showed no difference in refractive index or the tendency to crystallize. Temperatures lower than that of liquid nitrogen might have caused crystallization of one of the layers.

From a consideration of the properties of the 5 hydrocarbons known to boil between 102° and 108° C, ethylcyclopentane [4] and 2,2-dimethylhexane [8] are most likely to occur in this small volume.

3. DISTILLATE BETWEEN 108.5° AND 110.5° C

Though the boiling point of toluene is given in the literature as about 110.8° C, very little of it was found in this fraction. The maximum concentration of the aromatic hydrocarbon was actually found to correspond with the maximum in the refractive-index curve, A_1, which occurs at about 105° C. The material represented by curve B_2 contained practically no toluene, as evidenced by the fact that the refractive index was not changed by treatment with nitrating agents or filtration through silica gel. The fact that the refractive-index curve in this range rises with boiling point indicates, therefore, that the distillate contained paraffinic mixed with higher-boiling naphthenic constituents.

When cooled, none of the fractions could be crystallized without solvents, and distillation with acetic acid failed to separate the naphthene, as shown by figure 3. Curves A_1 and A_2 of this figure show the results obtained after about 15 distillations without acetic acid in stills ranging in type of construction from 12 bubbling plates to 3-meter chain-packed columns and curves B_1 and B_2 show the results obtained after two successive fractional distillations with acetic acid. The material was distilled in three batches of about 1.5 liters each, and the distillate was again divided according to refractive index for the second distillation. It is to be observed that curves indicate very little improvement in separation.

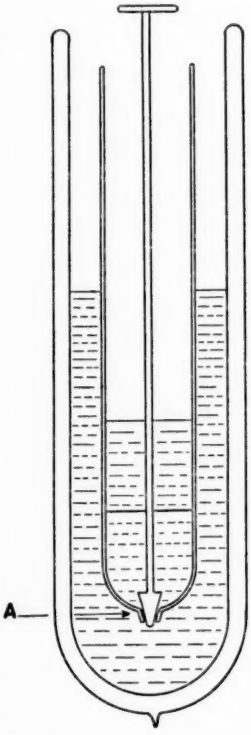

FIGURE 2.—*Separatory funnel for separating liquid layers formed when hydrocarbons are diluted with liquid methane and propane.*

A, drain orifice with ground stopper. Funnel removed from bath of liquid nitrogen to a cold test tube and lower layer drained through this opening.

Attempts to crystallize the material from methane and propane as solvents, as described above, resulted in two liquid layers, one of which was chiefly methane and the other propane, each containing petroleum hydrocarbon. The layers were separated but no differences in the properties of the fractions were observed.

The 2,5- [9], 2,4- [11], 3,3- [16], 3,5-dimethylhexanes [15], and 2,2,3-trimethylpentane [14] are shown in figure 1 as possible paraffinic constituents. The fact that the refractive-index curve rises with boiling point indicated that the naphthenic constituents were the higher-boiling components of the mixture. It appears that 1,2,3- [17], 1,1,3- [24], 1,1,2- [23], and 1,2,4-trimethylcyclopentane [19]

were the most likely possibilities, though their boiling points are higher than those of 1-methyl-1, 2-diethylcyclopropane [10] and 1-methyl-2-isobutylcyclopropane [12]. Since the total volume of material distilling between 108° and 111° C was less than 4 liters, it was estimated that the constituents of this fraction originally constituted not more than 0.1 percent of the crude petroleum. Of this, the major constituents appeared to be paraffinic. It is possible that the difficulty in separating the constituents sufficiently to obtain crystals may have been caused by the presence of a number of the isomeric octanes with nearly the same boiling points.

4. DISTILLATE BETWEEN 112° AND 116° C

This small volume of distillate, less than a liter, had a range of refractive indices which indicated that it was chiefly naphthenic in composition. The most likely constituents are the trimethylcyclopentanes [17, 19, 23, 24] mentioned above. Attempts to crystallize

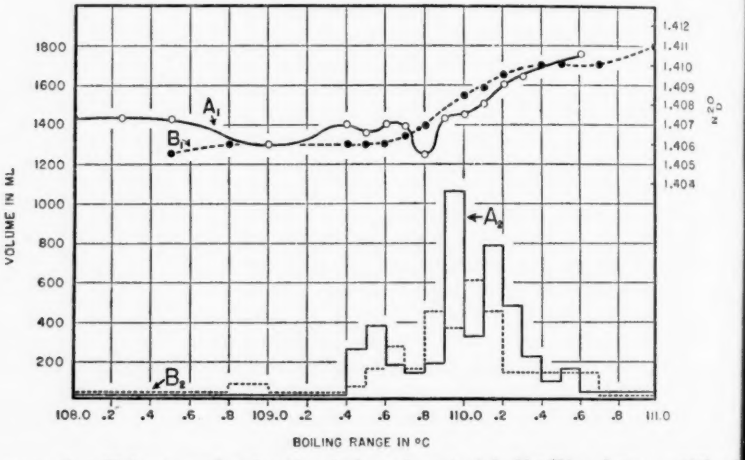

FIGURE 3.—*Volume and refractive index of material distilling between 108° and 110° C before and after distillation with acetic acid.*

A, April 1935, before distillation with acetic acid; *B*, December 1935, after distillation with acetic acid.

this material with methane and propane resulted in two liquid layers. Additional careful distillation should concentrate this fraction to the point where it will crystallize, unless it contains small quantities of many of the possible hydrocarbons.

5. DISTILLATE BETWEEN 117° AND 124° C

Because the proportion of the material which distilled between 117° and 124° C was large, most of the effort was devoted to separating constituents in this range.

The refractive-index and volume curves, A_1 and A_2 of figure 1, show that the fraction distilling between 114° and 128° C contained originally a large quantity of paraffinic material which had a slight tendency to separate into two large volumes. An amount of *n*-octane [44] equivalent to about 1 percent of the crude petroleum was removed by crystallization from the distillate between 123° and 126° C.[11] Sub-

[11] R. T. Leslie and S. T. Schicktanz, BS J. Research 6, 377 (1931) RP282.

sequent distillations resolved the fraction into two more or less distinct ones boiling between 116° and 124° C and between 124° and 128° C. The lower-boiling fraction appeared to have the more complex composition. In previous publications there has been described in detail the isolation of a relatively large quantity of 2-methylheptane [12] [26] (about 0.5 percent of the petroleum) boiling at about 117° C, a smaller quantity of a mixture of naphthenes [13] (about 0.2 percent) boiling between 119.2° and 120.8° C, and of a small quantity of a naphthene (about 0.04 percent), boiling at about 123.4° C.[14]

The photomicrographs at the bottom of figure 1 show the crystal behavior of fractions from this range. The photograph of the material boiling at 116.9° C shows material identified as 2-methylheptane [26]. Those of the fraction at 119.8° C probably show 1,1-dimethylcyclohexane [34]. The three photographs of the same fraction were made successively and show two crystal forms.[15] At 120.2° C the crystals still resemble those at 119.8° C. At 120.3° C, however, the crystals resemble *m*-dimethylcyclohexane [16] [36]. The naphthenic material boiling at 123.4° C, thought to be *trans-o*-dimethylcyclohexane [39], differs in appearance from the crystals of the lower-boiling naphthenes. The fine crystals which appear in one of the photographs may be a small amount of *n*-octane. The result of adding more octane from the higher-boiling fractions is shown by the photograph of the "mixture."

The residue shown by curve B_2 between 116° and 122° C represents the relatively small quantity of material which concentrated after removing, by crystallization as completely as practicable, the constituents discussed above. The refractive-index curve B_1, figure 1, indicates that the material contained lower-boiling paraffinic constituents and higher-boiling naphthenes, which were probably an additional small quantity of the hydrocarbons mentioned above.

In addition to the 2-methylheptane [26], it is possible that this fraction also contained small quantities of 3-ethylhexane [29], 3,4-dimethylhexane [27], 3-methylheptane [28], 4-methylheptane [31], and 3-methyl-3-ethylpentane [32]. If they were present they would be found in the residue shown by curve B_2 of figure 1. Of the seven naphthenes which are reported to boil in this range [30, 33, 34, 35, 36, 39, and 40], three were found and tentatively identified [34, 35, 39]. Cycloheptane [30], because of its high freezing point, and *p*-dimethylcyclohexane [33], because of the absence of the characteristic crystals which it forms, appeared to be absent. 1-methyl-3-ethylcyclopentane [35] and isopropylcyclopentane [40] may be present in small quantities but were not detected.

6. DISTILLATE BETWEEN 125° AND 126° C

The approximately 7 liters of distillate obtained in the narrow range, 125° to 126° C, as shown by the volume curve B_2 of figure 1, was probably *n*-octane, as indicated by the minimum in the refractive-index curve B_1. The photomicrographs of crystals from these fractions show that the chief constituent behaves like *n*-octane [17] [44]. It is possible, however, that small quantities of 2,2,4,4-tetramethylpen-

[12] R. T. Leslie, BS J. Research **10,** 609 (1933) RP552.
[13] R. T. Leslie, J. Research NBS **15,** 41 (1935) RP808.
[14] [15] R. T. Leslie, J. Research NBS **17,** 761 (1936) RP943.
[16] [17] R. T. Leslie and W. W. Heuer, J. Research NBS **18,** 639 (1937) RP1000.

tane [37], and 2,2,5-trimethylhexane [38], were also present since their boiling points are reported in this neighborhood. From the manner in which the refractive-index curve rises abruptly on either side of this narrow boiling range, it is apparent that the material also contained naphthenic constituents in small quantities, which were probably some of the *cis*-dimethylcyclohexanes [43, 46], 1-methyl-2-ethylcyclopentane [41], or isopropylcyclopentane [40]. The original 125° to 126° C distillate must have contained only a small percentage of naphthenic material, since the refractive-index of the large-volume fraction is very low and there are only small quantities of the fractions on either side which have high refractive indices.

7. DISTILLATE BETWEEN 127° AND 130° C

The material represented as "residue" in figure 1 was composed of "tailings" from several systematic fractionations and probably contained considerable cracked material. Treatment with silica gel, or other reagent for removing olefins, and distillation would return most of this material to lower-boiling fractions. Very little material actually distilled between 127° and 130° C. This might be expected since, as shown by figure 1, very few hydrocarbons are reported to boil in this range. If 2,3,5-trimethylhexane [45], *cis-o*-dimethylcyclohexane [46], and *n*-propylcyclopentane [47] were present, they must have been minor constituents. The next higher-boiling concentration of a constituent occurred at about 130° C, and the isolation of ethylcyclohexane from it has been reported by Rose and White.[18]

III. PROBABLE COMPOSITION OF A MIDCONTINENT PETROLEUM BOILING BETWEEN 100° AND 130° C

Most of the conclusions which have been reached in the investigation are summarized in table 2. This table presents, in addition to the relative quantities of constituents actually isolated, conclusions as to the probable presence or absence of each of the other hydrocarbons boiling between 98° and 131° C on which the author has found data in the literature. A column of the table also gives the approximate boiling ranges of the distillate from which constituents were isolated or in which constituents whose presence is uncertain might be expected to occur.

[18] F. W. Rose, Jr., and J. D. White, J. Research NBS **15**, 151 (1935) RP817.

TABLE 2.—*Known hydrocarbons boiling between 100° and 130° C (approximately) with relation to the corresponding naphtha fraction of a midcontinent petroleum*

Compound	Reference number to table 1	Normal boiling point of pure compound	Approximate boiling range in which material occurred, if present	Relative volume found, referring to *n*-octane as unity [1]	Occurrence [2]
		°C	°C		
n-Heptane	1	98.4	95 to 100	1.1	*P*
2, 2, 4-Trimethylpentane	2	99.3			*A*
Methylcyclohexane	3	101.2	98 to 102	0.3$_5$	*P*
Ethylcyclopentane	4	103.0 ±0.5	98 to 102		*S*
1, 1, 2-Trimethyl-2-ethylcyclopropane	5	103.5 to 104.5			*U*
1, 2-Dimethyl-1-ethylcyclopropane	6	104			*U*
2, 2, 3, 3-Tetramethylbutane	7	104 to 105.2			*U*
2, 2-Dimethylhexane	8	106 to 107	102 to 106		*S*
2, 5-Dimethylhexane	9	109.2 ±0.1	108.5 to 110.5		*S*
1-Methyl-1, 2-diethylcyclopropane	10	108 to 109			*U*
2, 4-Dimethylhexane	11	108 (750 mm)	108.5 to 110.5		*S*
1-Methyl-2-isobutylcyclopropane	12	109.5 to 110.5			*U*
Toluene	13	110.6$_4$	98 to 111	.3	*P*
2, 2, 3-Trimethylpentane	14	110.2	108.5 to 110.5		*S*
d-3, 5-Dimethylhexane	15	111 to 112	108.5 to 110.5		*S*
3, 3-Dimethylhexane	16	111 to 112	108.5 to 110.5		*S*
1, 2, 3-Trimethylcyclopentane	17	111.5 to 114	112 to 116		*S*
2, 3, 4-Trimethylpentane	18	112.8	108.5 to 110.5		*S*
1, 2, 4-Trimethycyclopentane	19	112.5 to 113	112 to 116		*S*
2, 3, 3-Trimethylpentane	20	113.6	112 to 116		*S*
2, 3-Dimethylhexane	21	115.9	112 to 116		*S*
2-Methyl-3-ethylpentane	22	114	112 to 116		*S*
1, 1, 2-Trimethylcyclopentane	23	113 to 114 (740 mm)	112 to 116		*S*
1, 1, 3-Trimethylcyclopentane	24	115 to 116	112 to 116		*S*
3, 3-Dimethylbicyclo-(0, 1, 3) hexane	25	115			*A*
2-Methylheptane	26	117.2	115 to 118	.2	*P*
3, 4-Dimethylhexane	27	118.7	116 to 122		*S*
3-Methylheptane	28	116.5 (748 mm)	116 to 122		*S*
3-Ethylhexane	29	118.8 to 119 (766 mm)	116 to 122		*S*
Cycloheptane	30	118 to 120			*A*
4-Methylheptane	31	118	116 to 122		*S*
3-Methyl-3-ethylpentane	32	118.5 to 119 (750 mm)	116 to 122		*S*
trans-1, 4-Dimethylcyclohexane	33	119.63	116 to 122		*S*
1, 1-Dimethylcyclohexane	34	119.8	116 to 122		*S*
1-Methyl-3-ethylcyclopentane	35	120.5 to 121 (756 mm)	116 to 122		*S*
trans-1, 3-Dimethylcyclohexane	36	120.40	118 to 122 [3]	.2	*P*
2, 2, 4, 4-Tetramethylpentane	37	122.30	120 to 126		*S*
2, 2, 5-Trimethylpentane	38	121 to 123	120 to 126		*S*
trans-1, 2-Dimethylcyclohexane	39	123.70	122 to 124	.04	*P*
Isopropylcyclopentane	40	123 to 124	122 to 126		*S*
1-Methyl-2-ethylcyclopentane	41	124	122 to 126		*S*
1, 1, 3, 3-Tetramethyl-2, 4-diethylcyclobutane	42	124 to 125			*U*
cis-1, 4-Dimethylcyclohexane	43	124.59	122 to 126		*S*
n-Octane	44	125.59	122 to 126	1.0	*P*
2, 3, 5-Trimethylhexane	45	129			*U*
cis-1, 2-Dimethylcyclohexane	46	130.04			*U*
n-Propylcyclopentane	47	130.6 ±0.2			*U*

[1] The numbers in this column give the estimated relative amounts by volume of the given hydrocarbons in the petroleum referred to normal octane as unity. To obtain the approximate magnitude of the percentage of hydrocarbon in the crude, these numbers should be multiplied by a factor which is roughly estimated, on the basis of the "over-all" losses, to lie between 1 and 1¼ (see abstract). Similarly, the approximate magnitude of the percentage in the 100° to 130° C fraction may be obtained by multiplying the numbers by a factor estimated to lie between 17 and 30. (Estimates in previous papers were made by doubling the actual quantities found in an attempt to compensate for losses. This factor is probably low.)

[2] Letters in this column have the following significance: *P*, present; *A*, presence in more than small amounts considered unlikely because of the properties of the compound; *S*, possibly present in amounts too small to be detected by the method used; *U*, presence considered unlikely because of structure or small quantity of distillate at its boiling point.

[3] This fraction also contained an unidentified naphthene boiling at about 119.8° C (possibly No. 34).

Of the distillate from the crude petroleum boiling between 100° and 130° C, *n*-octane [44] was by far the chief constituent. Reasonably careful distillation caused most of the *n*-octane to concentrate between 122° and 126° C. From this distillate a quantity of nearly pure hydrocarbon was isolated equal to about one-tenth of the volume with which the investigation was begun. Toluene [13] was the sole aromatic constituent and was present in a relatively large proportion. Distillation caused it to appear in a wide temperature range (98° to 111° C), and a quantity was isolated equal to about one-third the volume of *n*-octane. Methylcyclohexane [3] about equal in quantity to toluene was found in the distillate between 98° and 102° C. A quantity of 2-methylheptane [26] amounting to about one-fifth of the *n*-octane occurred in the material distilling between 115° and 118° C. At least three cycloparaffinic hydrocarbons were present in appreciable quantities in the distillate between the boiling range of the material containing the 2-methylheptane and that of the *n*-octane (*trans*-1,3-dimethylcyclohexane [36], *trans*-1,2-dimethylcyclohexane [39], and an unidentified hydrocarbon which may be 1,1-dimethylcyclohexane [34]). The other known hydrocarbons boiling in this range were in relatively small amounts, if at all. Between 126° and 130° C there was only a small quantity of distillate, indicating insignificant amounts of the few hydrocarbons whose boiling points are within the range. There was, however, distillate other than toluene between 102° and 115° C which though small, showed the presence of di- and trimethyl isomers of octane [8, 9, 11, 14, 15, 16, 18, 20, 21, 22] and possibly one or more of the cyclopentanes [4, 17, 19, 23, 24].

WASHINGTON, October 21, 1938.

U. S. Department of Commerce National Bureau of Standards

RESEARCH PAPER RP1175

Part of Journal of Research of the National Bureau of Standards, Volume 22, February 1939

GASOMETRIC METHOD AND APPARATUS FOR THE ANALYSIS OF MIXTURES OF ETHYLENE OXIDE AND CARBON DIOXIDE

By Joseph R. Branham and Martin Shepherd

ABSTRACT

A gasometric method for the analysis of ethylene oxide mixed with carbon dioxide is reported. Ethylene oxide is swiftly and quantitatively removed from the gas phase by a relatively small amount of sulfuric acid. This reagent absorbs over 5,000 times its own volume of ethylene oxide, and the quantity used (only 0.2 ml) dissolves no significant amount of carbon dioxide. The carbon dioxide is absorbed in a concentrated solution of potassium hydroxide. A reproducibility of ±0.05 percent is attained; the accuracy is commensurate. All gases are measured dry in a new apparatus designed to perform this type of analysis rapidly.

CONTENTS

	Page
I. Introduction	171
II. Previous investigations	172
III. Development of a gasometric method	172
1. Preliminary considerations	172
2. Reagent for ethylene oxide	174
3. Suitable desiccants	175
4. Design of the volumetric apparatus	176
5. Volumetric behavior of the dry apparatus	178
6. Analytical procedure	178
IV. Analyses of mixtures of ethylene oxide and carbon dioxide	179
1. Preparation of mixtures for analysis	179
2. Purity of the ethylene oxide	180
3. Purity of the carbon dioxide	180
4. Analysis of mixture 1	181
5. Analysis of mixture 2	182
V. Accuracy of the method	183
1. Pressure-volume considerations	183
2. Gravimetric determination of accuracy	185
(a) Apparatus	186
(b) Procedure	186
(c) Results	187
VI. Note on sampling	188

I. INTRODUCTION

The use of ethylene oxide as a fumigant has increased considerably in this country and abroad during the last 8 years. This substance is generally used with about 90 percent of carbon dioxide to produce a noninflammable mixture. The analysis of this simple mixture has caused some difficulty, in spite of the remarkable chemical reactivity

of the ethylene oxide. The methods so far reported have been limited in number and are not satisfactorily accurate. They have involved a combination of gravimetric or gasometric methods, always with a final estimation of the ethylene oxide alone by titrimetric procedure. The method here developed involves only direct gasometric measurements made with a standard burette-manometer-compensator unit. Its accuracy is commensurate with that obtained by the best of the former methods, and both components of the mixture may be determined in less time and with less effort than were required previously for the determinations of ethylene oxide alone.

II. PREVIOUS INVESTIGATIONS

Deckert [1] employed the reaction of ethylene oxide with hydrochloric acid and sodium chloride to form glycol chlorohydrin, titrating the excess acid with sodium hydroxide to determine ethylene oxide. Later, Deckert [2] reported a colorimetric method based upon the reaction of ethylene oxide with a concentrated solution of sodium chloride to form glycol chlorohydrin, phenolphthalein and bromothymol blue serving as indicators. He reported a third method (colorimetric) [3] for the examination of air containing traces of ethylene oxide, based on the reaction with potassium thiocyanate, with phenolphthalein as indicator.

According to Lubatti,[4] Deckert's titrimetric method indicated only 90 percent of the ethylene oxide present. Lubatti employed a nearly saturated acid solution of magnesium chloride as an analytical reagent for the examination of samples of liquid ethylene oxide, titrating with sodium hydroxide. The reaction was over 99 percent complete.

More recently the apparatus described by Page [5] was utilized by Lubatti,[6] who modified his original modification of Deckert's method to the extent of adding sodium, lithium, and magnesium chlorides to 0.1 *N* hydrochloric and sulfuric acids, titrating the excess acids with sodium hydroxide.

III. DEVELOPMENT OF A GASOMETRIC METHOD

1. PRELIMINARY CONSIDERATIONS

The reduction in gas volume which occurs when ethylene oxide reacts with reagents of these types was suggested by Deckert [7] as an obvious means of determining ethylene oxide. The gasometric procedure has been employed in several laboratories, but the results have not encouraged publication. The reagents used to absorb ethylene oxide have been aqueous solutions of various salts or mixtures of these prepared indiscriminately. It is not unlikely that these reagents reacted quantitatively with ethylene oxide, since water alone will do so, and with great rapidity if the gas is bubbled through it.[8] The major mistake apparent in these efforts has been the use

[1] W. Deckert, Z. anal. Chem. **82**, 297–307 (1930).
[2] W. Deckert, Z. angew. Chem. **45**, 559–62 (1932).
[3] W. Deckert, Z. angew. Chem. **45**, 758 (1932).
[4] O. F. Lubatti, J. Soc. Chem. Ind. **51**, 361 (1932).
[5] A. B. P. Page, J. Soc. Chem. Ind. **54**, 421 (1935).
[6] O. F. Lubatti, J. Soc. Chem. Ind. **54**, 424 (1935).
[7] See footnote 1.
[8] Several experimenters state that the reaction is slow. This is not true if an efficient absorbing pipette is employed.

of 100- to 200-ml portions of aqueous reagents in ordinary forms of absorption pipettes. Thus speed of reaction has been attained, but with a grievous sacrifice of accuracy, since carbon dioxide dissolves abundantly in such aqueous solutions. Elaborate precautions have been taken to saturate the reagent (at controlled temperature) with carbon dioxide. This prerequisite to actual analysis not only requires much time, but unfortunately does not accomplish its objective since the dissolved carbon dioxide wanders in two directions: Into the air through the atmospheric arm of the pipette, and into the gas sample during the absorption of ethylene oxide. The amount lost by the reagent to the gas sample may be tediously replaced by repeated passage into the pipette, but the amount lost to the air must be replaced by an equal amount from the gas sample itself, thus causing a proportionately high estimation of ethylene oxide.

A brief outline of a successful gasometric method for the analysis of a mixture of ethylene oxide and carbon dioxide should serve to make this problem clear.

To begin with, the sample taken for analysis must be measured in a dry burette. If the moist burette generally used were employed, water present would react with the ethylene oxide (hereinafter designated C_2H_4O) and alter the composition of the sample before its analysis.

Next, the dry sample must be transferred to a reagent which will quantitatively remove C_2H_4O, without removing CO_2.

Since the reagent which removes C_2H_4O will also add H_2O vapor to the residual gas, this gas must be returned through a suitable desiccant in order that it may reach the burette in a dry state. The difference between the measured dry sample and dry residue should then represent the C_2H_4O in the sample.

Finally, the CO_2 must be removed, and the residual gas returned (after drying) to the burette for measurement. The contraction observed will then represent the CO_2 in the sample.

Since the sample may consist entirely of C_2H_4O and CO_2, a measured volume of dried air must be added during the initial steps of the analysis. This will act as a transfer or "push" gas, and must be inert with respect to the reagents employed. The difference between its volume and the volume of the residual gas observed at the end of the analysis represents the inert content of the sample.

From this outline, it can be seen that the development of a successful gasometric method for the analysis of this mixture will resolve naturally into three separate problems, as follows:

1. Selection of a reagent which is chemically and physically selective with respect to C_2H_4O in the presence of CO_2 and air.

2. Selection of a desiccant which is chemically and physically passive with respect to CO_2 and air.

Since a satisfactory reagent for CO_2 (in the presence of air) already exists, the final problem becomes:

3. Design of a volumetric apparatus capable of performing the necessary procedures indicated.

These problems will be discussed in their order.

2. REAGENT FOR ETHYLENE OXIDE

A suitable reagent for the determination of C_2H_4O must possess the following qualifications:

1. The reagent must react quantitatively with C_2H_4O, completely removing this substance from the gas phase, or replacing it with a stoichiometrically definite volume not equal to its own.
2. The product or products of reaction must possess negligible vapor pressures (or vapors which can be removed chemically without affecting CO_2 or air).
3. The reaction must produce no gaseous by-product (unless this can be removed).
4. The reagent or products of reaction must not react with, or dissolve, significant amounts of CO_2 or air.
5. Since any reagent likely to be conceived will dissolve CO_2 to some extent, the volume of the reagent actually employed must be very small in order to reduce the attendant error to the order of magnitude of the required volumetric precision.
6. The above qualification at once imposes several additional and severe ones. Since the volume of the reagent must be reduced to 0.2 to 0.3 ml, it can most conveniently be confined over mercury. Therefore, it must not react with mercury to produce significant amounts of gas.
7. A pipette of the type mentioned above is at best an inefficient absorber, presenting little contact between gas and reagent. Accordingly, the rate of reaction between the reagent and C_2H_4O must be very rapid.
8. Finally, because of its small volume, and for the sake of convenience, the reagent should have an extremely large capacity for C_2H_4O, so that its frequent replacement may be avoided.

This list of qualifications would appear to be somewhat appalling to the gas analyst; but actually they were easily realized. The behavior of C_2H_4O with various substances was roughly studied in a preliminary set of experiments. C_2H_4O was observed to react readily with the contents of the reagent bottles at hand on the laboratory shelf, such as HNO_3, HCl, H_3PO_4, H_2SO_4, CrO_3, $H_2Cr_2O_7$, $HgNO_3$, etc., in various dilutions with water. As a matter of fact, since C_2H_4O reacts readily with H_2O alone, it seems likely that few inorganic reagents would prevent the formation of the glycol in the presence of water, although some accelerate the reaction. The apparent tendency of C_2H_4O to react with many such mixtures suggests the possibility of a number of satisfactory reagents.

Only one from this list of reagents was selected for extensive study. The reagent selected was a mixture of equal parts of H_2O and concentrated H_2SO_4. This met every one of the qualifications previously delineated. In the event other reagents develop, it would not seem worth-while to issue additional papers for each in turn.

Apparently, the reaction between the diluted H_2SO_4 and C_2H_4O goes through an intermediate state to form ethylsulfuric acid, which breaks down to H_2SO_4 and the first glycol. This in turn reacts with additional C_2H_4O to produce higher glycols, increasing enormously the capacity of the reagent.

The behavior of this reagent with C_2H_4O is interesting. If the gas is confined over mercury within a glass tube, and the reagent is admit-

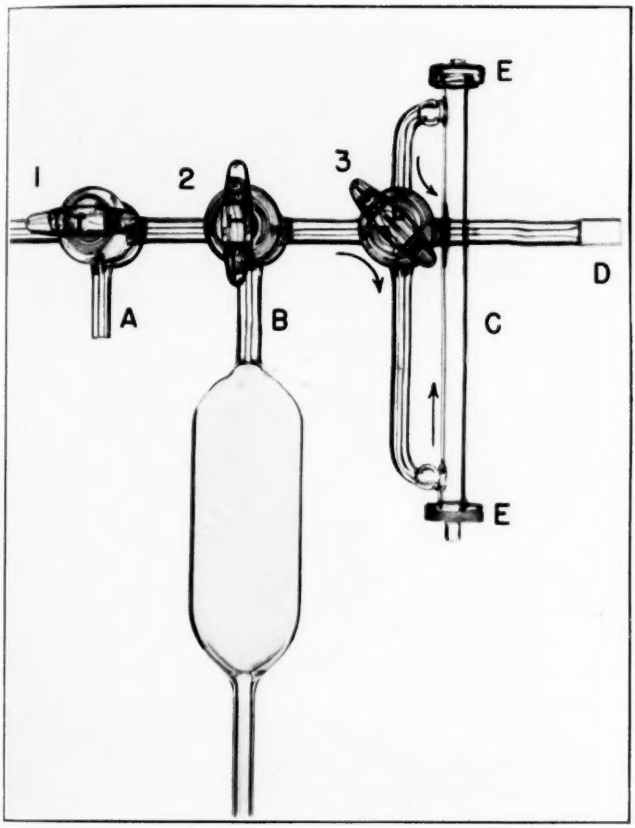

FIGURE 1.—*Reaction unit.*

ted in successive small portions of 0.2 ml each, the initial reaction is very rapid and the final reaction very slow with the addition of each portion of reagent. However, if the wall of the tube is coated with the reagent by shaking, the reaction thereafter is extremely rapid. The glycols which form drain slowly, producing a film or droplets of honey-like consistency over the entire wall of the tube.

Over 2,500 ml of C_2H_4O was passed (at a rate exceeding 200 ml per minute), into a tube containing 0.5 ml of the H_2SO_4 solution. At the end of this experiment, the reaction was still proceeding rapidly and completely. Approximately 2 ml of the glycols had been collected. The capacity of the reagent is accordingly over 1:5000, expressed as a ratio by volume of reagent:C_2H_4O, a novel behavior from the viewpoint of the gas analyst.

There was no direct evidence of the formation of interfering by-products of the reaction. Acetaldehyde was suspected, but only traces of it were found.

3. SUITABLE DESICCANTS

To qualify for occupancy of the drying tube within the analytical apparatus, a desiccant must possess the following characteristics:

1. It must leave somewhat less water vapor in the dried gas than corresponds to the volumetric accuracy of the apparatus. This limit with respect to the desiccant can be set at 0.02 ml.
2. It should dry the gas rapidly, preferably at the rate of 100 ml per 30 seconds or less.
3. It must not react with CO_2 or air, nor adsorb significant quantities of these gases.
4. It should not react objectionably with C_2H_4O in the event that this gas is accidently brought into contact with it through a mistake in operation.
5. It should be convenient to use.

Of the available desiccants initially suggesting themselves, P_2O_5, $Mg(ClO_4)_2$, $CaSO_4$, and $CaCl_2$ (fused, granular, anhydrous) seemed best suited. These were studied experimentally, and the following facts were ascertained:

1. All four met the first qualification, $CaCl_2$ in its best available form just passing.
2. All four met the second qualification.
3. P_2O_5, $Mg(ClO_4)_2$ and $CaCl_2$ met the third qualification. ($CaCl_2$ must, of course, be of reagent quality. Traces of alkaline impurities must be neutralized by treatment with CO_2+air before the gas analysis.) $CaSO_4$ adsorbed large amounts of CO_2 and was therefore discarded.
4. Of the remaining three desiccants, $CaCl_2$ alone met the fourth qualification completely. This is a "should" and not a "must" qualification, however, since C_2H_4O would not come into contact with the desiccant except by mistake.

If C_2H_4O is inadvertently passed over P_2O_5, the reaction is marked, as is the P_2O_5 with a visible deposit of carbon, which leaves no doubt as to the necessity of its replacement.

$Mg(ClO_4)_2$ is open to a curious objection. A double mistake might conceivably result in (a) bringing H_2SO_4 into contact with this desiccant, and later (b) bringing C_2H_4O into the same tube. It is not

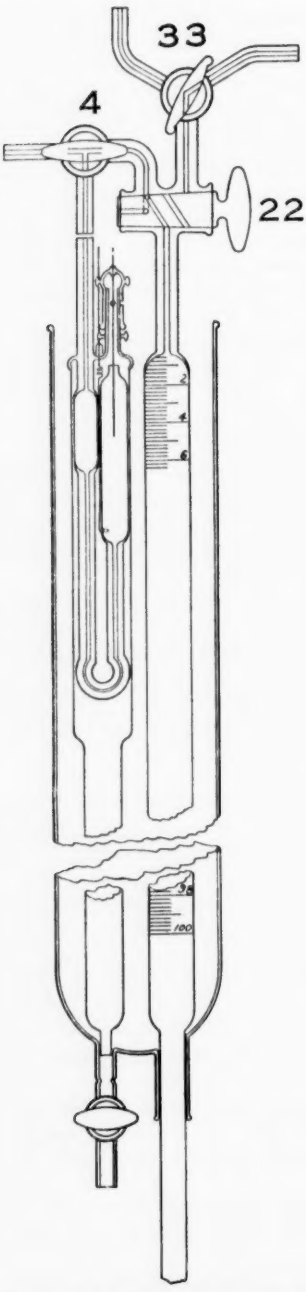

FIGURE 2.—*Volume-measuring unit.*

probable that such mistakes would be made; but if they were, a serious explosion might occur. $Mg(ClO_4)_2$ was actually used in the analytical work which follows. Since it demonstrated no marked superiority, it had probably best be laid aside in this instance.

5. Of the two remaining desiccants, $CaCl_2$ is by far more convenient to use. However, P_2O_5 may, without too great difficulty, be sifted onto glass wool within the drying tube of the apparatus. This is best done by plugging a tube (smaller than the drying tube) at one end with glass wool, drawing (by vacuum) P_2O_5 from the reagent bottle into this tube, and finally inserting the small tube into the desiccating tube of the apparatus, discharging its contents therein by means of a thin glass rod. Once this tube is filled, prolonged service is to be expected.

The analyst will probably make his own choice between P_2O_5 and $CaCl_2$. With respect to H_2O and CO_2, P_2O_5 offers the best chemical behavior. Both desiccants gave good analytical results. In any event, the same desiccant should be used in both drying tubes attached to the apparatus.

4. DESIGN OF THE VOLUMETRIC APPARATUS

In measuring the mixture of C_2H_4O+ CO_2 gasometrically, it is obvious that the burette must be dry. The dry burette accordingly should be complemented with a dry compensator. The burette and compensator-manometer unit of our standard gas-analysis apparatus [9] served satisfactorily.

Aside from measurement, it is necessary only to transfer the measured dry sample to the reagent which removes C_2H_4O and subsequently remove the water vapor which this reagent adds to the residual gas prior to returning it to the burette. Thereafter, the residue is to be passed into a reagent which removes CO_2, and the residual gas dried and measured.

[9] M. Shepherd, BS J. Research 6, 122-130 (1931) RP266.

An apparatus [10] by means of which these procedures may be easily achieved is shown in figure 1.

This unit is sealed directly onto the horizontal outlet of stopcock 4 of the burette-manometer-compensator assembly previously mentioned, which is reproduced here for convenience (fig. 2). A thermoplastic cement (pine tar and shellac) serves to make the joint at the sleeve, *D*, (fig. 1). According to tests made, rubber reacted with C_2H_4O too rapidly to permit its use. The cement reacted too slowly to cause significant error. Actually, the main concern is at the sampling inlet.

An ordinary bubbling pipette connected at the outlet, *A*, of T-stopcock 1 is filled with a concentrated solution of KOH to remove the CO_2. (A concentrated solution is used because of the low solubility of atmospheric inerts.)[11]

A reservoir, *B*, connected to T-stopcock 2 serves as the reaction pipette for the C_2H_4O. It is filled with mercury, and a leveling bulb is attached to its lower outlet. The small volume of reagent (0.2 to 0.3 ml of equal parts by volume of H_2O and concentrated H_2SO_4) may be conveniently introduced into *B* by means of a medicine dropper drawn out into a tip which is bent downward at a right angle. This tip may be inserted in the capillary inlet of *B* when the key of cock 2 is removed. One such charge will serve for a hundred or more analyses before it must be removed in the same manner.

The capillary inlet of *B* has a reference or zero mark etched around the stem just under cock 2. The lower outlet of *B* connects to a stopcock by means of nitrometer tubing, around which is placed a compression screw for adjusting the reagent meniscus to this zero mark.

The tube, *C*, contains a desiccant for drying the gases returned from *A* or *B*. Stopcock 3 is drilled with three bores, as indicated on the handle. When turned 45° counterclockwise to the position shown in figure 1, tube *C* is by-passed, and gas *from* the burette flows directly within the horizontal distributor to either *A* or *B*. When the cock is turned in the position shown, gas flowing from *A* or *B to* the burette must pass through *C*, entering at the bottom of this tube and leaving the top, as indicated by the directional arrows.

The tube, *C*, is closed by means of plates, *E–E*, which are ground flat to fit corresponding ground seats at the ends of *C*. A heavy lubricant serves to seal them. They are held in position by two coil springs fastened to saddles of sheet metal, which, in turn, fit over the glass knobs of the end plates, *E–E*. Thus, the tube, *C*, may be easily opened in position on the apparatus for supplying or removing desiccants. Plugs of glass wool at the ends of *C* keep the desiccants in place.

The gas volume of *C*, when filled with desiccant, is small enough so that changes of 0.2° C. in room temperature will produce no significant error in comparing volumes during an analysis. The time required for an analysis is so short that trouble from changing temperature should never occur.[12]

[10] This apparatus was designed by Shepherd. The unit comprising cock 3 and tube *C* is to be used in a multiple assembly in a new type of gas-analysis apparatus now under test.

[11] J. R. Branham and M. Sucher, J. Research NBS **21**, 63 (1938) RP1113.

[12] One of the most embarrassing questions asked the authors with respect to any type of analysis is, "How long does it take to do it?" There are so many factors involved—the accuracy desired, the composition of the mixture, and, of course, the analyst—that definite answers cannot be given. But in the present instance, it may be of interest to know that it is possible to complete an analysis in 15 minutes, operating carefully.

To complete the apparatus, a drying tube is connected to the left-hand outlet of stopcock 33 of the burette (fig. 2), and the source of sample to the right-hand outlet of the same cock. These connections were made with sleeve joints and thermoplastic cement in the present work, but ground joints would be preferable.

The apparatus described in figure 1, as previously noted, may be used in conjunction with the regular volumetric unit and with the supporting frame of our standard gas analysis apparatus. If, however, the number of samples to be analyzed would justify a separate apparatus for the purpose, the following modifications would improve the unit somewhat:

1. The burette should be blown with a 20-ml bulb at the top, with intervals on the stem from approximately 20 to 100 ml. This would (a) shorten the apparatus or (b) permit estimations of intervals of smaller volume if the apparatus were not shortened.

2. The two outlets of stopcock 33 of the burette (fig. 2) should terminate in interchangeable ground-glass joints (male members), to permit easy connection to an auxiliary drying tube and source of sample.

3. The sleeve, *D*, (fig. 1), should be tapered (female) to fit a corresponding taper (male) on the outlet of cock 4 (fig. 2).

5. VOLUMETRIC BEHAVIOR OF THE DRY APPARATUS

Before developing the analytical procedure, the volumetric behavior of the dry burette and compensator was studied experimentally. The following facts were ascertained:

1. With a desiccant in the tube, *C*, and with the reservoir, *B*, the burette and the compensator dried, a volume of dried air could be repeatedly measured, transferred from the burette to the reservoir and back, and even allowed to stand overnight, with no significant change in volume (± 0.02 ml). Indeed, there are indications that the dry system might prove more accurate than the saturated (wet) system ordinarily employed.

2. With water in the reservoir, *B*, dry air transferred to *B* and returned to the burette through *C* (containing any desiccant later employed) gained approximately 0.05 to 0.08 ml if the rate of return exceeded 70 ml per 20 seconds. However, no change of volume was noted at the lesser rates of gas flow employed. Returning a gas from *B* through *C* in 30 seconds insures drying.

3. If dried air is passed directly over water in *B* and returned to the burette, by-passing *C*, the volume is increased to correspond to the existing vapor pressure of water. Thereafter, if the moist air is passed back and forth between *B* and the burette through the desiccant, the volume gradually returns to its original dry value. Approximately 4 or 5 passages (2 minutes each) through the desiccant are required to restore the dry condition, since adsorbed water is apparently given up reluctantly by the burette wall. This illustrates the importance of always returning gas to the burette through the tube, *C*.

6. ANALYTICAL PROCEDURE

The following detailed procedure was developed during the course of a few preliminary analyses, and of the analyses reported in table 1.

Initial drying of apparatus.—The compensator was dried by alternate evacuation and filling with air dried over P_2O_5. (A small amount of desiccant left permanently in the bottom of the compensator would probably be desirable in an apparatus to be used for this type of analysis only.) The burette was dried by repeatedly passing air in and out through the desiccant connected to cock 33 (fig. 2). The distributor was dried by passing air through *C* to *A* and back. About 10 passages of 2 minutes each are required for drying, if no water was originally visible. Once dry, the apparatus should remain so.

Analytical technique.—The distributor, manometer, and *C* are filled with dried air and adjusted to the fixed pressure of the compensator.

Approximately 60 ml of the $C_2H_4O+CO_2$ mixture to be analyzed is drawn into the burette. With cock 22 closed the pressure is balanced against atmospheric with the leveling bulb, so that a minimum amount of gas will later flow between the burette and manometer. Cock 4 (fig. 2) is then turned to the position ⊢ to connect the manometer with the burette; the pressure is balanced against the compensator, cock 4 is turned to the position ⋎ to disconnect the burette from the manometer and train, and the volume of the sample is read. Cock 3 (fig. 1) is turned to the position $\frac{\vee}{\wedge}$, the leveling bulb attached to *B* is lowered slightly to reduce the pressure therein, cock 2 to the position ⊢, and cock 4 to the position ⊥. The sample is transferred to *B*, the leveling bulb being dropped to maintain approximately atmospheric pressure in *B*. When the mercury in the burette reaches cock 22, it is turned to connect to cock 33 and the line between them is flushed with mercury. Cock 33 is then turned to connect the burette to the source of dried air, 25 to 30 ml of which is taken into the burette and measured exactly as was the sample. The gas in the arm of the manometer connecting to the distributor is then displaced to the burette, cock 4 is turned to the position ⋎, the pressure of the gas in the burette adjusted to slightly in excess of atmospheric by the leveling bulb, and the air is then transferred to *B* with cock 4 in the position ⊥. The dry air has now swept the $C_2H_4O+CO_2$ into *B*, where the mixture is allowed to stand 1 minute. Agitation by means of mercury flow is not necessary after the first passage of the first analysis. Cock 3 is now turned to the position ⌐\⌙ and the residual gas (minus C_2H_4O) is returned through *C* to the burette, 30 seconds being taken for passage through *C*. The volume is measured as before, the contraction noted being computed as C_2H_4O.

The gas in the distributor arm of the manometer is again displaced to the burette, and thence transferred to the pipette, *A*, containing a solution of KOH, being routed through *C*, both back and forth. During the eighth and tenth passages *into A*, cock 3 is turned for a second to the position $\frac{\vee}{\wedge}$ to displace CO_2 trapped in the straight bore of this cock. At *no time* must gas by-pass *C* on the way *back* to the burette. After the tenth passage, the residual gas (minus CO_2) is measured and the contraction computed as CO_2. (Ten passages are used to insure complete removal of CO_2 from the tube, *E*, and the distributor, by dilution.) The difference in volume between this residue and the dry air originally taken for a transfer gas is computed as the inert content of the sample.

IV. ANALYSES OF MIXTURES OF ETHYLENE OXIDE AND CARBON DIOXIDE

1. PREPARATION OF MIXTURES FOR ANALYSIS

To test the method, apparatus, and procedure just discussed, two mixtures of C_2H_4O and CO_2 were prepared and analyzed. Both of these mixtures were made to contain approximately 10 percent of C_2H_4O by volume, which corresponds to the mixture used for fumigating. The mixtures were prepared in a 5-liter glass flask to which a barometric manometer was attached. The flask was evacuated, C_2H_4O was admitted until the manometer registered a pressure of approximately 75 mm, and CO_2 was then admitted until the pressure reached approximately 750 mm. The room temperature was observed to remain constant ($\pm 0.1°$ C). The two gases, of almost identical molecular weights, were allowed to mix for several days.

Convection was occasionally induced by local warming of the flask. The flask was then joined to the burette as previously described, and samples were withdrawn using the mercury within the burette as a pump.

The composition of the samples prepared in this manner was not necessarily expected to check the composition as determined by the analysis, even assuming absence of significant errors in both cases. Since the pressure-volume relationships existing during the preparation and during the analysis of these mixtures are different, the deviations of the gases and their mixtures from the behavior prescribed for ideal gases could account for differences in the composition as measured in the two cases.

2. PURITY OF THE ETHYLENE OXIDE

The C_2H_4O used in preparing the two mixtures was purified in a large commercial rectifying column. Approximately 10 liters of this was stored as a liquid in a cylinder. About one-third of the contents of this cylinder had been withdrawn before the present use of the gas.

The completeness of reaction between this C_2H_4O and the H_2O-H_2SO_4 reagent employed during the analyses was determined as follows:

1. 30.08 ml of dried air was measured in the burette and transferred to the reservoir, *B*, containing the reagent.
2. 274 ml of C_2H_4O was measured in three portions and transferred to *B*. (The reaction was so rapid that only with great difficulty could the mercury in *B* be prevented from being drawn into the horizontal distributor.)
3. The residual volume was passed through $CaCl_2$ in *C*, and measured in the burette as 30.53 ml.
4. The difference between the initial and final volumes corresponds to 0.017 ml of "inert" per 10 ml of C_2H_4O. Since 6 ml of C_2H_4O is the amount in the average sample, approximately 0.01 ml of the C_2H_4O used did not react or was inert during each analysis. This is less than the expected volumetric error.

The above test does not preclude the possibility that a compound other than C_2H_4O was present and reacted with the solution of H_2SO_4. The purification of the C_2H_4O by rectification makes such a possibility remote; and analyses of $C_2H_4O+CO_2$ mixtures obtained from the same source as that supplying the present C_2H_4O, made by isothermal fractional distillation in our laboratory, failed to disclose a notable impurity in the C_2H_4O fraction.

3. PURITY OF THE CARBON DIOXIDE

The carbon dioxide used was drawn from the last half of a cylinder of liquid obtained from a commercial source. Its "purity," so far as this work is concerned, was tested as follows:

1. Four volumes totalling 384 ml of CO_2 were measured; 30.43 ml of air was measured separately.
2. These gases were transferred to the pipette containing a saturated solution of KOH, first without bubbling, and finally with repeated bubbling passages.
3. The residual air was dried in *C* and measured as 30.54 ml. This corresponds to 0.03 ml of "inert" per 100 ml of CO_2, or about 0.016 ml per analysis. (A small amount of this inert may have been

air displaced from the solution of KOH during the absorption of CO_2.) This is of the same order of magnitude as the volumetric accuracy at its best.

4. ANALYSIS OF MIXTURE 1

According to the pressures observed in preparing this mixture, its composition was calculated to be:

	(%, *by volume; or mole %, assuming ideality*)
C_2H_4O	9.59 ±0.03
CO_2	90.15 ±.03
Air	0.26 ±.03

Correcting these for the amount of inert found in the C_2H_4O and CO_2:

C_2H_4O	9.57 ±0.03
CO_2	90.12 ±.03
Inert	0.31 ±.03

TABLE 1.—*Analyses of mixture 1*

Amount of reagent	Desiccant	Analysis number	Percentage, by volume Δ=deviation from average					
			C_2H_4O	Δ	CO_2	Δ	Inert	Δ
ml		1	9.91	0.05	89.91	0.12	0.19	0.07
2.0	$Mg(ClO_4)_2$	2	9.81	.05	89.98	.05	.22	.10
		3	9.84	.02	90.14	.11	.02	.10
		4	9.87	.01	90.07	.04	.06	.06
Average			9.86	±0.03	90.03	±0.08	0.12	±0.08
		5	9.66	0.04	90.08	0.08	0.27	0.04
0.3	$Mg(ClO_4)_2$	6	9.58	.04	90.12	.04	.30	.07
		7	9.63	.01	90.16	.00	.22	.01
		8	9.61	.01	90.27	.11	.12	.11
Average			9.62	±0.03	90.16	±0.06	0.23	±0.06
		9	9.55	0.04	90.17	0.02	0.28	0.02
0.3	$CaCl_2$	10	9.57	.02	90.20	.05	.24	.02
		11	9.60	.01	90.09	.06	.32	.06
		12	9.64	.05	90.15	.00	.20	.06
Average			9.59	±0.03	90.15	±0.03	0.26	±0.04
		13	9.73	0.06	89.99	0.17	0.28	0.11
0.3	P_2O_5	14	9.75	.08	90.15	.01	.09	.08
		15	9.64	.03	90.11	.05	.24	.07
		16	9.56	.11	90.39	.23	.05	.12
Average			9.67	±0.07	90.16	±0.12	0.17	±0.10
Average 5 to 16, incl.			9.63	±0.05	90.16	±0.07	0.22	±0.07
		17	17.3					
0.3	$CaSO_4$	18	16.6	(*)	(*)	(*)	(*)	(*)
		19	17.7					

* Not determined.

The analyses of this mixture are given in table 1. Determinations 5 to 16, inclusive, made with 0.3 ml of reagent and with three different desiccants, give the following average composition:

	(%, *by volume, as observed*)
C_2H_4O	9.63 ±0.05
CO_2	90.16 ±.07
Inert	0.22 ±.07

This agreement is closer than was to be expected.

A study of the data noted in table 1 discloses the following facts:

1. The value for C_2H_4O is apparently 0.2 percent too high, and that

for CO_2 correspondingly too low, if 2 ml of the H_2SO_4 reagent is used instead of 0.3 ml. (Compare the average of determinations 1 to 4 with the average of 5 to 8.) This illustrates the effect of the solubility of CO_2 in the aqueous reagent, and the importance of reducing the volume of the reagent to a working minimum.

2. The results obtained when the desiccants $Mg(ClO_4)_2$, $CaCl_2$ and P_2O_5 are used are concordant, since no significant differences occur between the averages for the determinations 5 to 8, 9 to 12, and 13 to 16, inclusive. When $CaSO_4$ is employed, the results are aberrant. (Note determinations 17 to 19.)

3. The reproducibility attained is adequate.

5. ANALYSIS OF MIXTURE 2

The analysis of this mixture was a slightly more extended effort than that of the first one. According to the pressures observed when preparing the mixture, the composition (corrected for inert found in C_2H_4O and CO_2) was as follows:

	%, by volume
C_2H_4O	9.97 ±0.03
CO_2	89.98 ± .03
Inert	0.05 ± .03

The average of 28 determinations reported in table 2 shows the composition of this mixture to have been:

	%, by volume
C_2H_4O	9.93 ±0.04
CO_2	90.02 ± .05
Inert	0.05 ± .04

TABLE 2.—*Analuses of mixture 2*

Desiccant	Analysis number	Percentage, by volume Δ=deviation from average						
		C_2H_4O	Δ	CO_2	Δ	Inert	Δ	Total
$CaCl_2$	1	9.96	0.03	89.84	0.15	0.20	0.12	100.00
	2	9.86	.07	90.01	.02	.12	.04	99.99
	3	9.82	.11	90.08	.09	.09	.01	99.99
	4	9.93	.00	89.99	.00	.08	.00	100.00
	5	10.08	.15	89.92	.07	.00	.08	100.00
	6	9.91	.02	90.07	.08	.02	.06	99.99
	7	9.83	.10	90.02	.03	.15	.07	100.00
	8	9.98	.05	89.99	.00	.04	.04	100.01
	9	9.98	.05	89.88	.11	.13	.05	99.99
	10	9.91	.02	90.02	.03	.07	.01	100.00
	11	9.93	.00	90.05	.06	.02	.06	100.00
	12	9.95	.02	90.00	.01	.05	.03	100.00
Average		9.93	±0.05	89.99	±0.05	0.08	±0.05	
$CaCl_2+P_2O_5$	13	9.93	0.01	90.01	0.04	0.06	0.03	100.00
	14	9.99	.07	89.95	.10	.06	.03	100.00
	15	9.90	.02	90.06	.01	.04	.01	100.00
	16	9.92	.00	90.05	.00	.03	.00	100.00
	17	9.85	.07	90.15	.10	.00	.03	100.00
	18	9.95	.03	90.05	.00	.00	.03	100.00
Average		9.92	±0.03	90.05	±0.04	0.03	±0.02	

TABLE 2.—*Analyses of mixture 2*—Continued

Desiccant	Analysis number	Percentage, by volume Δ=deviation from average						
		C_2H_4O	Δ	CO_2	Δ	Inert	Δ	Total
	19	10.01	0.07	89.99	0.06	0.00	0.02	100.00
	20	9.99	.05	90.01	.04	.00	.02	100.00
	21	9.93	.01	90.05	.00	.02	.00	100.00
	22	9.97	.03	90.03	.01	.00	.02	100.00
	23	9.96	.02	90.04	.01	.00	.02	100.00
P_2O_5								
	24	9.91	.03	90.07	.02	.02	.00	100.00
	25	9.83	.11	90.17	.12	.00	.02	100.00
	26	9.90	.04	90.10	.05	.00	.02	100.00
	27	9.93	.01	90.03	.02	.04	.02	100.00
	28	9.95	.01	89.97	.08	.08	.06	100.00
Average		9.94	±0.04	90.05	±0.04	0.02	±0.02	
Average of all analyses		9.93	±0.04	90.02	±0.05	0.05	±0.04	

The agreement in this case is about as close as before.

For the convenience of study, the data in table 2 include the deviation of each analysis from the average, the average and the average deviation of each of the three groups of analyses, and the total averages and deviations for the entire series. A study of these data gives the following information:

1. So far as the C_2H_4O is concerned, P_2O_5, $CaCl_2$, and a mixture of the two serving as the desiccant are equally good.

2. The CO_2 tends to be slightly lower when $CaCl_2$ alone is employed. However, the difference between the amount obtained when using this desiccant, and the amounts obtained when using P_2O_5 or $P_2O_5+CaCl_2$ is a matter of no concern.

3. The results on the whole are concordant, and the reproducibility attained should satisfy the general need (±0.05 percent). The maximum deviation noted was 0.15 percent, which should serve to indicate the desirability of check determinations.

It may be noted that the remarkable totals obtained (last column) have little significance other than to testify to the fact that no measurable amount of air leaked out of the apparatus during the analysis

V. ACCURACY OF THE METHOD

1. PRESSURE-VOLUME CONSIDERATIONS

So far we have made mention of reproducibility only. This is as far as the gas analyst has usually found it convenient to go. Reproducibility, often under the pseudonym of precision, has long masqueraded under the cloak of accuracy. It is a demonstrable entity, and can be captured by anyone with sufficient patience. Accuracy is not so easily demonstrated. This is unfortunately true in the present instance.

If two gases of known and satisfactory purity, which deviate by no significant amount from the formulas laid down for ideal gases either separately or mixed, had been mixed according to the pressure method employed in preparing the samples previously analyzed, then, indeed, a definite figure for the accuracy of this method could be expressed.

But these two gases, C_2H_4O and CO_2, are known to deviate from ideality as separate gases, and the extent of the deviation of C_2H_4O has not been measured. Worse yet, their behavior when together, and when mixed with air, has not been reported. It seems unreasonable to suppose that these two, noticeably imperfect with respect to Boyle's law *as individuals*, would strictly observe only *one* of the perfect gas laws when brought together. Thus it seems scarcely consistent to assume deviations from Boyle's law and ignore deviations from the unnamed laws of additive volumes—an assumption that has already served as the thesis in the development of some impressive formulas for correcting gasometric analyses.[13]

It will be worth while to show experimentally the behavior of these two gases when mixed, in order to illustrate the danger of making the above assumption.

C_2H_4O will vary from Boyle's law considerably more than will CO_2. For this reason, the samples were prepared by measuring C_2H_4O at a low pressure, in which state it could be expected to more nearly behave itself. Even so, it would not be safe to compute the gravimetric composition of this mixture from such pressure data. Reflection over the following data will serve to support this feeling in the matter.

Suppose 40 ml of dry air is measured in the burette of the apparatus used for these analyses. If it is then stored, and 40 ml of dry CO_2 is measured at the same temperature and pressure—and if, now, the 40 ml of air is returned to mix with the 40 ml of CO_2, what would the volume be? This experiment was performed, and the resulting volume (average of 10 determinations) was 80.06 ($\pm$0.02) ml. Next, 40 ml of air and 40 ml of C_2H_4O, measured separately as before, were mixed; the resulting volume (average of 10 determinations) was 80.37 ($\pm$0.04) ml. Now, 40 ml of CO_2 and 40 ml of C_2H_4O were measured separately, and mixed. If a law of ideal mixing prevailed, the expected volume would be 80.00 ml. On the other hand, it might be inferred from the above data that the combined volumes of these two gases would be either 80.43 or 80.21, depending on the particular assumption invoked. But the average of 10 determinations was 80.13 ($\pm$0.01) ml. (40 ml of air+40 ml of air were measured as above to check burette calibration and reproducibility.) It is true these measurements are not sufficiently accurate to justify formulation of equations defining the exact behavior on mixing; but the order of magnitude of the differences is certainly quite significant. The results are convincing enough evidence that the volume relationships on mixing in this gas analysis (and in others) should be investigated. Without such investigation, it is impossible to say whether or not such behavior on the part of gas mixtures will cause significant error.

To get a clearer picture of the pressure-volume relationships existing during this analysis, consider the volumes actually observed. These are (average values):

[13] Dalton's law, apparently an extension of the law of Henry, has been interpreted in modern textbooks as meaning that the total pressure of a mixture of gases is equal to the sum of the partial pressures of the components. The gases are, therefore, still thought of individually, and one is considered to have no physical effect on the others. This concept has been extended in some texts, and in the minds of many experimenters, to be the practical equivalent of the statement that the total volume of a mixture of gases is equal to the sum of the volumes of the components measured separately, and, of course, at the same temperature and pressure. The latter statement must necessarily involve Boyle's law, and, in the absence of a formal sponsor, it is difficult to name any law of additive volumes. The point so far not taken into account by gas analysts is that mixed gases may not behave as individuals. Thus, if two gases are each measured separately at the same temperature and pressure, the sum of their volumes may not be equal to the total volume of the mixed gases (measured at the same temperature and pressure); and the deviation from this sum may be significantly different from the deviation that might be expected from the law of Boyle alone.

1. The sample is composed of 54 ml of CO_2+6 ml of $C_2H_4O=V_1$.
2. 24 ml of air, measured separately from V_1, and used as an inert transfer gas$=V_2$.
3. 54 ml of CO_2+24 ml of air, the residue after absorption of $C_2H_4O=V_3$.
4. 24 ml of air, the residue after absorption of $CO_2=V_4$.

The analysis is computed:

$$\frac{V_1+V_2-V_3}{V_1}=C_2H_4O;\ \frac{V_3-V_4}{V_1}=CO_2.$$

Of these volumes, V_2 and V_4 are definite; but V_1 and V_3 must be evaluated, since they cannot be arrived at by simple arithmetic.

In order to evaluate V_1 and V_3, the following measurements were made:

1. 54 ml of CO_2 and 6 ml of C_2H_4O were measured separately and when mixed, both gases being dry and at the same condition of temperature and pressure (approx. 1 atm, 25° C). The average of 10 determinations gave this result:

54 ml of CO_2+6 ml of $C_2H_4O=60.07\ \pm0.03$ ml$=V_1$, above.

2. The above measurement was verified by 10 determinations of 54 ml of air+6 ml of air, which served to check the burette calibration and manipulation.
3. 54 ml of CO_2+24 ml of air, measured separately and mixed as before, gave as the average of 10 determinations:

54 ml of CO_2+24 ml of air$=78.04\ \pm0.02$ ml$=V_3$, above.

4. The above measurement was verified by 10 determinations of 54 ml of air+24 ml of air, to check the burette calibration and the manipulation.
5. The measurements made above were further authenticated by passing measured volumes of C_2H_4O and of CO_2 from the burette to the storage reservoir and back, without significant gain or loss of volume.

These evaluations of V_1 and V_3 at once disclose deviations whose order of magnitude (0.1 percent) could produce significant error. But fortunately in this particular instance the computation partially cancels the effect of deviation from ideality. Thus, the deviations, if taken into account, would increase the C_2H_4O by only 0.05 percent and the CO_2 by 0.07 percent.

2. GRAVIMETRIC DETERMINATION OF ACCURACY

While the above measurements give assurance that the accuracy of the method probably is commensurate with the reproducibility obtained, a definite experimental check is in order. The accuracy was, therefore, determined by preparing several mixtures of $C_2H_4O+CO_2$ ranging in composition from about 7 to 12 percent of C_2H_4O. These mixtures were made up as before by measurement of pressure at fixed volume and temperature, but at the same time the composition was determined gravimetrically, and by the analytical method here reported.

(a) APPARATUS

The apparatus employed is shown in figure 3. It comprises a 5-liter flask, *C*, to which is attached a barometric manometer, *B*. A small brass cylinder, *A*, fitted with a needle valve of the vacuum type, connects to *C* through an interchangeable ground joint. An auxiliary flask, *E*, may be attached at the same joint and serves as a sample pipette. The flask and connections may be evacuated by a pump through cock 1, and supplied with C_2H_4O and CO_2 through the two inlets of cock 4.

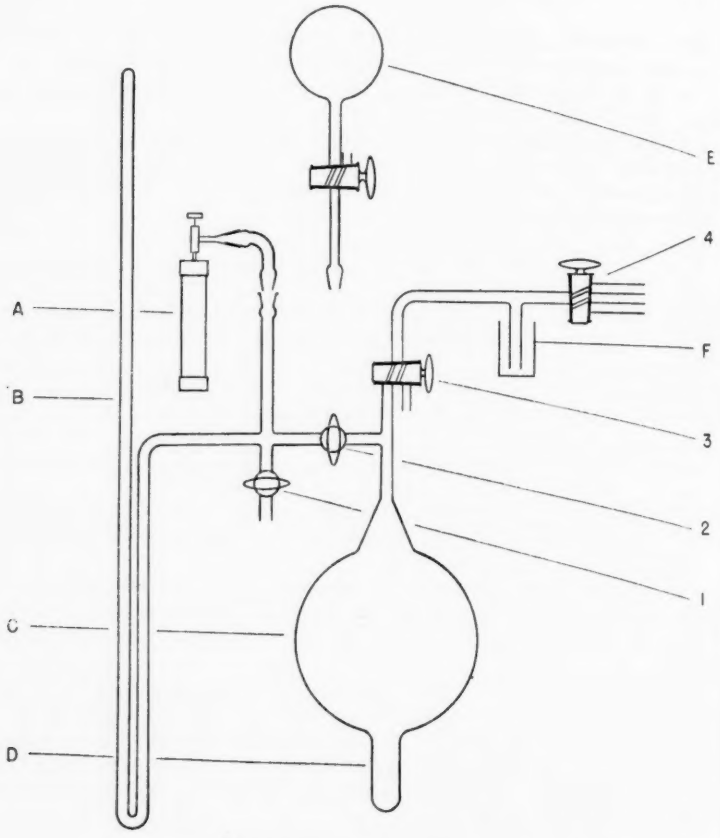

FIGURE 3.—*Apparatus for preparing known mixtures.*

(b) PROCEDURE

The procedure is as follows: Flask, connections, and cylinder *A* are thoroughly dried and evacuated. The manometer is read, *A* and 2 are closed, *A* is removed, weighed, replaced, and the connections evacuated. Cock 1 is then closed and 2 opened. C_2H_4O is allowed to purge through the atmospheric outlet of cock 3 and the safety seal, *F*, immersed in mercury, and then slowly admitted to the flask maintaining excess flow at *F*. Cock 3 is closed when the desired pressure is

attained, *A* is immersed in liquid air, its valve opened, and the C_2H_4O condensed therein. The pressure is observed, the valve closed, liquid air placed around the tube, *D*, at the bottom of the flask, and the pressure again observed. C_2H_4O and CO_2 will condense to negligible pressures at −190° C; but very small traces of air in these gases will prevent their complete transfer to *A* within reasonable time, by accumulating at the opening of the needle valve, and offering a plug of uncondensed gas through which the final small portions of C_2H_4O and CO_2 must diffuse slowly. Most of the gas condensed rapidly in *A*, but the final traces were transferred slowly. Rather than wait for the tardy diffusion to occur, a gravimetric correction was made for 0.2- to 4-mm residual pressure. Actually, this introduced the greatest uncertainty in the measurements, and would be avoided in more exacting work. Cock 2 and *A* are both closed, and *A* is removed and weighed. Repeated weighings were made to insure reproducible temperature and humidity conditions, and against leakage of valve.

After weighing cylinder *A* it is replaced, the connections are evacuated, and the C_2H_4O is condensed in *D*. A is closed, and the C_2H_4O is allowed to evaporate in *C*. The pressure and temperature are observed. CO_2 is now purged through 3 and the desired amount is then admitted into *C*. The pressure and temperature are observed. The two pressure observations from which the composition is calculated are thus made within a relatively short interval of time, and temperature conditions remain comparable. The $C_2H_4O+CO_2$ is then condensed into *A* at −190° C. The pressure is observed, *A* is closed, *D* is immersed in liquid air, and the pressure is again observed. Cock 2 is closed, and *A* is removed and weighed.

A is then replaced, the connections are evacuated, and the mixture is condensed in *D*. Cock 2 is closed, the mixture is allowed to evaporate and is stirred by thermal convection, *E* replaces *A*, the connections are evacuated, and a sample taken into *E* from *C* for analysis.

(c) RESULTS

The results of the determinations made with this apparatus and in this manner are given in table 3. Five mixtures were investigated, since some differences might be expected because of the different pressure-volume relationships existing. The mixtures were made up at different temperatures (26° to 30° C), and analyzed at different temperatures (25° to 31° C), so that any probable effect of temperature is accounted for in the data. The range studied covers what may be expected in commercial use.

TABLE 3.—*Comparison of the composition of five mixtures of* $C_2H_4O+CO_2$ *as determined by three methods:*

M=Amount of C_2H_4O, expressed as mole percent calculated from observed gravimetric data:

$$\frac{100\ N_{C_2H_4O}}{\text{Total } N}$$

P=Amount of C_2H_4O calculated from observed pressures:

$$\frac{100\ P_{C_2H_4O}}{\text{Total } P}$$

V=Amount of C_2H_4O, expressed as percent by volume as determined from gasometric analysis:

$$\frac{100\ V_{C_2H_4O}}{\text{Total } V}$$

If the ideal gas laws were obeyed, these three would all be expressions of mole percent, and would agree within the limits of error of the observations, assuming the reaction involved in the data V were quantitative.

Mixture number	Percentage of C_2H_4O			Percentage of C_2H_4O	
	M[a]	P	V	$M-P$	$M-V$
1	7.01	7.06	7.00	−0.04	+0.02
2	8.71	8.78	8.67	−.07	+.04
3	9.92	9.97	9.77	−.05	+.15
4	11.14	11.18	11.07	−.04	+.07
5	12.13	12.13	12.14	0	−.01
Algebraic averages				−0.04	+0.05

[a] Within the significance of the present work, these values may be taken directly as an expression of percentage by weight, since the molecular weights of the two gases are very nearly the same.

The data given show the differences existing between the composition, expressed as percentages of ethylene oxide, as determined (M) gravimetrically according to the method just described, (P) by the measurement of pressure at fixed volume, and (V) by actual gasometric analysis, according to the method described in this paper.

A glance at these data discloses the following facts:

1. The amount of C_2H_4O, as determined by observed pressures, is in general about 0.04 percent higher than that measured gravimetrically.

2. The amount of C_2H_4O as measured by the gasometric analysis, is in general about 0.05 percent lower than that measured gravimetrically.

3. The accuracy attained by the gasometric analytical method, in the range of compositions investigated, is commensurate with the reproducibility of the method. The average deviations observed over the range of composition investigated may be applied as corrections of the gasometric results (if desired) in computing mole percent or percent by weight.

VI. NOTE ON SAMPLING

The fumigant is usually obtained as a mixture of liquid C_2H_4O and CO_2 under pressure in a cylinder. Some cylinders are equipped with a connection leading from the valve to the bottom, so that the contents may be discharged from the liquid rather than the gas phase. Even so, one must not expect to open the cylinder valve slowly and draw off

a sample of gas whose composition approaches that of the liquid within the cylinder. The two gases have widely different boiling points, and will separate notably by distillation when vapor is drawn slowly from the cylinder; and vapor will be drawn from the cylinder if the seat of the valve is warm enough to vaporize CO_2. This vapor will push back liquid trying to escape, and so the C_2H_4O will be effectively separated from the mixture.

The tendency of liquified mixtures to separate under such conditions has long been known and has been studied experimentally. An interesting example of such behavior was observed during the gravimetric preparation of the mixtures here reported. After weighing one of these mixtures, the cylinder containing the liquid (at room temperature) was connected to the evacuated flask, the valve was opened, and the mixture allowed to vaporize into the flask. The pressure within the flask built up *immediately* to 10 to 20 mm in excess of the pressure of the CO_2 alone. Thereafter, the pressure increased *very slowly* to equal that originally observed for the mixture of $C_2H_4O+CO_2$.

The only recourse is an extremely rapid discharge of the cylinder (with valve opened wide) into a long pipe of sufficient diameter so that back pressure or cooling does not cause condensation. Samples may be taken from this discharge tube. Better yet, if the cylinder is discharged completely into a large dry evacuated container used for fumigating, samples from this may be treated with more confidence.

It is also necessary to take the sample in dry containers; and rubber tubing should not be used.

WASHINGTON, July 27, 1938.

118273—39——5

U. S. DEPARTMENT OF COMMERCE NATIONAL BUREAU OF STANDARDS

RESEARCH PAPER RP1176

Part of Journal of Research of the National Bureau of Standards, Volume 22, February 1939

ELASTIC PROPERTIES OF CAST IRON

By Alexander I. Krynitsky and Charles M. Saeger, Jr.

ABSTRACT

An optical method for measuring the deflection of cast-iron transverse-test bars during loading and up to the breaking strength has been developed. Transverse-strength properties were determined on test bars made from three types of cast iron heated to the maximum temperatures of 1,400°, 1,500°, 1,600°, and 1,700° C. Test bars were vertically cast bottom-poured in green-sand molds at 100°, 150°, 200°, and 250° C above the liquidus temperature. Total, plastic, and elastic deflection; modulus of rupture; modulus of relative elasticity; and total, plastic, and elastic resilience were determined and the microstructure of the test bars was examined.

CONTENTS

	Page
I. Introduction	191
II. Method of measuring deflection	192
III. Materials and preparation of test bars	193
IV. Testing procedure	194
V. Physical properties of test bars	195
1. Modulus of rupture	195
2. Plastic, elastic, and total deflection	196
3. Relative modulus of elasticity	198
4. Resilience	199
VI. Effect of maximum heating temperature on composition and structure	202
VII. Unusual structural features in cast iron	204
VIII. Summary	206
IX. References	207

I. INTRODUCTION

The term "elastic properties" as used in this discussion connotes those complex properties that determine the behavior of cast iron under load. They may be determined from the results of transverse bending tests.

All of the properties of cast iron are related to and, to a large extent, determined by the structure, which consists of a coherent metallic matrix throughout which particles of graphite are dispersed. The presence of these particles decreases the amount of metallic material available to resist stressing in a given section and causes nonuniform distribution of stresses, but the quantitative interpretation of these effects is as yet unsettled. In the consideration of the behavior of cast iron in compression, the question whether the spaces occupied by the graphite particles should be considered as voids or as spaces filled with compressible, partly compressible, or incompressible material,

has been discussed by several authors, for example, MacKenzie [1],[1] Thum and Ude [2], Meyersberg [2a], Pearce [3], and Bolton [4]. Aside from the general weakening or depreciation of properties, because of the presence of the relatively soft graphite flakes, the nonhomogeneous structure frequently leads to erratic results in determinations of the properties and renders their interpretation uncertain. Such factors as the composition, shape, size, and surface condition of the specimen, and the details of the testing procedure are of greater importance in determining the properties of cast iron than in similar determinations on other metals, steel, for example.

The determination of the elastic properties of cast iron is further complicated by the fact that even moderate stresses produce plastic as well as elastic deformation in this material. Attention was called to this fact approximately 50 years ago, by de Segundo [5] and by Bach [6]. The observations of these early investigators have been confirmed by subsequent workers, and it had been definitely established that plastic deformation of cast iron begins under low loads. In the determination of elastic properties by means of transverse tests it is necessary, therefore, to define complete stress-deflection curves by means of step-wise loading, and to determine for each load not only the total deflection under load but also the plastic deformation or permanent set that remains in the bar after the load has been removed. The difference between the total and the plastic deformation is the elastic deformation.

Interpretation of the results of transverse tests and of the data computed from these results, for example, modulus of elasticity, resilience, et cetera, in terms of properties such as brittleness, toughness, ductility, and energy required to break a bar has been widely discussed but the correlations have not been entirely satisfactory partly because of the difficulties of conducting transverse tests, with resultant uncertainty regarding the accuracy and reliability of the data obtained.

Preliminary results of this investigation, presented in a previous publication [7], showed that various properties, including the transverse strength and running quality during casting as well as the size and distribution of the graphite flakes in each of the irons used, were affected by the maximum temperature to which the liquid metal had been heated. Computations of the modulus of elasticity were made, based on the data obtained under loads of 1,200 pounds and also under the loads that caused rupture. These results clearly showed the need for a more detailed and systematic study of the stress-strain relations in cast iron. For the present investigation, it was decided to prepare test bars from each of several irons, representing different maximum heating and pouring temperatures, and to record, as accurately as possible, the complete stress-strain curves up to the breaking point of each bar, by means of observations of the successive deflections under increasing loads and the permanent set that accompanied the application of each load.

II. METHOD OF MEASURING DEFLECTION

One of the first requirements for the proposed investigation was an improved method of measuring the deflection of the bar under load

[1] Figures in brackets indicate the literature references at the end of this paper.

and the permanent set in the bar after the load was removed. Direct observation of the changing position in space of a reference mark on the bar is unsatisfactory because it involves a number of assumptions, for example, the supports and the testing machine as a whole must remain immovable and there must be no penetration of the supports into the specimen. To avoid these possibilities of error a new method of measuring deflection was devised, as follows:

In this new method of measuring deflection of bars under transverse loading, a rubber band, *B*, is stretched tightly along the length of the bar, *A*, and is held in position by two clamps, *C*, as shown in figure 1. Metal strips on the inner surface of the clamps keep the rubber band near to, but not in contact with the surface of the bar at all times. The spacing between the two clamps is the same as that between the supports for the bar in the testing machine, 18 inches in these experiments. Reference mark *D* is attached directly to the bar, midway between the clamps. The bar is placed in the testing machine and the micrometer telescope, *E*, mounted at a distance of 20 inches from the bar, is used to measure the distance between the lower edge of the rubber band and the top edge of the reference mark. When the bar deflects under load, the reference mark moves away from the rubber band which remains as a straight line connecting the central portions of the bar at the two supports. The distance between the rubber band and the reference mark therefore indicates the deflection of the loaded bar and a similar measurement after the load is removed indicates the permanent set. With this apparatus, the maximum error in reading deflections, including errors in the micrometer telescope and personal errors of the observer, was found to be less than ±0.002 inch.

The principal advantage of this simple method of measuring deflections is that the readings are made entirely independently of the testing machine and supporting fixtures. A further advantage is that observations can be continued up to and including the breaking load without danger to sensitive optical apparatus or to delicate instruments such as extensometers.

III. MATERIALS AND PREPARATION OF TEST BARS

Three types of iron, of the compositions shown in table 1, were used in this investigation. Iron *A* is a stove-plate pig iron remelted with the addition of 10 percent of open-hearth ingot iron. Iron *B* approximates the composition of a medium cylinder iron, although the carbon is slightly high and the phosphorus is somewhat low. Iron *C* represents a soft iron such as is used for general castings.

TABLE 1.—*Composition of stock pig irons*

Iron	Total carbon	Silicon	Manganese	Phosphorus	Sulfur
	Percent	*Percent*	*Percent*	*Percent*	*Percent*
A	3.44	1.40	0.15	0.46	0.020
B	3.79	1.40	.63	.181	.062
C	3.44	2.43	.77	.395	.050

Cylindrical bars for the transverse tests were cast in groups of four, as shown in figure 2. The pattern was molded in a three-part cylindrical flask with the full length of the test bars contained in the cheek. Each flask contained two groups, that is, eight bars. The patterns were molded in a mixture of eight parts of molding sand and one part of sea coal, tempered to approximately 7 percent of moisture. The mold cavities were faced with nongraphitic carbonaceous material [2] of commercial origin. The castings were bottom poured with the bars occupying vertical positions in the mold. By this procedure, as described in a previous publication [8], test bars can be produced which are satisfactorily uniform in diameter throughout their length and free from burnt-on sand or other surface defects. The cylindrical section of each bar was 21 inches in length and 1.2 inches in diameter.

Charges of 230 pounds of iron, in a commercial magnesia crucible, were melted in a high-frequency induction furnace of the tilting type. Each melt was heated to a predetermined maximum temperature of 1,400°, 1,500°, 1,600°, or 1,700° C and was maintained at this temperature for approximately 1 minute. The metal was then allowed to cool until the temperature was 250° C above the liquidus temperature [3] of the iron used in that particular melt. A set of four bars was then cast as a unit by pouring the metal directly from the tilted furnace into the mold. The metal remaining in the crucible was allowed to cool to the next pouring temperature, 200° C above the liquidus, and another set of four bars was cast. By continuing this procedure, a set of four bars was cast at 150° C above the liquidus, and a final set at 100° C above the liquidus. Sixteen test bars, representing four pouring temperatures, could be thus obtained from a 230-pound melt that had been heated to a definite maximum temperature. The bars were allowed to remain in the molds for at least 18 hours after casting.

Temperature measurements of the molten iron up to 1,600° C were made with a platinum–platinum 10-percent rhodium thermocouple that was protected by a closed-end, glazed porcelain tube inserted in a closed-end graphite tube. The portion of the graphite tube that came in contact with the molten iron was protected by a coating of aluminum oxide covered with a mixture of 95 percent of zirconium silicate and 5 percent of bentonite.

Temperatures above 1,600° C were measured with an optical pyrometer which had been previously calibrated with the thermocouple in the temperature range of 1,400 to 1,600° C.

IV. TESTING PROCEDURE

A universal testing machine of the hydraulic type of 50,000 pounds capacity was used for the transverse tests. The rate of loading of all bars corresponded to 0.12 inch per minute travel of the free cross head of the testing machine.

The test bar, equipped with the rubber band and reference mark, as shown in figure 1, was mounted in the testing machine on two supports of the roller type, at a span of 18 inches. The bar was adjusted until the rubber band lay in the horizontal plane of the neutral axis of the bar. A load of 50 pounds was sufficient to seat the bar firmly but was not enough to produce noticeable plastic deflection, was ap-

[2] Approximate analysis: 4 percent of volatile; 74 percent of fixed carbon; 22 percent of ash.
[3] The liquidus temperature of each iron was estimated from its composition, according to the procedure described in a previous publication [7].

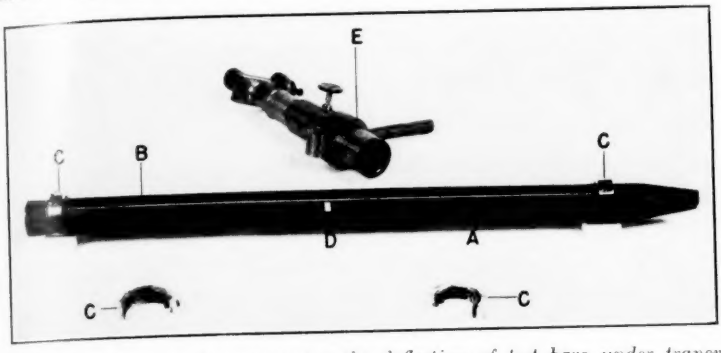

FIGURE 1.—*Apparatus for measuring the deflection of test bars under transverse loading.*

A, cast-iron test bar; *B*, rubber band; *C*, clamps; *D*, reference mark; and *E*, micrometer telescope.

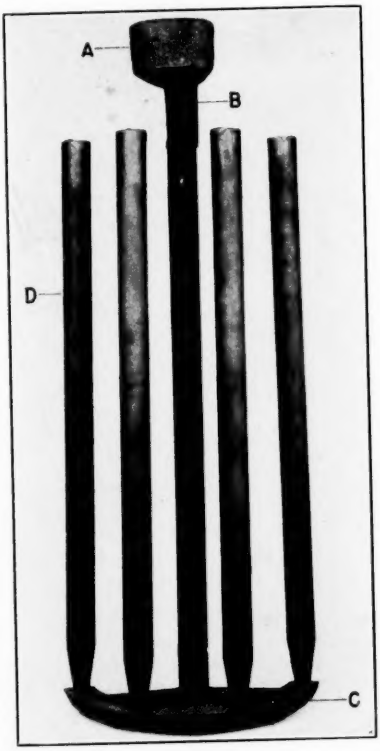

FIGURE 2.—*Transverse test bars, as cast.*

A, pouring basin; *B*, down gate; *C*, semicircular feeder for bottom pouring; and *D*, vertically cast bars.

plied and the distance between the edge of the rubber band and the top of the reference mark was determined as a zero reading. The bar was then loaded in a series of steps (100 or 200 pounds each) until the breaking load was reached and the deflection of the bar under each of the loads was recorded. After the load reached 800 or 1,000 pounds, each application of a load was followed by unloading to the original 50-pound load, and the permanent set in the unloaded bar was determined. Attempts to record the small permanent deformations that resulted from loads of less than 800 or 1,000 pounds were seldom made. Unloading the bars did not affect the deflection under subsequent loads; the breaking loads and the load-deflection curves of duplicate bars were practically identical when one of the bars was loaded in the manner just described and the other was progressively loaded without unloading between successive loads.

V. PHYSICAL PROPERTIES OF TEST BARS

The results of the transverse tests yielded information on the following properties of the cast iron bars: Modulus of rupture; plastic, elastic, and total deflection; relative modulus of elasticity; and resilience.

1. MODULUS OF RUPTURE

The modulus of rupture of each bar was calculated, according to the formula

$$M=\frac{2.546LS}{D^3},$$

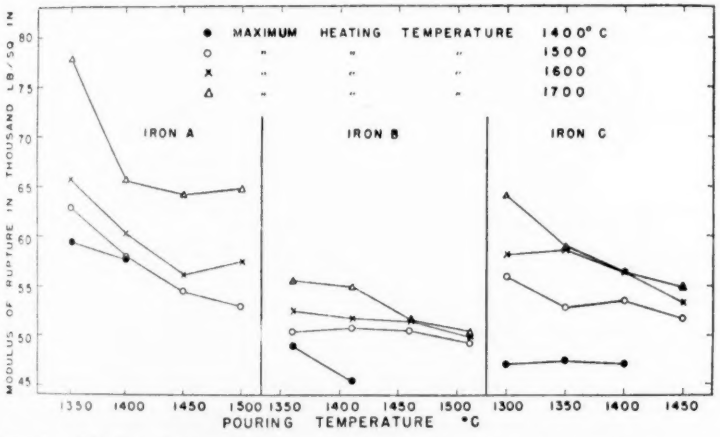

FIGURE 3.—*Effect of maximum heating temperature and pouring temperature on the modulus of rupture of three irons.*

where M is the modulus for round bars; L, the span of the bar between supports; S, the breaking load; and D, the diameter of the bar.

The modulus of rupture for each of the three irons and the effect on the modulus of varying the maximum heating and pouring temperatures are shown in figure 3. Each of the plotted points is an average of values derived from four companion bars.

The modulus of rupture of iron *A* was found to be considerably higher than that of either of the others; and that of iron *B* to be the lowest of the three. For all of the irons the modulus increased with an increase in the maximum heating temperature and tended to decrease with an increase in pouring temperature, the latter effect being more pronounced for iron *A* than for *B* and *C*.

2. PLASTIC, ELASTIC, AND TOTAL DEFLECTION

The total and plastic deflections or "set" of each bar under increasing loads, were determined and the elastic deflection was taken

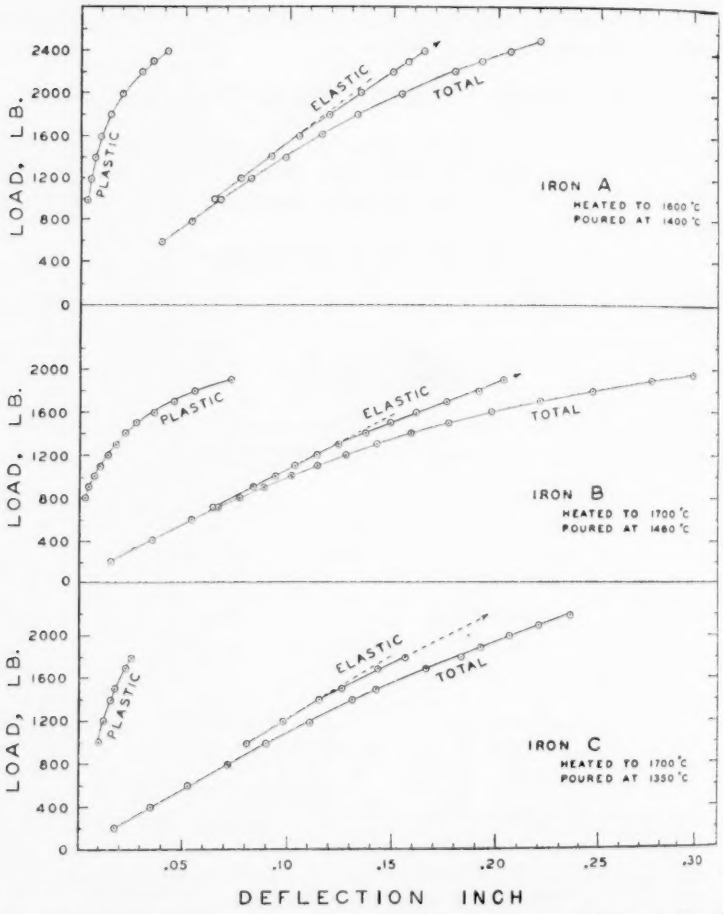

FIGURE 4.—*Typical plastic, elastic, and total deflection curves of irons A, B, and C.*

as the difference between the total and the plastic deflection for each load.

The relation between load and total, plastic, and elastic deflections of representative bars of irons *A*, *B*, and *C* is shown in figure 4. Iron *A* has the highest breaking strength of the three irons and has about

the same deflection at the breaking load as iron *C*. Iron *B* has about the same breaking load as iron *C* but considerably more deflection at rupture.

In all cases the total deflection curve is a continuous curve inclining progressively towards the deflection axis. If there is any linear portion in the total deflection curve it is confined to the region of very light loads. The curves for plastic deformation for loads of 800 pounds or more, likewise, are continuous curves without straight portions. These observations are in accord with those of previous investigators but the data for elastic deflection are not. Meyersberg [2a] concluded that the upper portions of the elastic elongation curves were slightly bent, whereas Pearce [3] found that the elastic deflection curve usually was a continuous straight line for all loads. The results of this study, illustrated in figure 4, show that the elastic deflection curve is linear only in its lower portion. For iron *A*, the linear portion extends to some load between 1,400 and 1,800 pounds for each of the bars. For irons *B* and *C* it extends to the range of loads from 1,200 to 1,400 pounds. Above the linear portion, each curve inclines toward the deflection axis.

The departure from linearity in these curves can be demonstrated mathematically by the method suggested by Tuckerman in the discussion of a paper by Templin [9]. Theoretical values for the elastic deflection for each load can be calculated from the equation for a straight line and from the modulus of elasticity of the bar at a load within the initial, straight portion of the curve. As long as the curve conforms to the equation for a straight line the observed and calculated values will be in agreement, within the limits of experimental error. Any systematic or appreciable divergence of the observed and calculated values indicates a deviation of the curve from the equation for a straight line.

TABLE 2.—*Observed and calculated elastic deflection for iron B*

Comparison of observed values for elastic deflection with values calculated from the relative modulus of elasticity, 12,445,000 lb/in.², of this bar under a load of 1,000 pounds.

Load	Elastic deflection		
	Observed	Calculated	Difference
Pounds	*Inches*	*Inches*	*Inches*
700	0.064	0.066	−0.002
800	.075	.075	.000
900	.083	.085	−.002
1,000	.094	.094	.000
1,100	.104	.104	.000
1,200	.115	.113	+.002
1,300	.124	.123	+.001
1,400	.137	.132	+.005
1,500	.150	.142	+.008
1,600	.161	.151	+.010
1,700	.176	.160	+.016
1,800	.192	.170	+.022
1,900	.204	.179	+.025

These computations were made for a number of the curves. The data in table 2 show the results obtained from a bar of iron *B* heated to a maximum temperature of 1,700° C and poured at 1,460° C. Loads were applied to this bar in increments of 100 pounds, to define

the curves more closely. It is evident that the observed and calculated values for elastic deflection are in agreement, within the limits of experimental error, ±0.002 percent, for loads of 1,300 pounds or less, but not for loads in excess of this figure. The elastic deflection curve of this bar, therefore, is a straight line only for loads of 1,300 pounds or less.

3. RELATIVE MODULUS OF ELASTICITY

In this investigation the term "relative modulus of elasticity" is used in place of "modulus of elasticity," because it is well known that cast iron does not follow Hooke's law exactly and the term "modulus of elasticity," as applied to cast iron, generally means the relative stiffness of the iron under the particular conditions of loading.

The relative modulus of elasticity, as determined in the transverse test for a single centrally applied load, is determined by the formula

$$E=\frac{Pl^3}{48ID},$$

where

E=relative modulus of elasticity in pounds per square inch,
P=load in pounds,
l=span in inches,
I=moment of inertia, and
D=deflection (at load P) in inches.

Values for D were taken from the elastic-deflection curves. In view of the fact that the elastic-deflection curve was found to be linear only in the lower portion, two values of the relative modulus of elasticity were computed for each bar; E_1 for the straight portion of the elastic-deflection curve, and E_2 for the second portion of the curve, at the point of rupture.

The data in table 3 show that the values for E_1 are consistently higher than for E_2. For irons A and B the difference between E_1 and E_2 is generally greater than 1,000,000 lb./in.^{2}; for iron C the difference is usually less than this figure.

Values for the relative modulus of elasticity, E_1, have been plotted in figure 5 to show the variations with different maximum and pouring temperatures. In general, values of E_1 for iron A are higher than those for either of the other irons and, under some conditions of heating and pouring, the values of E_1 for iron B are higher than those for iron C. A tendency for the values of E_1 to increase with an increase in maximum heating temperature is more evident in irons A and B than in iron C. The data for each iron show a slight and somewhat erratic tendency for the values of E_1 to decrease with increasing temperature of pouring.

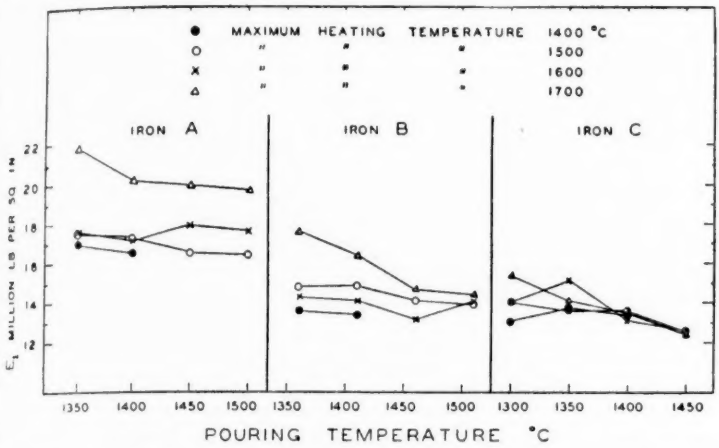

FIGURE 5.—*Effect of maximum heating and pouring temperature on the relative modulus of elasticity of cast iron.*

TABLE 3.—*Relative modulus of elasticity of cast iron*

Iron *A*				Iron *B*				Iron *C*			
Temperature		Relative modulus		Temperature		Relative modulus		Temperature		Relative modulus	
Maximum	Pouring	E_1	E_2	Maximum	Pouring	E_1	E_2	Maximum	Pouring	E_1	E_2
°C	°C	Million lb/in.²	Million lb/in.²	°C	°C	Million lb/in.²	Million lb/in.²	°C	°C	Million lb/in.²	Million lb/in.²
1,400	1,400	16.50	15.27	1,410	1,410	13.38	11.92	1,400	1,400	• 13.37	12.00
1,400	1,350	17.00	15.59	1,410	1,360	13.54	12.15	1,400	1,350	• 13.71	12.89
								1,400	1,300	• 13.08	12.31
1,500	1,500	16.40	15.14	1,510	1,510	13.85	12.51	1,500	1,450	• 12.58	11.69
1,500	1,450	16.51	15.75	1,510	1,460	14.09	12.63	1,500	1,400	• 13.57	12.33
1,500	1,400	17.27	16.35	1,510	1,410	14.84	13.47	1,500	1,350	• 13.58	13.01
1,500	1,350	17.49	16.46	1,510	1,360	14.79	13.08	1,500	1,300	• 13.97	13.01
1,600	1,500	17.57	16.73	1,600	1,510	14.07	12.30	1,600	1,450	• 12.55	11.67
1,600	1,450	17.89	17.04	1,600	1,460	13.13	12.40	1,600	1,400	• 13.17	12.34
1,600	1,400	17.17	16.08	1,600	1,410	14.07	12.80	1,600	1,350	• 15.10	14.09
1,600	1,350	17.56	16.21	1,600	1,360	• 14.22	12.95	1,600	1,300	• 13.97	13.50
1,700	1,500	19.65	18.60	1,700	1,510	• 14.39	13.01	1,700	1,450	• 12.42	11.64
1,700	1,450	19.95	18.46	1,700	1,460	• 14.64	13.17	1,700	1,400	• 13.48	12.41
1,700	1,400	20.17	18.95	1,700	1,410	16.34	14.47	1,700	1,350	• 14.10	13.20
1,700	1,350	21.82	19.73	1,700	1,360	17.55	15.63	1,700	1,300	• 15.36	14.69

• These data are average values of 2 bars. All other figures are averages of 4 bars.

4. RESILIENCE

The resilience of cast iron, the work absorbed by the specimen before rupture, is obtained by measuring the area below the deflection curve and between the origin and an ordinate to the deflection curve at the point of rupture. If the resilience of a specimen could be simply and adequately expressed there would be no need for discussion of "stiffness", "plasticity", "toughness", "brittleness", or similar indefinite but important properties of cast iron. These

values measure the total work but do not define the way in which it has been absorbed. It is necessary, therefore, to consider not only the area below the curve but also its shape, to determine whether a particular resilience value is the result of a high, low, or medium breaking strength coupled with high, low, or medium deflection. And, finally, a complete definition of resilience should differentiate between the work absorbed in elastic and in plastic deformation.

Measurements of the total resilience are best determined with a planimeter; determinations of the "triangular" resilience, based on the assumption that the total deflection curve is a straight line between the origin and the point of rupture, obviously only approximate the true resilience and the degree of approximation decreases as the curvature of the deflection curve increases.

Values of total resilience of the three irons, measured planimetrically, are shown in figure 6. The resilience values of irons *B* and *C* are

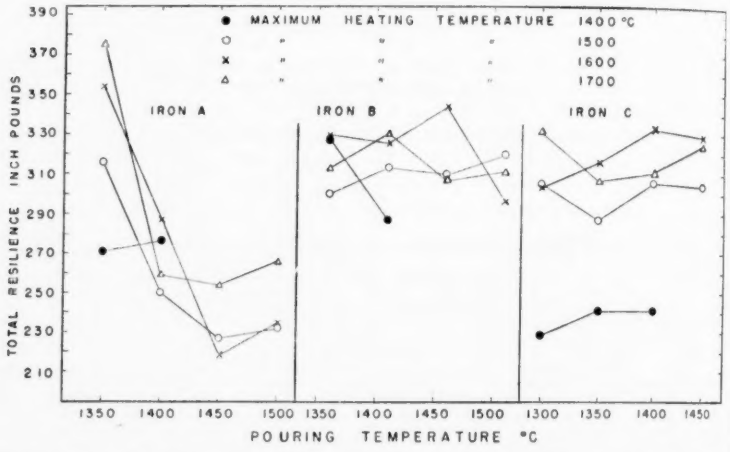

FIGURE 6.—*Effect of maximum heating and pouring temperatures on the total resilience of cast iron.*

similar. In neither case is there a definite relation to either the maximum heating temperature or the pouring temperature, except that very low resilience values were obtained from iron *C* that had been heated only to 1,400° C. The curves for iron *A* are quite different from those for irons *B* and *C*. For iron *A* there is a pronounced decrease in resilience with increasing pouring temperature, at least up to 1,450° C. An increase in resilience with increasing maximum heating temperature is evident in the bars that were poured at 1,350° C, but this effect is less evident at higher pouring temperatures. Iron *A* under some conditions of melting and pouring showed the highest resilience values of any of the three irons, but under other conditions of melting and pouring its resilience values were lower than any of those of irons *B* and *C*. These resilience values illustrate the marked effect on the characteristics of cast iron of an addition of 10 percent of ingot iron, as in iron *A*.

A number of attempts to establish more satisfactory criteria for evaluating the properties of cast iron have been made in recent years.

MacKenzie [10] found that there was a definite relation between the ratio of the true to the triangular resilience and the ratio of the secant modulus of elasticity at half load to the ultimate modulus of elasticity. These ratios were computed from the data in this investigation, by using values of E_1 for the secant modulus at half load and values of E_2 for the ultimate modulus, but no definite relation between the widely scattered plotted points could be established.

Attempts to correlate resilience values with the carbon and silicon contents also have been made. For example, MacKenzie [1] and Bolton [4] compared resilience values with those representing the carbon content, plus one-fourth of the silicon content. Values of C+Si/4, for irons *A*, *B*, and *C* were computed and were plotted against total resilience, as shown in figure 7. The plotted points for each iron are widely scattered, the spread of the resilience values being greater than that of the C+Si/4 values. However, there is some indication of an increase in total resilience with increasing values of C+Si/4, as is indicated in figure 7 by the two dotted lines that include the majority of the points for all three irons. A similar relation was found for plastic resilience values, but the elastic resilience tended to decrease with increasing values of C+Si/4. On the whole, it must be concluded that the relation between resilience and carbon-plus-silicon contents is not definite for these three irons.

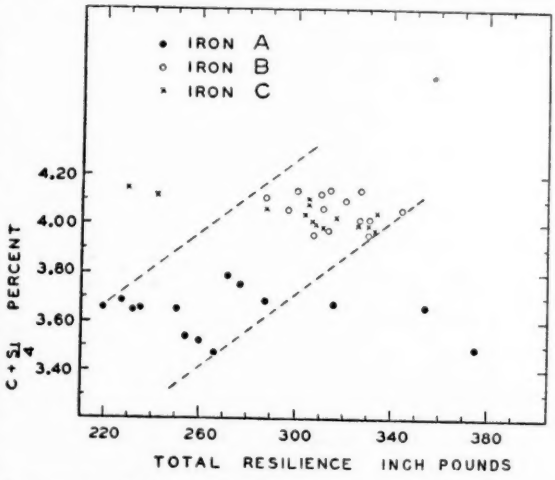

FIGURE 7.—*Relation of total resilience to carbon and silicon contents.*

Tucker [12] concluded that neither the breaking load, deflection, nor resilience values gave reliable indications of the resistance to thermal shock, but that the plastic resilience, expressed in percentage of the total resilience, furnished a measure of the relative toughness of the irons that he investigated. Such values of plastic resilience of the bars in the present investigation were obtained by subtracting from the total resilience the elastic resilience computed on the assumption that the elastic-deflection curve was a straight line between the origin and the breaking point. These values, expressed as percentage of the total resilience, are given in table 4. The data show that the plastic resilience values for each iron are slightly lowered when the maximum heating temperature is 1,600° or 1,700° C; the effect of varying the pouring temperature, after heating to a particular maximum temperature, is not definite.

According to the data in table 4, the ratio of plastic to total resilience (in percent) of iron *B* is definitely higher than that of either of

the other irons, with the values for iron *A* slightly lower than for iron *C*. According to Tucker's data this indicates that the medium cylinder iron *B* is definitely more resistant to thermal shock than either of the other two, and that the soft iron *C* is somewhat better than the high-strength iron *A* in this respect. It is interesting to note the grouping of the three irons classified in this way and according to the total resilience. On the basis of a comparison of the percentage plastic resilience, iron *B* is superior with irons *A* and *C* paired, whereas, if the comparison is based on the total resilience (fig. 6), irons *B* and *C* are quite similar and *A* is different. These results indicate the complexity of resilience determinations and the difficulty of their interpretation.

TABLE 4.—*Relation of plastic to total resilience of three irons*

Iron *A*			Iron *B*			Iron *C*		
Temperature		Ratio of plastic to total resilience	Temperature		Ratio of plastic to total resilience	Temperature		Ratio of plastic to total resilience
Maximum	Pouring		Maximum	Pouring		Maximum	Pouring	
°C	°C	%	°C	°C	%	°C	°C	%
1,400	1,400	32	1,410	1,410	46	1,400	1,400	34
1,400	1,350	28	1,410	1,360	49	1,400	1,350	*37
						1,400	1,300	*32
1,500	1,500	29	1,510	1,510	48			
1,500	1,450	29	1,510	1,460	46	1,500	1,450	*35
1,500	1,400	29	1,510	1,410	47	1,500	1,400	*35
1,500	1,350	32	1,510	1,360	45	1,500	1,350	*37
						1,500	1,300	*35
1,600	1,500	26	1,600	1,510	40			
1,600	1,450	26	1,600	1,460	46	1,600	1,450	*35
1,600	1,400	30	1,600	1,410	44	1,600	1,400	*33
1,600	1,350	35	1,600	1,360	*46	1,600	1,350	*33
						1,600	1,300	*32
1,700	1,500	27	1,700	1,510	*42			
1,700	1,450	26	1,700	1,460	*42	1,700	1,450	*28
1,700	1,400	26	1,700	1,410	43	1,700	1,400	*32
1,700	1,350	30	1,700	1,360	43	1,700	1,350	*25
						1,700	1,300	*29

* Average value of 2 bars. Other figures are average values from 4 bars.

VI. EFFECT OF MAXIMUM HEATING TEMPERATURE ON COMPOSITION AND STRUCTURE

After completing the transverse tests, the bars were sampled for chemical analysis and for microscopic examination. The analytical data are summarized in table 5, which gives average values, for each iron, for all the metal that was heated to a particular maximum temperature, irrespective of the temperatures at which the bars were poured. Although data on this point are not included in table 5, variations in pouring temperature did not appreciably affect the content of any of the elements determined.

The data show that there was no appreciable variation in the silicon, manganese, phosphorus, and sulfur contents with variations in maximum heating temperature. There was, however, a definite tendency for the total carbon to decrease with increasing temperature of the molten metal. The metal was melted in a magnesia crucible with the surface of the melt exposed to the air. Under these conditions some loss of carbon by oxidation at the higher temperatures

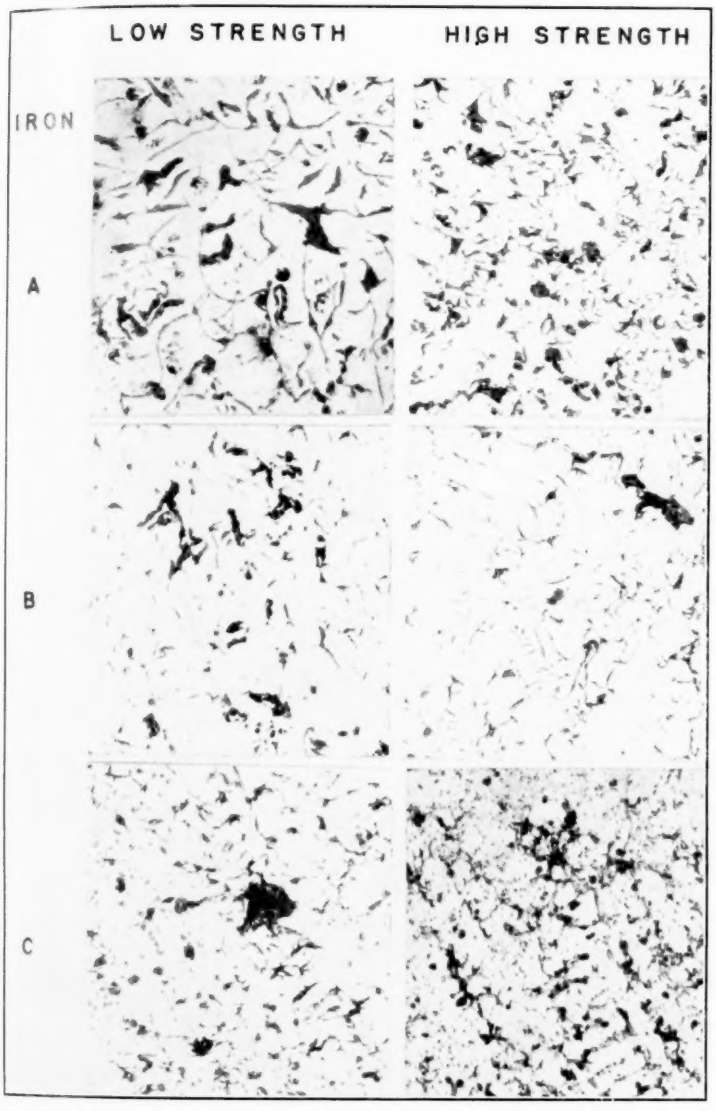

FIGURE 8.—*Structure of low- and high-strength bars of irons A, B, and C, unetched; ×100.*

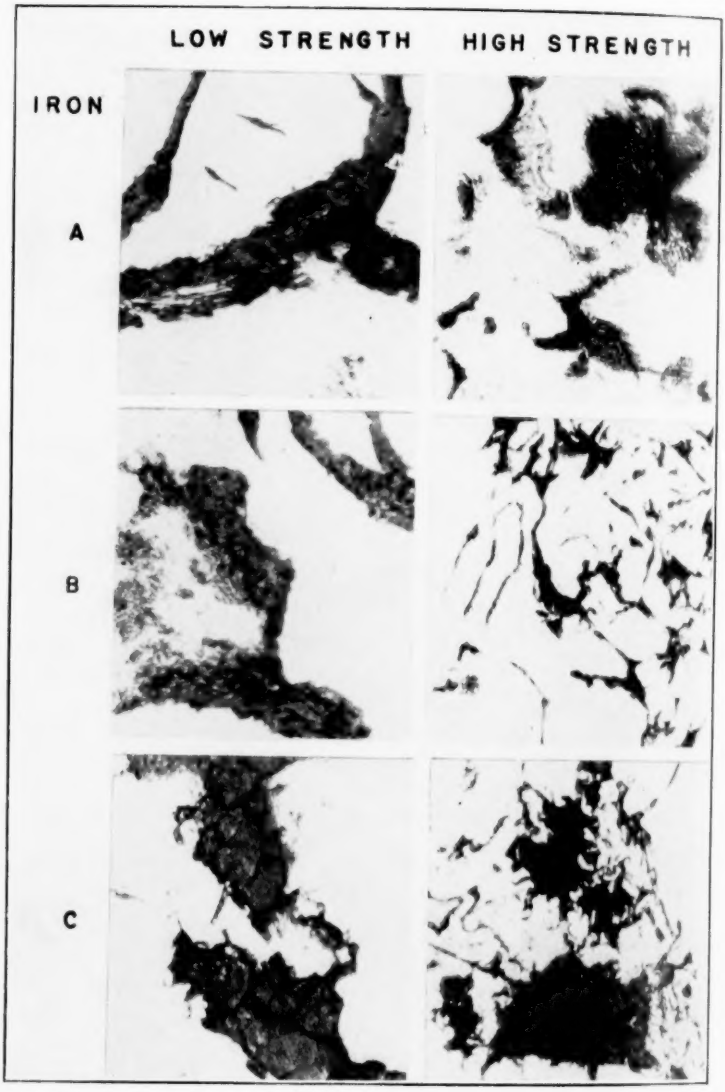

FIGURE 9.—*Graphite flakes in low- and high-strength bars of irons A, B, and C, unetched; ×500.*

would be expected. The total carbon contents of all the bars are close to or slightly less than the eutectic values computed from the amounts of silicon and phosphorus present. The combined carbon contents of bars of iron *A* are close to the eutectoid composition for the low-strength bars and exceed the eutectoid composition for the high-strength bars. In all bars of irons *B* and *C* the combined carbon is less than the eutectoid amount.

TABLE 5.—*Effect of maximum heating temperature on the composition of cast-iron bars*

Iron	Maximum heating temperature	Number of bars	Average composition							Breaking load [1]
			Total	Carbon combined	Graphite	Si	Mn	P	S	
	°C		%	%	%	%	%	%	%	*lb*
A	1,400	8	3.46	0.90	2.56	1.24	0.14	0.46	0.024	2,210
A	1,700	16	3.20	1.04	2.16	1.22	.15	.46	.025	2,567
B	1,410	8	3.82	0.74	3.08	1.25	.48	.172	.059	1,780
B	1,700	16	3.66	.72	2.94	1.29	.55	.170	.061	2,010
C	1,400	12	3.54	.58	2.96	2.36	.72	.39	.056	1,780
C	1,700	16	3.39	.64	2.75	2.38	.75	.40	.058	2,210

[1] Corrected to bar diameter of 1.2 inches.

In general, the strength of cast iron increases with decreasing amounts of graphitic (or total) carbon. Data for the breaking loads, in table 5, show that the bars of iron *A* had higher strengths and lower graphitic carbon contents than the corresponding bars of either *B* or *C*. Furthermore, in each of the three irons, an increase in maximum heating temperature decreased the amount of graphitic carbon and increased the strength. Evidently the strength and associated properties of these irons are affected by the amount of graphitic or total carbon but examination of the microstructure shows that there are variations in the size of the graphite flakes and in their distribution, as well as in the amount of graphitic carbon.

Cross sections of the test bars, from locations close to the fractures, were prepared for microscopic examination, according to the procedure described by Ellinger and Acken [13]. The specimens were ground on a surface grinder, lapped on a lead-tin plate charged with fine emery, further lapped on a second plate charged with finer emery, and, finally polished with an aqueous suspension of rouge, in an automatic polishing machine.

The micrographs in figure 8 show that the high-strength bars of each iron contained smaller and more uniformly distributed particles of graphite than did the low-strength bars of the same iron. The difference in particle size is more readily apparent in the micrographs of representative areas under higher magnification, in figure 9, and the structure of the nongraphitic matrix of each bar, revealed by etching the polished specimen, is shown in figure 10. The latter micrographs show that the matrix of the low-strength bars of iron *A* (heated to 1,400° C) is coarsely pearlitic, whereas in the high-strength bars of the same iron (heated to 1,700° C) large amounts of massive cementite are present, which, by stiffening and hardening the matrix, undoubt-

edly contributed to the high strength of these bars. Cementite is found only in iron that contains hypereutectoid amounts of combined carbon; pearlitic structures are associated with eutectoid and hypoeutectoid compositions. For iron *B*, the matrix of both high- and low-strength bars was found to be pearlitic, with small amounts of ferrite present and the structure of both high- and low-strength bars of iron *C* was found to consist of fine pearlite with areas of ferrite and of steadite.

The relations between the strengths, compositions, and structures of the three irons may be summarized as follows:

1. The increase in strength of each of the irons after it has been heated to a high temperature is associated with a decrease in the amount of graphitic carbon and in the size of the graphite particles and with an increase in the uniformity of their distribution.

2. The high strength of iron *A*, as compared to irons *B* and *C*, is associated with lower graphitic carbon and higher combined carbon contents.

VII. UNUSUAL STRUCTURAL FEATURES IN CAST IRON

An unusual structural condition was observed in many of the graphite flakes of iron *C*, in which an appreciable portion of the graphite appeared to be subdivided into roughly hexagonal grains. This condition is readily apparent in the micrograph of low-strength iron *C*, in figure 9, and is also evident, although less pronounced, in the micrograph of a high-strength iron *C*. Nipper [14] observed similar structures in samples of graphite laminas, but it is not entirely clear from his paper whether these laminas are natural graphite or have been isolated from cast iron. The present example of hexagonal graining in graphite refers definitely to the structure of graphite in cast iron.

Several of the specimens of iron *C* also showed a tendency towards a dendritic structure in the arrangement of graphite particles. This tendency is evident in portions of the micrograph of the high-strength bar of iron *C*, in figure 8, but in no case was the dendritic structure developed to such an extent that the properties of the bar were definitely affected.

Several of the micrographs in figure 9 suggest the existence of a laminated structure in some of the graphite particles. Examination under higher magnification confirmed this suggestion by showing that laminated areas existed in some of the large graphite particles and that the structure of some of the smaller particles was almost entirely laminated, as is shown by the micrographs in figure 11. This condition was most pronounced in specimens from high-strength bars of iron *A*, in which the combined carbon is hypereutectoid, but was also observed in hypoeutectoid, low-strength bars of iron *A* and occasionally in both high- and low-strength bars of iron *B*. These laminated structures were observed in specimens from the unstrained ends of the bars as well as in specimens from locations adjacent to the fractures and, therefore, were not caused by stress deformation of graphite particles during transverse loading. Furthermore, the laminated appearance persisted through repeated repolishings and hence was not an accidental or surface phenomenon.

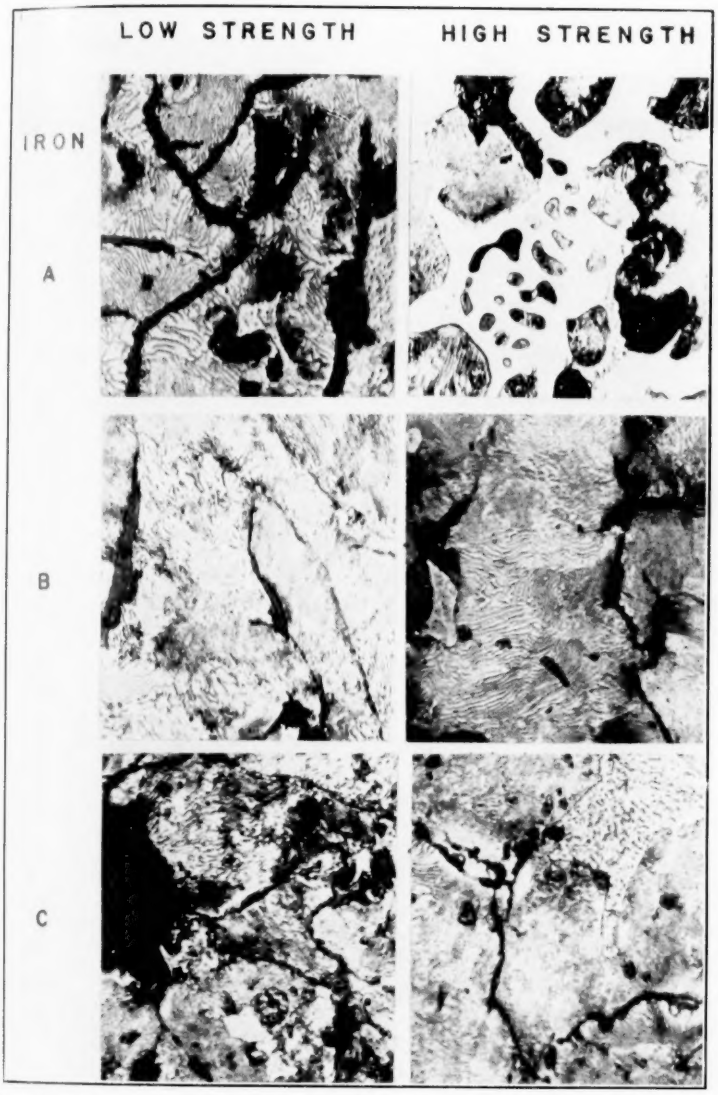

FIGURE 10.—*Matrix structure in low- and high-strength bars of irons A, B, and C.*
Etched with 1-percent solution of nitric acid in ethyl alcohol; ×500.

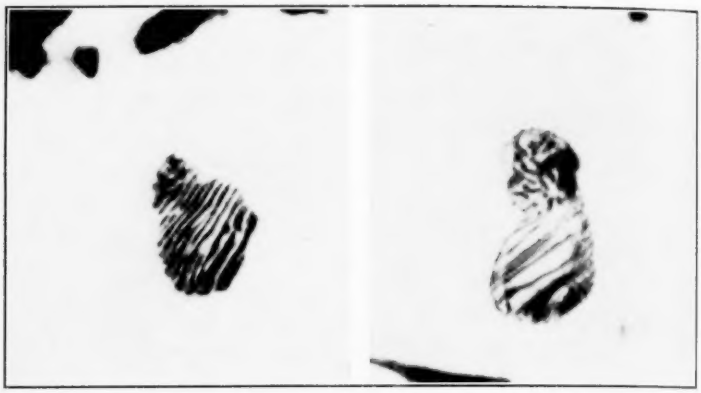

FIGURE 11.—*Laminated structure in small graphite particles, unetched;* ×2000.

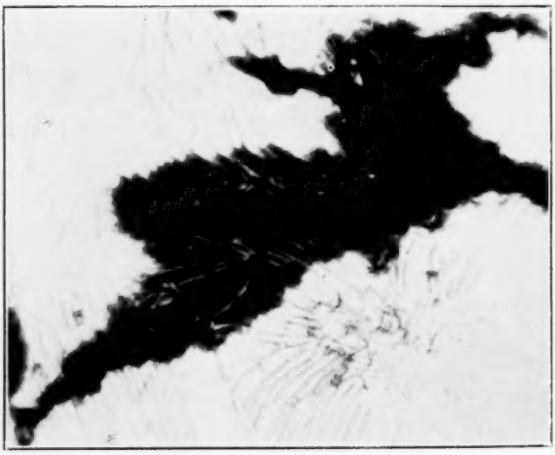

FIGURE 12.—*Eutectoid structure in a flake of graphite.*
Etched with 1-percent solution of nitric acid in ethyl alcohol; ×2000.

Discussion of the mechanism of formation of graphitic particles involves the controversial questions of the double iron-carbon diagram, that is, the question whether graphite in cast iron is formed at eutectic or eutectoid temperatures, or both. Arguments for and against the double diagram were reviewed by Epstein [15], who concluded that the existence of the iron-graphite eutectic had been confirmed by observations of eutectic-like structures and that the existence of the iron-graphite eutectoid had been indicated by the results of thermal analyses, although no one had been able to illustrate satisfactorily the appearance of the iron-graphite eutectoid. In a recent paper Wells [16] concluded that the iron-graphite eutectoid occurs at 738° C and 0.69 percent of carbon, and that the graphitization observed in high-purity alloys of iron and carbon resulted directly from decomposition of austenite as well as from decomposition of cementite. Boyles' recent paper [17] indicates that the large flakes of graphite in cast iron were formed during the solidification at eutectic temperatures and that subsequent decomposition of austenite or carbide at subeutectic temperatures produced finely divided graphite which had little effect on the flake structure.

The authors' conclusion that the laminated graphite structure, illustrated in figure 11, was formed by eutectoid decomposition of austenite or carbide is in agreement with the conclusions of these other investigators. Laminated structures have been observed in some examples of eutectic alloys, but the best-known example of laminated structure is pearlite, which consists of alternate laminations of ferrite and cementite in the proportions of the eutectoid composition. The appearance and structure of the laminated graphite are similar to those of pearlite, and it is reasonable to assume that the laminated graphite also is a result of a eutectoid decomposition, one in which austenite (or carbide) decomposes to form laminated graphite and ferrite. The micrographs in figure 11 therefore are offered as photographic evidence of the existence of the iron-graphite eutectoid.

Etching of specimens that contained laminated graphite revealed further unusual structures. Figure 12 shows the appearance of a flake of graphite and its surrounding areas in one of the high-strength bars of iron *A*, etched with a 1 percent solution of nitric acid in ethyl alcohol. The graphite flake is surrounded by pearlitic areas the structure of which extends into, and at one point entirely across, the graphite. The appearance suggests that the surface of the pearlitic area has been flowed over the graphite in the polishing operation, but there are objections to this suggested explanation. The flow of metal surfaces during polishing has been established by Beilby and subsequent workers, but it is generally agreed that such a flowed film is "amorphous," that is, structureless, and hence different in properties from those of the parent metal. It is difficult to believe that such a layer could preserve the patterns that are shown in figure 12. Moreover, a reasonable explanation of this structure can be developed if it is assumed that both pearlite and the laminated graphite are produced by the eutectoid decomposition of austenite or carbide. Apparently, in the area shown in figure 12, the same eutectoid decomposition that produced pearlite in the surrounding areas formed the laminated structure in the graphitic area. The fact that some of the laminations are common to both the pearlite and the laminated graphite,

indicates that the two structures were formed under the same conditions. These observations further indicate that the laminated graphite structure shown in figure 11 represents the iron-graphite eutectoid mixture. Furthermore, the suggested mechanism of simultaneous formation of pearlite and laminated graphite in adjacent areas accounts for the observation of the existence of the laminated structure in numerous small areas along the boundaries of large grains of graphite, as in figure 9. The structure of the pearlite is not revealed in these polished but unetched specimens.

Although Bolton [18], in a discussion of a somewhat similar structure, suggested that the black area might not be graphite, the authors believe that the black area in figure 12 is graphite, containing definite indications of a laminated structure closely related to the structure of pearlite. The present data do not indicate whether the laminated graphite is formed by eutectoid decomposition of austenite or of carbide. However, Wells [16] has shown that either of these reactions can produce graphite in high-purity iron-carbon alloys.

VIII. SUMMARY

1. A new method of measuring the deflection of test bars under transverse loading has been developed. Measurements of deflection under interrupted loading can be continued up to the breaking point of the bar and the accuracy of these measurements is entirely independent of the rigidity of the testing machine and the mountings of the bar.

2. The properties of three types of cast iron were determined by measurements under transverse loading. Iron *A* was a stove-plate pig iron to which 10 percent of basic open-hearth ingot iron had been added, iron *B* represented the medium cylinder type of cast iron, and iron *C* was a soft iron of the type used for general castings. The average breaking load of iron *A* was appreciably greater than the breaking load of either irons *B* or *C*, and consequently, the elastic properties of *A* were generally superior to those of *B* or *C*.

3. Variations in the maximum temperature to which the liquid metal was heated affected the composition, structure, and properties of the test bars. An increase in the maximum heating temperature decreased the amounts of total and graphitic carbon, decreased the size and increased the uniformity of distribution of the graphite particles, and in general increased the transverse strength and elastic properties. The properties of iron *A* were more susceptible than those of *B* or *C* to variations in the maximum heating temperature.

4. Variations in the temperatures at which the test bars were poured had less effect than variations in maximum heating temperature on the composition, properties, and structure. However, there was a tendency for some of the properties to decrease with increasing pouring temperature, particularly for iron *A*.

5. The results of the transverse tests indicate that the initial portion of the elastic-deflection curve is a straight line, but at approximately half of the breaking load the curve inclines towards the deflection axis. For all bars of iron *A* the points of inflection occurred at loads between 1,400 and 1,800 pounds, for irons *B* and *C* the limiting value lay between 1,200 and 1,400 pounds. Because of the curvature of the elastic-deflection curves, a value for the relative modulus

of elasticity, computed from the data for any point on the initial linear portion of the curve, is approximately 1,000,000 pounds greater than a similar value computed from the load and deflection at the point of rupture.

6. Two unusual structural conditions were observed, indications of the existence of hexagonal-like grains within some of the graphite particles of iron *C*, and evidence of the existence of a laminated structure, resembling that of pearlite, in many of the graphite particles of irons *A* and *B*, particularly the former. The laminated graphite structure is considered to be that of the iron-graphite eutectoid composition.

Grateful acknowledgment is made to L. D. Jones, C. E. Jackson, and G. W. Wells for assistance in this investigation and to H. L. Whittemore for his counsel.

IX. REFERENCES

[1] J. T. MacKenzie, *Elastic properties of cast iron*, Proc. Am. Soc. Testing Materials **29,** pt. 2, 94 (1929).
[2] A. Thum and H. Ude, *Die mechanischen Eigenschaften des Gusseisens*, Z. Ver. deut. Ing. **74,** 257 (1930).
[2a] G. Meyersberg, *Sur la signification du module d'élasticité de la fonte*, La Fonte, No. 14, 522 (1934).
[3] J. G. Pearce, *The elasticity, deflection, and resilience of cast iron*, J. Iron Steel Inst. (London) **129,** pt. 1, 331 (1934).
[4] J. W. Bolton, Gray Cast Iron (The Penton Publishing Co., Cleveland, Ohio, 1937).
[5] E. C. de Segundo, *Experiments on the strain in the outer layers of cast iron and steel beams*, Proc. Inst. Civil Engrs. (London) **98,** 308 (1888–1889).
[6] C. Bach and R. Baumann, Elasticität und Festigheit, 9th ed. (Julius Springer, Berlin, Germany, 1924).
[7] C. M. Saeger, Jr., and E. J. Ash, *Properties of gray iron as affected by casting conditions*, J. Research NBS **13,** 573 (1934) RP726; Trans. Am. Foundrymen's Assn. **39,** 449 (1933).
[8] A. I. Krynitsky and C. M. Saeger, Jr., *An improved method for preparing cast iron transverse test bars*, J. Research NBS **16,** 367 (1936) RP880; Trans. Am. Foundrymen's Assn. **45,** 753 (1937).
[9] R. L. Templin, *The determination and significance of the proportional limit in the testing of metals*, Proc. Am. Soc. Testing Materials **29,** pt. 2, 523 (1929)
[9a] Cast Metals Handbook (Am. Foundrymen's Assn. p. 88, 1935).
[10] J. T. MacKenzie, *Report of subcommittee 15 on impact testing*, Proc. Am. Soc. Testing Materials **33,** pt. 1, 87 (1933).
[11] J. T. MacKenzie, *The influence of phosphorus on iron*, Trans. Am. Foundrymen's Assn. **33,** 445 (1925).
[12] R. C. Tucker, *Pig iron*, Foundry Trade J. (London) **56,** 347 (1937).
[13] G. A. Ellinger and J. S. Acken, A Method of Preparation of Metallographic Specimens. Am. Soc. Metals, Preprint 22 (1938).
[14] H. Nipper, *Contribution to the study of graphite formation and structure in cast iron and its influence upon the properties of the cast metal*, Foundry Trade J. (London) **51,** 7 (1934).
[15] S. Epstein, The Alloys of Iron and Carbon, **1** (McGraw-Hill Book Co., Inc., New York, N. Y., 1936).
[16] C. Wells, *Graphitization in high-purity iron-carbon alloys*, Trans. Am. Soc. Metals **26,** 289 (1938).
[17] A. Boyles, The Freezing of Cast Iron, Metals Tech. **4** (April 1937) Tech. Pub. 809, published by American Institute of Mining and Metallurgical Engineers.
[18] J. W. Bolton, *Graphitization and inclusions in gray iron*, Trans. Am. Foundrymen's Assn. **45,** 467 (1937).

WASHINGTON, October 21, 1938.

U. S. Department of Commerce National Bureau of Standards

RESEARCH PAPER RP1177

Part of Journal of Research of the National Bureau of Standards, Volume 22, February 1939

RELATION OF CAMERA ERROR TO PHOTOGRAMMETRIC MAPPING

By Irvine C. Gardner

ABSTRACT

A portion of the errors in a map constructed from airplane photographs arises from differences between the actual performance of the airplane camera and the postulated performance as defined by the calibration constants. The different sources of errors of this nature are enumerated and equations are derived showing the relation between errors in the calibration constants of the camera and the resulting errors in the map.

Equations 3, 4, 10, 11, 18, and 19 give resulting errors in the map arising from incorrect value of the calibrated focal length, distortion, and incorrect location of the principal point. Other sources of error in the camera, such as failure of the film to lie in a plane, the character of performance of the shutter, and imperfect filters are considered and their effects upon the image evaluated.

CONTENTS

	Page
I. Introduction	210
1. General characteristics of the airplane camera	210
2. Differences between ideal imagery and actual camera performance	212
3. Sources of error in the map	213
4. General consideration of errors of the camera	214
II. Calibrated focal length	215
1. Permissible range in selection of calibrated focal length	215
2. Map errors resulting from error in determining calibrated focal length	216
3. Causes of variation in calibrated focal length	218
III. Distortion	219
1. Variation of distortion with selection of focal length	219
(a) Criterion for selecting the calibrated focal length	220
2. Error arising from distortion	221
3. Values of focal length and distortion reported for a lens not mounted in a camera	225
IV. Principal point of the focal plane	225
1. Index marks for principal point	225
2. Relation between the principal point and the axis of the lens	225
3. Error arising from incorrect location of the principal point	226
(a) Case in which the two overlapping photographs are from a single flightstrip	227
(b) Case in which the two overlapping photographs are from adjacent flightstrips	229
(c) Equations generalized to apply to the two preceding cases (a) and (b)	231
V. Departure of film from the focal plane	231

Page
VI. Types of shutters 232
1. Between-the-lens shutter 232
2. Focal-plane shutter 233
(a) Efficiency 233
(b) Distortion introduced by focal-plane shutter 234
VII. Accessories in optical path of camera 236
1. Filter 236
(a) Types of filters 236
(b) Distortion introduced by filter 237
(c) Effect of filter upon definition and camera calibration 237
2. Pressure plate 238

I. INTRODUCTION

1. GENERAL CHARACTERISTICS OF THE AIRPLANE CAMERA

The airplane mapping camera is a precision measuring instrument. Although fundamentally an optical instrument, it is dependent, for proper functioning, not only upon the proper design and installation of the optical parts but also upon the proper performance of a large number of elaborate and complicated mechanical auxiliary parts, among which are the mount which prevents the vibration of the airplane from affecting the definition of the photograph, the film mechanism by which the film is advanced and constrained to lie in the focal plane, the photographic shutter by which the exposure is timed, and the control devices by which the desired overlap is secured between the different negatives of a series. In this discussion consideration will be restricted to the fundamental requirements that are necessary in order that the resulting negatives may have the metrical characteristics suitable for the production of a map of the desired accuracy. These requirements relate to the precision with which the equivalent focal length must be determined, the distortion introduced by the objective, the location of the principal point of the focal plane, the planeness and shrinkage of the film, the type of shutter, and choice of focal length. After the tolerances connected with these characteristics have been derived and a suitable photographic objective has been chosen, it then becomes the problem of the camera designer to design the mechanical parts of the camera so that the photographic operations may be satisfactorily performed in a manner consistent with the maintenance of these tolerances. The requirements for the mechanical parts, except as they affect optical performance, will not be considered in this discussion.

When use is made of an airplane photograph for the construction of a map, it is commonly assumed that the photograph is a true perspective representation. Usually this is not rigorously true as distortion and other defects prevent the realization of a perfect perspective. Points A, B, O, C, D, and H in figure 1 are object points that are imaged on the photograph at A', B', O', C', D', and H', respectively. The point N' that brings the points of the photograph as nearly as possible into the correct perspective relationship should be chosen as the perspective center. The point O', at the foot of the perpendicular from N' to the plane of the photograph, is the principal point [1] and the length $N'O'$ is the principal distance. These terms are standard ones long used in the theory of perspective and are applicable to any representation in perspective, whether it is a photograph, painting, or

[1] This principal point of the photograph or of the focal plane is not to be confused with the principal points of the lens, a pair of points coincident with the nodal points in lenses of the types employed for photogrammetric purposes.

drawing. It will be noted that the definitions are in terms of the photograph and bear no reference to the camera.

The point N is the corresponding perspective center for the terrain that is photographed. If β is the angle at N, subtended by O and any point A, and if y' is the distance from O' to A', then since, ideally, $\beta=\beta'$, it is evident that

$$\tan \beta=\frac{y'}{p}, \qquad (1$$

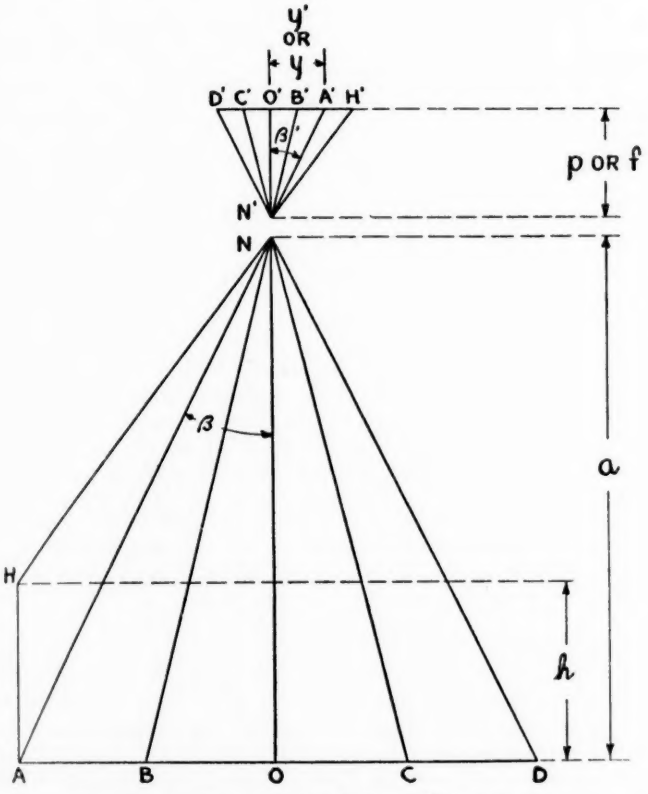

FIGURE 1.—*The metrical relations of the camera.*

The symbols y' and p designate the indicated lengths when D', C', O', B', A', and H' are assumed to be points on a print or diapositive. If they are assumed to be images of points, as formed in the camera (in which case they are unaffected by shrinkage of film or subsequent enlargement), the symbols y and f apply.

where p is the principal distance. This relationship enables the photograph to be utilized for the measurement of angles. In practice these angles may be determined either by computation, after a direct measurement of y', or, if a plotting machine is employed, the angle β is determined and utilized to transfer the desired result to the map in a semiautomatic manner without an intermediate reading or recording of the angle.

2. DIFFERENCES BETWEEN IDEAL IMAGERY AND ACTUAL CAMERA PERFORMANCE

Returning to figure 1, let it now be assumed that points A', B', O', C', D', and H' are no longer the points recorded on a photograph, as was the case in the discussion of the preceding paragraph, but that they are the image points as actually produced in the focal plane by the photographic objective. The distinction lies in the elimination of possible changes in the spacing of the points as a result of film and paper shrinkage, subsequent enlargement from the negative, etc. In order to make this distinction quite clear without making two separate drawings, alternate symbols, y' and y, and p and f, are shown in figure 1. When $\overline{D'H'}$ is assumed to represent the trace of a print, made either by contact or enlargement, y' represents a length measured on the print and p is the principal distance. When points D', C', O', B', A', and H' are assumed to be points of the aerial image as formed by the camera lens, the symbols y and f refer to the corresponding dimensions. The point N' is selected as before to correspond to the most nearly correct perspective. The point N remains the corresponding perspective center for the terrain. We now have the equation

$$\tan \beta = \frac{y}{f}, \tag{2}$$

which resembles eq 1, the difference being that f has been written instead of p and that y' in eq 1 is measured on the photograph and the y of eq 2 is measured on the image in the camera. In other words, eq 1 involves the properties of a finished negative, print, or enlargement, whereas eq 2 is restricted to the properties of the camera.

If it be assumed that the camera lens (not shown in the diagram) producing the imagery of figure 1 is free from aberrations and the inevitable minor errors of workmanship, and further, if the idealized rays of paraxial imagery are assumed, then N and N' are identical with the first and second nodal points or the camera objective and the quantity f of eq 2 is the equivalent focal length.[2]

Inevitable departures from the idealized conditions of paraxial imagery, however, cause differences, too large to be neglected, between the magnitudes that are actually used in the construction of maps and the corresponding quantities for the idealized case.

Ordinarily the surfaces of a lens are assumed to be surfaces of revolution having their axes of symmetry in coincidence. This common axis is referred to as the axis of the lens. When a lens is carefully examined on the test bench, it is often found, even though the lens is of excellent quality and repute, that the axes of the different surfaces fail to coincide exactly. In such a case it is difficult to define the axis of the lens or the positions of the nodal points with precision. If a line approximately coincident with the axes of the several surfaces is tentatively accepted as the axis of the lens, it may be found that a ray in the object space traveling along this line is deviated several min-

[2] This is based on the assumption that a, the altitude of the camera, may be considered infinite. When a is 15,000 feet and the focal length of the camera objective is 6 inches (150 mm), the displacement of the image from the rear focal plane, because of the finite, though large distance to the object, is approximately two ten-thousandths of an inch, an amount negligible in comparison with the other departures from the ideal condition that are to be considered.

utes by transmission through the lens. Consequently, N and N' of figure 1 have been referred to, not as nodal points of the lens but as centers of perspective in the object and image space. The principal point of the focal plane is not necessarily the point where the axis of the lens intersects the image plane but is at the foot of the perpendicular dropped from the center of perspective in the image space to the image plane. For the pair of conjugate points, N and N', angles β and β' are equal when distortion is absent. These points may, therefore, be termed the points of unit angular magnification, although they satisfy this condition rigorously only in the ideal case. As a consequence of this unit angular magnification, a lens may be tipped about N' through an appreciable angle without seriously affecting the metrical characteristics of the negative and, in such a case, the point O' will not coincide with the intersection of the axis of the lens and the focal plane.

The equivalent focal length is usually defined in textbooks on optics in terms of paraxial imagery, and it is treated as though it were a uniquely defined quantity associated with the lens. Actually, when the physical nature of light and other factors, such as the graininess of the photographic emulsion, are taken into consideration there is a considerable range of positions in which the image plane may be established without marked variation in definition. For each of these settings there is a different value of the f of eq 2, and this is but one reason why the f of eq 2 is not necessarily identical with the computed focal length. When distortion is present, eq 2 is not valid for all parts of the field unless it is modified by the addition of a correction term. If the plotting machine has no provision for the introduction of such a correction term, a partial correction can be secured by choosing a modified value of f in a manner that is more fully considered in a later section. In view of differences of this nature between the f of eq 2 and the equivalent focal length, the former will be referred to as the calibrated focal length, and it is defined as the value that best satisfies eq 2 for all points of the image.

According to this nomenclature, therefore, the equivalent focal length is an optical characteristic of a lens defined in terms of paraxial imagery; while the calibrated focal length is a property of the lens and camera, which not only depends upon the equivalent focal length of the lens and the amount of distortion present but is also governed by the manner in which the lens is adjusted in the camera. The principal distance is a property of the finished negative or print and differs from the calibrated focal length in that it is further affected by film shrinkage, by the shrinkage of the paper base, if a print has been made, and by any enlargement or reduction. If, for example, a photograph is enlarged any number of diameters, the principal distance is proportionately increased.

3. SOURCES OF ERROR IN THE MAP

Errors in the map may result from errors introduced into the photograph by the camera, from changes such as shrinkage of the film or paper, and from errors introduced during the process of making the map from the photograph. This last classification includes faulty enlargement; imperfect rectification or tilt elimination by projection; systematic errors introduced by the plotting machine as a consequence

of inaccurate gears, pantograph linkages, and projectors; errors systematic for each print but changing from print to print because of incorrect adjustment of photographs in the plotting machine; errors arising from lost motion in the plotting machine; and accidental errors arising from the inability of the operator to make pointings unaffected by accidental variations. Errors of a systematic nature may also arise because of errors in the system of control points.

This presentation is restricted to a consideration of the errors that have their origin in the camera. They are: a, a difference between the assumed and actual value of the calibrated focal length; b, distortion produced by the optical system; c, a difference between the assumed and actual position of the principal point; d, a departure of the film from a plane; e, distortion introduced by the shutter; and f, distortion introduced by filter or pressure plate.

4. GENERAL CONSIDERATION OF ERRORS OF THE CAMERA

In evaluating the effects of these sources of error upon the map it is necessary to consider the manner in which the photographs are used. It might at first appear necessary to consider only the displacement or apparent displacement of an image point as produced by those variations and then to determine the corresponding displacement upon the map. This procedure might be followed if the photographs could be used for map making without known control points. In airplane mapping, however, control points are necessary,[3] and consequently the introduction of residual errors in the final map is too subtle to be evaluated so easily by such a simple direct computation which would give estimates larger than the errors actually introduced.

In the interpretation of aerial photographs one makes direct use of the known control points in the picture. If (1) an automatic-plotting machine is used to interpret the negative, one adjusts the negative to fit the control points. In this operation it is usually assumed that there is no distortion and that the camera is correctly calibrated and collimated. Implicitly, this adjustment of the negative in the machine amounts to a determination of the position of the camera in space at the instant of exposure. If (2) the negative is to be interpreted by direct measurements and mathematical analysis, one first determines explicitly the position and tilt of the camera at the instant of exposure. In case (1) or case (2) the choice is made in such a manner that eq 1, with the assumed calibration, is valid, or made as nearly valid as possible for all control points. If these assumptions are incorrect an incorrect position for the camera at the time of exposure will be determined but, as has been noted, the error will be such that eq 1, with the incorrect values that have been assumed, applies to the control points. Consequently, this error in the location of the camera is of a compensatory nature and tends to correct the errors for other points on the negative.[4]

[3] One may be actually fitting a photograph to control points or, when "bridging" from one set of control points to another, there may be no control points on a given print, but it may be adjusted to have the proper relation to the preceding photograph of the series. For the purposes of this discussion, however, these two operations are essentially similar in character, whether the print is fitted to control points independently surveyed or to the points of the preceding print.

[4] This compensating effect occurs in all applications of airplane photography to mapping, and it considerably increases the allowable variations in the performance of the camera. It is interesting to note, that on the contrary when mapping is done by cameras on tripods at the ends of measured base lines the positions of the cameras are observed by direct surveying methods rather than by fitting the negatives to control points and therefore this compensation is not obtained.

The same idea may be expressed, from another viewpoint, by stating that the camera serves as a means for determining the positions of points in space by interpolating or extrapolating from the known control points. If control points lie at the extreme positions of the photographs and at maximum and minimum elevations, then all points are "bracketed" by the control points and the process is entirely interpolation. If this is not the case, some of the points to be located lie beyond the control points and are located by extrapolation. The exact functional relationship by which the interpolation or extrapolation is to be done is known and the only errors incidental to the process are the accidental errors arising from lack of precision in the different steps of the operation and the systematic errors (systematic in the results obtained from a given pair of photographs) arising from the use of incorrect constants, such as calibrated focal length and incorrectly located principal point. Consequently, the results obtained by extrapolation, although probably less accurate than those obtained by interpolation, are not so markedly inferior as may be the case when extrapolation is done by an entirely empirical method.

The distribution of the control points is governed by the nature of the region to be mapped and the results available from preceding surveys. Consequently, the distribution necessarily varies from photograph to photograph, with consequent changes in the errors resulting from departures of the camera from its calibrated values. In this discussion of errors the assumption is made that all the control points lie in a datum plane. The systematic errors arising from errors in the camera are largely independent of the distribution of the control points, but for points located from a given pair of photographs the systematic errors resulting from the necessarily imperfect fitting of the photographs to the control points increase rapidly if the control points are not distributed over the entire region included in the photographs. If all control points lie in a plane, the determination of all elevations is a result of extrapolation, and consequently the errors in stereoscopic parallax resulting from errors in the camera may be expected to be maximal. If the control points are distributed not only in the horizontal datum plane but also over the range of elevation presented by the terrain, it is probable that the errors of stereoscopic parallax will be less than those embodied in the conclusions of this presentation.

II. CALIBRATED FOCAL LENGTH

1. PERMISSIBLE RANGE IN SELECTION OF CALIBRATED FOCAL LENGTH

It has already been suggested that the value of f in eq 2 that makes this equation most nearly valid for all parts of the negative be designated as the "calibrated focal length" and that this can be expected to differ from the equivalent focal length. For lenses that are not assembled in cameras when submitted to the National Bureau of Standards for test, the reports give values of the equivalent focal length and of the back focal length. If distortion were absent and if, light consisted of rays that could be represented by geometric lines, these values would each be unique. Actually, however, there is considerable depth of focus, and the values given in a report are self-

consistent values lying near the middle of a range of two or more tenths of a millimeter, the total variation without marked change in definition depending upon the lens and the relative aperture. If a lens that has been tested is mounted in a camera, and if a depth gage is used to make the distance from the vertex of the last surface of the lens to the plane of the emulsion, equal to the reported back focal length, then, in the absence of distortion or tipping of the lens, the calibrated focal length should be equal to the equivalent focal length given in the report. If, however, the distance of the lens from the focal plane is selected by trial exposures made as this distance is varied, it will be fortuitous if the adopted distance from lens to film is the same as the back focal length given in the report. Consequently, even in the absence of distortion, the calibrated focal length of a lens mounted in a camera may not be the same as the equivalent focal length as measured on the same lens submitted unmounted.

A portion of this depth of focus, which results in an image equally good along a considerable range of the optic axis, arises because of the diffraction resulting from the wave character of light. This contribution to the depth of focus varies as the square of the "f number" and, for an ideal lens, has the values given in table 1.

TABLE 1.—*Depth of focus as a function of aperture*

Relative aperture	Depth of focus
	mm
f/2	±0.004
f/2.8	.008
f/4	.016
f/5.6	.032
f/8	.064
f/11	.128
f/16	.256
f/22	.512

These limits are considerably extended in actual practice because of the graininess of the photographic emulsion, which limits the resolving power of the film. For testing purposes at the National Bureau of Standards, a special spectrographic plate with an emulsion designated by the Eastman Kodak Co. as type *V* is used. This emulsion has a very fine grain with high resolving power but is too slow for use in the field. Even with this emulsion, exposures made with a relative aperture of *f*/8 and spaced 0.3 mm along the axis show scarcely distinguishable differences in sharpness between consecutive positions. This corresponds to a possible variation of ±0.15 mm in the value of *f*, depending upon the adopted setting of the lens in the camera.

The presence of this depth of focus is often very advantageous. When a lens has considerable curvature of field, it is possible to locate the focal plane in a compromise position for which the definition is greatly improved at the edge of the photograph without materially reducing the quality of definition at the center.

2. MAP ERRORS RESULTING FROM ERROR IN DETERMINING CALIBRATED FOCAL LENGTH

To determine how precisely the calibrated focal length need be determined and the magnitude of allowable variations arising from

temperature change of camera, from removal and replacement of magazine, etc., it is necessary to consider the effect resulting from using an erroneous value of f in constructing a map. A little consideration leads to the conclusion, somewhat startling at first, that so long as the camera is vertical and the terrain a horizontal plane, an error in the value of f introduces no error at all in the map. All such pictures, taken with lenses of different focal lengths or at different heights, are rigorously geometrically similar, and consequently the negatives differ only in scale. When the negative is adjusted in the plotting machine to fit the control points the scale is adjusted to the correct value and the representation is correct.

However, if the terrain is not plane, the relief parallax [5] will be different for photographs taken from different heights because, as the elevation of the camera is changed, the displacement on the negative, for the points nearer the camera, that is, for the more elevated points, changes disproportionately to that for the less elevated points.

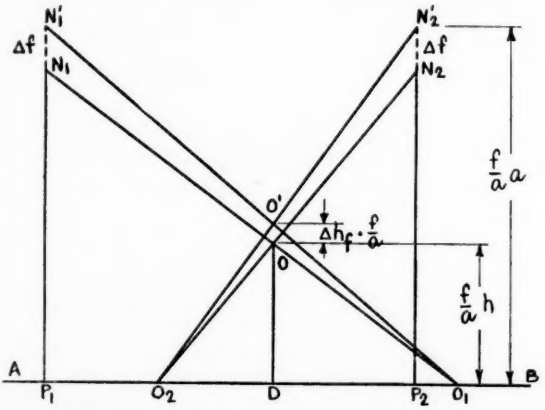

FIGURE 2.—*The error arising from an incorrect value of the calibrated focal length.*

The correct centers of perspective are at N_1 and N_2. Because of the error Δf in the calibrated focal length, points N_1' and N_2' are assumed to be the centers of perspective and the elevated point O is incorrectly located at O', a point displaced vertically but not horizontally.

The effect of an incorrect value of the calibrated focal length is illustrated in figure 2, which is an elevation, $\overline{AB}$ being the trace of two overlapping photographs, 1 and 2, assumed to be so placed that the common control points coincide.[6] The principal points are at P_1 and

[5] The relief parallax is the apparent relative lateral displacement of a point because of its elevation or depression from an assumed reference plane. In figure 1, the point H, is directly over A, but, in the focal plane, H' is laterally displaced with respect to A'. The displacement, $\overline{H'A'}$, is the relief parallax and always extends in a radial direction from the principal point. When two overlapping photographs are properly arranged for stereoscopic viewing, the relief parallax gives rise to the stereoscopic relief by which the elevation of a point common to the two photographs can be determined.

[6] In this figure and the similar figures that follow, when reference is made to two overlapping photographs, this expression is used because of its brevity. Actually, if two photographs were superposed, the overlapping part of one would prevent the observation of points under the other. The superposition is accomplished optically in the plotting machine. The ordinary stereoscope presents a common example of such optical superposition. Futhermore, if photographs are used, the distances $\overline{N_1P_1}$ and $\overline{N_2P_2}$ are principal distances instead of calibrated focal lengths. If the photographs are contact prints from the negatives, and if there is no shrinkage in negative or print, the principal distance of the photograph and calibrated focal length of the camera become identical. The lengths are referred to as calibrated focal lengths because the errors of the camera are being considered and it seems advisable to exclude, so far as convenient, effects arising from the processing of the film or subsequent methods of reproduction.

P_2, and $\overline{P_1N_1}$ and $\overline{P_2N_2}$ are the two principal distances, assumed equal to the calibrated focal length. If the photographs are viewed stereoscopically from N_1 and N_2, one has a true stereoscopic model, of which the scale factor is f/a, where a is the altitude of the camera at the time of the exposure. The point O is the correct position in the model, in accordance with the scale, of a point at an elevation h above the reference plane. It is imaged on photographs 1 and 2 at points O_1 and O_2. With the correct value of the calibrated focal length, the two photographs, when mounted in the plotting machine, are viewed from points N_1 and N_2, and O is correctly located at the intersection of lines $\overline{N_1O_1}$ and $\overline{N_2O_2}$. Because of the error Δf in the value of the calibrated focal length, the photographs will be so mounted in the plotting machine that the two photographs are viewed from points N_1' and N_2' and the point O is incorrectly located at O', the intersection of lines $\overline{N_1'O_1}$ and $\overline{N_2'O_2}$. The displacement $\overline{OO'}$ is equal to $\Delta h_f f/a$, where Δh_f is the consequent error in elevation of the point O'. From similar triangles it is readily seen that

$$\Delta h_f = \frac{ha}{af}\Delta f = \frac{h}{f}\Delta f. \tag{3}$$

From the similar triangles it is also apparent that O' is directly over 0. Therefore, if Δl_f denotes the horizontal displacement arising from the error in the calibrated focal length,

$$\Delta l_f = 0. \tag{4}$$

In eq 3, if $\pm\Delta f$ is the probable error of the calibrated focal length, $\pm\Delta h_f$ will be the resulting contribution to the probable error of the elevation of a point on the map.

3. CAUSES OF VARIATION IN CALIBRATED FOCAL LENGTH

Although the calibrated focal length of a camera may be correctly determined for certain given conditions, it must be remembered that changes in the scale of the negative can arise from various causes such as failure of the film to always occupy the same position in the camera because of poorly designed or poorly constructed devices for removing and replacing the magazine, failure of the lens to return precisely to its original position after it is removed for cleaning, expansion of the camera cone with change of temperature, and other similar causes. All of these can be considered and their effects evaluated as if they were changes in the calibrated focal length arising from changes in the dimensions of the camera.

For a camera with a lens having a focal length of 150 mm and a cone made of brass or aluminum, it is interesting to note that a change of 50° F in temperature will introduce a change in the length of the cone of 0.08 mm. If the photographic film showed tne same percentage change in its dimensions it would largely compensate for the change in the cone and the camera would require little or no correction for temperature. If the cone and film have different coeffi-

cients of expansion the resulting coefficient for the camera will depend upon their difference.[7]

However, the great uncertainty in the determination of the temperature coefficient and its application lies in the lack of information as to whether or not the camera and its spool of film have time to attain temperature equilibrium during the period required for ascent of the plane and before the exposures are begun. It is fortunate that preliminary considerations indicate that the temperature correction is so small that an approximate estimate of its value should be sufficiently accurate.

III. DISTORTION

1. VARIATION OF DISTORTION WITH SELECTION OF FOCAL LENGTH

A photographic objective is designed to be symmetrical about its axis and, although the errors of workmanship and assembly necessarily imply departures from this symmetry, it is commonly assumed that the distortion of a photographic objective is also symmetrical about the axis of the lens. In such a case the displacement of any point from its distortion-free position is along a radius, either from or toward the center of the plate. In the presence of distortion no value of f can be found that will satisfy eq 2 for all parts of the negative. Consequently, when distortion is to be considered, it is customary to modify eq 2 by the addition of a correction term, writing it

$$\tan \beta = \frac{y - \Delta y}{f} \tag{5}$$

In this equation, y is the measured distance from the principal point to the image point, Δy is the linear distortion, and $y - \Delta y$ is the distortion-free position of the image point. The angle β is the angular distance of the point from the center of the field.

The distortion Δy is not a constant but is different for points in different parts of the field. If it is assumed that the distortion can be satisfactorily represented as symmetrical about the center of the field, it will be the same for all points at a given distance from the center and therefore will be a function of β only. In accordance with this assumption, in the reports of the National Bureau of Standards, in the table headed "Distortion" the values of Δy are tabulated for intervals of 5°, measured from the center of the plate.

Equation 5 can be written

$$\Delta y = y - f \tan \beta, \tag{6}$$

where $f \tan \beta$ is the distance from the center of the plate to the distortion-free position, as given by eq 2. This equation shows that the distortion-free position $(y - \Delta y)$ is a function of the value of f that has been chosen and that, in consequence, y being fixed in value, Δy can be modified at will by changing the value of f. After any value of f is chosen, the corresponding values of Δy can be obtained from eq 6, and a consistent description of the image is obtained. For lenses of usual

[7] This argument is not rigorously exact because there will be a change in the position of the second nodal point of the lens resulting from the change in the index of refraction of the lens components with temperature. However, in most, if not in all cases, this will be relatively unimportant in comparison with the expansion of the camera cone and film.

construction there will, in general, be a small range of values of f for which the values of Δy vary approximately as the cube of tan β over the field of view that is utilized. When Δy varies as $\tan^3 \beta$, it follows that its value is relatively small for points in the neighborhood of the center of the field and over this region, therefore, for these values of f, eq 2 with no correction term applies with fair accuracy.

When f is so chosen that Δy varies approximately as $\tan^3 \beta$, Δy has the same sign over the entire field and it has its maximum value at the extreme edge of the field. But values of f can be chosen for which the distortion has one sign for values of β less than some given value and the opposite sign for points beyond. With such an adjusted value of f the distortion is distributed more uniformly, so to speak, over the entire negative and never equals in magnitude the value that would exist at the edge of the field if the equivalent focal length of geometric optics were selected.

Either system of values describes the imagery correctly and will lead to the same final result in the map, provided no quantities are neglected when the computations are made. If, however, the plotting machine has no provision for introducing the term Δy, or if the distortion is only partially compensated by the machine, the two systems of values may be expected to lead to different results. To determine the proper value of f to be selected as the calibrated focal length, it is necessary to consider the method by which a map is constructed.

(a) CRITERION FOR SELECTING THE CALIBRATED FOCAL LENGTH

When adjusting the negative in a machine an attempt is made to fit certain points on the negative to the corresponding control points that have been carefully surveyed. In the presence of distortion an exact fit cannot be secured. The calibrated focal length should have the value that will lead to the least error in the map as a whole. This requirement does not lead directly to a criterion governing the choice of the calibrated focal length, because the distribution of the control points and the overlap of the photographs govern the manner in which the distortion introduces error into the map. Fortunately the distortion of the modern lens is so small that the different methods of adjusting the focal length lead to results which do not differ greatly. A simple and satisfactory basis for adjustment is afforded if the calibrated focal length is chosen to make the maximum value of the distortion in the photograph as small as possible.

This criterion can be applied by means of eq 6. If Δy of this equation is defined as a function of β, by differentiation and the usual method of determining a maximum or minimum, one can determine the value of f for which the maximum value of Δy within a field of given angular extent is a minimum. To illustrate this, let it be assumed that a lens covers a field having a half-angle of 35° and that the distortion, referred to the equivalent focal length, varies as the cube of the tangent of the angular distance from the center of the field. If D is the maximum distortion, when referred to the equivalent focal length, then the calibrated focal length will be $1.06D$ greater than the equivalent focal length. The maximum absolute value of the distortion will be $0.25D$, and this value will be attained for the values $\beta = 19.3°$ and $\beta = 35°$.

It should perhaps be mentioned that this change from the equivalent to the calibrated focal length in order to vary the distribution of the distortion over the field has no relation to the depth of focus. In this respect it is quite different from an alteration of the back focal length because of the presence of curvature. Such an adjustment was mentioned (section II–1) as possible, because the focal plane can be shifted over an appreciable range without seriously affecting the definition at the center of the field. When, however, the equivalent focal length is changed to compensate for distortion, the position of the focal plane is not altered. The change relates to computations only, the constant of eq 2 being changed in order to obtain a scale factor that better fits the photograph, but no change is made in the distance from camera lens to photographic film.

2. ERROR ARISING FROM DISTORTION

After the calibrated focal length has been adjusted to reduce the maximum value of the distortion as much as possible, the effect of the remaining distortion upon the map must be considered. If the maximum value of this residual distortion is Δr, this will represent the maximum error in the horizontal location of any point lying in the datum plane. The error, in general, will be less than Δr, not only because the point in question may be located at a position on the photograph where the distortion does not attain this maximum value but also because, when the best possible fit is secured between the control points and the distorted system of image points on the photograph, the adjustment that gives the best fit distributes the distortion and yields a further compensatory action beyond that secured by adjusting the focal length.

If the point under consideration does not lie in the datum plane the determination of the resulting error is more involved. One such case is represented in figure 3, which is an elevation, $\overline{AB}$ being the trace of the photographs 1 and 2 assumed to be so placed that the common control points coincide. The principal points are at P_1 and P_2, and $\overline{P_1N_1}$ and $\overline{P_2N_2}$ are the two principal distances assumed equal to the calibrated focal length. If the photographs are viewed stereoscopically from N_1 and N_2, one has a true stereoscopic model of which the scale is f/a, where a is the altitude of the camera at the time of exposure. The point O is the correct position, in the model, in accordance with this scale, of an elevated point that, as a consequence of the relief parallax, is imaged on photographs 1 and 2 at points O_1 and O_2 when there is no distortion.

Actually, because of the distortion, O is imaged at O_1' and O_2'. In the present illustration it is assumed that the displacement arising from distortion in each photograph is positive, that is, the point O_1' is displaced outward from point P_1, and O_2' is displaced outward from point P_2, the two displacements being Δr_1 and Δr_2, respectively. If O were imaged at points O_1 and O_2 on the two photographs, observations from points N_1 and N_2 upon points O_1 and O_2 would correctly locate O at the intersection of lines $\overline{N_1O_1}$ and $\overline{N_2O_2}$. Actually, however, the observations are made on points O_1' and O_2', and O is erroneously located at O'. The point O' is at the vertex of the triangle $O'EG$, of which the base, by similar triangles, is $(\Delta r_1+\Delta r_2)\ (a-h)/a$, and the angles at the two ends of the base may, without important

error, be assumed to be $90°-\beta_1$ and $90°-\beta_2$. (These values differ from the true values by the angles $O_1N_1O_1'$ and $O_2N_2O_2'$, angles of a few minutes of arc, shown much exaggerated in the drawing.)

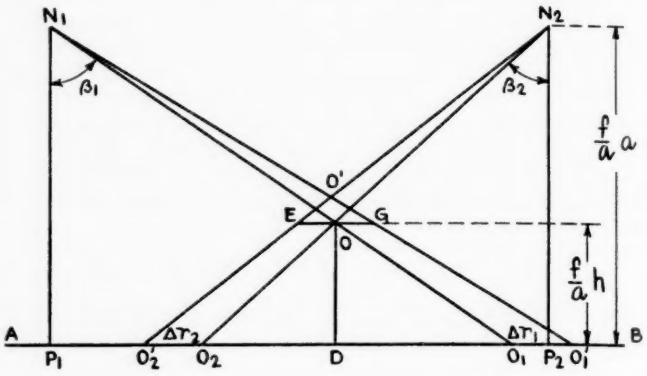

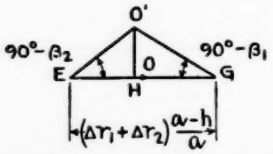

FIGURE 3.—*The error arising from distortion.*

The elevated point O is imaged at O_1' and O_2' instead of at O_1 and O_2 because of the distortions Δr_1 and Δr_2. Consequently the point O is erroneously determined to be at O', displaced vertically and horizontally from its true position.

For greater clearness, this triangle is shown to a much larger scale, below the main figure. The length $\overline{O'H}$ is $\Delta h_d' f/a$, where $\Delta h_d'$ is the error in elevation resulting from the presence of distortion. To obtain a convenient expression for $\Delta h_d'$, one writes

$$\frac{\overline{EH}}{\overline{HG}}=\frac{\cot E}{\cot G}=\frac{\tan \beta_2}{\tan \beta_1}$$

$$\frac{\overline{EH}+\overline{HG}}{\overline{HG}}=\frac{(\Delta r_1+\Delta r_2)(a-h)}{\overline{HG}a}=\frac{\tan \beta_1+\tan \beta_2}{\tan \beta_1}$$

$$\overline{HG}=\frac{(\Delta r_1+\Delta r_2)\tan \beta_1}{\tan \beta_1+\tan \beta_2}\quad\frac{(a-h)}{a}$$

$$\Delta h_d'\frac{f}{a}=\overline{HG}\cot \beta_1=\frac{(\Delta r_1+\Delta r_2)}{\tan \beta_1+\tan \beta_2}\quad\frac{(a-h)}{a} \tag{6}$$

If $\overline{O_1O_2}$ (greatly exaggerated in fig. 3) is neglected as small in comparison with $\overline{P_1P_2}$, this equation may be written

$$\Delta h'_d = \frac{\overline{N_1P_1}}{\overline{P_1P_2}} \frac{(a-h)}{f} (\Delta r_1 + \Delta r_2). \tag{7}$$

In constructing figure 3, it was assumed that the distortions at O_1 and O_2 are positive in the two photographs. If it should occur that the distortion is positive in one photograph and negative in the other, the quantity $(\Delta r_1 + \Delta r_2)$ becomes the difference of the absolute values of the two distortions. In all cases the value of $(\Delta r_1 + \Delta r_2)$ will be less than $2\Delta r$, where Δr is the maximum value of the distortion. Furthermore, the ratio $(a-h)/a$ for any point lying above the datum plane will not exceed 1. If the ratio $\overline{N_1P_1}/\overline{P_1P_2}$ is denoted by k, eq 7 may be written

$$\Delta h'_d \leq \frac{2ka}{f} \Delta r. \tag{8}$$

This inequality will be true for all points that lie above the datum plane.

The ratio $\overline{N_1P_1}/\overline{P_1P_2}$ is equal to the ratio of camera altitude to stereoscopic base and is a function of the focal length of the camera objective and the amount of overlap. The values for a film 9 by 9 inches and for different percentages of overlap are given in table 2.

TABLE 2.—*Values of k (or k'), the ratio of altitude to stereoscopic base for different percentages of overlap*

Percentage of overlap	Focal length of objective		
	6 in.	7 in.	8 in.
10	0.74	0.86	0.99
20	.83	.97	1.11
30	.95	1.11	1.27
40	1.11	1.29	1.48
50	1.33	1.54	1.77
60	1.66	1.95	2.22
70	2.22	2.59	2.96
80	3.34	3.88	4.44
90	6.66	7.77	8.89

In a flight strip the customary overlap is 60 percent. The value of k for an overlap of this amount or less does not exceed 1.7, 2.0, and 2.2, for camera objectives with focal lengths of 6, 7, and 8 inches, respectively. This illustrates the advantages of the lens of shorter focal length, for a given scale factor, f/a, in minimizing the error in elevation that arises from the presence of distortion.

The horizontal displacement arising from the presence of distortion will be denoted by $\Delta l'_d$. Referring to figure 3, it is evident that a vertical through O' will always cut $\overline{EG}$, the base of the triangle $O'EG$. Furthermore, the length $\overline{OE}$ or $\overline{OG}$ will never exceed $(a-h)\Delta r/a$. Therefore,

$$\Delta l'_d \leqq \Delta r. \tag{9}$$

In eq 8 and 9, Δr is the maximum distortion on a photograph, and, consequently, $\Delta h'_d$ and $\Delta l'_d$ are the maximum errors resulting from the distortion. It is convenient to have these equations in a form

suitable for dealing statistically with the resulting errors of the map. The distortion in a photograph assumes all values from $-\Delta r$ to $+\Delta r$, with the maximum values in two zones, one near the edge of the field, the other at an intermediate distance. For a given object point, the distortion on the two photographs will, in general, be different, because the images will not fall in homologous positions on the two photographs. Given the distortion measurements for a lens, it is possible to compute the error of location and elevation for any given object point. This error will vary with the elevation of the object point as well as with the projected position of the point upon the datum plane and will range in value from the maximum positive value, through zero, to maximum values in the opposite sense, the maximum error occurring only when the distortion for the images of a given object point has its maximum value in each of the two photographs that are combined to produce a stereoscopic model. In a general discussion of this nature it is not possible to consider these errors independently, but they must be dealt with by a statistical method.

For errors that are truly "accidental" and follow the normal frequency curve, the error whose probability is one in one hundred, is approximately four times the probable error. Consequently, if the magnitudes of the errors resulting from distortion followed such a distribution law the probable error, the error that is equal to or larger than the errors for 50 percent of the points, could be assumed, with satisfactory precision, to be one fourth the maximum error that has just been deduced. Actually, however, the errors arising from distortion are systematic and this is evidenced by the regular distribution of the errors over the photograph. A typical distortion curve for a lens has been assumed and, for a large number of points, the resulting horizontal and vertical errors arising from distortion have been computed. A study of these errors indicates that 50 percent of the errors may be expected to be less than or equal to 0.4 of the maximum error. Accordingly, in order to treat the errors arising from distortion in the same manner as those arising from variation of calibrated focal length or location of principal point, the maximum error arising from distortion, multiplied by 0.4, will be considered to be a measure of the error arising from distortion and will be applied in the same manner as a probable error. This error is analogous to the probable error in that it is a "50-percent error" but differs from it in that it relates to errors that are not "accidental" in origin.
Accordingly,

$$\Delta h_d \leqq 0.8 \frac{ka}{f} \Delta r \tag{10}$$

$$\Delta l_d \leqq 0.4 \Delta r, \tag{11}$$

where $\pm \Delta h_d$ and $\pm \Delta l_d$ are contributions made by the distortion to the probable errors of elevation and horizontal displacement of a point on the map.

It should be noted that eq 10 has the reciprocal of the scale factor f/a in the right-hand member and $\pm \Delta h_d$, consequently, is the probable error of the elevation. Equation 11, on the other hand, gives probable error as a displacement on the photograph or on a map having the same scale as the photograph. These are the convenient forms of these equations because of the manner in which the allowable errors of

a map are commonly specified. If one wishes to obtain an inequality similar to that of eq 11 giving the error on a map having a scale different from that of the photograph, the right-hand member must be divided by the scale factor of the photograph and be multiplied by the scale factor of the map.

3. VALUES OF FOCAL LENGTH AND DISTORTION REPORTED FOR A LENS NOT MOUNTED IN A CAMERA

In the reports of the National Bureau of Standards on lenses submitted for test unassembled in cameras the equivalent focal length is given rather than an adjusted focal length. Several advantages result from this. Lenses are frequently submitted for test before acceptance and, when the distortions of all lenses are referred to the paraxial value of the focal length, the values permit a more direct comparison of different lenses, because no question arises as to whether or not the difference in distortion may be the consequence of a better choice of focal length rather than of greater freedom from distortion. In many cases, when a large number of lenses have been submitted for test at the same time, a measurement of the distortion at a single point, usually 30° from the axis, has been considered sufficient to classify a lens. In such cases some convention, of which the choice of the paraxial value of the focal length seems to be the simplest, is particularly necessary, as otherwise, by a modification of the value of the focal length, the distortion for the one point could be made to have any desired value. The measurement of the distortion in this manner also permits direct comparison of the values with the computed values of distortion, as given and plotted in many publications dealing with photographic objectives.[8]

IV. PRINCIPAL POINT OF THE FOCAL PLANE

1. INDEX MARKS FOR PRINCIPAL POINT

Mapping cameras utilize various devices for locating the principal or collimation point. When a glass pressure plate is employed, a cross may be etched on the side of the plate in contact with the film to register on the negative at the time of the exposure. When a pressure plate is not used, four projections in the focal plane are placed so that they are registered on the negative and are so located that lines joining the two pairs of opposite points determine the position of the principal point by their intersection. Sometimes the four index marks are registered on the film by four small optical projectors attached to the interior of the camera cone, this method giving sharper and finer lines than can be obtained by the simpler silhouette.

2. RELATION BETWEEN THE PRINCIPAL POINT AND THE AXIS OF THE LENS

It has already been mentioned that the principal point is located at the foot of the perpendicular from the center of perspective to the focal plane, and that this will not correspond with the intersection of the focal plane and the axis of the lens, if the lens is tipped from its

[8] V. Rohr, Theorie und Geschichte des Photographischen Objektivs (Julius Springer, Berlin, 1899). Handbuch der Wissenschaftlichen und Angewandten Photographie, vol. I, Das Photographische Objektiv (Julius Springer, Wien, 1932).

normal position. The errors resulting from such a tipping of the lens are not as serious as is perhaps commonly considered. In most cases the only error introduced by such a maladjustment arises from the possible blurring of the image because the plane of best focus is inclined with respect to the plane of the film. If there is a great deal of distortion a further error may be introduced because the distortion will not be symmetrical about the principal point.

3. ERROR ARISING FROM INCORRECT LOCATION OF THE PRINCIPAL POINT

When adjusting a negative in a plotting machine an error in the location of the principal point, as registered on the negative, causes the negative to be located in the machine in a position displaced in its own plane from the true position. This is illustrated in figure 4. The drawing on the left is assumed to illustrate the actual condition at the time of the exposure. The true principal point is at O'. The image of O, the point directly below the camera, coincides with the principal point. If the camera is assumed to be incorrectly calibrated, so that C' is indicated as the principal point, the final adjustment in the plotting machine leads to the implicit conclusion that the camera was vertically over the point C at the time of the exposure. This corresponds to a displacement of the camera from its actual position through the horizontal distance $\Delta ca/f$, where Δc is equal to the distance $\overline{O'C'}$, the error in the location of the principal point. As long as the camera is vertical and the terrain plane and horizontal, the photographs taken with the camera in the two positions will be identical except for the displacement of each point of the picture through the distance $\overline{C'O'}$, a characteristic that has no bearing upon the accuracy of the map. Since the two negatives are identical the control points, if lying in the reference plane, can be fitted accurately when O', C', or any other point is assumed to be the principal point. Therefore, just as an error in the focal length introduces no error when the terrain is plane

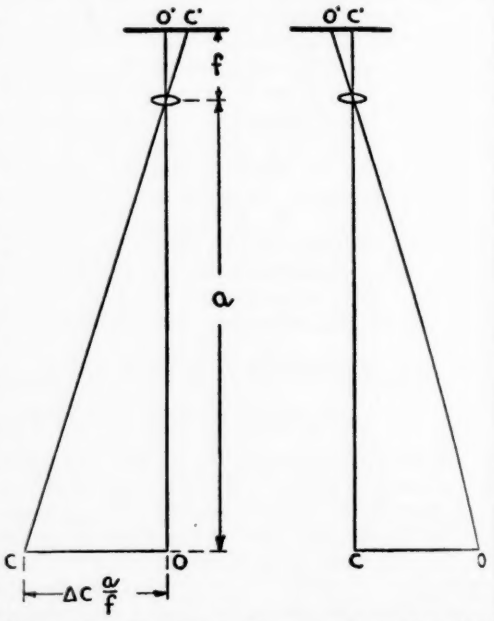

FIGURE 4.—*The error in the assumed position of the camera arising from an incorrect position of the principal point.*

The exposure was made with the camera above O, but it is assumed to have been above C because of the error in the indicated location of the principal point.

and horizontal, so an error in the location of the principal point introduces no error under similar simplified assumptions.

(a) CASE IN WHICH THE TWO OVERLAPPING PHOTOGRAPHS ARE FROM A SINGLE FLIGHT STRIP

The region to be mapped usually has depressions and elevations which produce relief parallax. In order to determine the error that results from an incorrectly located principal point, it is necessary to consider the interpretation made from two photographs that serve as members of a stereoscopic pair when the map is being made. If these photographs are successive photographs from a flight, it may be assumed, without serious error, that the camera underwent no rotation in azimuth between the two exposures. Consequently, not

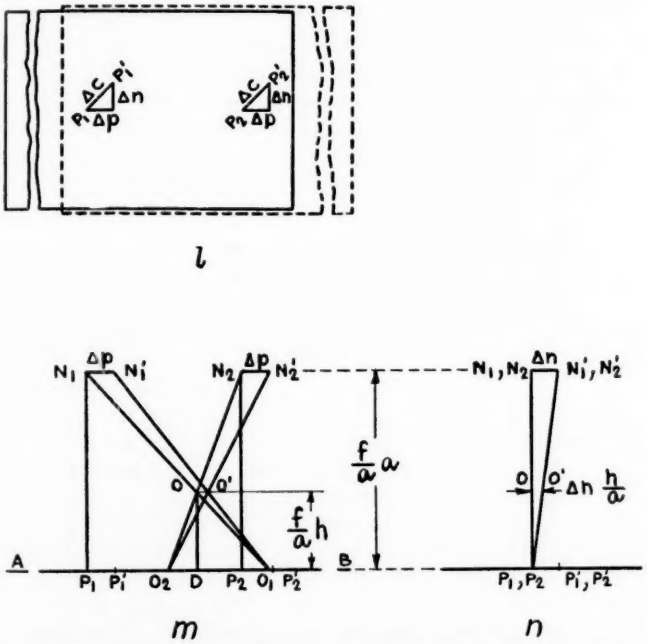

FIGURE 5.—*The error arising from an incorrectly located principal point.*

When the two overlapping photographs are selected from a single flight-strip, the displacements of the principal points, denoted by Δc, are similarly oriented in the two photographs and the elevated point at O is incorrectly located at O', a point displaced horizontally but having the correct elevation. Diagrams m and n are projections. A projected point that corresponds to two or more original points is designated by the symbols of the several points, separated by commas.

only the magnitude of the displacement of the principal point, but also the azimuth of a line joining the true principal point with the assumed principal point will have the same value for the two exposures. This is illustrated in figure 5 (l) which is a diagrammatic representation of the two photographs with the overlapping portions superposed to bring the common control points (in the datum plane) into coincidence. The two principal points are at P_1 and P_2, the assumed incorrect principal points are at P'_1 and P'_2. The displacements,

Δc, may be resolved into components Δp and Δn, parallel and normal to the stereoscopic base, $\overline{P_1P_2}$.

Figure 5(m) is an elevation in which significant points are projected on a vertical plane parallel to the stereoscopic base. $\overline{AB}$ is the trace of the plane of the photographs, and lines $\overline{P_1N_1}$ and $\overline{P_2N_2}$ represent the principal distances of the two photographs, assumed equal to the calibrated focal length. If the photographs are viewed stereoscopically from N_1 and N_2 one has a true stereoscopic model, of which the scale is f/a, where a is the altitude of the camera at the time of exposure. The point O is the position, in the model, in accordance with this scale, of an elevated point that, because of relief parallax, is imaged at O_1 and O_2 in the two photographs.

When these two photographs are mounted in a mapping machine, if the correct positions of the principal points are utilized, the point O will be correctly located at the intersection of the lines $\overline{N_1O_1}$ and $\overline{N_2O_2}$. If the principal points are assumed to be at P_1' and P_2' the photographs are viewed stereoscopically from N_1' and N_2' and the point O will be located at O', the intersection of lines $\overline{N_1'O_1}$ and $\overline{N_2'O_2}$. The lengths $\overline{N_1N_1'}$ and $\overline{N_2N_2'}$ are equal to Δp, and from similar triangles it is seen that

$$\Delta h_p=0, \tag{12}$$

where Δh_p is the error in elevation, and

$$\Delta l_p=\frac{h}{a}\Delta p, \tag{13}$$

where $\Delta l_p=\overline{OO'}$ is the component, parallel to the stereoscopic base, of the displacements of the point O on the photographs.

In figure 5(n) a second elevation is shown in which the significant points are projected on a vertical plane normal to the stereoscopic base. With this projection the points N_1 and N_1' are superposed on N_2 and N_2', respectively, and lines $\overline{N_1'O_1}$ and $\overline{N_2'O_2}$ are superposed, appearing as a single line. These two superposed lines actually intersect at the height hf/a above AB. The lengths $\overline{N_1N_1'}$ and $\overline{N_2N_2'}$ are equal to Δn and, from similar triangles it is evident that

$$\Delta l_n=\frac{h}{a}\Delta n, \tag{14}$$

where $\Delta l_n=\overline{OO'}$ is the component, normal to the stereoscopic base, of the displacements of the point O on the photographs. The component Δn, like Δp, produces no error in elevation.

From eq 13 and 14 it follows that

$$\Delta l_c=\frac{h}{a}\Delta c, \tag{15}$$

where Δl_c may be considered to be the vector displacement of the point O from its true position resulting from the vector displacement

Δc of the assumed position of the principal point from its true position. These are actual displacements measured on the stereoscopic model constructed from the photographs.

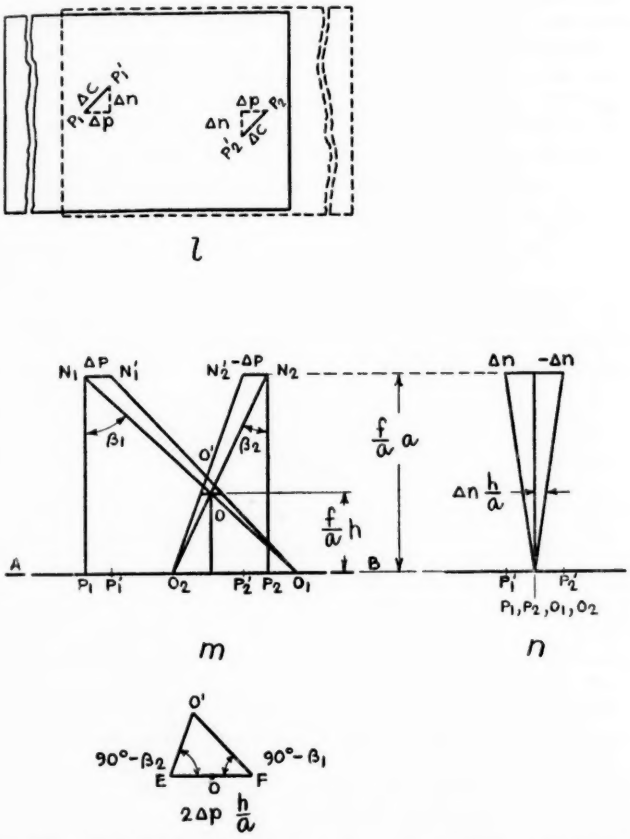

FIGURE 6.—*The error arising from an incorrectly located principal point.*

When the two overlapping photographs are selected from two adjacent flight-strips flown in opposite directions, the displacements of the principal points, denoted by Δc, differ in azimuth 180°, and the elevated point at O is incorrectly located at O', the elevation and the horizontal position both being in error. Diagrams *m* and *n* are projections. A projected point that corresponds to two or more original points is designated by the symbols of the several points, separated by commas.

(b) CASE IN WHICH THE TWO OVERLAPPING PHOTOGRAPHS ARE FROM ADJACENT FLIGHT STRIPS

If the two pictures under stereoscopic examination are overlapping photographs from two adjacent flight strips, the plane will have been flying, in most instances, down one strip and up the other. Consequently, the azimuths of the displacements of the principal points from their true positions in the two photographs will differ by 180°. This is illustrated in figure 6(l), which is a diagrammatic representation of the two photographs with the overlapping portions superposed to bring the common control points (assumed to lie in the datum plane) into coincidence. As in figure 5, the two principal points are at P_1 and

P_2, the assumed principal points at P'_1 and P'_2. The vector displacements of the points P'_1 and P'_2 from P_1 and P_2 are Δc and $-\Delta c$, respectively, the negative sign resulting from the 180° difference in sign of the two values. The displacement of P'_1 may be resolved into the components Δp and Δn, parallel and normal to the stereoscopic base, $\overline{P_1P_2}$. Similarly, the displacement of P'_2 can be resolved into the components $-\Delta p$ and $-\Delta n$.

Figure 6(m) is an elevation, similar to that shown in figure 5(m). The point O is correctly located at the intersection of lines $\overline{N_1O_1}$ and $\overline{N_2O_2}$. When points P'_1 and P'_2 are assumed to be the principal points, N'_1 and N'_2 becomes the assumed centers of perspective and O is located at O', the intersection of lines $\overline{N'_1O_1}$ and $\overline{N'_2O_2}$. Also it is evident from the figure that O' will, in general, be displaced from its true position both in vertical and horizontal directions. The point O' is at the upper vertex of a small triangle with the base horizontal and point O located at its midpoint. The length of the base is $2\Delta ph/a$. By geometrical analysis similar to that used in connection with figure 3, it can be shown that

$$\Delta h_p = 2\frac{h\overline{N_1P_1}}{f\overline{P_1P_2}}\Delta p$$

$$= 2\frac{k'h}{f}\Delta p. \tag{16}$$

In this equation, Δh_p is the error in elevation resulting when the principal points of two overlapping photographs are displaced a distance, Δp, in opposite directions along the stereoscopic base. Also k' is the ratio $\overline{N_1P_1}/\overline{P_1P_2}$, as tabulated in table, 1, and is distinguished from k of eq 10 because the customary overlap for successive flight strips is 30 percent instead of 60 percent, as in a given strip. Values of k' are 0.95, 1.11, and 1.27, respectively, for focal lengths of 6, 7, and 8 inches.

In the triangle $EO'F$ the horizontal displacement of the point O' will be less than one-half the base, provided O lies vertically over a point falling between P_1 and P_2. Consequently, one may write

$$\Delta l_p \leq \frac{h}{a}\Delta p, \tag{17}$$

where Δl_p represents the actual displacement of O' from O, as measured on the photograph.

Figure 6(n) is an elevation in which the significant points are projected on a plane normal to the stereoscopic base. Unlike figure 5(n), the components Δn and $-\Delta n$ are here turned in opposite directions. The lines $\overline{N_1'O_1}$ and $\overline{N_2'O_2}$ do not intersect at all (their projections intersect in figure 6(n), but at this point the lines themselves are separated by the distance $\overline{O_1O_2}$). One line lies on one side of the vertical plane containing the stereoscopic base (the trace of this plane is $\overline{N_1O_1}$) and the other line lies on the other side. The point of nearest approach for these two lines has approximately the same elevation as the point O' in figure 6(m). It is evident from this figure, where Δn and $-\Delta n$ are shown greatly exaggerated, that strict stereoscopic fusion cannot

be attained for this condition, but it is attainable in satisfactory degree even though the two fields in the viewing instrument will be at slightly different heights. Reference to figure 6(n) shows that neither line departs from the correct position for the intersection more than $\Delta n\, h/a$, and it appears reasonable to assume that the horizontal position of the point will be obtained with a horizontal error not exceeding this amount. The components Δn and $-\Delta n$ do not introduce any significant error in the elevation.

(c) EQUATIONS GENERALIZED TO APPLY TO THE TWO PRECEDING CASES (a) AND (b)

A consideration of eq 12 and 15 of case (a) and eq 16 and 17 of case (b) shows that one may write

$$\Delta h_c \leqslant 2\frac{k'h}{f}\Delta c \tag{18}$$

$$\Delta l_c \leqslant \frac{h}{a}\Delta c. \tag{19}$$

These equations are applicable to either case (a) or case (b) and cover all errors arising from incorrectly located principal points. In eq 18 and 19, Δh_c and Δl_c are the errors of elevation and horizontal displacement corresponding to the error Δc in the location of the principal point. The constant k' is taken from table 1, the overlap being that for adjacent flight strips. As for the previous pairs of equations, eq 18 gives the actual error in elevation and eq 19 gives the displacement as measured on the photograph.

In eq 18 and 19, if $\pm\Delta c$ is the probable error of the location of the principal point, $\pm\Delta h_c$ will be the resulting contribution to the probable errors of the elevation and $\pm\Delta c$ the contribution to the probable error of the location of a point on the photograph.

V. DEPARTURE OF FILM FROM THE FOCAL PLANE

Photographic film, rather than plates, is commonly used for photogrammetric purposes and the assumption, in all the foregoing discussion, has been that the sensitive photographic emulsion lies in a plane. A suction or pressure back, or a pressure plate is commonly used to flatten the film. If this does not operate perfectly, it is to be expected that the film will be concave toward the objective, and it seems probable that the curvature will be different in the direction in which the film is rolled and in a direction at right angles to it. If a portion of the film is in advance of or behind the position that it should occupy, the image falling upon this portion of the film will be displaced the distance $\Delta d \tan \beta$ toward or from the center of the negative, when Δd is assumed to be the displacement of the film. If the film is curved in an approximately symmetrical manner from the focal plane there will be a systematic displacement over the field somewhat resembling that arising from distortion, and it is a reasonable assumption that this will be a maximum at the edge of the field. If the curvature of the film were quantitatively known and sufficiently uniform from exposure to exposure, a change in the value of the calibrated focal length could be made in order to secure compensation, as was done for distortion. For distortion, with a field of view of 60°, the correction

to the calibrated focal length is approximately equal to the distortion at the edge of the field referred to the paraxial focal length, and, as a first assumption, it appears that a somewhat similar relation might exist between a regular departure of the emulsion from a plane and the change in the calibrated focal length to compensate for it. If, therefore, it is assumed that the film curves from the nominal plane surface by 0.1 mm, the resulting error is approximately the same as would result from an error of 0.1 mm in the calibrated focal length, but it is not the same in all parts of the field and cannot be readily compensated.

By decreasing focal length and film size one can increase the expectancy of obtaining planeness of film, but unfortunately the error introduced by a given departure from planeness increases with decrease of focal length, so that exact information regarding the manner in which the departure from planeness diminishes with size of the film is necessary before it can be said whether or not reduction of focal length is advantageous in respect to the error arising from curvature of film. It is important to note that when a 9- by 9-inch film is retained and the angular field increased by the use of a lens of shorter focal length, the planeness of the film must be improved if the error from this source is not to increase.

All of these considerations indicate that the planeness of the film at the time of exposure is an important requirement of the precision camera and that any increase in the accuracy of the precision camera may require a more complicated or better designed device for holding the film flat. This immediately suggests the use of plates rather than films in the photogrammetric camera. However, plates as commercially manufactured are not plane, and, in many cases, the holders are of such a nature that the plate is bent by the springs that serve to retain them in the focal plane. Arnulf and Perrin [9] have made measurements on photographic plates and report departures from planeness as great as 0.26 mm when the plate is in the plateholder of an airplane camera. P. Lafouasse [10] presents data indicating that the films measured by him were somewhat more nearly plane than the photographic plates that he measured. It is probably advisable that additional quantitative data be secured regarding the planeness of films and plates in the types of airplane cameras that are used in this country, and the curvature of the film or plate may be one of the important factors setting a limit to the precision that can be obtained with the photogrammetric cameras now in use.

VI. TYPES OF SHUTTERS

1. BETWEEN-THE-LENS SHUTTER

The type of shutter having its leaves mounted within the lens and between the components, is the one most favored for airplane photography. With this type of shutter all portions of the film are exposed at the same time. Consequently, if the duration of the exposure is too great, with respect to the translatory or angular velocity of the plane, the resulting negative may lack definition because of the movement of the plane, but in no case will there be distortion analogous to that to be considered later in connection with the focal-plane shutter.

[9] Arch. Int. Photogrammetry **7**, 2d part, 202 (1930–31).
[10] Bul. soc. franç. phot. **24**, 29–35(1937).

The fundamental requirement for a between-the-lens shutter is that it should open as rapidly as possible to its maximum opening, remain open for a given period of time, and then close in the shortest possible time. An ideal shutter would consume zero time in its opening and closing. In such a case the exposure may be considered equal to the product of the area of the shutter aperture by the elapsed time from the opening to the closing of the shutter. During the actual performance of a shutter one does not have the aperture of the shutter completely open during the entire period that elapses between the beginning of the opening and the end of the closing of the shutter. Consequently, one obtains the effective exposure by integrating the area of the varying shutter opening with respect to the time, the integration being extended to cover the over-all length of the exposure. The ratio of the effective exposure to the ideal exposure is defined as the efficiency of the shutter. It is evident that the efficiency of the shutter, in general, will decrease as the exposure is shortened because a proportionately greater time is consumed in opening and closing. It is also evident that the efficiency of a given shutter will increase as a lens is stopped down because, with the smaller diaphragm, the shutter requires less time to open to the full extent of the smaller diaphragm. The motion of the plane sets a limit to the maximum duration of an exposure that can be made without blurring, and a high efficiency is important because it permits more light to reach the film for an exposure of given duration. Lutz and Doyle [11] describe a shutter with an efficiency of 93 percent for a one-fiftieth second exposure and 80 percent for an exposure of one one-hundred-fiftieth second.

It is important that successive exposures for a given setting of the speed control should be identical, and desirable that the actual speeds do not depart greatly from the nominal speeds. For a precise camera the shutter should be so designed that the lenses can be removed for cleaning or disassembly of the shutter and replaced without necessitating a recalibration of the camera. Some users of cameras desire a shutter sufficiently simple and robust to be repaired in the field and others consider that a shutter should give the minimum of trouble, but that it is desirable to permit no alteration or adjustment of the shutter except when it is returned to the home office.

2. FOCAL-PLANE SHUTTER

(a) EFFICIENCY

The focal-plane shutter consists of an opaque blind or curtain containing a transverse slit that travels across the face of the photographic film, approximately in the focal plane. The light reaches the film through the slit and the exposure can be varied by altering the velocity of travel or varying the width of the slit. Adhering to the usual assumptions of geometric optics, the cone of rays proceeding from an object point has its vertex at the film. Therefore, a section of the light cone lying in the focal plane shrinks to a point, and if the curtain cuts the cone in this plane, the cone is entirely intercepted by the curtain or entirely transmitted by the slit at any given instant. Consequently, any small area of the film is illuminated by the entire aperture of the lens during the entire period of the exposure and no time

[11] Photogrammetric Engineering **3**, No. 3, 1–6 (1937).

is lost by the process of opening or closing the shutter. Therefore, if the traveling slit could be placed exactly in the focal plane the efficiency of the shutter would be 100 percent and this type of shutter would be realized in its ideal form.

Obviously, however, it is impracticable to place the curtain of the shutter in the focal plane and it is not unusual to find it a centimeter or more from the surface of the film. In this case the section of the cone of light in the plane of the curtain is a circle of appreciable diameter and the aperture of the lens is not entirely unobstructed until the curtain has travelled a distance equal to the diameter of this section. Consequently, the efficiency of the shutter in its practicable form is not 100 percent and, in important cases, may be quite as low as for the between-the-lens type of shutter. The efficiency of the shutter decreases as the section of the cone of light in the plane of the curtain increases, and this increases as the aperture of the lens is increased or as the distance from focal plane to plane of shutter curtain increases. For the shorter exposures, for which the slit width is narrow, the time required for uncovering the entire aperture of the lens is greater with respect to the total time of exposure than for a wider slit. Consequently, the departure from ideal efficiency is greater for the narrower slit widths. For typical values, the efficiency of the focal plane shutter as a function of the slit width, lens aperture, and distance of curtain from film is given in table 3.

TABLE 3.—*Efficiency of focal-plane shutter*

Distance from curtain to focal plane	Width of slit, in millimeters, with *f*/4 aperture			Width of slit, in millimeters, with *f*/8 aperture			Width of slit, in millimeters, with *f*/16 aperture		
	10	20	30	10	20	30	10	20	30
mm	%	%	%	%	%	%	%	%	%
10	80	89	92	89	94	96	94	97	98
20	67	80	86	80	89	92	89	94	96
30	57	73	80	73	84	89	84	91	94

A focal-plane shutter with a 20-mm slit, 20 mm from the focal plane, may be considered as typical of modern practice for shutters on airplane cameras. For such a shutter the efficiencies for lens apertures of *f*/4, *f*/8, and *f*/16 are shown in table 3 to be 80, 89, and 94 percent, respectively.

(b) DISTORTION INTRODUCED BY FOCAL-PLANE SHUTTER

In the preceding section the efficiency has been expressed as the ratio of the actual exposure to the exposure obtained with an ideal shutter having the same over-all duration of exposure for a given point on the photographic film. This over-all duration of the exposure, for a given movement of the airplane, has a maximum value that cannot be exceeded without the presence of blur and loss of definition resulting from the movement of the plane. With the focal-plane shutter, unlike the between-the-lens shutter, different portions of the film are exposed successively as the slit travels across the field of the lens. Consequently, although the exposure for a restricted area of the film is sufficiently short to "stop" the motion and eliminate blur, it is still possible that the plane may move appreciably before the time

required for exposing the entire area of the film has elapsed. If this is the case, different parts of the photograph are made from different positions in space and the photograph is distorted.

The typical values for a focal plane shutter that were used in the preceding section will again be considered. If the slit is 20 mm wide and the exposure is 1/75th second, the curtain travels with a speed of 1,500 mm per second. The direction of travel is the short dimension of the photograph, and it therefore requires somewhat more than a tenth of a second for the curtain to travel 175 mm (7 in.), the width across the picture. If the plane is traveling at a speed of 200 miles per hour, it travels nearly 30 feet in a tenth of a second. Consequently, the extreme edges of the film are exposed from positions 30 feet apart. There is no true center of perspective for a picture taken under these conditions, because the portion of the negative exposed by the initial movement of the shutter curtain has a center of perspective 30 feet distant from that corresponding to the portion of the negative exposed as the shutter slit left the field of view. If the focal length of the lens is 6 inches and the altitude of the plane is 15,000 feet, this corresponds to a progressive displacement of the principal point of 0.3 mm on the photograph. Even if the curtain speed is increased so that the same slit width gives a speed of 1/225th second, the displacement of the principal point for different parts of the negative is 0.1 mm.

A similar displacement of the principal point will also arise from the angular velocity (rolling or pitching) of the airplane. Estimates, based on several intervals of 30 seconds each in smooth air, indicate a value of $\frac{1}{8}°$ per second (0.002 radian per second) as the maximum value that was encountered, although large variations from this value may be anticipated for different types of planes and for different pilots. With this value of the angular velocity, if the elapsed time for an exposure is 0.1 second, the airplane will swing through an angle of 0.0002 radian during its progress. The corresponding displacement of the principal point for a lens with a focal length of 150 mm is 0.03 mm. This indicates that the distortion arising from the angular velocity of the plane will not be as great as that arising from the velocity of translation when one is flying over smooth and uniform terrain. When an airplane is flying over nonuniform territory, where upward air currents and bumpiness result, angular accelerations exceeding these values are probable and may introduce serious and unpredictable amounts of distortion in the photographs.

If the direction of travel of the curtain shutter is parallel to the direction in which the airplane moves, it will introduce a distortion consisting of a lengthening or shortening of the picture in the direction of travel. If the curtain travels in a direction at right angles to the motion of the airplane, the distortion will be of a different character in which a square is photographed as a rhombus.

The large ratio of the time that elapses during the exposure of the entire picture to the length of exposure for a given small area of the picture is the fundamental disadvantage of the focal-plane shutter. This ratio decreases as the width of the slit is increased but, with the wider slit, it is necessary to correspondingly increase the velocity of travel of the curtain, a matter of some difficulty, if a short exposure is to be secured. The ratio of total elapsed time to exposure time for a series of slit widths follows. In this tabulation it has been assumed that the film is 7 by 9 inches and that the direction of travel of the

slit is parallel to the short dimension of the film. It will be noted that even for a 100-mm (4-in.) slit the elapsed time is three times the exposure time. With a between-the-lens shutter, for all speeds and apertures, the value of this ratio is 1.

Slit width	Ratio
mm	
20	10
40	5
60	4
80	3
100	3

VII. ACCESSORIES IN OPTICAL PATH OF CAMERA

1. FILTER

(a) TYPES OF FILTERS

In airplane photography the exposures are commonly made through filters selected to absorb the light of shorter wave length in order to eliminate the loss of contrast produced by the blue haze that results from the scattering of light by the atmosphere. These filters are light yellow in color and, as the speeds of the available photographic emulsions increase, it is probable that filters of deeper color will be employed. (For special purposes deep-red filters and infrared sensitive film are now used.) The filters are of three materials (a) gelatine film, unsupported and unprotected, and usually placed within the lens, between the components, (b) gelatine film mounted with canada balsam between two plates of plane parallel glass, and (c) filters of colored glass, ground and polished with the surfaces plane and parallel.

The gelatine film is commonly mounted within the lens between the components in order to protect it from the effects of varying humidity. It is only the extreme thinness of the film that permits its use in this manner. Placing the filter between the components has the same effect, optically, as changing their spacing. Furthermore, the two surfaces of the filter, although approximately parallel, always depart greatly from planeness. Even under the most favorable conditions the use of a filter in this manner may be expected to affect the definition unfavorably. There is also the further danger that moisture will eventually reach the filter, even when mounted between the components, and that the filter will develop pronounced wrinkles that may ruin a series of exposures before their presence is detected. The necessary removal of the lens cells from the shutter for replacement of the gelatine filter from time to time is an additional undesirable feature. In view of these disadvantages, filters of gelatine film should not be used for photographic mapping purposes although, for experimental work in connection with the selection of a filter shade for a given emulsion, the use of gelatine filters is a convenient and inexpensive procedure.

The gelatine filter, mounted between glass plates, has one disadvantage. The balsam tends to deteriorate with age, the glass plates partially separate, and the filter assumes a nonuniform shade, or a feathery structure resulting from crystallization appears.

A filter of colored glass performs exactly as the filter composed of a gelatine film cemented between two plates, but offers the advantage that it is entirely unaffected by humidity and does not deteriorate with age. For some purposes for which filters are required, it is not possible to obtain glass of the desired color and a cemented type of filter must be used. For eliminating atmospheric haze, satisfactory filters of colored glass are available, and this form of filter is preferable to the cemented type.

(b) DISTORTION INTRODUCED BY FILTER

Filters, either of colored glass or of the cemented type, are several millimeters thick and should never be placed between the components of a lens unless the manufacturer has designed the lens to be used in this manner. If the filter is placed between the lens and the focal plane, it will introduce appreciable amounts of negative distortion. The resulting distortion is of the same amount as that introduced by a pressure plate of the same thickness and this can be ascertained by reference to table 5, which gives the distortion at different angular distances from the axis for several glass thicknesses. Lenses have been built with a filter permanently mounted on the lens barrel, following the last component with the entire system designed to form a unit free from distortion. If a filter of good quality is mounted in front of a lens it will not introduce any distortion. If the surfaces of the filter are plane but not parallel it will act as a weak prism and deviate the rays slightly before they enter the lens. The angular deviation will be approximately equal to half the angle between the two surfaces. As a result of this deviation, the camera, when in a true vertical position, will make a photograph as though it were tilted through the angle of deviation produced by the prismatic filter. To illustrate this, the difference in thickness at opposite edges of a prism is 0.5 mm for a filter 50 mm square (a relatively large deviation from parallelism) a photograph taken with the camera in a vertical position will show a tilt of approximately 15 minutes. If the resulting photograph is properly adjusted in the plotting machine this will cause no error, as the effect of this tilt arising from the filter will be eliminated in the same manner that tilt arising from a nonvertical position of the camera is eliminated. If a filter is always to be used with a given camera, it is feasible to adjust the level with respect to the camera so that a picture without tilt is obtained when the level indicates horizontality.

(c) EFFECT OF FILTER UPON DEFINITION AND CAMERA CALIBRATION

It should be clearly understood that a filter, used with a photographic lens, is just as much a part of the optical system as any component of the lens and that defects in its quality are just as detrimental to good definition as are similar defects of the lens. Consequently, it is not good practice to purchase an expensive photographic objective with precisely polished surfaces and equip it with a filter of indifferent quality. An interference test, applied to the surfaces of the filter, should show plane surfaces of the same quality as lens surfaces, and the glass should be equally free from internal heterogeneities. If the filter has slightly spherical surfaces, its use will change the focal length and therefore affect the calibration of the camera but this

defect will not be appreciably present in filters of good quality. A wedge-shaped filter in front of the lens does not alter the position of the principal point. If a filter is of good quality and is to be used in front of the lens it is not necessary to calibrate the camera with the filter in position, although the National Bureau of Standards does calibrate cameras in this manner upon request. This method of test is advisable when it is suspected that the filter may impair the definition.

2. PRESSURE PLATE

The newer types of cameras are equipped with suction or pressure backs to hold the film plane during the exposure. Nevertheless, it seems advisable to discuss the action of the pressure plate of glass against which the film is pressed by a spring because many cameras with this equipment are still in use. There is a loss of light amounting to approximately 10 percent of that which would otherwise reach the photographic emulsion because of reflection at the two surfaces of the pressure plate. Unfortunately, a portion of this "lost" light will undergo multiple reflection at the two surfaces of the pressure plate and ultimately reach the emulsion as stray light, tending to reduce the contrast and detract from the brilliance of the image. If the pressure plate does not have surfaces of good quality, this will be somewhat detrimental to the quality of the image but the pressure plate is so close to the focal plane that its surfaces can affect definition relatively little as compared with the surfaces of the lens components.

Probably the most serious objection to the pressure plate has been the large amount of negative distortion that it introduces. This distortion is proportional to the thickness of the plate and increases from the center of the field outward. Values of the distortion for a pressure plate having the refractive index 1.52 are given in table 4.[12]

TABLE 4.—*Linear distortion (in millimeters) produced by a plane parallel plate behind the lens*

Angular distance from center of field (degrees)	Thickness of plate (in millimeters)				
	3	5	10	15	20
0	0.00	0.00	0.00	0.00	0.00
10	.00	.00	−.01	−.02	−.02
20	−.03	−.04	−.08	−.13	−.17
30	−.10	−.16	−.31	−.47	−.63
40	−.26	−.43	−.85	−1.28	−1.71

The large amount of distortion introduced by the pressure plate can be entirely and satisfactorily eliminated if the lens with which it is used has a corresponding amount of positive distortion. To design such a lens does not offer any great difficulty but this method of compensation for a pressure plate has not been employed. Such a procedure would necessitate the production of a greater variety of lenses for pressure plates of different thicknesses with consequent increased cost and the use of the suction or pressure back has become the more convenient and desirable construction.

WASHINGTON, October 24, 1938.

[12] For a 7- by 9-inch negative the angular distances to the extreme corners of the field are 55.4°, 44.0°, and 35.9°, respectively, for focal lengths of 100, 150, and 200 mm. For a 9- by 9-inch negative the corresponding angular distances are 58.2°, 47.1°, and 38.9°, respectively.

U. S. DEPARTMENT OF COMMERCE NATIONAL BUREAU OF STANDARDS

RESEARCH PAPER RP1178

Part of Journal of Research of the National Bureau of Standards, Volume 22, February 1939

MUTUAL INDUCTANCE AND FORCE BETWEEN TWO COAXIAL HELICAL WIRES

By Chester Snow

ABSTRACT

A formula is found for the mutual inductance and force between two coaxial helical wires which, in addition to the well-known current-sheet formula, contains small correction terms, one of which represents the axial components of current; one the finite diameters of the wires; and another ω_a, which depends upon the relative azimuths of the helices, arises, naturally, from the actual helical form of the windings. The pitch of the windings may be different in the two, but each is considered so small in comparison with the cylindrical radii that terms relatively smaller than the square of this ratio may be neglected. The number of turns is not necessarily an integer.

CONTENTS

		Page
I.	Introduction	239
II.	Formal expressions for the mutual inductance and force between two coaxial helices	241
III.	The principal terms ω_0 and ω'_0	247
IV.	Effect of axial current in helices and lead wires	251
V.	The azimuthal terms	255
VI.	The helix equivalent to a helical wire	263
VII.	Application to the current balance used in the National Physical Laboratory	266
VIII.	Summary	268

I. INTRODUCTION

A formula of precision sufficient for absolute electrical measurements of the mutual inductance or force between two coaxial helical wires does not appear to have been developed to the same degree of precision as in the case of a self inductance. The principal part corresponding to current sheets is well known, but even if the construction were perfect, there remain certain small correction terms which must be found by starting with an idealization of the coils which is nearer the actual than a current sheet. The procedure here adopted as the most natural is to formulate the mutual inductance as Neumann's double-line integral and to expand the integrand in a Fourier's series as a function of the difference of the angular parameters of the two helices. The constant term of this series gives the current sheet formula, provided both angular and axial components of current are included in this term. The remainder of the series gives a correction depending upon azimuth of the two helices, which is relatively small for such closely wound coils as are used in practice. By restricting the problem to cases where the windings of the one do not come too close to those

of the other, we avoid most of those evaluations of proximity effect so troublesome in deriving a formula for self inductance.

The equations defining the first helix, h_1, may be taken as the three equations which express the rectangular coordinates, x_1, y_1, z_1, of any point, P_1, on it, in terms of a single independent parameter. The most suitable line parameter in this case is the angle θ_1, where x_1, r_1, and θ_1 are the cylindrical coordinates of P_1. If the rectangular axes are right-handed, a positive pitch, $2\pi p_1$, corresponds to a right-handed helix. If the plane $x=x_{i_1}$ and the azimuth $\theta=\theta_{i_1}$ are those of its initial point, and $x=x_{e_1}$, $\theta=\theta_{e_1}$ its end point, and if r_1 is its cylindrical radius, the equations of h_1 are

$$\left.\begin{aligned} x_1&=x_{i_1}+p_1(\theta_1-\theta_{i_1})\\ y_1&=r_1\cos\theta_1\\ z_1&=r_1\sin\theta_1 \end{aligned}\right\}, \text{ where } \theta_{i_1}\leqq\theta_1\leqq\theta_{e_1}. \tag{1}$$

Its axial length, l_1, is given by

$$l_1=x_{e_1}-x_{i_1}=p_1(\theta_{e_1}-\theta_{i_1})\equiv 2\pi p_1 N_1. \tag{2}$$

Its element of length has the magnitude

$$ds_1=\sqrt{r_1^2+p_1^2}\,d\theta_1 \tag{3}$$

and the direction cosines

$$\frac{dx_1}{ds_1}=\frac{p_1}{\sqrt{r_1^2+p_1^2}},\ \frac{dy_1}{ds_1}=-\frac{r_1\sin\theta_1}{\sqrt{r_1^2+p_1^2}},\ \frac{dz_1}{ds_1}=\frac{r_1\cos\theta_1}{\sqrt{r_1^2+p_1^2}}. \tag{4}$$

If two helices of the type in eq 1 differ only in the values of their two constants, x_{i_1} and r_1, they may be considered as filaments of the same helical wire, w_1, where, for the purpose of this paper, a "helical wire" is defined as follows:

To specify a helical wire, w_1, of pitch $2\pi p_1$ and axial length l_1 and with a wire radius, ρ_1, whose central filament has the cylindrical radius r_1, the initial plane and azimuth of this central filament being x_{i_1} and θ_{i_1}, the plane and azimuth of its end point, x_{e_1} and θ_{e_1}, we define it as the totality of all helices, h_1', represented by eq 1 with (x_{i_1}' and r_1' in place of x_{i_1}, r_1), provided that the two constants, x_{i_1}' and r_1', lie in the range

$$(x_{i_1}'-x_{i_1})^2+(r_1'-r_1)^2\leqq\rho_1^2 \tag{5}$$

All azimuthal planes cut this wire in circular sections of radius ρ_1, the initial face of the wire in the plane $\theta=\theta_{i_1}$, and its end face in the plane $\theta=\theta_{e_1}$. All its filaments have the same terminal azimuths and the same axial length l_1. Giving θ_{i_1} a variation while holding l_1 constant corresponds to a rigid rotation of the wire about the x axis, while a variation in x_{i_1} with l_1 constant is a translation parallel to that axis.

The second helical wire, w_2, coaxial with w_1 is specified, as above, with subscripts 2. It is assumed that p_1 and p_2 are both positive; that is, w_1 and w_2 are both right-handed helical axes or both left-handed, depending upon whether the coordinate axes are chosen right-handed or left-handed.

The total "number of turns," N_1 and N_2, are not necessarily integers, as no essential simplification in the final formulas would be obtained by placing such a restriction upon the generality of their application.

The associated current sheet of a helix is defined as a circular cylindrical surface coaxial with it, having the same radius and end planes, on which the linear density of current has the angular component $j_\theta = n = 1/2\pi p$ and the axial component $j_x = 1/2\pi r$. The mutual inductance between the sheets of the two helices will be denoted by $m_{s_1 s_2} = m_\theta + m_x$.

The mutual inductance between one helix and the current sheet of the other is identical with that of the two sheets, and this statement holds for each component of $m_{s_1 s_2}$ separately, the part m_θ being due to their angular components of current and m_x due to their axial currents. The latter, m_x, may also be interpreted as the mutual inductance between one of the sheets and any straight line which is a generator of the other.

A definition will be given later of a helix which is equivalent to a helical wire, so that the associated current sheet of a helical wire is that of its equivalent helix.

The equivalent helix of a wire has the same pitch, terminal end planes, (and hence axial length), as the central filament of the wire, but a slightly different cylindrical radius, depending upon the wire radius and the nature of the current distribution in the wire, which is assumed to flow everywhere in the direction of the generating helical filament, its magnitude being a function of r.

Hence the axial length adopted here for that of the current sheet of a helical wire is in harmony with that generally accepted. All single-layer solenoids are, in fact, helical wires, but when N is an integer they have generally been treated by idealizing them as N equal coaxial circular turns of wire, their central planes equally spaced at $x = 2\pi pn$, $n = 0, 1, 2, 3, \ldots N-1$, so that the distance between central planes of the first and last turn is $2\pi pN - 2\pi p$. If all these circular turns are cut by a plane through the x axis and each given a shear, they go exactly into the "helical wire" here defined. The current sheet associated with this series of circular turns of wire is generally taken with length $2\pi p$ plus the axial distance $2\pi pN - 2\pi p$ between central planes of the first and last wire, that is, $2\pi pN$, which is the length adopted here in general, although we do not restrict N to be integral.

II. FORMAL EXPRESSIONS FOR THE MUTUAL INDUCTANCE AND FORCE BETWEEN TWO COAXIAL HELICES

The mutual inductance, m, between the helix h_1, and that h_2 is here defined by the Neumann's double-line integral

$$m = \int ds_1 \int ds_2 \frac{\cos(ds_1, ds_2)}{\sqrt{(x_2-x_1)^2+(y_2-y_1)^2+(z_2-z_1)^2}}.$$

Letting

$$R^2(\psi) = r_1^2 + r_2^2 - 2r_1 r_2 \cos\psi, \tag{6}$$

this becomes

$$m=\int_{x_{i_1}}^{x_{e_1}} dx_1 \int_{x_{i_2}}^{x_{e_2}} dx_2 \frac{\frac{r_1 r_2}{p_1 p_2}\cos\psi(x_1,x_2)+1}{\sqrt{(x_2-x_1)^2+R^2[\psi(x_1,x_2)]}}, \tag{7}$$

where $\psi(x_1,x_2)$ is a function of (x_1,x_2) given by

$$\psi(x_1,x_2)=\frac{x_2}{p_2}+\left[\theta_{i_2}-\frac{x_{i_2}}{p_2}\right]-\frac{x_1}{p_1}-\left[\theta_{i_1}-\frac{x_{i_1}}{p_1}\right] \tag{8}$$

The part of m which is due to the angular components of current in the two helices is that part of the integral in eq 7 attributable to the first part of the numerator $r_1 r_2 \cos\psi/p_1 p_2$; the part coming from the item 1 in the numerator is due to their x-components or axial components of current. The latter is a small quantity compared with the former (in general, of second order, when p_1/r_1 and p_2/r_2 are both small quantities of the first order).

Writing eq 7 in the form

$$m=\int_{x_{i_1}}^{x_{e_1}} dx_1 \int_{x_{i_2}}^{x_{e_2}} dx_2 f[x_2-x_1,\psi(x_1,x_2)]$$

and changing the variable x_2 to x' by the substitution $x'=x_2-x_1$ gives

$$m=\int_{x_{i_1}}^{x_{e_1}} dx_1 \int_{x_{i_2}-x_1}^{x_{e_2}-x_1} f[x',\psi(x_1,x'+x_1)]dx'$$

Next, changing the variable x_1 to x'' by the substitution $x''=x_{e_2}-x_1$ gives

$$\begin{aligned}
m&=\int_{x_{e_2}-x_{e_1}}^{x_{e_2}-x_{i_1}} dx'' \int_{x''-(x_{e_2}-x_{i_2})}^{x'} f[x',\psi(x_{e2}-x'',x'-x''+x_{e2})]dx' \\
&=\int_{x_{e_2}-x_{e_1}}^{x_{e_2}-x_{i_1}} dx'' \left\{\int_0^{x'} f[x',\psi(x_{e2}-x'',x_{e2}-x''+x')]dx' \right. \\
&\qquad \left. -\int_0^{x'-(x_{e_2}-x_{i_2})} f[x',\psi(x_{e2}-x'',x_{e2}-x''+x')]dx'\right\} \\
&=\int_0^{x_{e_2}-x_{i_1}} dx'' \int_0^{x'} f[x',\psi(x_{e2}-x'',x_{e2}-x''+x']dx' \\
&-\int_0^{x_{e_2}-x_{e_1}} dx'' \int_0^{x'} f[x',\psi(x_{e2}-x'',x_{e2}-x''+x']dx' \\
&-\int_{x_{e_2}-x_{e_1}}^{x_{e_2}-x_{i_1}} dy \int_0^{y-(x_{e_2}-x_{i_2})} f[x',\psi(x_{e2}-y,x_{e2}-y+x')]dx'
\end{aligned}$$

In the last double integral, the variable of integration x'' has merely been replaced by y in order that the symbol x'' may be used in another sense, so that the four integrals into which m is resolved in eq 9 below shall each have the same designation of their two variables, and shall have limits of the same general form. In the last double integral we next change the variable y to x'' by the substitution $x''=y-(x_{e_2}-x_{i_2})$,

and it becomes $+\int_{x_{i_2}-x_{e_1}}^{x_{e_2}-x_{e_1}} dx'' \int_0^{x'} f[x', \psi(x_{i_2}-x'', x_{i_2}-x''+x')]dx'$.

Writing the x'' integral of this in the form

$$\int_0^{x_{i_2}-x_{e_1}} (\quad)dx'' - \int_0^{x_{i_2}-x_{i_1}} (\quad)dx''$$

gives

$$\begin{aligned} m = &\int_0^{x_{e_2}-x_{i_1}} dx'' \int_0^{x'} f[x', \psi_{e_2 i_1}(x', x'')]dx' \\ &- \int_0^{x_{e_2}-x_{e_1}} dx'' \int_0^{x'} f[x', \psi_{e_2 e_1}(x', x'')]dx' \\ &+ \int_0^{x_{i_2}-x_{e_1}} dx'' \int_0^{x'} f[x', \psi_{i_2 e_1}(x', x'')]dx' \\ &- \int_0^{x_{i_2}-x_{i_1}} dx'' \int_0^{x'} f[x', \psi_{i_2 i_1}(x', x'')]dx', \end{aligned} \tag{9}$$

where

$$\left.\begin{aligned} \psi_{e_2 i_1}(x', x'') &= \frac{x'}{p_2} + \left(\frac{1}{p_1} - \frac{1}{p_2}\right)x'' + \theta_{e_2} - \theta_{i_1} - \left(\frac{x_{e_2}-x_{i_1}}{p_1}\right) \\ \psi_{e_2 e_1}(x', x'') &= \frac{x'}{p_2} + \left(\frac{1}{p_1} - \frac{1}{p_2}\right)x'' + \theta_{e_2} - \theta_{e_1} - \left(\frac{x_{e_2}-x_{e_1}}{p_1}\right) \\ \psi_{i_2 e_1}(x', x'') &= \frac{x'}{p_2} + \left(\frac{1}{p_1} - \frac{1}{p_2}\right)x'' + \theta_{i_2} - \theta_{e_1} - \left(\frac{x_{i_2}-x_{e_1}}{p_1}\right) \\ \psi_{i_2 i_1}(x', x'') &= \frac{x'}{p_2} + \left(\frac{1}{p_1} - \frac{1}{p_2}\right)x'' + \theta_{i_2} - \theta_{i_1} - \left(\frac{x_{i_2}-x_{i_1}}{p_1}\right) \end{aligned}\right\} \tag{10}$$

In what follows we shall use x (positive or negative) to represent one of the following four x-differences, and θ_x for the associated constant azimuth-difference.

$$\left.\begin{aligned} x &= x_{e_2}-x_{i_1},\ x_{e_2}-x_{e_1},\ x_{i_2}-x_{e_1},\ \text{and}\ x_{i_2}-x_{i_1} \\ \theta_x &= \theta_{e_2}-\theta_{i_1},\ \theta_{e_2}-\theta_{e_1},\ \theta_{i_2}-\theta_{e_1},\ \text{and}\ \theta_{i_2}-\theta_{i_1} \end{aligned}\right\} \tag{11}$$

These four differences represent the four possible axial distances between a terminal plane of h_1 and a terminal plane of h_2. The corresponding azimuth differences, θ_x, are those of the respective pairs of terminals (having the same subscripts). Equation 10 may by a similar notation be condensed into

$$\psi_x(x_1, x_2) = \frac{x_1}{p_2} + \left(\frac{1}{p_1} - \frac{1}{p_2}\right)x_2 + \theta_x - \frac{x}{p_1}, \tag{12}$$

where $\psi_x = \psi_{e_2 i_1}$, $\psi_{e_2 e_1}$, $\psi_{i_2 e_1}$, and $\psi_{i_2 i_1}$.

From the definitions given in eq 11 and 12 it is found by the use of eq 1 and 2 that $\psi_{e_2 i_1} = \psi_{e_2 e_1}$ and $\psi_{i_2 e_1} = \psi_{i_2 i_1}$.

Hence eq 9 shows that the mutual inductance between two helices is of the form

$$m=\omega(x_{e_2}-x_{i_1})-\omega(x_{e_2}-x_{e_1})+\omega(x_{i_2}-x_{e_1})-\omega(x_{i_2}-x_{i_1}) \tag{13}$$

Consequently, the x-component, f, of the attraction of h_2 for h_1, when each carries unit current in the same direction, is given by

$$f=-\omega'(x_{e_2}-x_{i_1})+\omega'(x_{e_2}-x_{e_1})-\omega'(x_{i_2}-x_{e_1})+\omega'(x_{i_2}-x_{i_1}), \tag{13}'$$

where primes denote derivatives with respect to the x-argument and

$$\omega(x)=\int_0^x dx_2\int_0^{r_1}\frac{\dfrac{r_1r_2}{p_1p_2}\cos\psi_x+1}{\sqrt{x_1^2+R^2(\psi_x)}}dx_1, \tag{14}$$

where R is a function of ψ_x defined by eq 6 and ψ_x is defined by eq 12. It will be found that ω is an even function and ω' an odd function of the x-argument, both vanishing with it.

It is necessary to evalute the integral $\omega\ (x)$ for positive and negative values of x in order to treat all possible coaxial helices. To do this we note that the integrand in the integral of eq 14 is an even periodic function of ψ, with period 2π, and may therefore be developed in a Fourier's cosine series. To find this series, consider the function $k/4\sqrt{1-k^2\cos^2\theta}$, where the modulus, k, is a positive real in the range $0\leqq k\leqq 1$. This function has the development

$$\frac{k}{4\sqrt{1-k^2\cos^2\theta}}=\frac{1}{2}\phi_0(k)+\sum_{n=1}^{\infty}\phi_n(k)\cos 2n\theta, \tag{15}$$

where the functions $\phi_n(k)$ are given by

$$\phi_n(k)=\phi_{-n}(k)=\frac{k}{\pi}\int_0^{\frac{\pi}{2}}\frac{\cos 2n\theta}{\sqrt{1-k^2\cos^2\theta}}d\theta=\frac{(-1)^n k}{\pi}\int_0^{\frac{\pi}{2}}\frac{\cos 2n\theta}{\sqrt{1-k^2\sin^2\theta}}d\theta. \tag{16}$$

They may be expressed in terms of the hypergeometric series

$$\phi_n(k)=\frac{k^{2n+1}}{2\pi}\frac{\Gamma\left(n+\frac{1}{2}\right)\Gamma\left(n+\frac{1}{2}\right)}{\Gamma(2n+1)}F\left(n+\frac{1}{2},n+\frac{1}{2},2n+1,k^2\right). \tag{17}$$

When $k\to 1$ every $\phi_n\to\infty$, its principal part being $\phi_n\cong\frac{1}{\pi}\cdot\log\frac{1}{k'}$, where k' is the complementary modulus. These functions satisfy the differential equation

$$k^3\frac{d}{dk}\left[\frac{1-k^2}{k}\phi_n'(k)\right]=(4n^2-1)\phi_n(k),$$

where $\phi_n'=\dfrac{d}{dk}\phi_n$. (18)

The first two functions of the series, ϕ_0 and ϕ_1, are expressible in terms of the two complete elliptic integrals of the first and second kind with modulus k.

$$\phi_0(k)=\frac{k}{\pi}K(k) \text{ and } \phi_1(k)=\frac{2}{\pi}\left(\frac{K(k)-E(k)}{k}\right)-\frac{kK(k)}{\pi} \tag{19}$$

Any other function, $\phi_n(k)$, could be computed in terms of ϕ_0, and ϕ_1 by successive application of the recurrence relation

$$\left(n+\frac{1}{2}\right)\phi_{n+1}+\left(n-\frac{1}{2}\right)\phi_{n-1}=2n\left(\frac{2}{k^2}-1\right)\phi_n \tag{20}$$

The derivative, ϕ_n' is given by

$$\frac{1-k^2}{k}\phi_n'(k)=\left(n-\frac{1}{2}\right)\left[\phi_{n-1}-\left(\frac{2}{k^2}-1\right)\phi_n\right] \tag{21}$$

When k is a function of x, r_1, and r_2 defined by

$$k^2=\frac{4r_1r_2}{x^2+(r_1+r_2)^2}. \tag{22}$$

the mutual inductance of two coaxial circles of radii r_1 and r_2 (the distance between their planes being x) is $M=4\pi^2\sqrt{r_1r_2}\phi_1(k)$
Their attraction, F, with unit currents is $F=-D_xM$, so that

$$Y_1(k)\equiv 4\pi^2\phi_1(k)=\frac{M}{\sqrt{r_1r_2}} \text{ and } Y_2(k)\equiv\pi^2k^3\phi_1'(k)=\frac{\sqrt{r_1r_2}}{x}F \tag{23}$$

These are convenient for finding $\phi_1(k)$ and $\phi_1'(k)$, because the functions $Y_1(k)$ and $Y_2(k)$ are tabulated against k^2 in table 2 of the Scientific Papers of the Institute of Physical and Chemical Research (Komagome, Hongo, Tokyo, 1927) by Nagaoka and Sakurai.

When k is given by eq 22, the functions $\phi_n(k)$ satisfy the partial differential equation

$$\left\{D_x^2+D_{r_1}^2+\frac{1-2\alpha}{r_1}D_{r_1}+\frac{\alpha^2-n^2}{r_1^2}\right\}(r_1^{\alpha-\frac{1}{2}}\phi_n)=0$$

$$=\left\{D_x^2+D_{r_2}^2+\frac{1-2\alpha}{r_2}D_{r_2}+\frac{\alpha^2-n^2}{r_2^2}\right\}(r_2^{\alpha-\frac{1}{2}}\phi_n), \tag{24}$$

where α is any constant.

There are also the integral representations

$$\frac{\phi_n(k)}{\sqrt{r_1r_2}}=\frac{1}{2\pi}\int_0^{2\pi}\frac{\cos n\psi}{\sqrt{x^2+R^2(\psi)}}d\psi=\int_0^\infty e^{-s|x|}J_n(r_1s)J_n(r_2s)ds, \tag{25}$$

where J_n is Bessel's function. The modulus, k, in all that follows, will be understood as the function of x, r_1, and r_2 defined by eq 22. unless otherwise stated. When x is replaced by x_1 it will be called k_1, and k_0 means the modulus for $x=0$.

Hence, as shown by eq 15,

$$\frac{1}{\sqrt{x_1^2+R^2(\psi_x)}}=\frac{1}{\sqrt{r_1r_2}}\left\{\phi_0(k_1)+2\sum_{n=1}^{\infty}\phi_n(k_1)\cos n\psi_x\right\}, \tag{26}$$

so that the required Fourier's series for the integrand of eq 14 is

$$\frac{\frac{r_1r_2}{p_1p_2}\cos\psi_x+1}{\sqrt{x_1^2+R_1^2(\psi_x)}}=\frac{1}{\sqrt{r_1r_2}}\left\{\frac{r_1r_2}{p_1p_2}\phi_1(k_1)+\phi_0(k_1)\right.$$
$$\left.+\sum_{n=1}^{\infty}\cos n\psi_x\left[\frac{r_1r_2}{p_1p_2}(\phi_{n-1}(k_1)+\phi_{n+1}(k_1))+2\phi_n(k_1)\right]\right\} \quad (27)$$

Hence eq 14 may be put in the form

$$\omega(x)=\omega_\theta(x)+\omega_x(x)+\omega_a(x,\theta_x), \quad (28)$$

where

$$\omega_{s1s2}=\omega_\theta+\omega_x=\frac{\sqrt{r_1r_2}}{p_1p_2}\int_0^x dx_2\int_0^{x_2}\left[\phi_1(k_1)+\frac{p_1p_2}{r_1r_2}\phi_0(k_1)\right]dx_1$$
$$=\frac{\sqrt{r_1r_2}}{p_1p_2}\int_0^x(x-x_1)\left[\phi_1(k_1)+\frac{p_1p_2}{r_1r_2}\phi_0(k_1)\right]dx_1 \quad (29)$$

$$\omega_a(x,\theta_x)=\sum_{n=1}^{\infty}\omega_n(x,\theta_x)$$

$$\omega_n(x,\theta_x)=\frac{1}{\sqrt{r_1r_2}}\int_0^x dx_2\int_0^{x_2}dx_1\cos n\psi_x(x_1,x_2)$$

$$\left[\frac{r_1r_2}{p_1p_2}(\phi_{n-1}(k_1)+\phi_{n+1}(k_1))+2\phi_n(k_1)\right] \quad (30)$$

The term ω_θ is the part of the integral of eq 29 involving ϕ_1; the term ω_x the small part involving ϕ_0.

To prove that the ω_{s1s2} defined by the integral of eq 29 is the ω function which, if used in the general formula, eq 13, would give the m_{s1s2} previously defined as mutual inductance of the two associated current sheets, we may start with the elementary formulation which is

$$m_{s1s2}=\int_{x_{i_1}}^{x_{e_1}}dx_1\int_{x_{i_2}}^{x_{e_2}}dx_2\int_0^{2\pi}\frac{d\theta_1}{2\pi}\int_0^{2\pi}\frac{d\theta_2}{2\pi}\frac{\frac{r_1r_2}{p_1p_2}\cos(\theta_2-\theta_1)+1}{\sqrt{(x_2-x_1)^2+R^2(\theta_2-\theta_1)}}$$
$$=\int_{x_{i_1}}^{x_{e_1}}dx_1\int_{x_{i_2}}^{x_{e_2}}dx_2\int_0^{2\pi}\frac{d\psi}{2\pi}\frac{\frac{r_1r_2}{p_1p_2}\cos\psi+1}{\sqrt{(x_2-x_1)^2+R^2(\psi)}} \quad (31)$$

By transformation similar to those used in passing from eq 7 to eq 13 (but much simpler) one finds that

$$\int_{x_{i_1}}^{x_{e_1}}dx_1\int_{x_{i_2}}^{x_{e_2}}dx_2 f(x_2-x_1)=\omega(x_{e2}-x_{i1})$$
$$-\omega(x_{e2}-x_{e1})+\omega(x_{i2}-x_{e1})-\omega(x_{i2}-x_{i1}) \quad (32)$$

where

$$\omega(x)=\int_0^x dx_2\int_0^{x_2} f(x_1)dx_1=\int_0^x (x-x_1)f(x_1)dx_1=\int_0^{-x} dx_2\int_0^{x_2} f(-x_1)dx_1, \quad (33)$$

provided f is such a function that these integrals converge. This shows that $\omega(x)$ is an even function of x, an odd function, or neither, according as $f(x)$ is. Also $\omega(0)=0$, and $\omega'(0)=0$, where $\omega'(x)=D_x\omega(x)$. In eq 31 $f(x)$ is an even function of x, so $\omega(x)$ is an even function of x, and m_{ss} is therefore reduced to the general form of eq 13, where the $\omega-$function is

$$\omega_{s_1s_1}=\omega_\theta+\omega_x=\int_0^x dx_2\int_0^{x_2} dx_1\int_0^{2\pi}\frac{d\psi}{2\pi}\frac{\frac{r_1r_2}{p_1p_2}\cos\psi+1}{\sqrt{x_1^2+R_1^2(\psi)}}$$

$$=\int_0^x (x-x_1)dx_1\int_0^{2\pi}\frac{d\psi}{2\pi}\frac{\frac{r_1r_2}{p_1p_2}\cos\psi+1}{\sqrt{x_1^2+R^2(\psi)}} \quad (34)$$

Using the expansion eq 27 for this integrand, the Ψ integral vanishes for all terms except $n=0$, so that eq 34 becomes identical with eq 29, thus proving that the latter corresponds to current sheets.

It is useful to notice the two following partial differential equations satisfied by the components ω_θ and ω_x, which are derivable from the definition 29 together with eq 24.

$$\Delta^2\omega_x=\left(D_{x_1}^2+D_{r_1}+\frac{1}{r_1}D_{r_1}\right)\omega_x=\left(D_x^2+D_{r_2}^2+\frac{1}{r_2}D_{r_2}\right)\omega_x=\frac{\phi_0(k_0)}{\sqrt{r_1r_2}} \quad (35)$$

$$\left(\Delta^2-\frac{2}{r_1}D_{r_1}\right)\omega_\theta=\left(D_x^2+D_{x_1}-\frac{1}{r_1}D_{r_1}\right)\omega_\theta$$

$$=\left(D_x^2+D_{r_2}^2-\frac{1}{r_2}D_{r_2}\right)\omega_\theta=\frac{\sqrt{r_1r_2}}{p_1p_2}\phi_1(k_0) \quad (36)$$

III. THE PRINCIPAL TERMS ω_θ AND ω_θ'

The equation 29 gives

$$\omega_\theta(x)=x\omega_\theta'(x)-\frac{\sqrt{r_1r_2}}{p_1p_2}\int_0^x x_1\phi_1(k_1)dx_1$$

where

$$\omega_\theta'(x)=\frac{\sqrt{r_1r_2}}{p_1p_2}\int_0^x \phi_1(k_1)dx_1$$

Now, by eq 22

$$\frac{1}{k_1^2}-\frac{1}{k_0^2}=\frac{x_1^2}{4r_1r_2},$$

so that

$$x_1dx_1=-4r_1r_2\frac{dk_1}{k_1^3}$$

Hence

$$\frac{-\sqrt{r_1r_2}}{p_1p_2}\int_0^x x_1\phi_1(k_1)dx_1=\frac{-4(r_1r_2)^{\frac{3}{2}}}{p_1p_2}\int_k^{k_0}\phi_1(k_1)\frac{dk_1}{k_1^3}.$$

By eq 18

$$\frac{\phi_1(k_1)}{k^3}=\frac{1}{3}\frac{d}{dk_1}\left[\frac{1-k^2}{k}\phi_1'(k)\right]=\frac{1}{6}\frac{d}{dk_1}\left\{\phi_0(k_1)-\left(\frac{2}{k_1^2}-1\right)\phi_1(k_1)\right\}$$

$$=\frac{1}{3\pi}\frac{d}{dk_1}\left[\frac{K(k_1)}{k_1}-\left(\frac{2}{k_1^2}-1\right)\frac{K(k_1)-E(k_1)}{k_1}\right]$$

Hence

$$\frac{-\sqrt{r_1r_2}}{p_1p_2}\int_0^x x_1\phi_1(k_1)\,dx_1=\frac{4(r_1r_2)^{\frac{3}{2}}}{3\pi p_1p_2}\left[\frac{K}{k}-\left(\frac{2}{k^2}-1\right)\left(\frac{K-E}{k}\right)\right]$$

minus the same function of k_0, which, being independent of x, may be discarded from the ω function as it always cancels from eq 13. Hence, placing

$$\frac{1}{\pi p_1p_2}=\frac{4\pi N_1N_2}{l_1l_2}$$

$$\omega_\theta(x)=x\omega_\theta'(x)$$

$$+\frac{2\pi N_1N_2}{l_1l_2}\left(\frac{4r_1r_2}{3}\right)\sqrt{x^2+(r_1+r_2)^2}\left[K-\left(\frac{2}{k^2}-1\right)(K-E)\right] \tag{37}$$

To find $\omega_\theta'(x)$ we use eq 16.

$$\omega_\theta'(x)=\frac{\sqrt{r_1r_2}}{\pi p_1p_2}\int_0^{\frac{\pi}{2}}\cos 2\theta d\theta\int_0^x\frac{k_1dx_1}{\sqrt{1-k_1^2\cos^2\theta}}$$

$$=\frac{2r_1r_2}{\pi p_1p_2}\int_0^{\frac{\pi}{2}}\cos 2\theta d\theta\int_0^x\frac{dx_1}{\sqrt{x_1^2+R^2(2\theta)}}$$

$$=\frac{2r_1r_2}{\pi p_1p_2}\int_0^{\frac{\pi}{2}}\cos 2\theta\log\left[\frac{x+\sqrt{x^2+R^2(2\theta)}}{R(2\theta)}\right]d\theta.$$

Integrating this by parts gives

$$\omega_\theta'(x)=\frac{2(r_1r_2)^2x}{\pi p_1p_2}\int_0^{\frac{\pi}{2}}\frac{\sin^2 2\theta d\theta}{R^2(2\theta)\sqrt{x^2+R^2(2\theta)}}$$

$$=\frac{x\sqrt{r_1r_2}}{4\pi p_1p_2}kk_0^2\int_0^{\frac{\pi}{2}}\frac{\sin^2 2\theta d\theta}{(1-k_0^2\cos^2\theta)\sqrt{1-k^2\cos^2\theta}}$$

$$=\frac{\sqrt{r_1r_2}}{\pi p_1p_2}xk\int_0^{\frac{\pi}{2}}\frac{\sin^2\theta(1-\sin^2\theta)d\theta}{\left(\frac{1}{k_0^2}-\sin^2\theta\right)\sqrt{1-k^2\sin^2\theta}}$$

$$=\frac{\sqrt{r_1 r_2}}{\pi p_1 p_2} x \int_0^{\frac{\pi}{2}} \frac{d\theta}{\sqrt{1-k^2\sin^2\theta}} \left\{ \frac{1-(1-k^2\sin^2\theta)}{k} + \frac{k(1-k_0^2)}{k_0^2}\left[1-\frac{1}{1-k_0^2\sin^2\theta}\right]\right\},$$

so that

$$\omega_\theta'(x)=\frac{(r_1+r_2)k_0 k}{2\pi p_1 p_2} x, \left\{\frac{K-E}{k^2}+\frac{k_0'^2}{k_0^2}\left[K-\Pi\right]\right\},$$

where

$$\Pi=\int_0^{\frac{\pi}{2}} \frac{d\theta}{(1-k_0^2\sin^2\theta)\sqrt{1-k^2\sin^2\theta}}$$

$$=\int_0^K \frac{du}{1-k_0^2 sn^2(u,k)}=K+\int_0^K \frac{k_0^2 sn^2 u}{1-k_0^2 sn^2 u}du.$$

The equation may also be put in the form

$$\omega_\theta'(x)=\frac{2\pi N_1 N_2}{l_1 l_2}\left\{x\sqrt{x^2+(r_1+r_2)^2}(K-E)+\frac{x(r_1-r_2)^2}{\sqrt{x^2+(r_1+r_2)^2}}[K-\Pi]\right\}$$

For computing, it is sometimes preferable to introduce the Jacobian zeta-function, Z.

$$K-\Pi=\frac{k_0}{k_0'\sqrt{k_0^2-k^2}}\left[K\mathrm{Z}(\theta_0,k')+\frac{\pi F(\theta_0,k')}{2K'}-\frac{\pi}{2}\right] \tag{38}$$

where

$$0<\theta_0=\sin^{-1}\frac{k_0'}{k'}<\frac{\pi}{2}$$

Hence

$$\omega_\theta'(x)=\frac{2\pi N_1 N_2}{l_1 l_2}\left\{x\sqrt{x^2+(r_1+r_2)^2}(K-E) \pm\left|r_1^2-r_2^2\right|\left[K\mathrm{Z}(\theta_0,k')+\frac{\pi F(\theta_0,k')}{2K'}-\frac{\pi}{2}\right]\right\} \tag{39}$$

Where the plus sign belongs with positive x and the minus with negative x, the bracket multiplied by $\pm$ vanishing when $x=0$. (Also the absolute value $|r_1^2-r_2^2|$ must be observed.) The zeta-function is expressible in terms of $E(\theta, k')$ and $F(\theta, k')$ for

$$\mathrm{Z}(\theta,k')=E(\theta,k')-\frac{E'}{K'}F(\theta,k'). \tag{40}$$

Using the AGM method of computation,[1] and finding a_n, b_n, and c_n by the formulas

[1] L. V. King, On the Direct Numerical Calculation of Elliptic functions and Integrals, page 8.

$$\left.\begin{aligned} a_n=\frac{1}{2}(a_{n-1}+b_{n-1}),\ b_n=\sqrt{a_{n-1}b_{n-1}},\ c_n=\frac{1}{2}(a_{n-1}-b_{n-1}) \\ \tan\ (\theta_{n+1}-\theta_n)=\frac{b_n}{a_n}\tan\ \theta_n \end{aligned}\right\}, \quad (41)$$

and starting with the initial values

$$a_0=1,\ b_0=k,\ c_0=k',\ \text{and}\ \theta_0=\sin^{-1}\frac{k_0'}{k'}$$

then

$$\frac{\pi F(\theta_0,\ k')}{2K'}=\frac{\theta_n}{2^n}\ \text{and}\ Z(\theta_0,\ k')=c_1\sin\theta_1+c_2\sin\theta_2\ \ldots\ .\ c_n\sin\theta_n. \quad (41')$$

Using the initial values $a_0=1$, $b_0=k'$, and $c_0=k$,

gives

$$K=\frac{\pi}{2a_n}\ \text{and}\ K-E=(c_0^2+2c_1^2+4c_2^2\ \ldots\ .\ 2^nc_n^2)\frac{K}{2}$$

The formulas 41′ are the result of successive applications of Landen's transformation which increases the amplitude and decreases the modulus. Hence, they will be most suitable when k' is small.

If, however, k' is large it is easier to work the transformation in the opposite direction of increasing modulus, in which case the formula is

$$KZ(\theta_0,\ k')+\frac{\pi F(\theta_0,\ k)'}{2K'}-\frac{\pi}{2}=-\frac{\pi}{2}(1-\sin\ \psi_n)+K\sum_2(\psi_n,\ c_n), \quad (41'')$$

where

$$a_0=1,\ b_0=k',\ c_0=k$$

and

$$\sin\ (2\psi_{n+1}-\psi_n)=\frac{b_n}{a_n}\sin\ \psi_n\ \text{(beginning with}\ \psi_0=\theta_0)$$

and

$$\sum_2(\psi_n,\ c_n)=2c_2\frac{\tan\ (2\psi_2-\psi_1)}{\cos\ (2\psi_3-\psi_2)}+6c_3\frac{\tan\ (2\psi_3-\psi_2)}{\cos\ (2\psi_4-\psi_3)}+14c_4\frac{\tan\ (2\psi_4-\psi_3)}{\cos\ (2\psi_5-\psi_4)}$$

$$+\ \ldots\ .\ +2(2^{1+n}-1)c_{n+2}\frac{\tan\ (2\psi_{n+2}-\psi_{n+1})}{\cos\ (2\psi_{n+3}-\psi_{n+2})}\ \ldots\ .$$

King[2] also gives an alternative to this with the same a_n, b_n, and c_n, and the same recurrence formula between ψ_{n+1} and ψ_n, as above, except that it starts with

$$\sin^2\ \psi_0=\frac{1}{k'^2}\left(1-\frac{k^2}{k_0^2}\right)=\frac{x^2}{x^2+(r_1-r)^2}$$

[2] There is evidently a misprint in King's formula 7 see eq 75 or 75 defining $\Sigma_2(\psi_n c_n)$. The general term should contain the factor $2(2^{1+n}-1)c_{n+2}$ and not $2(2^n-1)c_{n+2}$.

in which case

$$\Pi=\frac{2K\cos\ (2\psi_1-\psi_0)}{k'^2\ \sin\ 2\psi_0}\Big[a_n\ \sin\ \psi_n+\sum_2(\psi_n,\ c_n)\Big] \qquad (41)'''$$

To interpret the function $\omega_\theta'(x)$ in eq 39 it will be found that if the factor $N_2/l_2=1/2\pi p_2$ is omitted and x replaced by l_1 in eq. 39 the result is the mutual inductance between the helix h_1 (or its sheet) and a circle of radius r_2 in its end plane. This is found from eq 13 by letting $l_2\to 0$. The formulas for $\omega_\theta(x)$ and $\omega_\theta'(x)$ when used in eq 13 or 13′ are equivalent to the formulas derived by Jones[3] for the mutual inductance of two sheets and the force between them. The principal part of the force comes from the ω_θ' function and is, by eq 13′,

$$f_\theta=[\omega_\theta'(x_{t_2}-x_{t_1})-\omega_\theta'(x_{t_2}-x_{e_1})]-[\omega_\theta'(x_{e_2}-x_{t_1})-\omega_\theta'(x_{e_2}-x_{e_1})].$$

By the above interpretation of the function $\omega_\theta'(x)$ it is evident that the first bracket is N_2/l_2 times the mutual inductance between helix h_1 (or its sheet) and the initial circle of sheet 2 (in the plane $x=x_{t_2}$). The second bracket is N_2/l_2 times the mutual inductance between h_1 and the end circle of sheet 2 (in the plane $x=x_{e_2}$).

IV. EFFECT OF AXIAL CURRENT IN HELICES AND LEAD WIRES

From eq 29

$$\omega_x(x)=\frac{x}{\sqrt{r_1r_2}}\int_0^x\phi_0(k_1)dx_1-\frac{1}{\sqrt{r_1r_2}}\int_0^x x_1\phi_0(k_1)dx_1=x\omega_x'(x)$$
$$-\frac{1}{\sqrt{r_1r_2}}\int_0^x\phi_0(k_1)x_1dx_1.$$

Now, by eq 19 and 22

$$\frac{1}{\sqrt{r_1r_2}}\int_0^x\phi_0(k_1)x_1dx_1=\frac{1}{\pi\sqrt{r_1r_2}}\int_0^x k_1K(k_1)x_1dx_1=\frac{4\sqrt{r_1r_2}}{\pi}\int_k^{k_0}\frac{K(k_1)}{k_1^2}\,dk_1$$
$$=\frac{4\sqrt{r_1r_2}}{\pi}\Big[\frac{E(k)}{k}-\frac{E(k_0)}{k_0}\Big].$$

Hence, we may take

$$\omega_x(x)=x\omega_x'(x)-\frac{4\sqrt{r_1r_2}}{\pi}\frac{E(k)}{k}, \qquad (42)$$

dropping the term in k_0, which is independent of x, and therefore always cancels from eq 13.

[3] J. V. Jones, Proc. Roy. Soc. (London) [A] **63**, 198 (1898).

To find $\omega_x'(x)$ we may use eq 17

$$\omega_x'(x)=\frac{1}{\sqrt{r_1r_2}}\int_0^x \phi_0(k_1)dx_1=\frac{1}{\pi}\sum_{s=0}^{\infty}\frac{\Gamma^2\left(s+\frac{1}{2}\right)}{\Gamma^2(s+1)}(4r_1r_2)^s\int_0^x\frac{dx_1}{[x_1^2+(r_1+r_2)^2]^{s+\frac{1}{2}}}$$

$$=\frac{1}{2}\log\frac{1+\sin\gamma}{1-\sin\gamma}+\sin\gamma\, S(\gamma, k_0^2)$$

where

$$\gamma=\tan^{-1}\frac{x}{r_1+r_2}$$

and

$$S(\gamma, k_0)=\frac{1}{\pi}\sum_{s=1}^{\infty}\frac{\Gamma^2\left(s+\frac{1}{2}\right)}{\Gamma^2(s+1)}k_0^{2s}F\left(1-s, \frac{1}{2}, \frac{3}{2}, \sin^2\gamma\right)$$

Now, $\sin\gamma S$ is, in general, small compared to the logarithm, except when $\gamma=0$, in which case they both vanish; but as x becomes large, γ approaches $\pi/2$, and the logarithm becomes infinite, while the series approaches the finite limit $S\left(\frac{\pi}{2}, k_0\right)=\log\frac{2}{1+k_0'}$, which vanishes if $k_0=0$, and has its greatest value, $\log 2=0.69$, when $k_0=1$. Also S vanishes when $k_0=0$, so that, since the term $\sin\gamma S(\gamma_1 k_0)$ is a small correction to a second-order term, a good approximation is obtained (sufficient for all cases with which this paper is concerned) by taking

$$\sin\gamma S(\gamma, k_0)=\sin\gamma\log\frac{2}{1+k_0'},$$

so that

$$\omega_x'(x)=\log\left[\frac{x+\sqrt{x^2+(r_1+r_2)^2}}{r_1+r_2}\right]+\frac{x}{\sqrt{x^2+(r_1+r_2)^2}}\log\left(\frac{r_1+r_2}{r_m}\right), \quad (43)$$

where r_m is the greater of r_1 and r_2 $\left(\text{since } \frac{2}{1+k_0'}=\frac{r_1+r_2}{r_m}\right)$. It may be noted that the method used to obtain $\int_0^x\phi_1(k_1)dx_1$ in the preceding section leads to

$$\int_0^x\phi_0(k_1)dx_1=\frac{1}{\pi}\int_0^{\pi}\log\left[\frac{x+\sqrt{x^2+R^2(\theta)}}{R(\theta)}\right]d\theta.$$

An approximation similar to this may be obtained from eq 17 in the form

$$\frac{1}{\sqrt{r_1r_2}}\int_0^x\phi_n(k_1)dx_1=\sin\gamma k_0^{2n}S_n(\gamma, k_0),$$

where

$$S_n(\gamma,k_0)=\frac{1}{\pi}\sum_{s=0}^{\infty}k_0^{2s}\frac{\Gamma^2\left(s+n+\frac{1}{2}\right)}{\Gamma(s+1)\Gamma(s+2n+1)}F\left(1-s-n,\frac{1}{2},\frac{3}{2},\sin^2\gamma\right).$$

when

$$\sin^2\gamma=1,\ F\left(1-s-n,\frac{1}{2},\frac{3}{2},1\right)=\frac{\sqrt{\pi}}{2}\frac{\Gamma(s+n)}{\Gamma\left(s+n+\frac{1}{2}\right)},$$

so that

$$\begin{aligned}k_0^{2n}S_n\left(\frac{\pi}{2},k_0\right)&=\frac{1}{2n}\left(\frac{k_0}{2}\right)^{2n}F\left(n,n+\frac{1}{2},2n+1,k_0^2\right)\\&=\frac{1}{2n}\left(\frac{k_0}{1+k_0'}\right)^{2n}=\frac{1}{2n}\left(\frac{r_1}{r_2}\right)^n\text{ if }r_2>r_1\\&=\frac{1}{2n}\left(\frac{r_2}{r_1}\right)^n\text{ if }r_2<r_1.\end{aligned}$$

Hence an approximation sufficient for use in second order terms is obtained by placing

$$k_0^{2n}\sin\gamma S_n(\gamma,k_0)=\frac{\sin\gamma}{2n}\left(\frac{k_0}{1+k_0'}\right)^{2n},$$

so that the following approximation analagous to eq. 43 is obtained:

$$\frac{2}{\sqrt{r_1r_2}}\int_0^x\phi_n(k_1)dx_1=\frac{x}{\sqrt{x^2+(r_1+r_2)^2}}\frac{1}{n}\left(\frac{r_1}{r_2}\right)^n\text{ if }n>0\text{ and }r_2>r_1.\qquad(44)$$

When the lead wire of length l_1 for the return current of h_1 lies parallel to a generator of the current sheet but at a slightly greater distance from the axis, say $r_{l_1}=r_1+\Delta r_1$, the mutual inductance between this lead wire, l_1, and the helix, h_2, is (as far as second-order terms are concerned) equal to that between l_1 and the current sheet of h_2, the corresponding ω-function being

$$-\omega_x(x,\,r_{l_1},\,r_2)=-\omega_x(x,\,r_1,\,r_2)-\Delta r_1D_{r_1}\omega_x(x,\,r_1,\,r_2).$$

If the lead wire of No. 2 is similarly situated at a distance $r_{l_2}=r_2+\Delta r_2$ its mutual inductance with h_1 has the ω-function

$$-\omega_x(x,\,r_1,\,r_{l_2})=-\omega_x(x,\,r_1,\,r_2)-\Delta r_2D_{r_2}\omega_x(x,\,r_1r_2).$$

This arrangement, of course, implies that the number of turns, N_1 and N_2, are integers, so that the azimuths of the two lead wires are θ_{l_1} and θ_{l_2}. Their mutual inductance with each other is determined by the ω-function, $\omega_{l_1l_2}$, as in eq 13, and their force by $\omega'_{l_1l_2}$, as in eq 13′, where

$$\omega_{l_1l_2}(x,\,\alpha,\,r_{l_1},\,r_{l_2})=x\omega'_{l_1l_2}-\sqrt{x^2+R^2_{l_1l_2}(\alpha)}\qquad(45)$$

$$\omega'_{l_1l_2}(x,\ \alpha,\ r_{l_1},\ r_{l_2})=\log\frac{\sqrt{x^2+R^2_{l_1l_2}(\alpha)}+x}{R_{l_1l_2}(\alpha)}=\int_0^x\frac{dx_1}{\sqrt{x_1^2+R^2_{l_1l_2}(\alpha)}} \tag{45'}$$

where

$$\alpha=\theta_{l_2}-\theta_{l_1}$$

$$R^2_{l_1l_2}(\alpha)=r^2_{l_1}+r^2_{l_2}-2r_{l_1}r_{l_2}\cos\alpha.$$

The additive constant, $R_{l_1l_2}$, has been omitted from eq 45, being independent of x, so that it cancels from eq 13. When the radial distances, Δr_1 and Δr_2, of the lead wires from the helices are small, the axial currents in the lead wires and helices almost compensate in their effects upon inductance and force, the residual being a very small term, depending upon the azimuth, α, of the coils. If $\bar{\omega}_x(x,\ \alpha)$ represents the total ω-function due to x-components of current in lead wires and helices, then

$$\bar{\omega}_x(x,\ \alpha)=\omega_x(x,\ r_1,\ r_2)+\omega_{l_1l_2}(x,\ \alpha,\ r_1+\Delta r_1,\ r_2+\Delta r_2)$$
$$-\omega_x(x,\ r_1+\Delta r_1,\ r_2)-\omega_x(x,\ r_1,\ r_2+\Delta r_2).$$

When Δr_1 and Δr_2 are small, this becomes

$$\bar{\omega}_x(x,\ \alpha)=\omega_{l_1l_2}(x,\ \alpha,\ r_{l_1},\ r_{l_2})-\omega_x(x,\ r_1,\ r_2)-(\Delta r_1D_{r_1}+\Delta r_2D_{r_2})\omega_x(x,\ r_1,\ r_2)$$

Since, however, these ω-functions are themselves of second order, the terms in Δr are smaller than second order and therefore negligible. Hence, for this arrangement of lead wires, the ω-function and its derivative, which takes account of all axial components of current in helices and lead wires, are given by

$$\bar{\omega}_x(x,\alpha)=x\omega'_*(x,\alpha)+\frac{4\sqrt{r_1r_2}}{\pi}\frac{E}{k}-\sqrt{x^2+R^2(\alpha)}, \tag{46}$$

where

$$\bar{\omega}'_x(x,\alpha)=\log\frac{x+\sqrt{x^2+R^2(\alpha)}}{R(\alpha)}-\omega_x'(x)=\sum_{n=1}^{\infty}b_n\cos n\alpha, \tag{46'}$$

the constant term in this Fourier's cosine series being zero. The coefficients b_n for $n>0$ are given by

$$b_n=\frac{2}{\sqrt{r_1r_2}}\int_0^x\phi_n(k_1)dx_1= \tag{46''}$$

$$=\frac{x}{\sqrt{x^2+(r_1+r_2)^2}}\frac{1}{n}\left(\frac{r_1}{r_2}\right)^n$$

by the approximation in eq. 45, if $r_2>r_1$. On summing this Fourier's series we find the following finite form as an approximation for eq 46'

$$\bar{\omega}'(x,\alpha)=\frac{x}{\sqrt{x^2+(r_1+r_2)^2}}\log\frac{r_2}{R(\alpha)} \tag{46'''}$$

when $r_2>r_1$.

V. THE AZIMUTHAL TERMS

To integrate eq 30, we may place (by reference to eq 10′)

$$\cos n\psi_x = e^{in\psi_x} = e^{in\left(\theta_x - \frac{x}{p_1}\right) + \frac{inx_1}{p_1} + \left(\frac{1}{p_1} - \frac{1}{p_2}\right)inx_2},$$

with the understanding that the real part of the result is to be taken. Using the abbreviation

$$J(n,s) = J_{n-1}(r_1 s)J_{n-1}(r_2 s) + J_{n+1}(r_1 s)J_{n+1}(r_2 s) + \frac{2p_1p_2}{r_1r_2}J_n(r_1 s)J_n(r_2 s).$$

eq 30 becomes, by use of eq 25,

$$\omega_n(x,\theta_x) \equiv \frac{r_1r_2}{p_1p_2}\, e^{in\left(\theta_x - \frac{x}{p_1}\right)} \int_0^\infty ds J(n,s) \int_0^x e^{in\left(\frac{1}{p_1} - \frac{1}{p_2}\right)x_2} dx_2 \int_0^{x_2} e^{\frac{inx_1}{p_1} - s|x_1|} dx_1.$$

If $x > 0$, then x_1 and x_2 are both positive in the range of integration of the x_1x_2 double integral, so that $e^{-s|x_1|} = e^{-sx_1}$. When $x < 0$, then x_1 and x_2 are both negative in the range of the integral, so that $e^{-s|x_1|} = e^{+sx_1}$, and the result of the integration in the latter case is found by changing the sign of s in the result of the integration for the first case.

It is thus found that both results are included in the following:

$$\omega_n(x,\theta_x) = \frac{r_1r_2e^{in\theta x}}{n^2(p_2 - p_1)} \int_0^\infty ds J(n,s) \left\{ \frac{p_2\left(e^{-\frac{inx}{p_2}} - e^{-s|x|}\right)}{1 \pm \frac{ip_2 s}{n}} - \frac{p_1\left(e^{-\frac{inx}{p_1}} - e^{-s|x|}\right)}{1 \pm \frac{ip_1 s}{n}} \right\}$$

$$= \frac{r_1r_2e^{in\theta x}}{n^2} \int_0^\infty ds J(n,s)$$

$$\left\{ \frac{p_2 e^{-\frac{inx}{p_2}}}{(p_2 - p_1)\left(1 \pm \frac{ip_2 s}{n}\right)} - \frac{p_1 e^{-\frac{inx}{p_1}}}{(p_2 - p_1)\left(1 \pm \frac{ip_1 s}{n}\right)} - \frac{e^{-s|x|}}{\left(1 \pm \frac{ip_1 s}{n}\right)\left(1 + \frac{ip_2 s}{n}\right)} \right\},$$

where the upper sign belongs with positive x and the lower with negative x.

The real part of this is

$$\omega_n(x,\theta_x)=\frac{r_1r_2}{n^2}\int_0^\infty ds J(n,s)\left\{\frac{1}{p_2-p_1}\left[\frac{p_2\cos n\left(\theta_x-\frac{x}{p_2}\right)}{1+\frac{p_2^2s^2}{n^2}}-\frac{p_1\cos n\left(\theta_x-\frac{x}{p_1}\right)}{1+\frac{p_1^2s^2}{n^2}}\right]-\frac{\left(1-\frac{p_1p_2s^2}{n^2}\right)e^{-|x|}\cos n\theta_x}{\left(1+\frac{p_1^2s^2}{n^2}\right)\left(1+\frac{p_2^2s^2}{n^2}\right)}\right\}$$

$$\pm\frac{r_1r_2}{n^3}\int_0^\infty sds J(n,s)\left\{\frac{1}{p_2-p_1}\left[\frac{p_2^2\sin n\left(\theta_x-\frac{x}{p_2}\right)}{1+\frac{p_2^2s^2}{n^2}}-\frac{p_1^2\sin n\left(\theta_x-\frac{x}{p_1}\right)}{1+\frac{p_1^2s^2}{n^2}}\right]-\frac{(p_1+p_2)e^{-|x|}\sin n\theta_x}{\left(1+\frac{p_1^2s^2}{n^2}\right)\left(1+\frac{p_2^2s^2}{n^2}\right)}\right\} \tag{47}$$

The terms in the first integral which do not contain the exponential factor $e^{-s|x|}$ may be discarded, as they will all cancel in eq 13 because, as shown by reference to eq 2 and 11, the values of $\theta_x - x/p_1$ will be the same for the first and second x-differences, $(x_{e_2} - x_{i_1})$ and $(x_{e_2} - x_{e_1})$. These first and second x-values enter eq 13 with opposite signs. Similarly, the values of $\theta_x - x/p_1$ are the same for the third and fourth x-values, $x_{i_2} - x_{e_1}$ and $x_{i_2} - x_{i_1}$, which enter eq 13 with opposite signs. Hence the term in eq 47, $\cos n(\theta_x - x/p_1)$, disappears by the second x-term canceling the first and the fourth canceling the third. It is also found that $\cos n(\theta_x - x/p_2)$ disappears by the fourth canceling the first and the third canceling the second. The corresponding terms in the second integral, $\sin n(\theta_x - x/p_1)$ and $\sin n(\theta_x - x/p_1)$, do not always cancel because of the $\pm$ factor which has the sign of x. If the associated current sheets are wholly external to each other the cancelation is complete, but if one lies wholly or partly within the other the terms $\sin n(\theta_x - x/p_1)$ and $\sin n(\theta_x - x/p_2)$ of eq 47 do not disappear from eq 13.

Hence eq 47 may be written

$$\omega_n(x,\theta_x) = -\frac{r_1 r_2}{n_2} \cos n\theta_x \int_0^\infty \frac{e^{-s|x|} J(n,s)\left(1 - \frac{p_1 p_2 s^2}{n_2}\right)}{\left(1+\frac{p_1^2 s^2}{n^2}\right)\left(1+\frac{p_1^2 s^2}{n^2}\right)} ds$$

$$\mp \frac{r_1 r_2 (p_1 + p_2)}{n^3} \sin n\theta_x \int_0^\infty \frac{s e^{-s|x|} J(n_1 s)}{\left(1+\frac{p_1^2 s^2}{n^2}\right)\left(1+\frac{p_2^2 s^2}{n^2}\right)} ds \pm \omega_n^*(x,\theta_x), \quad (48)$$

plus terms which cancel in eq 13, where

$$\omega_n^*(x,\theta_x) = \frac{r_1 r_2}{n(p_2 - p_1)}$$

$$\left\{ \sin n\left(\theta_x - \frac{x}{p_2}\right) \int_0^\infty \frac{s J(n,s) ds}{s^2 + \frac{n^2}{p_2}} - \sin n\left(\theta_x - \frac{x}{p_1}\right) \int_0^\infty \frac{s J(n,s) ds}{s^2 + \frac{n^2}{p_1^2}} \right\}.$$

We may now show that by limiting the application of the results of this section to those cases where the $\omega_n^*(x)$ are all negligible, we do not impose a serious restriction as far as practical mutual inductances are concerned, with the exception of a bifilar-wound coil in which one of the windings is used as primary, the other as secondary. Such a coil has never been used for absolute measurements, but we see no reason why it should not be used in the future. It would possess certain advantages from the point of view of accurate construction and measurement and would give the greatest possible mutual inductance. The formula for its mutual inductance has never been evaluated with precision as it has for a self inductance, but the problem would present no greater difficulty.

It is easy to foretell that this limitation is that the helices, h_1 and h_2 shall not through a finite part of their lengths be separated from each other by a distance which is small (of the order of p/r).

If H_n denotes the first Hankel's function then

$$\int_0^\infty \frac{sJ_m(r_1s)J_m(r_2s)ds}{s^2+\frac{n^2}{p^2}} = \frac{\pi}{2}J_m\left(\frac{inr_1}{p}\right)iH_m\left(\frac{inr_2}{p}\right).$$

when $r_2 > r_1$. In case $r_2 < r_1$, the two are interchanged in this equation. Since r_1/p and r_2/p are large, the asymptotic expansions of H_m and J_m show that this expression is very close to

$$\frac{p}{2n\sqrt{r_1r_2}}e^{\frac{-n|r_2-r_1|}{p}} \text{ in cases } r_2 > r_1 \text{ or } r_2 < r_1.$$

Hence, approximately,

$$\omega_n^*(x,\theta_x) = \frac{\sqrt{r_1r_2}}{n^2(p_1-p_2)i}\left\{p_2e^{-\frac{n}{p_2}[|r_2-r_1|+i(x-p_2\theta x)]} - p_1e^{-\frac{n}{p_1}[|r_2-r_1|+i(x-p_1\theta_x)]}\right\},$$

where the real part is to be taken.

When $p_2=p_1=p$, this becomes

$$\omega_n^*(x,\theta_x) = \frac{\sqrt{r_1r_2}}{i}\left\{\frac{1}{n^2}+\frac{|r_2-r_1|+ix}{np}\right\}e^{-\frac{n}{p}[|r_2-r_1|+i(x-p\theta_x)]}$$

Since the entire ω_a function with the factor r_1r_2 is of second order in general, compared with the principal term, ω_θ, which has the large factor $\frac{r_1r_2}{p_1p_2}$, it is evident that $\sum_1^\infty \frac{e}{n}^{-\frac{n}{p}|r_2-r_1|}$ will be utterly negligible when r_2-r_1 is finite (not a small quantity of the order of p). Since ω_n^* is only different from zero when one coil lies wholly or partly within the other, this means that the two must not approach very close to each other if ω_n^* is to be neglected.

The remaining integrals in eq 48 cannot be similarly integrated in finite terms, but it is evident that when $|x|$ is finite (not small of the order p/r), we may (on account of the convergence factor $e^{-s|x|}$ of the integrand) obtain the principal part of ω_n by placing $p_1=p_2=0$ in the integrand, as the resulting integrals still converge, even if $r_1=r_2$. We cannot be content, however, with this restriction on x, as we must evaluate ω_n for cases where $x=0$. In this case, if we place $p_1=p_2=0$, the integrals in eq 48 then converge only if $r_1 \neq r_2$, but if r_1-r_2 is a finite quantity, the principal part of ω_n is thus obtained. The limitation is therefore evident—*the helices must be everywhere separated from each other by finite distances.* Assuming this to be the case, and noting that the last term in the definition of $J(n, s)$ is negligible, we obtain the result

$$\omega_n(x,\theta_x) = -\frac{\sqrt{r_1r_2}}{n^2}[\phi_{n-1}(k)+\phi_{n+1}(k)]\cos n\theta_x,$$

so that

$$\omega_a(x,\theta x) = -\sqrt{r_1r_2}\sum_{n=1}^{\infty}[\phi_{n-1}+\phi_{n+1}]\frac{\cos n\theta_x}{n^2}, \tag{49}$$

and

$$\omega_a'(x,\theta_x)=\frac{xk^3}{4\sqrt{r_1r_2}}\sum_{n=1}^{\infty}[\phi_{n-1}'+\phi_{n+1}']\frac{\cos\ n\theta_x}{n^2}. \tag{49'}$$

(In finding the self inductance of a helix, the ω_a rises in rank from a second order to a first order quantity, from which originates the most important correction term—the evaluation of which was the only difficult part of that problem. The same remark would apply to a bifilar mutual inductance). Eq 49 holds of course when $r_1=r_2$, provided the end planes of the two coils are not close together and the coils wholly external to each other (so that k is not close to unity).

The series 49 and 49′ may be evaluated by finding ϕ_0 and ϕ_1 in terms of elliptic integrals by eq 19, and then finding all other ϕ_n or ϕ_n' by the recurrence relation 20 or 21.

Since the series represent second-order terms, it is evident that some simpler approximation will be sufficient. To obtain such, consider the even, continuous function of θ, $f(\theta)$, which is never negative and is a periodic function of θ, with period 2π, defined by the series

$$f(\theta)\equiv\frac{2}{3}-\frac{4}{\pi^2}\sum_{n=1}^{\infty}\frac{\cos\ n\theta}{n^2}\text{ for all real values of }\theta. \tag{50}$$

$f(\theta)$ vanishes when $\theta=2n\pi$, where n is any integer. It has the maximum value unity when $\theta=(2n+1)\pi$. It consists of a succession of parabolic arcs for

$$f(\theta)=\left(2-\frac{\theta}{\pi}\right)\frac{\theta}{\pi}\text{ ---------- when }0\leqq\theta\leqq\ 2\pi, \tag{51a}$$

and

$$f(\theta)=\left(4-\frac{\theta}{\pi}\right)\left(\frac{\theta}{\pi}-2\right)\text{------ when }2\pi\leqq\theta\leqq 4\pi. \tag{51b}$$

Now,

$$f(\theta+\theta_x)=\frac{2}{3}-\frac{4}{\pi^2}\sum_{n=1}^{\infty}\frac{\cos\ n(\theta+\theta_x)}{n^2}. \tag{52}$$

Also from eq 15 one finds

$$\frac{k}{2}\ \frac{\cos\ \theta}{\sqrt{1-k^2\cos^2\ \frac{\theta}{2}}}=\phi_1(k)+\sum_{n=1}^{\infty}[\phi_{n-1}(k)+\phi_{n+1}(k)]\ \cos\ n\theta. \tag{53}$$

Multiplying eq 52 by eq 53, and integrating the product from $\theta=0$ to $\theta=2\pi$, gives

$$\frac{k}{2}\int_0^{2\pi}\frac{f(\theta+\theta_x)\ \cos\ \theta d\theta}{\sqrt{1-k^2\cos^2\ \frac{\theta}{2}}}=\frac{4\pi}{3}\phi_1(k)-\frac{4}{\pi}\sum_{n=1}^{\infty}(\phi_{n-1}+\phi_{n+1})\frac{\cos\ n\theta_x}{n^2},$$

so that eq 49 becomes

$$\omega_a(x,\theta_x)=-\sqrt{r_1r_2}\left\{\frac{\pi^2}{3}\phi_1(k)-\frac{\pi k}{8}\int_0^{2\pi}\frac{f(\theta+\theta_x)\cos\theta d\theta}{\sqrt{1-k^2\cos^2\frac{\theta}{2}}}\right\}$$

$$=-\sqrt{r_1r_2}\left\{\frac{\pi^2}{3}\phi_1-\frac{\pi k}{8}\int_0^{2\pi-\theta_x}\frac{f(\theta+\theta_x)\cos\theta d\theta}{\sqrt{1-k^2\cos^2\frac{\theta}{2}}}-\frac{\pi k}{8}\int_{2\pi-\theta_x}^{2\pi}\frac{f(\theta+\theta_x)\cos\theta}{\sqrt{1-k^2\cos^2\frac{\theta}{2}}}d\theta\right\}.$$

It is sufficient to evaluate this for the range $0\leqq\theta_x\leqq\pi$ since its value for any other range of θ_x is obtainable from this by inspection, remembering that ω_a is an even function of θ_x with period 2π. (This restriction disappears from the end result.) With this restriction the argument of f in the integral from 0 to $2\pi-\theta_x$ lies in the range $0\leqq\theta+\theta_x\leqq2\pi$, so that by eq 51a

$$f(\theta+\theta_x)=\left(2-\frac{\theta+\theta_x}{\pi}\right)\left(\frac{\theta+\theta_x}{\pi}\right).$$

In the integral last written, as eq 51b shows,

$$f(\theta+\theta_x)=\left(4-\frac{\theta+\theta_x}{\pi}\right)\left(\frac{\theta+\theta_x}{\pi}-2\right).$$

Making these substitutions, and then changing the variable of integration in the last integral to θ', where $\theta=2\pi-\theta'$, gives

$$\omega_a(x,\theta_x)=-\sqrt{r_1r_2}\left\{\frac{\pi^2}{3}\phi_1(k)-\frac{\pi k}{8}\int_0^{2\pi-\theta_x}\left[2-\frac{\theta_x+\theta}{\pi}\right]\frac{\theta_x+\theta}{\pi}\frac{\cos\theta d\theta}{\sqrt{1-k^2\cos^2\frac{\theta}{2}}}\right.$$

$$\left.-\frac{\pi k}{8}\int_0^{\theta_x}\left[2-\frac{\theta_x-\theta}{\pi}\right]\frac{\theta_x-\theta}{\pi}\frac{\cos\theta d\theta}{\sqrt{1-k^2\cos^2\frac{\theta}{2}}}\right\}$$

or

$$\omega_a(x,\theta_x)=-\sqrt{r_1r_2}\left\{\frac{\pi^2}{3}\phi_1-\frac{\pi k}{8}\int_0^{2\pi-\theta_x}\frac{f(\theta_x+\theta)\cos\theta d\theta}{\sqrt{1-k^2\cos^2\frac{\theta}{2}}}-\frac{\pi k}{8}\int_0^{\theta_x}\frac{f(\theta_x-\theta)\cos\theta d\theta}{\sqrt{1-k^2\cos^2\frac{\theta}{2}}}\right\},\quad(54)$$

where both of the arguments $\theta_x+\theta$ and $\theta_x-\theta$ lie in the positive range of less than 2π. For this range, instead of the cosine series 50, we find a sine series for $f(\theta)$

$$f(\theta)=\frac{32}{\pi^3}\left[\sin\frac{\theta}{2}+\frac{\sin\frac{3\theta}{2}}{27}+\frac{\sin\frac{5\theta}{2}}{125}\ldots.\right]\text{ for }0\leqq\theta\leqq2\pi.\quad(55)$$

Since $32/\pi^3=1.032$, it is evident that a good approximation for the integrals in eq 54 is given by placing $f(\theta)=\sin\frac{\theta}{2}$ for $0\leqq\theta\leqq2\pi$, that is,

$$f(\theta_x+\theta)=\sin\left(\frac{\theta_x+\theta}{2}\right) \text{ and } f(\theta_x-\theta)=\sin\left(\frac{\theta_x-\theta}{2}\right).$$

This gives after some simple transformations

$$\omega_a(x,\theta_x)=-\sqrt{r_1r_2}\left\{\frac{\pi^2}{3}\phi_1(k)+\frac{\pi k}{2}\sin\frac{\theta_x}{2}\int_{\left(\frac{\pi-\theta_x}{2}\right)}^{\frac{\pi}{2}}\frac{\sin\theta\cos 2\theta}{\sqrt{1-k^2\sin^2\theta}}d\theta\right.$$
$$\left.+\frac{\pi k}{2}\cos\frac{\theta_x}{2}\int_0^{\left(\frac{\pi-\theta_x}{2}\right)}\frac{\cos\theta\cos 2\theta}{\sqrt{1-k^2\sin^2\theta}}d\theta\right\}. \quad (56)$$

Now,

$$k\int\frac{\sin\theta\cos 2\theta}{\sqrt{1-k^2\sin^2\theta}}d\theta=\frac{1}{k^2}[\log(k\cos\theta+\sqrt{1-k^2\sin^2\theta})$$
$$-k\cos\theta\sqrt{1-k^2\sin^2\theta}]$$

and

$$k\int\frac{\cos\theta\cos 2\theta}{\sqrt{1-k^2\sin^2\theta}}d\theta=\frac{1}{k^2}[-k'^2\sin^{-1}(k\sin\theta)+k\sin\theta\sqrt{1-k^2\sin^2\theta}],$$

so that

$$\omega_a(x,\theta_x)=-\frac{\sqrt{r_1r_2}\pi^2\phi_1(k)}{3}-\frac{\pi\sqrt{r_1r_2}}{2}\left[\frac{1}{k}\sqrt{1-k^2\cos^2\frac{\theta_x}{2}}\right.$$
$$\left.-\frac{k'^2}{k^2}\cos\frac{\theta_x}{2}\sin^{-1}\left(k\cos\frac{\theta_x}{2}\right)-\frac{1}{k}\sin\frac{\theta_x}{2}\log\frac{k\sin\frac{\theta_x}{2}+\sqrt{1-k^2\cos^2\frac{\theta_x}{2}}}{k'}\right]. \quad (57)$$

Differentiating this with respect to x gives

$$\omega_a'(x,\theta_x)=\frac{x}{12\sqrt{r_1r_2}}\cdot\pi^2k^3\phi_1'(k)$$
$$+\frac{\pi x}{4\sqrt{r_1r_2}}\left\{\cos\frac{\theta_x}{2}\sin^{-1}\left(k\cos\frac{\theta_x}{2}\right)-\frac{k\left(1-\frac{k^2}{2}\right)}{k'^2}\sqrt{1-k^2\cos\frac{\theta_x}{2}}\right.$$
$$\left.+k\sin\frac{\theta_x}{2}\log\left[\frac{k\sin\frac{\theta_x}{2}+\sqrt{1-k^2\cos^2\frac{\theta_x}{2}}}{k'}\right]\right\} \quad (57')$$

These equations hold for any value of θ_x since they are even periodic functions of θ_x, with period 2π.

The four azimuthal differences in eq 11 may be written.

$$\theta_{e_2i_1}=\alpha+2\pi N_2, \theta_{e_2e_1}=\alpha+2\pi(N_2-N_1),$$

$$\theta_{i_2e_1}=\alpha-2\pi N_1, \theta_{i_2i_1}\equiv\alpha\equiv\theta_{i_2}-\theta_{i_1} \quad (58)$$

so that when the number of turns, N_1 and N_2, are integers, every θ_x may be taken equal to α. It is evident that no essential simplification would have resulted in the formulas eq 57 and 58 had we restricted N_1 and N_2 to integral values at the beginning.

To obtain an interpretation of the term $\omega_a(x,\theta_x)$, let $M(x,\theta_x,r_1,r_2)$, or, more briefly, $M(\theta_x)$, denote the mutual inductance between the two incomplete circular arcs which are the parts of the two coaxial circles of radii $r_1 r_2$ (the distance between their planes being x) included between the azimuth planes $\theta=0$ and $\theta=\theta_x$.

When the circles are complete we have by eq 23

$$M(2\pi)=4\pi^2\sqrt{r_1 r_2}\phi_1(k)$$

In general, if $0<\theta_x<2\pi$

$$M(\theta_x)=r_1 r_2\int_0^{\theta_x}d\theta_1\int_0^{\theta_x}d\theta_2\frac{\cos(\theta_2-\theta_1)}{\sqrt{x^2+R^2(\theta_2-\theta_1)}}$$

which may be transformed into

$$\frac{M(\theta_x)}{2\sqrt{r_1 r_2}}=\int_0^{\theta_x}d\theta_2\int_0^{\theta_1}\frac{k\cos\theta_1 d\theta_1}{2\sqrt{1-k^2\cos^2\frac{\theta_1}{2}}}.$$

Using the expansion in eq 53 for this integrand gives

$$\frac{M(\theta_x)}{2\sqrt{r_1 r_2}}=\frac{\theta_x^2}{2}\phi_1(k)+\sum_{n=1}^{\infty}\frac{\phi_{n-1}(k)+\phi_{n+1}(k)}{n^2}(1-\cos n\theta_x). \quad (59)$$

Equations 49 and 59 are equivalent to

$$\omega_a(x,\theta_x)=\omega_a(x,0)+\frac{1}{2}\left[M(\theta_x)-\left(\frac{\theta_x}{2\pi}\right)^2 M(2\pi)\right] \text{ when } 0\leqq\theta_x\leqq 2\pi.$$

Since, by eq 57,

$$\omega_a(x,0)=-\frac{M(2\pi)}{12}-\frac{\pi\sqrt{r_1 r_2}k'}{2k}\left(1-\frac{k'}{k}\sin^{-1}k\right),$$

this may be written

$$\omega_a(x,\theta_x)=-\frac{M(2\pi)}{12}+\frac{1}{2}\left[M(\theta_x)-\left(\frac{\theta_x}{2\pi}\right)^2 M(2\pi)\right]$$

$$-\frac{\pi\sqrt{r_1 r_2}k'}{2k}\left[1-\frac{k'}{k}\sin^{-1}k\right], \quad (60)$$

which furnishes an interpretation for part of the term $\omega_a(x,\theta_x)$, although this form has no advantage in computation since the mutual induc-

tance $M(\theta_x)$ of the two incomplete circular arcs is not a well-known or tabulated function as in the case $M(2\pi)$ when the arcs are complete circles. In fact, the foregoing formulas give for it

$$M(\theta)=\left(\frac{\theta}{2\pi}\right)^2 M(2\pi)-\pi\sqrt{r_1 r_2}\left\{\frac{\sqrt{1-k^2\cos^2\frac{\theta}{2}}-k'}{k}\right.$$
$$-\frac{k'^2}{k^2}\left[\cos\frac{\theta}{2}\sin^{-1}\left(k\cos\frac{\theta}{2}\right)-\sin^{-1}k\right]$$
$$\left.-\frac{1}{k^2}\sin\frac{\theta}{2}\log\left[\frac{k\sin\frac{\theta}{2}+\sqrt{1-k^2\cos^2\frac{\theta}{2}}}{k'}\right]\right\}. \quad (61)$$

When the series 49 and 49′ are known to converge so rapidly that only the first two terms need be retained, there is no need to use eq 57 and 57′.

VI. THE HELIX EQUIVALENT TO A HELICAL WIRE

Consider the unit current in wire w_1 to have the vector volume density whose magnitude is a function of the distance r_1' from the x axis, say $u_1\ (r_1')$. Its direction is that of the generating helical filament.

An axial plane cuts the wire in a circular section of radius ρ_1, as specified in eq 5. If dS_1 is an element of area of this circular section, a helical tube whose (oblique) section is dS_1 carries the current,

$$dI_1=\frac{u_1(r_1')dS_1}{\sqrt{1+\left(\frac{p_1}{r_1'}\right)^2}}$$

since

$$\frac{1}{\sqrt{1+\left(\frac{p_1}{r_1'}\right)^2}}$$

is the cosine of the angle between the normal to dS_1 and the direction of the current-density vector or tube. The total current carried by the wire is unity, so that

$$\int\int\frac{u_1(r_1')dS_1}{\sqrt{1+\left(\frac{p_1}{r_1'}\right)^2}}=1 \quad (62)$$

integrated over the circular section of the wire.

In place of the rectangular coordinates $x_{i_1}'-x_t$ and $r_1'-r_1$ of a point of this section referred to the center of the circle as origin (as used in eq 5), we may use the polar coordinates ρ_1' and ϕ_1, where

$$x_{i_1}'-x_{i_1}=\rho_1'\cos\phi_1 \text{ and } r_1'-r_1=\rho_1'\sin\phi_1,$$

in terms of which

$$dS_1=\rho_1' d\rho_1' d\phi_1.$$

Expanding the current density, $u_1(r_1')=u_1(r_1+\rho_1' \sin \phi_1)$, about the value r_1 (corresponding to the central filament of the wire) by Taylor's theorem and applying the condition 62, we obtain (to the second order, inclusive, in ρ_1)

$$dI_1=\frac{\rho_1' d\rho_1' d\phi_1}{\pi\rho_1^2}\left[1+A_1\rho_1' \sin \phi_1+B_1\left(\rho_1'^2 \sin^2 \phi_1-\frac{\rho_1^2}{4}\right)\right],$$

where

$$A_1=\frac{u_1'(r_1)}{u_1(r_1)} \text{ and } B_1=\frac{u_1''(r_1)}{2u_1(r_1)}.$$

With similar definitions of A_2 and B_2, etc., the current, dI_2, in a helical current tube of the second wire is

$$dI_2=\frac{\rho_2' d\rho_2' d\phi_1}{\pi\rho_2^2}\left[1+A_2\rho_2' \sin \phi_2+B_2\left(\rho_2'^2 \sin^2 \phi_2-\frac{\rho_2^2}{4}\right)\right],$$

so that

$$dI_1 dI_2=\frac{\rho_1' d\rho_1' d\phi_1 \rho_2' d\rho_2' d\phi_2}{\pi^2\rho_1^2\rho_2^2}\Big\{1+(A_1\rho_1' \sin \phi_1+A_2\rho_2' \sin \phi_2)$$
$$+B_1\left(\rho_1'^2 \sin^2 \phi_1-\frac{\rho_1^2}{4}\right)+B_2\left(\rho_2'^2 \sin^2 \phi_2-\frac{\rho_2^2}{4}\right)+A_1A_2\rho_1' \sin \phi_1 \cdot \rho_2' \sin \phi_2\Big\}. \quad (63)$$

The mutual inductance, $m_{w_1 w_2}$, between the two helical wires, w_1 and w_2, is found by multiplying this expression for $dI_1\, dI_2$ by m and integrating over both circular sections of the wire, an operation which is equivalent to multiplying by 1 when applied to any terms of m except the finite part m_θ since the operation only alters the subject by a second-order fraction of itself.

Now, by eq 13, replacing the x by x'

$$\iint dI_1 \iint dI_2 m_\theta=\iint dI_1 \iint dI_2 \omega_\theta(x_{e_2}'-x_{i_1}')-\iint dI_1 \iint dI_2 \omega_\theta(x_{e_2}'-x_{e_1}')$$
$$+\iint dI_1 \iint dI_2 \omega_\theta(x_{i_2}'-x_{e_1}')-\iint dI_1 \iint dI_2 \omega_\theta(x_{i_2}'-x_{i_1}').$$

Also

$$\omega_\theta(x_{e_2}'-x_{i_1}')=\omega_\theta(x'_{e_2}-x'_{i_1}, r_1', r_2')$$
$$=\omega_\theta(x_{e_2}-x_{i_1}+\rho_2' \cos \phi_2-\rho_1' \cos \phi_1, r_1+\rho_1 \sin \phi_1, r_2+\rho_2 \sin \phi_2), \quad (65)$$

where $x_{e_2}-x_{i_1}$, r_1, and r_2 refer to the central filaments of the wires. The expansion of this by Taylor's theorem for a function of three variables may be written symbolically (to the second order in ρ_1' and ρ_2')

$$\omega_\theta(x_{e_2}'-x_i')=\Big\{1+[(\rho_2' \cos \phi_2-\rho_1' \cos \phi_1)D_x+\rho_1' \sin \phi_1 D_{r_1}+\rho_2' \sin \phi_2 D_{r_2}]$$
$$+\frac{1}{2}[(\rho_2' \cos \phi_2-\rho_1' \cos \phi_1)D_x+\rho_1' \sin \phi_1 D_{r_1}+\rho_2' \sin \phi D_{r_2}]^2\Big\}\omega_\theta(x, r_1 r_2), \quad (66)$$

where $x=x_{e_2}-x_{i_1}$.

Multiplying eq 63 by eq 66 and integrating gives

$$\iint dI_1 \iint dI_2 \omega_\theta(x'_{e_1} - x'_{i_1}) = \left\{1 + \frac{\rho_1^2}{8}(D_x^2 + D_{r_1}^2 + 2A_1 D_{r_1}) + \frac{\rho_2^2}{8}(D_x^2 + D_{r_2}^2 + 2A_2 D_{r_2})\right\}\omega_\theta(x, r_1 r_2),$$

where $x = x_{e_2} - x_{i_1} = z =$ the distance between end plane of the central filament of wire w_2 and the initial plane of the central filament of wires w_1. On making use of the partial differential 36, this becomes so that

$$\int\int dI_1 \int\int dI_2 \omega_\theta(x'_{e_2} - x'_{i_1}) = \omega_\theta(x_{e2} - x_{i1})$$

$$+\frac{1}{8}\left[\rho_1^2\left(\frac{1}{r_1} + 2A_1\right)D_{r_1} + \rho_2^2\left(\frac{1}{r_2} + 2A_2\right)D_{r_2}\right]\omega_\theta + \frac{\rho_1^2 + \rho_2^2}{8}\frac{\sqrt{r_1 r_2}}{\rho_1 \rho_2}\phi_1(k_0). \quad (67)$$

The expansion of the three remaining integrals of eq 64 is the same as this with the appropriate x-arguments.

The result is that, to the second order, the mutual inductance of the two wires is given by

$$m_{w1w2} = m + \frac{1}{8}\left[\rho_1^2\left(\frac{1}{r_1} + 2A_1\right)D_{r_1} + \rho_2^2\left(\frac{1}{r_2} + 2A_2\right)D_{r_2}\right]m_\theta, \quad (68)$$

where h_1 and h_2 are their central helical filaments, with radii r_1 and r_2. This may be written

$$m_{w1w2} = m_\theta(\bar{r}_1, \bar{r}_2) + m_x + m_a, \quad (69)$$

where

$$\bar{r}_1 = r_1 + \frac{\rho_1^2}{8}\left(\frac{1}{r_1} + 2A_1\right) \text{ and } \bar{r}_2 = r + \frac{\rho_2^2}{8}(1 + 2A_2), \quad (70)$$

where all the m's except the principal one refer to the central helices of the two wires, and every m is expressed in terms of its w-function, as in eq 13, with corresponding subscripts.

The sole effect of giving the wires a radius is to increase the effective radii of their current sheets from r to $\bar{r}$ (to the second order), the length of the sheets being unaltered. The latter fact is explained in part by the particular manner in which their lengths have been defined, and in part by the fact that the wire sections are circular, so that the terms which would represent an increase in effective length—being proportional to $D_x^2\omega_\theta$—have entered the result together with $D_r^2\omega_\theta$ and their combined effects have been expressed in terms of $D_{r_1}\omega_\theta$ and $D_{r_2}\omega_\theta$ by means of the partial differential eq 36.

For distributions of current in both wires whose r-derivative vanishes at the central filament, the constants A_1 and A_2 are both zero.

The uniform current distribution is an example of this class. A correction equal to the above but opposite in sign is obtained for distributions in which $A_1=-1/r_1$, and $A_2=-1/r_2$, an example of this class being the "natural" distribution ($B_1=1/r_1^2$), where the current density varies inversely as the linear length $\sqrt{r^2+\rho^2}$ of the helical current filaments. A distribution for which $A_1=-1/2r_1$, $A_2=-1/2r_2$ would have no correction of this order of magnitude.

Whatever assumption be made as to the current distribution, it will still be necessary to evaluate $D_{r_1}m$ and $D_{r_2}m$ roughly in order to estimate the effects of errors in determination of the mean radii, r_1 and r_2.

At present we are ignorant of the current distribution in such wires, so that for simplicity it would seem better to ignore altogether this correction for finite thickness of the wires. The assumption usually made of uniform current density carries with it a spurious precision.

We can, however, allow for future increase of knowledge as to current distribution, with no less simplicity of treatment, by defining the helix which is equivalent to a helical wire as one having the same pitch and end planes as its central filament, but a cylindrical radius

$$r=a+\frac{\rho^2}{8}\left(\frac{1}{a}+2A\right),$$

where a is the mean cylindrical radius of the helical wire and ρ is the wire-radius—the interpretation of the constant A being the value at the central filament of the r-derivative of the current density, which was assumed to be a function of r only and in the direction of the helical filament.

As far as we are concerned here, this disposes of the difference between helices and helical wires. All the formulas in the preceding sections regarding mutual inductance of two helices and the force between them are valid for the helical wires to which they are equivalent.

VII. APPLICATION TO THE CURRENT BALANCE USED IN THE NATIONAL PHYSICAL LABORATORY

If the x axis be taken vertically upward, the lower (or suspended) helix, called No. 1, has a mean radius $r_1=10$ cm and length $l_1=15.2$ cm. The upper helix has radius $r_2=16$ cm and length $l_2=11.0$ cm. Both helices have the same pitch, $2\pi p_1=2\pi p_2=0.2$ cm and an integral number of turns, $N_1=76$ and $N_2=55$ turns. Hence, every $\theta_x=\alpha=\theta_{i_2}-\theta_{i_1}$ the azimuth of the helices. The upper end of No. 1 projects into No. 2, so that the third x-difference of eq 11 is negative.

$$x_1\equiv x_{e_2}-x_{i_1}=+20.1 \text{ cm}\rightarrow k_1^2=0.5926$$

$$x_2\equiv x_{e_2}-x_{e_1}=+4.9 \text{ cm}\rightarrow k_2^2=0.9143$$

$$x_3\equiv x_{i_2}-x_{e_1}=-6.1 \text{ cm}\rightarrow k_3^2=0.8974$$

$$x_4\equiv x_{i_2}-x_{i_1}=+9.1 \text{ cm}\rightarrow k_4^2=0.8434$$

The force, f, acting on the suspended helix when both carry unit current is

$$f=f_\theta+\bar{f}_x(\alpha)+f_a(\alpha), \tag{71}$$

where f_θ is the principal part due to angular components of current in the helices and by eq 13′.

$$f_\theta = -\omega_\theta'(x_1) + \omega_\theta'(x_2) - \omega_\theta'(x_3) + \omega_\theta'(x_4), \tag{72}$$

where the $\omega\theta'(x)$ are given by eq 39. The small part $\bar{f}_x(\alpha)$ denotes the residue due to x-components of current in helices and lead wires together and is given by

$$\bar{f}_x(\alpha) = -\bar{\omega}_x'(x_1,\alpha) + \bar{\omega}_x'(x_2,\alpha) - \bar{\omega}_x'(x_3,\alpha) + \bar{\omega}_x'(x_4,\alpha), \tag{73}$$

where the $\bar{\omega}_x'(x,\alpha)$ are given by eq 46′.

The last part, $f_a(\alpha)$, is given similarly by

$$f_a(\alpha) = -\omega_a'(x_1,\alpha) + \omega_a'(x_2,\alpha) - \omega_a'(x_3,\alpha) + \omega_a'(x_4,\alpha), \tag{74}$$

where the $\omega_a'(x,\alpha)$ may be computed by eq 49′ or 57′. Both $\bar{\omega}_x'(x,\alpha)$ and $\omega_a'(x,\alpha)$ are even periodic functions of α, with period 2π, so the same is true of $\bar{f}_x(\alpha)$ and $f_a(\alpha)$.

In the actual coils, however, there are two helices on each cylinder differing in azimuth by π, so that when each carries unit current the force on the suspended coil is F, where

$$F = F_\theta + \bar{F}_x(\alpha) + F_a(\alpha), \tag{75}$$

where

$$\left.\begin{aligned} F_\theta &= 4f_\theta \\ \bar{F}_x(\alpha) &= 2[\bar{f}_x(\alpha) + \bar{f}_x(\alpha+\pi)] \\ F_a(\alpha) &= 2[f_a(\alpha) + f_a(\alpha+\pi)] \end{aligned}\right\} \tag{76}$$

This makes the azimuthal terms, $\bar{F}_x(\alpha)$ and $F_a(\alpha)$, each even periodic functions of α, with period π, so that

$$\bar{F}_x(\alpha) + F_a(\alpha) = \sum_{n=1}^{\infty} C_{2n} \cos 2n\alpha. \tag{77}$$

P. Vigoureux of the National Physical Laboratory of England has recently reported to this Bureau that in the absence of a formula for the coefficients C_{2n} he has evaluated experimentally the first coefficient, C_2, assuming the first term to be the only one of the series of practical importance. This he did by measuring the force for three different azimuths $\alpha = 3°$, $15°$, and $85°$.

In order to see what part of C_2 is due to axial components of current and what part is due to the azimuth terms ω_a', let

$$C_{2n} = C_{2n}^x + C_{2n}^a. \tag{78}$$

Reference to eq 72, 76, and 46″ shows that the effect of axial currents is given by

$$C_{2n}^x = \frac{1}{\sqrt{r_1 r_2}} \cdot \frac{1}{n} \left(\frac{r_1}{r_2}\right)^{2n} \{-x_1 k_1 + x_2 k_2 - x_3 k_3 + x_4 k_4\}, \tag{79}$$

and eq 49′ shows that

$$C_{2n}^{a}=\frac{1}{\sqrt{r_1r_2}}\frac{1}{4n^2}\{-x_1k_1^3[\phi'_{2n+1}(k_1)+\phi'_{2n-1}(k_1)]+x_2k_2^3[\phi_{2n+1}(k_2)+\phi_{2n-1}(k_2)]$$
$$-x_3k_3^3[\phi'_{2n+1}(k_3)+\phi'_{2n-1}(k_3)]+x_4k_4^3[\phi_{2n+1}(k_4)+\phi_{2n-1}(k_4)]\} \quad (80)$$

Placing $n=1$

$$C_2^z=\frac{1}{\sqrt{r_1r_2}}\left(\frac{r_1}{r_2}\right)^2[-x_1k_1+x_2k_2-x_3k_3+x_4k_4]=+0.103 \text{ dynes} \quad (81)$$

$$C_2^a=\frac{1}{\sqrt{r_1r_2}}\Bigg\}-x_1k_1^3\left[\frac{\phi'_1(k_1)+\phi'_3(k_1)}{4}\right]+x_2k_2^3\left[\frac{\phi'_1(k_2)+\phi'_3(k_2)}{4}\right]$$
$$-x_3k_3^3\left[\frac{\phi'_1(k_3)+\phi'_3(k_3)}{4}\right]+x_4k_4^3\left[\frac{\phi'_1(k_4)+\phi'_3(k_4)}{4}\right]\Bigg\} \quad (82)$$

From the recurrence relations 20 and 21, it is found that

$$k^3\left[\frac{\phi'_1(k)+\phi'_3(k)}{4}\right]=\frac{1}{\pi^2}\left\{\left[\frac{1}{2}+\frac{8k'^2}{3k^4}\right]\pi^2k^3\phi'_1(k)-\left(\frac{2}{k^2}-1\right)4\pi^2\phi_1(k)\right\}$$
$$=\frac{1}{\pi^2}\left\{\left[\frac{1}{2}+\frac{8k'^2}{3k^4}\right]Y_2(k)-\left(\frac{2}{k^2}-1\right)Y_1(k)\right\}\equiv\frac{1}{\pi^2}Y(k), \quad (83)$$

where Y_1 and Y_2 are the functions defined in eq 23, which may be taken from tables.

$Y_1(k)=2.086,\quad 9.100,\quad 8.165,$ and 6.072 for k_1, k_2, k_3, and k_4

$Y_2(k)=1.490,\quad 25.663,\quad 20.049,$ and 10.796

$Y(k)=0.401,\quad 9.04,\quad 6.57,$ and 3.41

$$C_2^a=\frac{1}{\pi^2\sqrt{r_1r_2}}\{-x_1Y(k_1)+x_2Y(k_2)-x_3Y(k_3)+x_4Y(k_4)\}=0.86 \text{ dyne.}$$

Hence

$C_2^a+C_2^z=0.86+0.10=0.96$ dyne, which differs from the observed value 1 dyne by less than the experimental error.

The force $F_\theta=94{,}527.22$ dynes, so that

$$F=94{,}527.22+0.96\cos 2\alpha$$

For azimuth $\alpha=0$ or π, this azimuthal term amounts to 10 parts in a million.

VIII. SUMMARY

The self inductance between two coaxial helices and the force between them are given in terms of four ω-functions, and their x-derivatives, respectively, as in eq 13 and 13′, the four x-distances being defined in eq 11 with their respective azimuthal differences θ_x. Resolving these functions into three components, $\omega(x)=\omega_\theta(x)+\omega_z(x)+\omega_a(x,\theta_x)$, the principal part corresponds to the mutual inductance

between the two associated current sheets, with angular components of current, and $\omega_x(x)$ with axial components. The last term, $\omega_a(x,\theta_x)$, is like $\omega_x(x)$, a second-order correction term applied to the finite term, $\omega_\theta(x)$, where the ratio of pitch to cylindrical radius is considered a first-order infinitesimal.

The principal term, $\omega_\theta(x)$, is given by eq 37 and $\omega_x(x)$ by eq 39. The first is equivalent to Jones' formula for current sheets. The terms $\omega_x(x)$ and $\omega'_x(x)$ are given by eq 42 and 43.

The azimuthal terms, $\omega_a(x,\theta_x)$ and $\omega'_a(x,\theta_x)$, are given by the series eq 49 and 49′ and in finite terms by eq 57 and 57′.

These formulas are not restricted to the case where the helices have an integral number of turns but are quite general. They need not have the same pitch. For the case most common in practice where the numbers of turns are integers and the lead wires are straight lines parallel and close to the generator of the cylindrical current sheet, the total effect of all axial components of current in helices and lead wires together is represented by a function $\overline{\omega}_x(x)$ which is given by eq 46, and its x-derivative by eq 46′.

It is shown in section VII that the azimuthal variation of the force computed by these equations agrees (within experimental errors) with that observed at the National Physical Laboratory.

The correction terms given in section VI take account of the finite diameter of helical wires. They require a knowledge of the current distribution in the wires.

These formulas are valid to the second order, inclusive, provided no parts of the two helices lie very close to each other, that is, at distances of the order of magnitude of the pitch of the windings.

WASHINGTON, December 21, 1938.

118278—39——10